Differences between a 3 dimensional probabilistic method of berthing structure design and the traditional method of a berthing structure design

J.Kool
01-09-2011

Thesis Committee:
Prof.drs. Ir. J.K. Vrijling   TU Delft, section Hydraulic Engineering
Prof.ir. A.Q.C. Van der Horst   TU Delft, section Design and Construction,
                                               BAM Infraconsult
dr.ir. J.G. De Gijt   TU Delft, section Hydraulic Engineering,
                                               Gemeentewerken Rotterdam
dr.ir. P.H.A.J.M. van Gelder   TU Delft, section Hydraulic Engineering
ir. L. Groenewegen   Delta Marine Consultant
ir. D. Dudok van Heel   Gemeentewerken Rotterdam

Differences between a 3 dimensional probabilistic method of berthing structure design and
the traditional method of a berthing structure design

J.J. Kool

Differences between a 3 dimensional probabilistic method of berthing structure design and the traditional method of a berthing structure design

Job Kool
Tel: 06-41428837
E-mail: jobkool@gmail.com

Delft University of Technology
Faculty of Civil Engineering and
Geosciences
Stevinweg 1
2628 CN Delft
The Netherlands
+31 (0) 15 278 54 40

Public Works of Rotterdam
Engineering Section
Galvanistraat 15
3029 AD Rotterdam
The Netherlands
+31 (0)10 489 69 22

Preface

This document is the thesis for the Master of Science Hydraulic engineering curriculum of the Delft University of Technology. This report is titled "The differences between the design of a berthing structure according a 3 dimensional probabilistic method and the design according the standards". The research was carried out by Job Kool at the office of Public works of Rotterdam at the Engineering section in Rotterdam

I would like to thank my family for their attention, patients, time and support in writing this thesis. I would like to thank the employers of the Harbour and Transport Group of the Engineering Section of Public Works of Rotterdam for their hospitality. My sincere thanks to all members of my committee for their professional guidance, patience and support during this final thesis.

Thesis Committee:

Prof.drs. ir. J.K. Vrijling   TU Delft, Section Hydraulic Engineering
Prof. ir. A.Q.C. Van der Horst TU Delft, Section Design and Construction, BAM Infraconsult
dr.ir.J.G. De Gijt   TU Delft, Section Hydraulic Engineering
dr.ir. P.H.A.J.M. Van Gelder   TU Delft, Section Hydraulic Engineering
ir. L. Groenewegen   Delta Marine Consultants
ir. D. Dudok van Heel   Gemeentewerken Rotterdam

Hilversum, October 2011

Job Kool

Differences between a 3 dimensional probabilistic method of berthing structure design and
the traditional method of a berthing structure design

J.J. Kool

CONTENTS

List of symbols

Symbol	Units	Description
$\varnothing$	[mm]	diameter of the tubelar section
t	[mm]	wall thickness
E	[kNm]	berthing energy
$F(y)$	[kN]	fender force
y	[m]	deformation
m_s	[tonnage]	mass of vessel
$F_{construction}$	[kN]	forces of structure
F_{tugs}	[kN]	forces due to tugs
F_{wind}	[kN]	forces due to wind
$F_{currents}$	[kN]	forces due to current
$F_{hydraudinamic}$	[kN]	forces due to additional mass
I_s	[m^4]	moment of inertia
ψ	[rad]	angle
$M_{construction}$	[kNm]	moment due to structure
M_{tugs}	[kNm]	moment due to tugs
M_{wind}	[kNm]	moment due to wind
$M_{currents}$	[kNm]	moment due to currents
$M_{hydraudinamic}$	[kNm]	moment due to added mass
C_e	[-]	eccentricity factor
C_m	[-]	virtual mass factor
C_s	[-]	softness factor

C_c	[-]	berth cinfiguration factor
v	[m/s]	velocity
M	[tonnage]	vessel mass
DWT	[tonnage]	death weight tonnage
k	[m]	radius of gyration
r	[m]	radius between the centre of mass of the vessel and the point of collision between the vessel and the structure
γ	[^{0}]	angle between the radius r and the velocity of the vessel
ρ	[tonnage/m^3]	density of water
L	[m]	length of vessel
B	[m]	width of vessel
D	[m]	draft of vessel
$\gamma_{m;\varphi}$	[-]	partial factor for soil characteristics tangent of the angle of internal friction
$\gamma_{m;c2}$	[-]	partial factor for cohesion
$\gamma_{m;cu}$	[-]	partial factor for undrained shear strength
$t_{99\%}$	[min]	time of 99% of total consilidation
c_v	[m^2/s]	consolidation coefficient
k	[m/s]	permeability coefficient
m_y	[N/mm^2]	compressibility coefficient
Δh	[m]	infinite settlement
ε	[-]	strain
σ_{zz}	[N/mm^2]	vertical stress
σ_1	[N/mm^2]	initial pressure
K_p	[-]	passive soil pressure coefficient
D	[mm]	diameter of the pile
K_a	[-]	Active soil pressure coefficient
c	[N/mm^2]	cohesion
E_y	[N/mm^2]	Young's modulus
k_h	[1/m^2]	bearing resisstance
z	[m]	depth beneath the soil surface
K_q	[-]	φ dependent term
K_c	[-]	cohesive term
$\sigma_v{}'$	[N/mm^2]	vertical grain stress
$\sigma_p{}'$	[N/mm^2]	passive grain pressure
p_{rs}	[kN/m]	shallow lateral soil resistance
p_{rd}	[kn/m]	deep lateral soil resistance
X	[m]	depth below the sea floor
k_ϕ	[kPa/m]	coefficient of the horizontal sub grade reaction below the water table

p_u	[kN/m]	ultimate lateral resistance
c_u	[kN/m^2]	undrained shear strength
p_0'	[kN/m^2]	effective overburden stress
J	[-]	empirical constant
X_R	[m]	depth below sea floor reduced resistance zone for uniform soils
ε_{cr}	[N/mm^2]	critical strain
f_y	[N/mm^2]	yield stress
γ_{plooi}	[-]	partial laod safety factor for local buckling
Z_e	[mm^4]	elastic section modulus
M_d	[Nm]	design moment
P	[kN]	test load
f_e	[m]	deformation due to laoding
α	[-]	magnification factor
$\psi(y)$	[-]	structure function
P_i	[-]	failure chance
u_{admis}	[m]	admisable deformation
Z	[-]	reliability function
M_{admis}	[kNm]	admisable Moment
β	[-]	reliability index
μ	[-]	mean value
σ	[-]	standard deviation
R_{rep}	[-]	representative resistance
R^*	[-]	design resistance
S_{rep}	[-]	representative load
S^*	[-]	design load
P_f	[-]	chance of failure
n_f	[-]	number of faults
n	[-]	amount of total simulations
$v_{average}$	[m/s]	average velocity

1 Abstract

In this study the emergence of overcapacity is examined, in the design of a continuous berthing structure designed using the semi-probabilistic standards, by using a Monte Carlo simulation. By developing a three dimensional model using Scia engineer, a finite element software, it is relatively easy to pinpoint where the weaknesses in the design are and what the critical variables in the application of the model are. In this study the applicability of the model, the probability of failure of the structure, possible over-capacity and the critical factors and variables related to failure are discussed and examined.

2 Summary

The jettie is designed by the guidance of the deterministic standards. These standards are based on the standardized values of safety factors (semi-probabilistic). The level 1 method takes the load and the capacity of every element as a standard value. The interaction of every separate element as a part of a whole is not taken in to account in this method. The use of deterministic standards can result in a design that is not economically optimal. A probabilistic approach gives a better insight in the occurrence of an unwanted events and leads to more insight of the optimizing of the structure.

The "Lyondell jetty" in the Europort in Rotterdam is used as reference structure. This jetty is constructed in 1997 and is in use of ARCO Chemie Nederland, a manufacturer of chemical derivatives for all kinds of synthetic products such as paints, foam and anti freeze). It concerns a berthing structure with a double deck that offers space to berth two large sea vessel and two smaller barges. The vessel berth at a continues berthing structure founded on piles and is covered with fender wood.

Considering the failure mechanisms of the jetty it appeared that the failure of the berthing structure is a conditional chance for functioning of the jetty. It was decided to submit the actual berthing structure to further examination by means of a Monte Carlo simulation. Using the Monte Carlo simulation a measure of failure of an event is expressed in strength and resistance. In this study this event consists of reaching the yielding stress in the structure or the exceeding of a determined boundary of deformation of the structure during the berthing of a vessel.

The energy loading in the calculation is introduced with the help of the equation of Saurin. When using the model it is necessary that the soil can be modelled as a spring. This has to meet the requirements of the Winkler model. In analysing the deformations of the structure the soil needs to have elasto-plastic characteristics. The function of the springs are described as p-y curves that were developed by Reese et al. (API accepted).

The actual berthing structure that was designed with the Blum method, the design was recalculated, using help of p-y curves. The piles have been extended to ensure that sufficient fixity can be achieved to develop full plastic moment, such as a simplified approach within the

framework of this study. The new and much simpler design is based on the terms of reference of the Lyondell jetty. This becomes the new reference model that is used for comparison with the results of the Monte Carlo simulation.

In this thesis only the berthing of the mooring point 2 (large sea vessel) is considered and two main objectives are researched. First the question if the developed 3 dimensional simulation technique is applicable for running a Monte Carlo simulation. The second question is whether the application of the model leads to differences in capacity between the reference design of the Lyondell jetty and the design according to the probabilistic method.

The first stated question was positively answered. The soil model developed in Scia engineer has the same behavior as in M-pile and the structure shows the expected behavior according the rules of mechanics. In the model relating to the energy load the variables of length, width, depth, mass, angle of berthing and the coordinates of impact are described as a stochastic. In the resistance of the structure the volume weight, internal angle of friction, cohesion, yielding stress and wall thickness of the tubular segments are described as a stochastic.

From the results it appears that the loads occurs only very locally. Consequently there appears an over capacity in the reference design relating to the length of all the piles and the diameter of the piles. The five most loaded piles in the structure are checked (due to the energy loading of the bow at Mooring Point 1). It appeared that the diameter of these piles (1820 [mm]) can have a fitted diameter of 1720 [mm] to 1760 [mm] (this will become 1820 [mm] again). But in length a reduction of 9% is found over the fifth most loaded piles. A trend can be distinguished that indicates a large reduction of capacity in length over the whole structure.

The most critical variable in the design is the velocity of the vessel. The most critical element in the structure is the berthing beam self. The sensitivity analysis of strength indicates that the chance of failure in strength can be diminished by the strengthening of the berthing beam and reducing the thickest wall thicknesses of the piles.

3 Introduction

The costs to build a jetty is relative low compared to the loss of income when the jetty is taken out of production. It is important to know the chance of occurrence of every basic failure mechanism. The whole berthing process depends on many different variables.

Jetties are used for berthing vessels, in order to provide more space and to facilitate the transfer of goods to the land. Traditionally jetties are designed by using standards based on normative parameters (semi-probabilistic).

The level 1 method incorporates the loads and the capacity of every element as a standard. The structure is designed by normative loads. Interaction of every separate element as part of the whole are not taken into account.

In general two types of jetty designs are constructed. In type 1 the vessel berths directly to the jetty. In type 2 the berthing structure is separate from the platform in order to avoid fender loads leading to movements and vibrations of the operational structures as loading platforms. In this way operation structures are kept intact in case of overloading. In this thesis the investigation is limited to a separate berthing structure (fender beam guiding structure).

Berthing introduces a reaction force due to energy interaction between the berthing structure and the vessel and are transferred to the soil by piles. The kinetic energy, described by the equation of Saurin, from the vessel and the motion of the water is transferred into potential energy of the berthing structure, the piles and the soil. How the energy is absorbed and distributed by the structure depends on the local stiffness of the structure itself and on the location of the loading.

Some of the recommended literature in jetty design was developed around the fifties of last century. Nowadays this literature still is the foundation of standards used in jetty design. Consequently some of this literature may not be up to date anymore, considering the increase of scale of the vessel size and re-evaluation of the standards is needed by appropriate investigation. This has become a point of debate.

In an early study commissioned by Rijkswaterstaat, "Aanvaarrisico's voor remmingwerken" written by G. van Driel and A. Vrijburcht, a Monte Carlo simulation is done in which the variables in the deterministic function for energy loading were replaced by stochastic. In this analyses the total berthing structure is modeled deterministic as an elastic spring. With this assumption are the differences in resistance over length neglected. The possible human error is taken implicitly in the variables.

In contrast to the design approach according to the standards, methods in this thesis use values of loads and strength directly as a stochastic. Jetty design according to probabilistic methods, aims to calculate the chance of structure failing of the system as a function of all possible failure mechanisms of the (sub) systems or functions.

In this thesis the applicability of the developed probabilistic method to berthing structure design is investigated by means of deterministic design formulas and finite element software to consider the structure as 3 dimensional. A comparison is made between a simplified reference design based on the already constructed "Lyondell jetty" according to the standards, with a design based on the probabilistic method (Monte Carlo simulation). Implicitly the amount of material is considered as a parameter of safety control and capacity. Consequently this could mean that in order to reach an equal level of safety less or more material is needed. With the developed method the exact capacity in relation to the loading can be calculated. This prevents overcapacity and so this results in lower costs. However this was not elaborated in detail.

Failure of the berthing structure is linked to exceeding the maximum deformation and reaching the plastic stress. Using a failure tree makes it possible to display the full failure mechanism as one system.

After construction of the whole system, some of the failure mechanisms are taken for further analysis. Making use of a 3 dimensional deterministic finite element software model, in which some of the parameters can be replaced by a stochastic, it is possible to introduce the structure and the loads as a three dimensional system.

3.1 Problem description

The main interest is a comparison and secondly possible reduction of costs but this will not be explicitly examined in this thesis.

In this thesis there are actually two mean objectives. To solve the actual primary objective, first the following conditional question relating to the developed technique has to be answered positively:

1. "Is the developed technique applicable for running a Monte Carlo simulation?"

In order to answer this stated question it is necessary to consider the following sub-questions:

    1.1. Is it possible for Scia to simulate the soil model?

    1.2. Are the reactions and relations of the model physically correct?

Subsequently the primary objective will be investigated:

2. "Is there a difference in amount of material needed between a jetty designed according to the standardized method in comparison to a jetty designed according to the probabilistic method, assuming the same terms of reference and natural conditions as the Lyondell jetty (the reference jetty)?"

An analysis will be made of the magnitude of reliability of each component in the total failure system. In order to answer the stated question the following sub questions are investigated:

2.1. What are the basic failure mechanisms and what are the relations to the head event?

2.2. What is the reference period of the Lyondell jetty and at what safety level is the Lyondell jetty build?

2.3. What is the actual safety level of the Lyondell jetty?

2.4. What is the relation between the safety level and the used capacity?

2.5. What is the influence of every variable on the safety level?

3.2 Layout of this report

This thesis contains 9 chapters. For each chapter a brief description is given in this section:

Chapter 1
Chapter 1 gives an introduction of this research project. It explains the motivation behind this research and introduces all the questions that are to be answered and explained.

Chapter 2
 In chapter 2 the boundary conditions and requirements of the reference project are introduced. These assumptions are the base of further designs and analyses. Also the actual Lyondell jetty is considered and analyzed.

Chapter 3
In chapter 3 the design rules are introduced. These parameters are explained, considered and worked out in ultimate and users design limits.

Chapter 4
Because of use of a soil model different from the one used for the original Lyondell jetty, a new design is made. In chapter 4 the new calculated dimensions are introduced

Chapter 5
In chapter 5 the used and related theory of probability rules are introduced. The first explanations are given of the applied theory. The fault tree of the project is introduced.

Chapter 6
In chapter 6 the used design rules are written as a stochastic. All the design rules make use of variables and they are introduced as distributions. Also further considerations are explained.

Chapter 7
In chapter 7 the model for the Monte Carlo simulation is discussed. The introduction of scia engineer as a finite element software. And the behavior, schematizations and limits of the model are discussed.

Chapter 8

In chapter 8 the results are discussed and the first conclusions are drawn.

Chapter 9

In chapter 9 the conclusions of the stated questions are presented. Discussion and the recommendations are done.

Differences between a 3 dimensional probabilistic method of berthing structure design and
the traditional method of a berthing structure design

J.J. Kool

4 'Lyondell jetty'

4.1 Introduction

The probabilistic design will be compared with a jetty that is already designed and build. This jetty is designed according the deterministic way using the NEN-codes.

In the port of Rotterdam a jetty is build in 1997, commissioned by 'ARCO Chemie Nederland Ltd' (ACNL). The 'ARCO Chemie Nederland Ltd' is a company that produces several kinds of derivatives and other intermediate chemicals, with a worldwide market[1.]. The products are used in a wide range of consumer goods for instance foam cushioning, paints, coatings, antifreeze and reformulated gasoline.

In order to make it possible for the chemical plant to operate, a possibility for importing commodities and exporting goods should be realized. For this mooring facilities for seagoing and inland vessels are constructed. Vessels can be unloaded and loaded by means of loading arms and transport pipes that are located on the jetty.

On behalf of Rotterdam Municipal Port Management (RMPM) a program of requirements is produced by the Port Engineering Division of Rotterdam Public Works. In the program of requirements are the boundary conditions defined that are imposed by environment and requirements in the port of Rotterdam.

In an early stage of this thesis the jetty structure self is considered as well. However this is not relevant for the objectives investigated in this thesis (see appendix B).

4.2 Overall description of the geometry 'Lyondell jetty'

The jetty is located in the Europe port in the north-west area of the Europe Port (see Figure 1). The area is relatively un-sheltered. The wind has a very large influence on the applied forces on the jetty. This is why the jetty is orientated on coordinates were the hardest wind is expected from, the north-west.
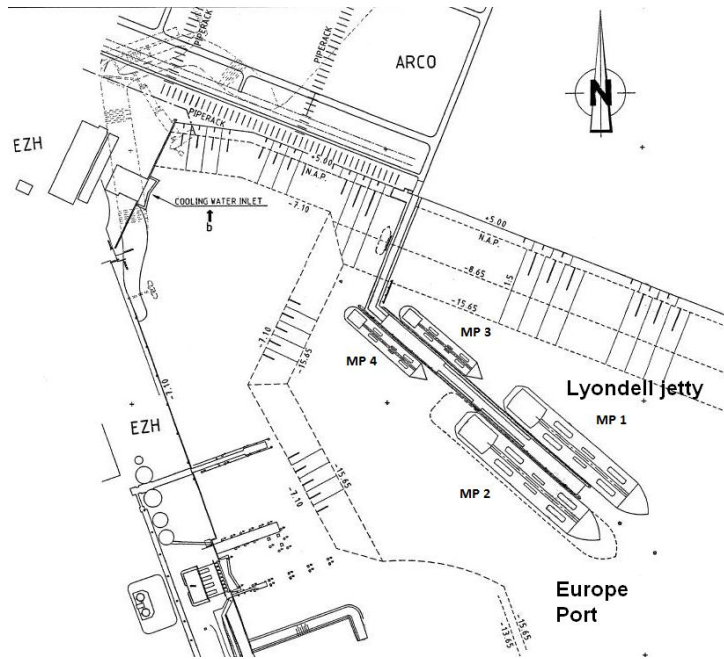
**Figure 1: overview drawing of the Lyondell jetty, in the Europe Port.
the mooring point 1 till 4 are marked.**

The jetty consists of two separate types of structures. The jetty structure and the fender structure in front of the jetty (**see** Figure 2). These structures will be considered later in this chapter.

Figure 2: cross section of the Lyondell jetty

Making sure that design vessels will not run into the ground a guaranteed depth (up to NAP-15.65 m) is determined. The jetty that is constructed consists of a main jetty (length of approximately 254 [m]) which is connected to shore with a rush jetty (length of 131 [m]) **(see** Figure 1**)**. To ensure the stability of the whole jetty, the jetty is founded on steel piles. The piles are placed vertical or with a slope of 5:1. The semi vertical piles are there to resist the horizontal forces caused by the wind forces and traffic. The concrete upper structure consists of an upper deck (for mobile traffic and loading-arms) and a lower deck (for transport pipes).

Differences between a 3 dimensional probabilistic method of berthing structure design and
the traditional method of a berthing structure design

J.J. Kool

4.2.1 Fender structure

The fender structure is build in front of the jetty to protect the jetty for the berthing and mooring loads of vessels. Designing the structure three different vessels are considered (see table below). The fender structure consists[3.] of a continuous fender frame of steel piles (with a slope of 20:1) and steel girders. The continuous horizontal girder has a grid of vertical bars, with a c.t.c. of approximately 5 [m]. The contact surface of the fender construction is covered with azobé wood (**see** Figure 3).

The piles are dimensioned using the Blum method (with multiple layers). The piles have, over the entire length, the same outer diameter (∅= 1820 [mm]), with a different wall thickness. The exact wall thickness differs over depth and varies in between t=35 [mm] and t=25 [mm]. The centre to centre distance of the piles are approximately 25 [m].
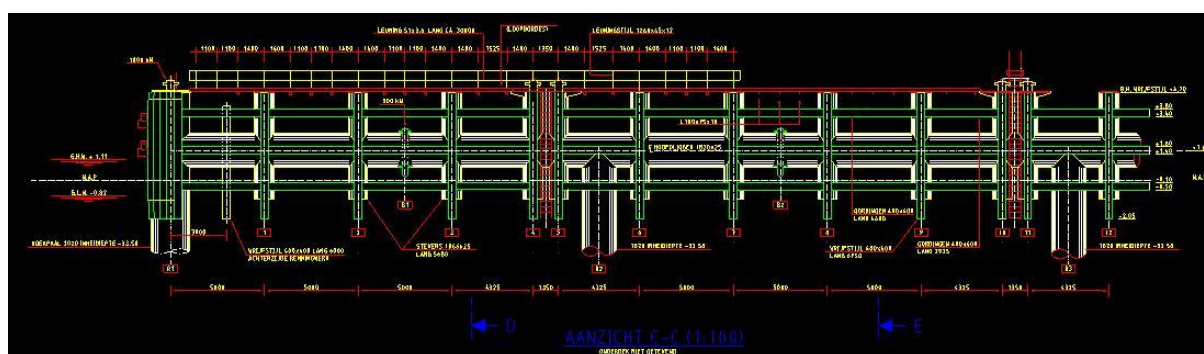
Figure 3: Fender construction

The continues, horizontal beam (berthing beam), on top of the piles, has a diameter of 1820 [mm] with a wall thickness of t= 25 [mm] (see Figure 3). Eventually the piles are filled with sand. The smaller elements in the structures are left out in this scope. The entire fender is 58% of the total building costs[3.].

4.2.2 Foundation piles

The foundation piles of the jetty are founded in the Pleistocene sand layer. The diameter of the piles is 1220 [mm] with a wall thickness of 14.2 [mm] with a length that varies between 29,20 [m] and 51,40 [m]. The working procedure is described in Appendix B.

Differences between a 3 dimensional probabilistic method of berthing structure design and
the traditional method of a berthing structure design

J.J. Kool

4.3 Boundary conditions

Geotechnical Boundary conditions

The 'Ingenieursbureau Havenwerken' (IH) commissioned a geotechnical advice concerning the construction of the Lyondell jetty. In the early 70 at the north side of the Europe port some partly ground reclamation has been done until a level of NAP+5 [m]. Before the reclamation, the sea bottom level used to be at a level of NAP-4 or NAP-5 [m]. Several sounding tests were done by a cone penetration and a soil profile was constructed (**see appendix O**). At a part of the location were the jetty is build there used to be a marine deposit for extracting of sand and transshipment of predominantly sandy material. As a result of dredging activities at this location, the soil is touched to a depth of about NAP-54 [m].

		[m]
Normal high water	N.A.P.	+1.05
Normal low water	N.A.P.	-0.65
High water (once a year)	N.A.P.	+2.90
Low water (once a year)	N.A.P.	-1.50
Extreme high water (once in 10 years)	N.A.P.	+3.54
Extreme high low water (once in 10 years)	N.A.P.	-1.70
Extreme high water (once in 33 years)	N.A.P.	+3.89
Extreme high water (once in 50 years)	N.A.P.	+4.00
Extreme high water (once in 100 years)	N.A.P.	+4.20

Table 1: Hydraulic boundary conditions

4.4 Requirements

Dimensions

Elevation top upper deck NAP+5.95 [m]

Width upper deck loading arm platform 13.00 [m]

Width upper deck approach jetty and between platforms 6.50 [m]

Length jetty 275.00 [m]

Length approach jetty 110.00 [m]

Height between top lower deck and bottom upper deck minimum 1.80 [m]

Height between bottom girder and lower deck minimum 1.40 [m]

Technical requirements

The expected life time of the jetty is 50 years.

Further specifications of the Lyondell jetty

Deck material specifications:

- Minimum quality of B35 (C28/35)

Foundation of the jetty:

- Steel piles (Ø=1220 [mm], t=14,2 [mm]) 115 stuks

Fender system:

- Continuous framework of piles c.t.c. approx. 25 [m]. and girders on both sides of the jetty. Length of the inner side approx. 295 [m] (extra length of 22 [m] because of fire boat) outer side approx. 285 [m]. (Ø=1820 [mm], Ø=2020 [mm], Ø=914,4 [mm])

Dredging depth:

- minimum N.A.P. -16.15 m (0.50 m deeper then contract depth because of maintenance) also depending on thickness of bottom protection layer.
-

Scour protection:

- The option of rock fill around the jetty and freestanding dolphins is included in the terms of reference.

Loads

Loads on the upper level:

a) Traffic class 60
b) Live load of 15 [kN/m^2]
c) Mobile crane of 150 [kN]
   (which is not representative compared to 'a)' and 'b)'.)
d) Loading arms:
   Vertical load of 460 [kN]
   Horizontal load of 52 [kN]
   Momentum of 560 [kN]
e) Service crane:
   Vertical load of 90 [kN]
   Momentum of 350 [kNm]
f) Gangway:
   Vertical load of 110 [kN]
   Moment of 475 [kNm]
g) Shelter
   distributed load (q) of 15 [kN/m^2]

Loads on the lower level:

a) Static load of cables and transport pipes of 2 [kN/m^2]
Live load of 10 [kN/m^2]

Nautical requirements

	Largest seagoing vessels (mooring point 1 and 2)	Small seagoing vessels (mooring point 3 and 4)	Exceptional and no design case, Seagoing vessel
Length [m]	180.00	105.00	230.00
Beam [m]	32.00	17.00	36.00
Draft [m]	13.00	6.20	13.5
Dead weight [kN]	550,000	90,000	850,000
Head engine power [kW]	13,000	3,000	17,000
Propeller diameter [m]	6.50	3.45	7.00
Distance between shaft and keel [m]	3.50	1.75	3.75
Bow thrusters power [kW]	883	350	1,000
Propeller diameter [m]	3.00	1.10	3.00
Distance between propeller [m]	3.00	1.50	3.00

Table 2: characteristics of the vessels to be considered[3].
See for the mooring point Figure 1.

Reference:

[1.] www.prnewswire.co.uk/cgi/news/release ?id29104
[2.] Recommendations of the Committee for waterfront structures harbours and waterways, EAU, 2004
[3.] Program of requirements, code A98.030, ir Broeken, 1997

5 Deterministic approach

5.1 Introduction

During the berthing process the vessel will collide into the berthing structure. At that moment the kinetic energy of the vessel will be absorbed by berthing structure and will be divided over several elements as potential energy (see Figure 4).
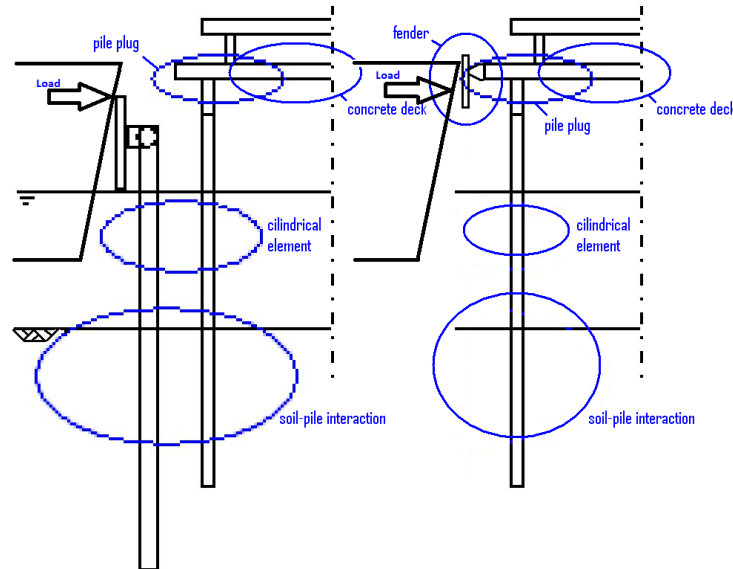
Figure 4: Overview of elements

In the next chapter all the design formulas are analyzed and considered. By analyzing the design formulas of every element, some assumptions can be made and there is something to say about the reaction of the whole structure. The relation of energy and force will be introduced because most design equations use not the dimension of energy [kNm] but on force [kN]. The kinetic energy of the vessel is absorbed by lateral deflection of the structure. The amount of energy absorbed by the structure by lateral deflection is determined by:

$$E = \int_{y0}^{y1} F(y)dy$$

In which:

E   absorbed energy [kNm]

F(y)   contact force of vessel and structure [kN]

y   horizontal deflection of the structure [m]
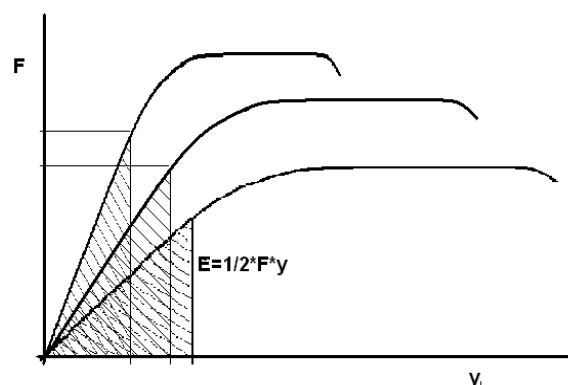
Figure 5: Energy relation between force and deformation in the elastic track.

The equation says that the amount of energy is equal to the space under the curve (see Figure 5). As known is the deformation a function of the force and the stiffness of the structure. It can be concluded that a stiffer structure that absorbs the same amount of energy produces higher forces (see Figure 5). To predict the forces it is important to know the structural behavior in the elastic and the plastic state.

In the first part of this chapter the vessel behavior and the applied loads of the berthing vessel are considered. In the second part the design formulas of every element of the berthing structure are considered in relation to strength capacity and deformation. In earlier stage of this thesis the behavior of the concrete structure is considered as well, but eventually this is left out of the scope (see appendix).

5.2 Loads caused by the vessel

5.2.1 Introduction

During the berthing process a vessel will load the structure with energy and the gross of this energy will be absorbed by the structure. During the berthing process the accuracy of first contact of the vessel with the structure is influenced by several external influences (**see appendix D**). The vessel is guided by so called tugs in order to minimize the inaccuracy and control the movement. This procedure will be explained in the next paragraph. The movements that a vessel makes can be described with a couple integral equations (see Figure 6). Eventually the load is calculated by use of the formula of Saurin (the kinetic method). This formula is discussed in the second paragraph.

5.2.2 Behavior of a berthing vessel

During the process of a berthing vessel, the vessel is subjected to a large amount of different elements. A large vessel is almost rudderless when at low speed (**see appendix E**)[2.]. Tugs are applied to keep the movements of the vessel in line and tow the vessel to its berthing location.
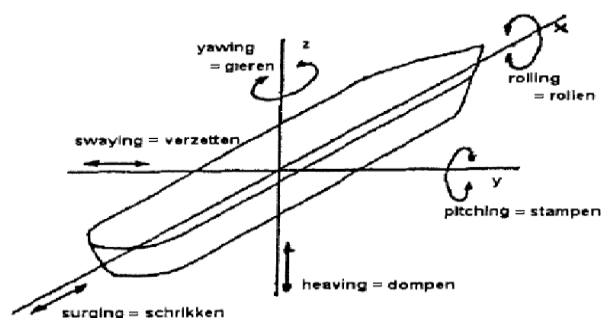
Figure 6: different degrees of freedom of a vessel

In the model some assumptions are made. Like the vessel is assumed to be infinitely stiff and
the water is assumed to be a liquid with constant parameters of temperature, salt, sediment and
has no elastic volume[4.].

Two equations can be established using the second law of Newton[1.]. To make an appropriate
description of the movement it is important to know the behavior over time of the external
forces. A force causes acceleration in line with the force and due to exocentric forces a moment
will be created. This causes the following equations:

For translation:

$$m_s \frac{d^2 y}{dt^2} = F_{constructie} + F_{sleepboten} + F_{wind} + F_{stroming} + F_{hydrodinarisch}$$

For rotation:

$$I_s \frac{d^2 \psi}{dt^2} = M_{constructie} + M_{sleepboten} + M_{wind} + M_{stroming} + M_{hydrodinarisch}$$

In practice the berthing process is described by the "Long wave theory" or the equation of
Saurin[5.]. The "long wave theory" has the advantage that it describes the whole berthing process
over time, but is very complex. In comparison to the equation of Saurin where only the maximum
amount of energy is considered, and the equation is relative easily used.

Because the maximum of energy loading is normative for the structure design the equations are
considered at the moment that the energy is at his maximum, this at the moment that the
maximum of deflection of the structure is reached.

5.2.3 Tug assistance

The Brolsma curves which are recommended as indication for the parameter 'velocity' in the
equation of Saurin by the PIANC 2002, are based on berthing records of vessels that are tug
assisted[13.]. Large vessels will require tugs for safe ship handling, sailing at small velocities (see
appendix E). In the 'Port of Rotterdam' large vessels will have an escort of tug boats entering
the port. In the turning basin the vessel is turned [2.] with the bow aimed towards the port exit.
So in case of emergency the vessel can sail away.

In this paragraph one tug handling strategy is introduced. Often a different tug handling strategy is used. Which requires less tugs. Approximately 100 to 150 meters from the jetty, the vessel will be positioned [1.] parallel to the 'berthing line' (jetty). From this position the vessel will be pushed towards the jetty (see Figure 7).
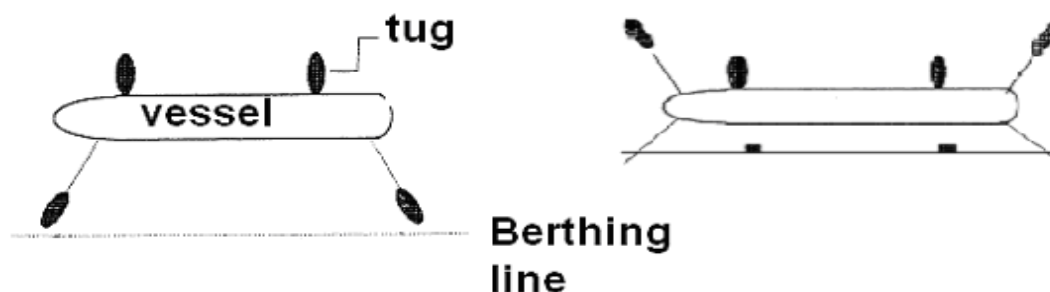
Figure 7: vessel during berthing process near the berthing line

At a distance of about 30 m of the 'berthing line' the tug boats take a more favorable position, to slow the vessel down in its velocity (see Figure 7). To secure the vessel a rope will be fixed between the jetty and the vessel. During the process the vessel will berth under a small angle therefore the vessel will always collapse initially on one fender with the bow or the stern (see Figure 8). Depending on the kind of fender and the distance between two fenders it is possible for a vessel to activate two fenders at the same time (see Figure 8).

The fender and the jetty are considered to be relatively flexible. After contact, the vessel loads the fender and will lose a part of his kinetic energy. The fender will primarily convert the kinetic energy in potential energy. In means of the eccentric applied reaction force the vessel experiences a moment that will change the rotation velocity causing the vessel to lose more kinetic energy, in to the water.
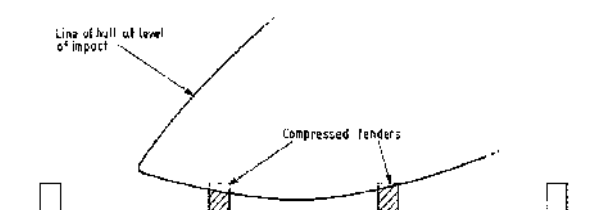
Figure 8: plan showing hull and cope geometry at impact [3.]

When the velocity of the vessel approaches the zero the reaction force will reach its maximum. Due to the rotation of the vessel the second fender will be activated. The longer the vessel will turn the more energy will be dissipated by the water. The tug boats will keep on pushing till the vessel stays in place.

## 5.2.4 Formula of Saurin (kinetic method)

The PIANC [3.] gives a deterministic approach for the design energy that has to be absorbed by the structure at moment of impact. The equation represents the standard equation of energy of mass:

$$E_d = \frac{1}{2}M * v^2$$

This energy equation is under ideal conditions where a lot of processes are neglected. Since the berthing of a vessel is not ideal, extra influence coefficients are added in the Saurin formula.
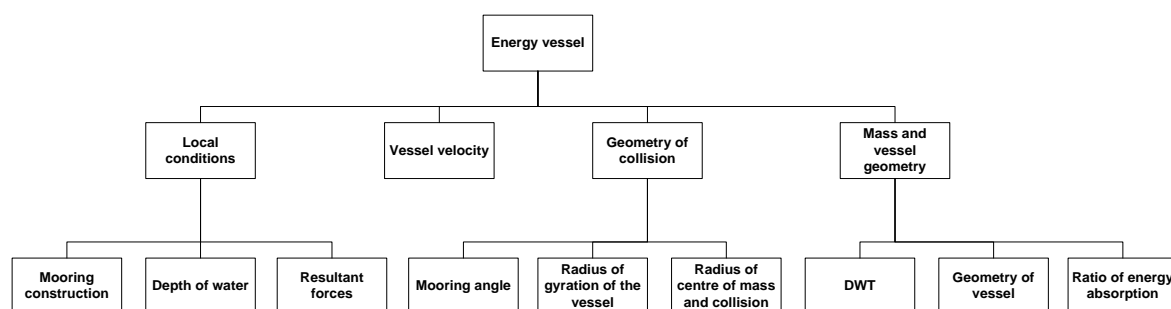
All the relations between the basic functions and the vessel energy according the formula of Saurin are displayed in the tree above. Using equation for the kinetic energy:

$$E_{rep} = \frac{1}{2}Mv^2 C_e C_m C_s C_c$$

E_rep   Design energy (under normal conditions) to be absorbed by fender system [kNm]
M   Mass of design vessel (displacement in tonnes), at chosen confidence level.
        (usually 95 [%] confidence level)

v   Approach velocity of the vessel perpendicular to the berth [m/s] (use 50[%] confidence level)

C_e Eccentricity factor

C_m Virtual mass factor

C_s Softness factor

C_c Berth configuration factor or cushion factor

For the energy calculation the water displacement tonnage is used for mass. The displacement tonnage of a vessel is the total mass of the vessel and can be calculated from the volume of water displacement multiplied with the water density. The PIANC gives some guidance of displacement tonnage factors. The total mass of cargo, fuels, crews and reserves with which a vessel is laden is called the DWT. From these values a relations is made between the DWT and the displacement of water:

$$Displacement mass = 1.128 * DWT + 2385.6 [tonnes]$$

Differences between a 3 dimensional probabilistic method of berthing structure design and
the traditional method of a berthing structure design
J.J. Kool

The PIANC advises a safety factor between 1.1 and 2.0 with in specific a factor of 1.25 for
tankers for abnormal berthing. According to the PIANC the designer should be aware in
determining the appropriate factor. Instead of the displacement mass the DWT is used for mass
in this calculation.

Eccentricity factor (C_E)

The coefficient of eccentricity takes the dissipation of energy into account caused by the
yawing of the ship. Important in this function is the berthing angle of the vessel, shown as in the
Figure 9. For this two scenarios have to be distinguished:

- A berth with continuous fendering
- A berth with breasting dolphins
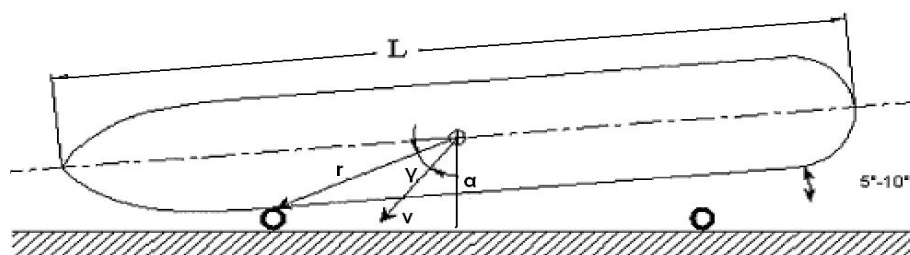
Figure 9: Overview of the mooring eccentricity [10]

The coefficient of eccentricity can be calculated (by this simplified formula without considering
the yaw motion upon arrival):

$$C_E = \frac{k^2 + r^2 \cos^2(\gamma)}{k^2 + r^2}$$

In which:

k   Radius of gyration of the ship [m]
r   The radius between the centre of mass of the ship and the point of collision
         between the ship and the structure [m]
γ   The angle between radius r and the velocity of the ship [m]

The radius of gyration of the ship is given by:

$$k = (0.19 C_b + 0.11) * L$$

In the gyration of the ship the bloc coefficient is defined as a ratio between the actual water
displacement and the displacement of a rectangle.

$$C_b = \frac{M}{L * B * D * \rho}$$

Differences between a 3 dimensional probabilistic method of berthing structure design and
the traditional method of a berthing structure design

J.J. Kool

In which
C_b Bloc coefficient
M   Mass of the vessel [displacement in tonnes]
L   Length of vessel [m]
B   Width of vessel [m]
D   Draft of vessel [m]
ρ   Density of water [ton/m³]

The smaller the value of C_b the larger the load F. The following approximation applies:

0.6 (slender ships)<C_b< 0.95 (container ships).

''r' is defined[5.] as the distance between the contact point and the centre of rotation.

$$r = \sqrt{(\frac{B}{2\cos\alpha} + \frac{hoh/2 - excentricity}{\cos\alpha}\sin\alpha)^2 + (\frac{hoh}{2} - excentricity)^2}$$

With the use of a berthing beam the point of collision is assumed fixed and the collision point is assumed at 0.25*L[3.].

$$r = \sqrt{(\frac{L}{2} - \frac{L}{4})^2 + (\frac{B}{2})^2}$$

With the angle γ [⁰]

$$\gamma = 90 - angleofspeed - \sin^{-1}(\frac{B}{2*r})$$

Softness factor (C_s)
The softness factor is an approximation of the ratio of energy absorption from the vessel and the total energy of the vessel and mooring structure together. For a very flexible pier with fenders a factor of C_s=1 is given as for a hard and a stiff structure the energy absorbed by the ratio absorbed energy of the skin of the vessel will be 10% (C_s=0.9).

Berth configuration factor (C_c)
The berth configuration factor gives an indication of the possibility for water that is between the vessel and the structure, to flow away. The enclosed water can have the effect of a cushion and absorb a part of the kinetic energy. The berth configuration factor depends on the following elements:

- Structural support

- Keel clearance

- Velocity and angle at approach

- Thickness of the fender

- Vessel's hull shape

The Lyondell jetty is an open structure. The PIANC gives, based on experience, a factor for open berths and corners of quay walls C_s=1.0

Virtual mass coefficient (C_m)
The factor represents the ratio between both the mass of the vessel and the water moving along with it and the mass of the vessel self. Over the years there are developed several formula that can be used.

According to Block and Dekker (1979) and the PIANC (1984) [1.] the virtual mass is a function of:

- The stiffness of the fender
- The increase with draft

But has only little relation with:

- the initial speed
- the angle of approach

C_m is generally defined as:

$$C_m = \frac{m_s + m_w}{m_s}$$

The hydrodynamic coefficient can be calculated:

$$m_s = \rho LBDC_b$$

In this equation the simplified assumption for the blocking coefficient[5.] is used:

$$C_b \approx \frac{\pi}{4}$$

There are many models to determine the additional mass, based on the potential theory or on theory of preservation of impulse. Over the years a lot of different equations are developed.

In practice[5.] the equation of Vasto Costa[6.] (1964) is used, although Vrijburcht[7.] considered this one as not preferable when the draft and depth can play an important role. Vasto Costa formula:

$$C_m = 1 + 2\frac{D}{B}$$

In which

B   Width of the ship [m]
D   Draught of the ship [m]

The Vasco Costa is valid under the following circumstances:

- The keel clearance shall be more than 0.1*D
- The vessel's velocity shall be more than 0.08 [m/s].

The influence of the depth is only included in the equation of Giraudet, this is the equation that A. Vrijburcht prefers:

$$C_m = 1,2 + 0,12 \frac{D}{(H-D)}$$

5.3 Structure reaction

5.3.1 Introduction

When a vessel berths, the energy from the vessel and the water, that is moving along, has to be absorbed. For most part the structure elements will absorb the energy and distribute the energy over the following major parts:

- The foundation and structure cylindrical piles of steel
- The upper structure of concrete
- The fender
- The soil

A small part of the energy will be absorbed by the deformation of the vessels hull and the energy left will be dissipated by the movement and the friction of the water along the bottom, the vessel and the structure itself. These phenomena will be left out in the discussion and their contribution will be neglected.
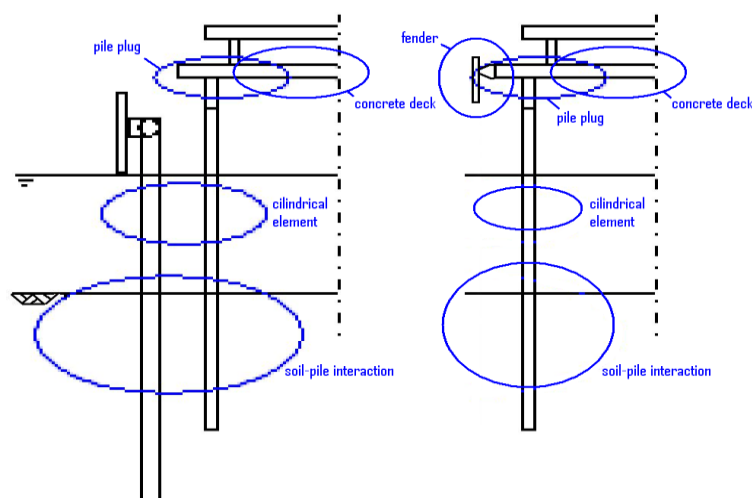
Figure 10: Schematization of jetty construction, with and without separate mooring construction

In this chapter all the structure parts will be discussed separately (see Figure 10). The discussion will be focused on the procedure of calculations in the deterministic approach. By exploring the behavior of every individual structure element, eventually it is possible to say something about the way all the construction parts will work together as one whole (see Figure 11).
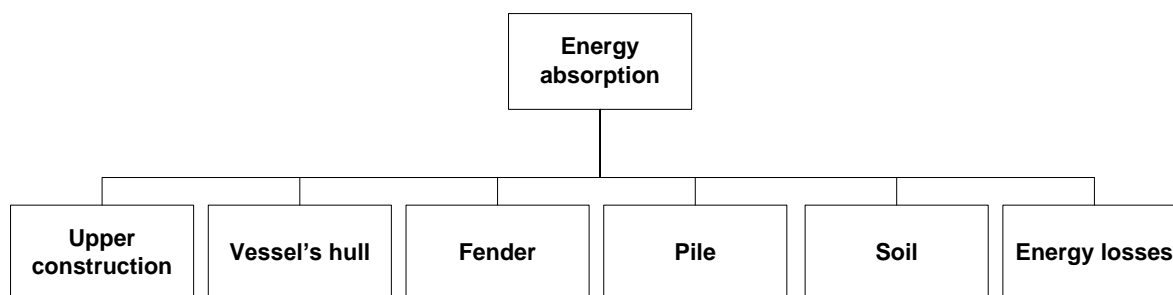
Figure 11: Schematization of all the elements that will participate in absorbing the energy

The load is applied as a point load [kN] therefore a deformation-force graph is constructed (see Figure 5). From this relation the absorbed energy is extracted.

5.3.2 Soil model for a laterally loaded pile

From a mechanical point of view, a laterally loaded pile has three kinds of behavior (see Figure 12):

- A fully clamped connection (flexible pile)
- A flexible connection (rigid pile)
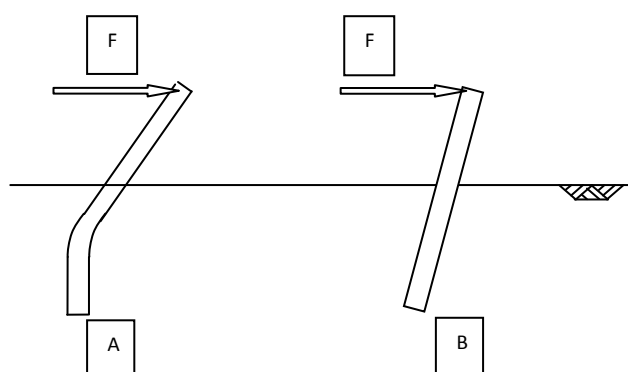
Figure 12: Pile with a plastic hinge (A) and a pile with a

relative too large stiffness (C)

In case of a flexible connection, the soil wedge in front of the pile completely fails and the pile can be considered as too short. With a fully clamped connection, the pile is long enough to develop equilibrium between the forces of the pile and the reaction forces of the soil.
There are a couple methods developed to model this type of system. The PIANC advices three methods for pile analysis:

1. The methods based on the earth pressure theory under ultimate equilibrium condition of the soil, e.g. BLUM's method or Brinch Hansen's method
2. An elastic approach (sub grade reaction), as proposed by Matlock and Reese and conform the API standards using p-y curves;
3. The best method to describe the soil- pile interaction is a three dimensional finite element model that takes plastic deformation into account. However this approach is elaborate and requires specific soil data.

Additional to these methods Fugro[8.] suggests a MSheet Single Pile as well.

The vessels energy is absorbed by the structure by deformation. Since virtually all deformations of soil cause the grains to replace and slide over each other and then absorbs energy. This process makes sure the energy will not be transferred back in to mechanical energy. How the soil reacts depends on a several different components. The permeability and the nature of the loads have a great impact on the soil behavior. With a fast impact it will take some time for the groundwater to spread out. The strain depends on the speed of the groundwater and is relieved over time (drained). Until the soil is considered drained, the load will be absorbed by groundwater and the grains. The behavior of the soil and its groundwater is described by the consolidation theory. The dynamic behavior is also explained (cyclic behavior) in the case that a pile is loaded with relative short loads and will waggle till they reach equilibrium.

The Brinch Hansen method is used in the original calculation of the Lyondell jetty. The Brinch Hansen method only considers the ultimate strength capacity of the system soil. In this thesis the service ability state is investigated as well. Therefore the soil reaction has to be described in an elastic and plastic mode. Originally the theory of Poulos (see appendix H) is considered as well but eventually the p-y curves of the NEN-EN ISO 19902 are used.

The NEN 6740 advices a factor for soil characteristics for retaining structures and embankments (see Table 3).

Partial factor for soil characteristics (γ_m)	Ultimate state (favourable)	Service ability state
$\gamma_{m;\varphi}$ tangent of the angle of internal friction	1.2	1
$\gamma_{m;c2}$ cohesion	1.5	1
$\gamma_{m;cu}$ undrained shear strength	1.5	1

Table 3: Partial factors (NEN 6740)

The function of the undrained shear strength is a function of the angle of internal friction and the cohesion. In the calculations is chosen to use apply direct the safety coefficient for undrained shear strength ($\gamma_{m;cu}$) instead of the partial factors of the internal friction ($\gamma_{m;\varphi}$) and cohesion ($\gamma_{m;c2}$). Using the partial factors of the internal friction and cohesion would be very conservative compared to the factor for undrained shear strength.

5.3.2.1   Consolidation theory

The berthing of a vessel can be considered as relative short and sudden loading. Due to sudden loading of wet soil, the deformation can be delayed caused by a volume reduction in which the contained water is pushed out, this is called consolidation. Instead of describing the soil deformation only as a function of stress the behavior of soil has then an obvious time depended element [22.] . In the appendix G the effects of this process is worked out. This consideration will be limited to an brief and one dimensional case. The elastic coefficient is assumed to be linearly elastic. Therefore it is assumed that the amount of stress difference is very small.

The grains are assumed non compressible so the volume of soil is only reduced when the porosity is reduced or by extracting water. In practice is calculated with drained soil unless it matters high soil with a high porosity. In theory the consolidation process is an infinitely long process . In practice only the 99% of the settlement is reached. In that case:

$$t_{99\%} = \frac{1.784h^2}{c_v} \approx \frac{1.8h^2}{c_v} = \frac{1.8h^2(m_v + n\beta)\gamma_w}{k}$$

In which

c_v Consolidation coefficient

k Permeability coefficient $k = \gamma_w m_v c_v$

m_v Compressibility coefficient $m_v = \dfrac{\Delta h_\infty}{hq}$

Δh_∞ Infinite settlement

5.3.2.2 Cyclic loading

The loading of the piles due to the berthing of a vessel has a oscillating character (cyclic loading). This will make the soil to react with some specific behavior. Because all deformation of soil are caused by the rearranging of the soil grains. It can be expected that with releasing of pressure the deformations will be permanent. With reloading less bonds and contacts between

grains will be broken than with the first loading (virgin loading) and can be expected to have a stiffer reaction.
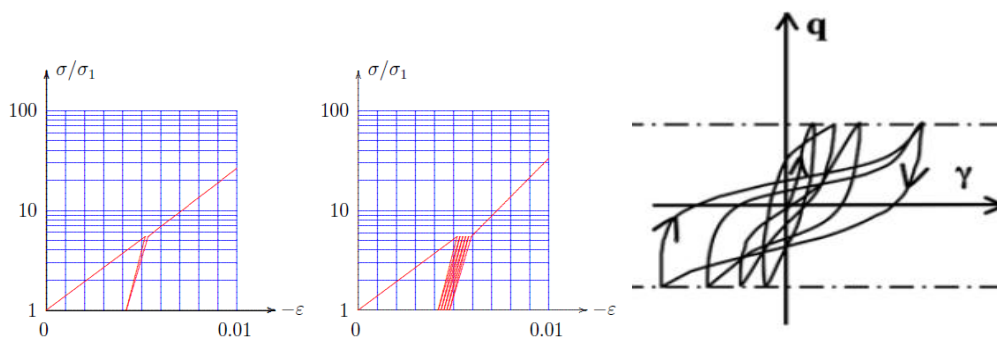
Figure 13: Left:stress and strain track of cyclic behavior, Right: cyclic behavior applied to p-y curves.

Figure 13 shows the relation between the strain (ε) and the load of the sample in case of a vertical stress (σ_{zz}) of an included sample. For every double tension a similar strain will occur. Therefore the graph will be put on logarithmic paper.

$$\varepsilon = \frac{1}{C}\log(\frac{\sigma}{\sigma_1})$$

In which

σ loaded pressure

Differences between a 3 dimensional probabilistic method of berthing structure design and
the traditional method of a berthing structure design

J.J. Kool

σ_1 initial pressure

5.3.2.3   Depth

The design depth of the guaranteed or nominal depth is set to NAP-15.65 [m]. This is determined by adding the draught of the design vessel, the tidal elevation above reference level, the net keel clearance and some depth for the vertical motion due to wave response. Due to currents in the port there is a possible scour around the piles. The depth of the scour hole is assumed to have a maximum of 0.5 [m]. So the maximum local depth is NAP-16.15 [m].

5.3.2.4   Soil elastic and plastic behavior

The soil response behavior to loading is characterized by a elastic and a plastic phase. In the approach of Prof. A. Verruijt[24.] the elastic part of the soil behavior is minimized, as it was originally developed by Blum (1931).
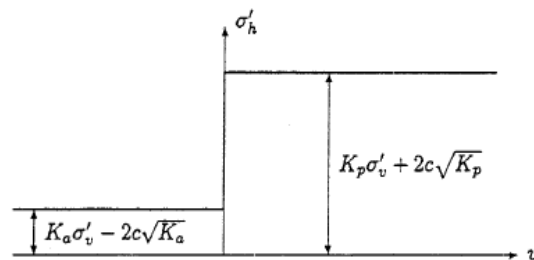
Figure 14: Perfectly plastic soil response

With any displacement the response will be either maximum or minimum. When a force is applied on a pile as in the situation below, the response is given by:

$$f = -(K_p - K_a)D\sigma'_v - 2cD(\sqrt{K_p} + \sqrt{K_a})$$

This term is included in the integral:

$$EI\frac{d^4u}{dz^4} = f = -(K_p - K_a)D\gamma'z$$

Elastic-plastic springs

Prof. A. Verruijt[24.] describes an approximately analytic solution for the problem of a laterally loaded pile in a homogeneous sandy soil (where cohesion c=0). In the solution the plastic deformation of the soil is taken into account (see figure below).
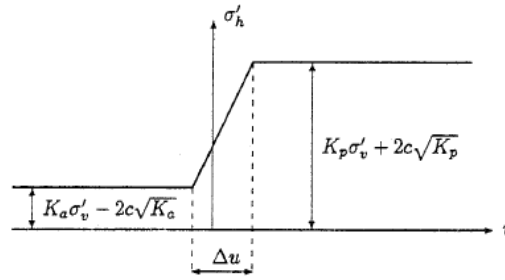
Figure 15: Elastic-plastic soil response in calculation

When soil is activated it knows two types of deformations. The first response is elastic for small deformations. The second response is plastic for large deformations. The elastic deformation is a small part of the track and only occurs in small deformations. There are two plastic tracks in the relationship, these parts are called the 'stroke'. At the right side the maximum value (the passive lateral soil pressure) relates to large positive deformations. This is described with the equation:

$$\sigma'_{h-\max} = K_p \sigma'_v + 2c\sqrt{K_p}$$

At the left side the active lateral soil pressure, when the displacement reaches a certain negative value. The minimum track is described by:

$$\sigma'_{h-\min} = K_a \sigma'_v - 2c\sqrt{K_a}$$

In these equation used:

c   Cohesion of the soil

$$K_a = \frac{1-\sin\phi}{1+\sin\phi} \qquad\qquad K_p = \frac{1+\sin\phi}{1-\sin\phi}$$

Φ Friction angle of the soil
K_p Passive soil pressure coefficient
K_a Active soil pressure coefficient

5.3.2.5   Winkler

In the PIANC of 1984 the Winkler method is advised [4.]. In this method the pile is assumed to be supported by springs (soil is discontinues). All the springs have no interaction with each other. The soil pressure has a linear relation with the deflection of the pile:

$$E_s(z,y) = k_h * D_{pile}$$

In which:

E_s the Young's modulus [kN/m^2]
k_h bearing resistance [1/m^2]
D   diameter of the pile [m]
z   depth beneath the soil surface [m]

The value of k_h differs in the application. When k_h is in mean of cohesive soil the value is assumed to be as a constant. When k_h is used for sand soil it increases linearly with depth.
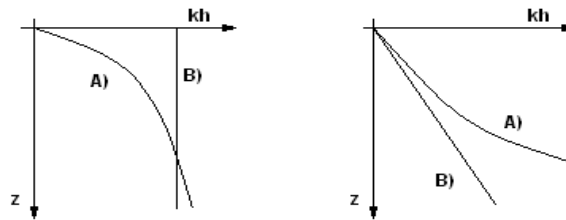
Figure 16:variation of k_h in depth [z]. A) is the actual value, B) is the assumed value of k_h. Left is graph of cohesive soil and right sand soil

For a better fit of k_h a parabolic or hyperbolic functions is often applied. This is given by:

$$k_h = A * z^{n_x} \qquad \text{or} \qquad k_h = k_{kl}(\frac{z}{l})^{n_x}$$

In which
A   Coefficient
L   Length of the pile
k_{hl} bearing resistance at the tip of the pile
n_z Parameter varying between 0 for clay, up to 2 for sand soil

5.3.2.6   Blum method and Brinch Hansen's method

The Brinch Hansen and Blum method are methods to describe the behavior of a horizontally loaded pile [9.] (see Figure 80). The Blum method is very fast and simple to execute. It is developed for non-cohesive soil like sand. And assumes the soil to behave plastic (this was mentioned earlier in the chapter) . The pile is considered to be fixed against deflections at an assumed penetration depth, t_0. The moment at this depth is assumed to be zero. And when the real length is taken $1,2*t_0$ there can still be some lateral force at a depth of t_0.

Figure 17: Left Blum's schematization and right earth pressure diagram for a laterally loaded pile model according to Brinch Hansen

Differences between a 3 dimensional probabilistic method of berthing structure design and
the traditional method of a berthing structure design
J.J. Kool

The wedge of soil in front of the pile will make equilibrium with the applied force at the head of the pile. It is assumed that the pile mobilizes the full passive resistance of the wedge. The wedge is pushed upwards due to the lateral force and is assumed to be independent of deformation.
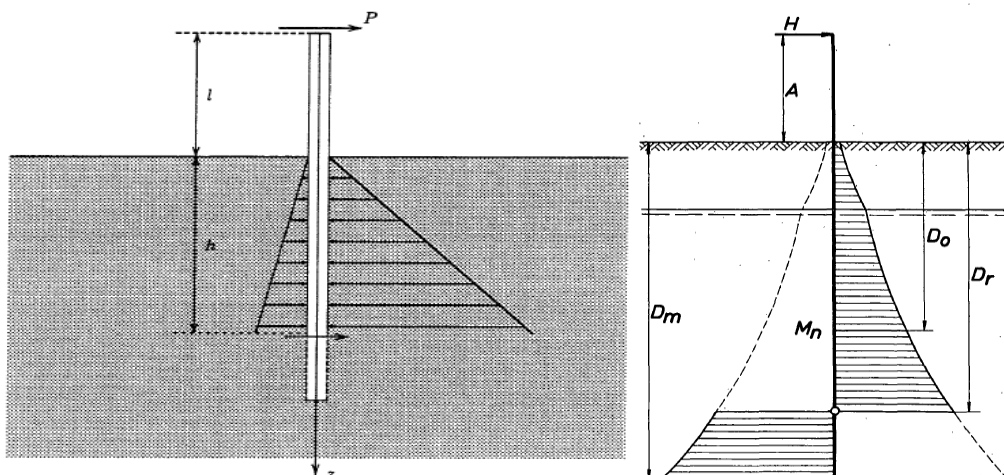
The Brinch Hansen method is also an ultimate limit state model and uses only the passive soil pressure. Brinch Hansen separates the soil resistance at different depths and allows the term of cohesion. The model is suitable for layered soil with different characteristics. When the load and the pile width are known, the pile length and the location of the rotation point can be found. The shape of the wedge depends on the shape, depth and diameter of the pile and is already taken into account in the soil pressure coefficient. The Brinch Hansen method takes cohesive soil and layered soil into account as well (see Figure 17). Above the rotation centre at the right side the soil is assumed to be an active ground pressure and at the left passive ground pressure. Below the rotation centre it is reversed. There are two unknown parameters the depth (D_r) of the rotation centre and the ultimate value of the force H. The two parameters are determined by two equilibrium conditions (horizontal forces and moment equation).

In this method the elastic deformations are not taken into account. Under impact force, the determination of the short-term resistance has to be calculated with undrained parameters. The earth pressure can be found using a graph. With these values the lateral earth pressure can be calculated:

$$\sigma' = K_q \sigma_v' + K_c c$$

In which
K_q φ dependent term [-]
K_c Cohesive term [-]
σ_v' Vertical grain stress [N/mm^2]
σ_p' Passive grain pressure [N/mm^2]
c   Cohesion [N/mm^2]

Both the Blum and the Brinch Hansen method have some disadvantages. They are both quite suitable for calculations of rigid piles. But both are actually not suitable to calculate the deflection of the pile in the service ability state. And it is not possible to include time dependent behavior or use non-linear soil behavior and cyclic loading or axial loading.

Because the wedge is considered as one body and the only thing that makes equilibrium to the pile, the shear force in the soil is taken into account. Therefore this model is not considered as favorite for a model of beam with springs.

5.3.2.7   P-Y curve

In case of including the elastic track as well the use of the p-y curves is recommended. The PIANC[3.]**Error! Reference source not found.** recommends for pile analysis in an elastic approach the use of p-y curves according to the 'American Petroleum Institute' standards. The same method is described in the NEN-EN ISO 19902. In the NEN-EN ISO 19902 a distinction is made in three different types of soil:

- sand soil

- soft clay
- stiff clay

The soundings (**see appendix I**) made for the original Lyondell jetty, show that the ground is not homogeneous. So instead of only one type of soil all the layers are considered.

The method of the p-y curves is based on a mass-spring model with non-linear springs. The curves are based on field tests. The shape of the curves depends on the parameters of the soil. Calculations can be done in both the ultimate limit state and the serviceability limit state. It is possible to implement the p-y curves in a computer program (M-pile) and model the non-linear track of soil behavior. Using the p-y curves it is possible to change the stiffness of the pile over depth and add a sloping surface.

Sand soil

In this method it is assumed that the strength of sand is depth depended. According to Reese, Cox and Koop[11.] (1974) the soil behavior can be modeled by a force-displacement graph. In sand modeling it is assumed that two failure mechanisms can occur:

- A wedge of soil provides a horizontal resistance. A straight sliding surface is assumed.
- The soil flows around the pile to the sides where a gap is likely to occur as a result of horizontal displacement.

The ultimate resistance of the soil depends on the type of failure mechanism a difference is made between shallow and deep depths. Where these two meet is called the transition depth (X_r).

If there are more than one ground layer the transition depth has to be taken in to account using the effective soil stress for each layer.

$$p_{rs} = (C_1 X + C_2 D)\gamma' X \qquad \text{shallow}$$

$$p_{rd} = C_3 D\gamma' X \qquad \text{deep}$$

In which
s	Signifies shallow
d	Signifies deep
p_r	Representative lateral capacity in units of force per unit length [kN/m]
γ'	Submerged unit weight of soil [kN/m^3]
X	Depth below the sea floor [m]
$C_1, C_2,$ C_3	Dimensionless coefficients [-]
D	Pile diameter

$$p = A p_u \tanh(\frac{kX}{A p_u} y)$$

In which
p	Lateral soil resistance per unit length of the pile [kN/m]
A	Factor to account for loading condition (cyclic or non-cyclic) [-]
X	Depth below seabed [m]
k_φ	Coefficient of the horizontal sub grade reaction below the water table, dependent on the

Differences between a 3 dimensional probabilistic method of berthing structure design and
the traditional method of a berthing structure design

J.J. Kool

angle of internal friction [kPa/m]

p_u Ultimate lateral resistance per unit length [kN/m]

Soft clay

The failure lateral actions of soft clay, when charged with statically forces is assumed to be between $8C_uD$ and $12C_uD$. Cyclic actions cause a reduction of the lateral capacity as compared to static forces.

As the depth increases from 0 to X_R, p_r will increase from $3c_uD$ to $9c_uD$. According a rule of thumb it can be assumed that X_R is at least 2,5 times the pile diameter.

$$p_r = 3 * c_u D = p_0'D + Jc_u X$$ and limited by $$p_r = 9c_u D \quad for \quad X > X_R$$

In which

p_r The representative lateral capacity [kN/m]

c_u The undrained shear strength of undisturbed clay soil sample [kN/m²]

D   Pile diameter [m]

p_0' Effective overburden stress [kN/m²] at depth X

J   Dimensionless empirical constant with values between 0.25 and 0.5.

X   depth below sea floor [m]

X_R Depth below sea floor reduced resistance zone for uniform soils

$$X_R = \frac{6c_u D}{\gamma'D + Jc_u}$$

γ' Submerged unit weight of soil [kN/m³]
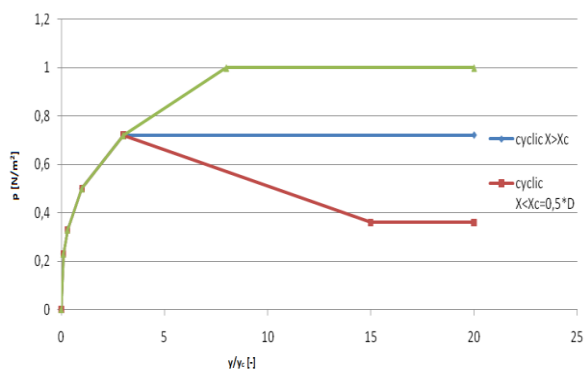
Like the sand curve the clay strength curve is non linear. For static forces the resistance will first be high and decreases when deformation increases. For dynamic loads the strength will increase with the depth. Below the depth of X_R the strength will be constant.

Figure 18: P-y curve for soft clay. With Stiff clay cyclic and non cyclic curves.

In the NEN-EN ISO 19902 distinguishes stiff clay from soft clay based on the cohesion. But in behaviour they should be the same. And that the representative unit lateral capacity, p_r, of stiff clay is similar to that for soft clay. Stiff clay (c>96 kPa) has also a non-linear stress strain relationship as the soft clay does. Only stiff clay is more brittle than soft clay is. This will lead

to possibly fast deterioration of the lateral capacity at large displacements and cyclic actions. For this the representative lateral capacity shall be reduced[19.].
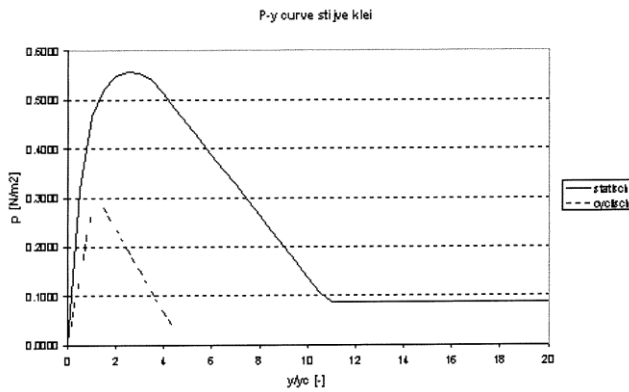
Figure 19: P-y curve of stiff clay[5.]

 However in the original paper, where the p-y curves of the NEN-EN ISO 19902 is based on, the p-y curve is found for stiff clay (see Figure 19)[5.]. The ultimate soil resistance at the surface is described as a function of

$$p_{ct} = 2c_{u,mean}D_{pile} + \gamma'D_{pile}H + 2{,}38c_{u,mean}H$$

The soil will be pushed out as a wedge at the surface.

At a certain depth the stresses near the pile are so high that the soil will fail and the soil will "flow" horizontally around the pile:

$$p_{c2} = 11c_{u,mean}D_{pile}$$

The undrained shear force, in the equation, is given at a certain depth. As with sand the lowest of the two equations is the normative ultimate strength of the soil. The calculated values are somewhat higher than the values of the experiments. This is why is the ultimate empirical strength is adjusted. The observed ultimate strength is divided by the calculated ultimate strength:

$$A = \frac{(p_u)_s}{p_c} \quad \text{and} \quad B = \frac{(p_u)_c}{p_c}$$

Where A is included for statically loads and B for cyclic loads. To make it possible to describe the behavior analytically, the track is divided in a couple of pieces (see appendix I).

5.3.3 Steel cylindrical elements

The cylindrical elements will be checked for tension and compressive strain due to moment loads. Since the system, in this model will only be loaded by the forces of the vessel in a horizontal plane, the vertical loads will be left out. A cylindrical element is considered as very stiff for normal and torsion buckling. The use of cylindrical elements has many advantages. The closed

shape without sharp corners extends the corrosion protection [17.]. The circular hollow section also has the advantage of very low drag coefficients if exposed to wind or water forces, in comparison with other shapes (see Appendix J). In the structure the cylindrical pile/girder are used as foundation of the jetty and berthing structure and for the berthing beam. All these elements have to satisfy the requirements set for the stresses and deformations.

5.3.3.1   Corrosion
The piles are situated in a wet environment and are expected to corrode. The level of corrosion depends on the moisture and oxygen level. This is why different regions are distinct [5.] of the length of the pile:

- Above MLWS-1.0 [m] a corrosion of 0.003 [m]
- Between MLWS-1.0 [m] and bottom level – 1.0 [m] a corrosion of 0.002 [m]
- Under bottom level- 1.0 [m] a corrosion of 0.001 [m]

5.3.3.2   Check of Cylindrical elements
The cylindrical member is loaded by normal, moment and shear loads. To explore the ultimate strength of the members, a stress check is done. The tubular members have to be checked [19.] for the stresses that occur due to the applied loads. A distinction is made between axial stresses and bending stresses. The shear stresses are left out of this scope since the normal stresses are much larger than the shear stresses. There are two different types of tubular members that are used in the foundation of the jetty, completely vertical and tilted piles. These piles are loaded with normal forces in combination of moment forces (see Figure 20). The members of the fender structures are checked for moment forces.
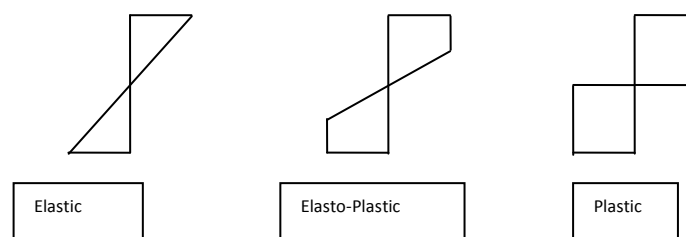
Figure 20: Stress behaviour due to bending force

There are 3 different representative bending stresses to distinguish:

- fully elastic and plastic hinge development
- fully elastic and then partly plastic hinge development
- fully elastic and the local buckling failure

The buckling is considered as full failure of the structure and hard to predict in behavior therefore is taken out for further considerations. It is very common to use the rule of a limitation of the wall thickness of 1/80 of the diameter and following this rule should buckling be prevented. Some short hand calculations show that this is not always the case (see appendix L).

This is done for NEN 6770, NEN 3650 and the NEN-EN ISO 19902. Eventually is chosen to use the method of NEN 3650.

However according to the NEN 3650 developed by Prof. Gresnigt the critical strain of tubes (D/t<120) depends on geometric shape[23.] :

$$\varepsilon_{cr} = 0.5 * (\frac{t}{D}) - 0.0025$$

Using the linear elastic rule of Hooke:

$$\varepsilon_y = \frac{f_y}{E_{steel}}$$

To make sure this will stand in the ultimate limit state a coefficient of γ_{plooi}= 2 is used.

$$\gamma_{plooi}\varepsilon_{rep} \leq \varepsilon_{cr}$$

From this can be concluded that the with a decreasing steel quality a smaller allowable D/t ratio is found (see appendix M).

Eventually the tubular members are checked by the NEN 3650 using the notation of ir. P.Heijndijk[23.] of the "Ingenieurs Bureau Gemeente Rotterdam" who developed a graph with all the ultimate ratio for specific steel qualities.

$$\frac{M_d}{Z_e} < f_y$$

In which
f_y yielding stress allowed with corresponding D/t ratio by the notation of ir. P.Heijendijk
Z_e Elastic section modulus

Elastic-plastic steel behavior
The full capacity of the steel element is limited by elastic and plastic behavior. The elastic theory gives a linear relation between the stresses and the strains and after loading the steel goes back to its original shape. In the first part of the curve an elastic strain relation is recognizable. At the right of the curve a complete different behavior is seen. The bi-linear model is a schematized curve of the actual stress-strain curve (see Figure 21).
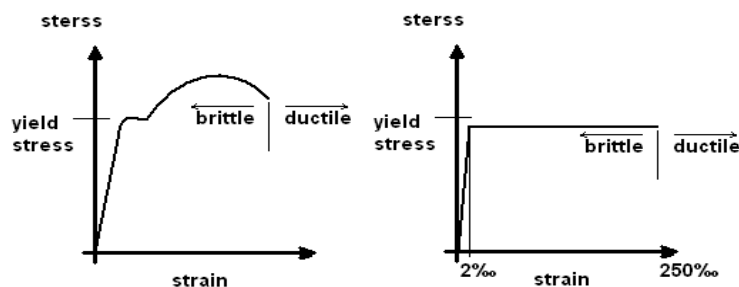
Figure 21: stress-strain relation of tests (left) and according to the bi-linear model

In the bi-linear model the first part of the curve, up to the reach of the yielding stress, shows an elastic behavior. In the second part the maximum stress has been reached but as the strain

grows it will break. This kind of behavior is called plastic behavior. In the part of the plastic behavior, the steel will deform permanently. The length of the plastic part of the curve tells if the material is brittle or ductile.

Deformation

The cylindrical member is loaded by a moment. Due to this moment the member will experience a deformation. This deformation can be described by the formula:

$$E = \int_0^l \frac{M(x)^2}{2EI} dx \Rightarrow \delta = \frac{M(x)^2}{2EI}$$

in which:
E   Absorbed energy [Nm]
M(x)   A function of the moment of the length [Nm]
E_y The Young's modulus [N/mm^2]
I   Moment of inertia [mm^4]

5.4 Design approach

Initially the original structure of the Lyondell was supposed to be. The piles have been extended to ensure that sufficient fixity can be achieved to develop a full plastic moment, such as a simplified approach within the framework of this study. Therefore the structure is designed again using the original design as a template. In the new design the original design is somewhat simplified. Making it more suitable to use in the Monte Carlo simulation. In this chapter the design strategy and consideration are treated. At the end of the chapter the actual reference design is calculated.

5.4.1.1   Berthing beams

In cases where a large range of vessel sizes is expected the use of a berthing beam could be desirable. This is also true in cases where it is not advantageous to design the jetty for large horizontal forces [17.]. The berthing beam is an ongoing beam that is welded on top of all the fender piles and connects the fender piles in this way. The distance between the piles should be chosen to assure an equal forces distribution between the piles, considering the dead load. The advantage of a berthing beam is found in the distribution of the loads. Nor does a vessel any longer have to moor or berth any longer on one specific point. Also it is not possible for a vessel to go in between fenders and miss out on the fender and still hit the actual jetty.

The height of the fender construction related to N.A.P. is determined by the water level and the freeboard of the vessels. Three conditions are considered:

- A small vessel that is empty during high water can berth
- A small vessel that carries load during low water can berth
- It must be possible to reach the seam of the welding under dry conditions.

Also some extra attention has to be paid in considering the driving inaccuracies and damage due to the driving activities. The way the berthing beam distributes the loads over the piles depends

on the relative stiffness of the beam. With a rigid beam the loads will be distributed over a lot more piles than using a flexible beam. How a beam is classified is shown in Appendix K.

5.4.1.2   Design of berthing construction

The strength and stiffness (energy absorption) of the berthing construction is checked using the M-Pile and Scia-engineering. The geometry of this model is very simplified. The wooden grid is left out and the forces apply in the mass centre of the beam. This will rule out additional torsion stresses in the beam due to eccentric loading (see Figure 22) and consequently additional moment at the head of the pile (see Figure 23).
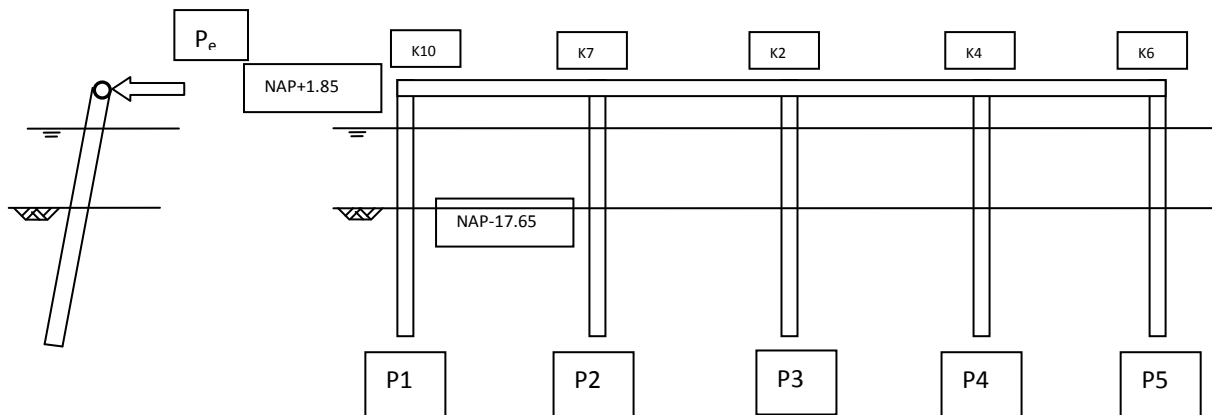
Figure 22: geometry of the construction and the loading

In the first run the piles are designed as separate elements, as it were a fender pile (see in the paragraph above). Because the beam will redistribute the forces over the piles a different mechanical scheme has to be applied. This will influence the moment distribution of the pile (see Figure 23).

 Using the M-pile program the clamping height is determined. For the unit load a force of 1000 [kN] is used. This load is placed in K10, K7, K2 and in between the joints (see Figure 23). For this calculation a mechanical scheme is used with clamped piles. From the results the occurring forces are calculated.
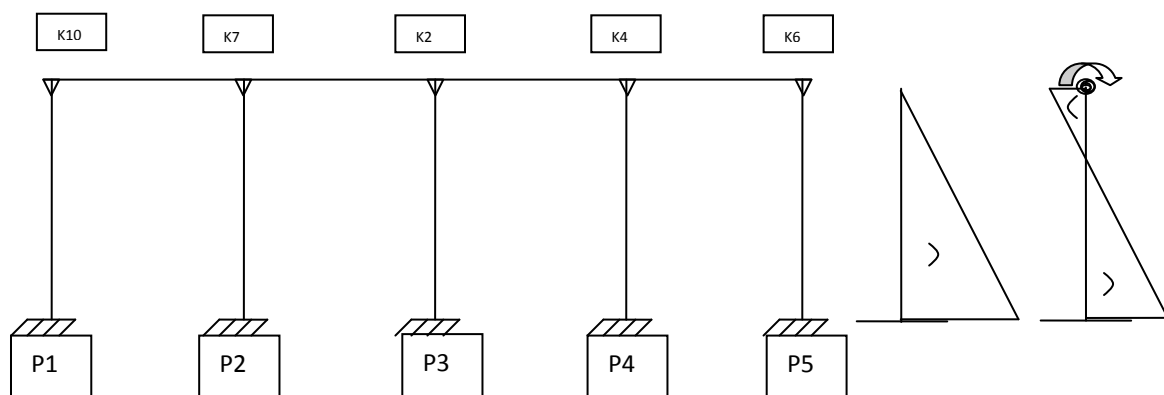
Figure 23: Mechanical scheme of the berthing structure with reaction moment

The energy delivered by the berthing structure is calculated in the elastic track:

$$E = \frac{1}{2} * P * f$$

The deformation f_e first is calculated. Using the energy equation the 'a' magnification factor in relation to the unit factor is calculated (see Figure 24). For the first calculation the clamping height is estimated. After determination of the local deformation, moment force and the shear force of the nearest piles the energy equation is used to distribute the ratio factor ('a').
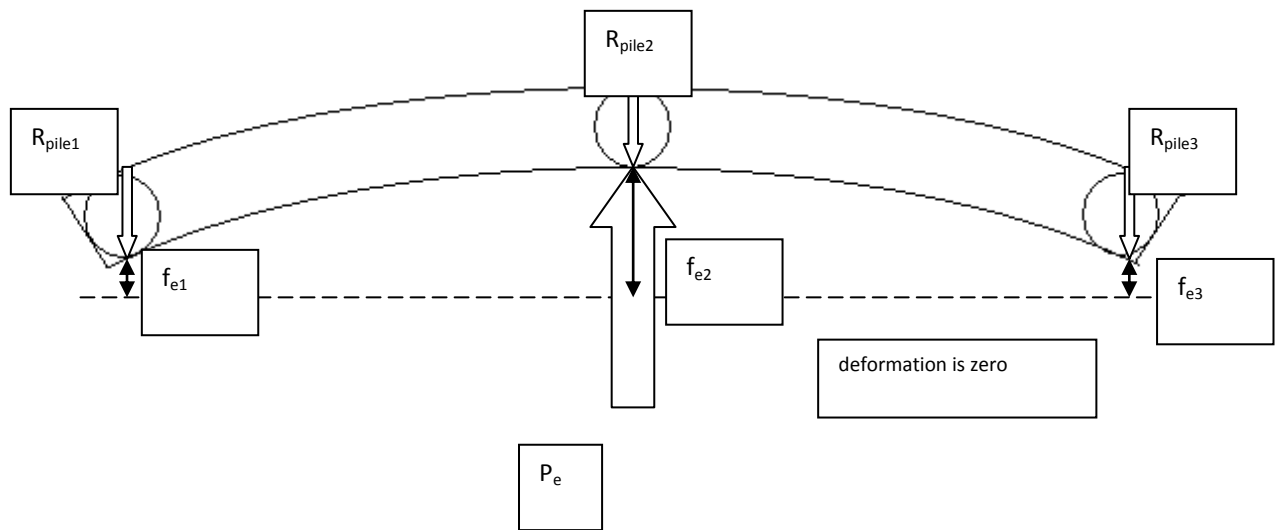
Figure 24: Overview schematization of collision

From this the new representative forces can be calculated and applied. The equilibrium:

$$P_e f_{e2} = R_{pile1} f_{e1} + R_{pile2} f_{e2} + R_{pile3} f_{e3}$$

The fender pile consists of sections of six or three meters of length. The wall thickness of every section can differ, but the outer diameter is always the same (see Figure 25). During placement the driving tolerances and the deformation due to driving of the upper part of the pile has to be taken in to account. Therefore the piles have some extra length and are adjusted after placement.
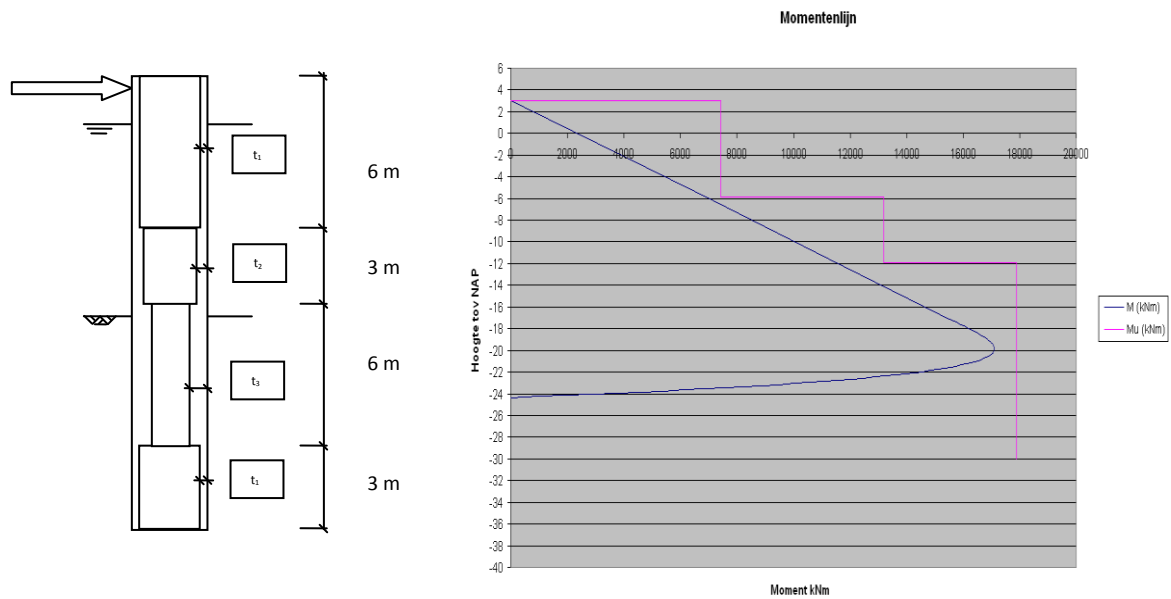
Figure 25: Schematization of wall thickness varying over a pile. An example of bending moment due to loads combined with ultimate moment resistance

By an iterative process the length is found. From the shape and values of the moment in the pile a wall thickness and diameter can be found. Every section is designed for ultimate strength for the applied bending moment (see Figure 25).

The relative stiffness of the pile is a very important factor in finding the length of the pile (see Figure 12). When the pile has too little of depth the end of the pile will shift, will have a rotation and the soil around the pile will fail. The steel member can also reach his ultimate bending resistance and develop an plastic hinge. This is described in the previous chapter. It is preferable that in case of overloading the pile will develop a plastic hinge instead of the surrounding soil to fail (see Figure 12).

In the geotechnical report the soil characteristics are given. Using M-pile, these characteristic will be entered into M-pile. The M-pile software will generate corresponding P-y curves. Using these methods the displacement can be calculated and the maximum absorption of energy can be determined. The length of the pile should be deep enough to prevent that the displacement of the top of the pile could be effected by the depth of the pile base (see Figure 26). This depth is found by varying the length of the pile and monitoring the deformation at the top of the pile (see Figure 26).
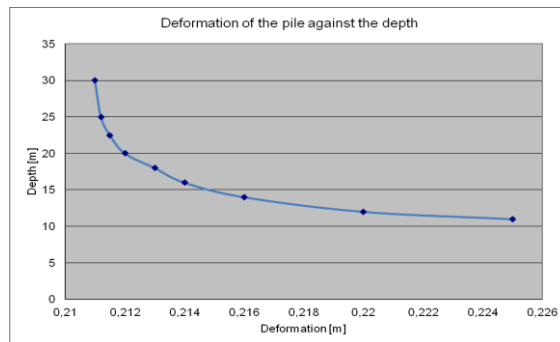
Figure 26: Results of the deflection of The maximum deflection [10.] of a fender construction is set on 1.5 m. the pile in the top per length. Model with a constant load.

In this thesis this assumed to be 0,7 [m]. When the deflection is larger the impact between ship and dolphin will be too gentle. The helmsman will not be able to judge the position and movement of the vessel in relation to the fender. At 'Ingenieursbureau Gemeentewerken Rotterdam' it is common to set the maximum deflection to 0.7 [m], to make sure there won't develop a large gap at the feet of the pile caused by plastic deformation of the soil.

Reference:

[1.] Dynamische analyse afmeerkrachten, Koopmans, 1998
[2.] Ports and Terminals (Ctwa 4330-5506), H. Ligteringen, TU Delft, 2009
[3.] Guidelines for the Design of Fenders Systems, PIANC, 2002
[4.] Dynamische analyse van afmeerkrachten van schepen, Koopmans, 1998
[5.] Probabilistische beschouwing van het afmeer proces, Van der Horst, 2000
[6.] Maritime Structuresm BS-6349 part 4, 1994
[7.] Loads on fender strutures and dolphings by sailing ships, dr ir A. Vrijburcht, Delft Hydraulics, 1991
[8.] Rapportage: Door grond horizontaal belaste palen bestaande ontwerpmodellen, ir F.J.M. Hoefsloot, FUGRO, 2008
[9.] GEO.DGI.Bulletin, No. 12, Brinch Hansen
[10.] Recommendation of the committee for waterfront structures harbours and waterways, EAU, 2004
[11.] Vergelijking van berekeningsmethoden voor dukdalven, P. van der Vorm, 1993
[12.] Ultimate resistance of rigid piles against transversal forces, Bulletin No. 12, Geoteknisk institut, Danish Geotechnical Institute, 1961
[13.] BR Paper Review of Berthing Condition Definitions, T.Becket, April 2010
[14.] Het berekenen van horizontaal belaste paalgroepen, ir.J.L.Bijnagte, ir. H.J. van der Graag, ir H.J. Luger, Geotechniek, 2005
[15.] M-Pile manual, J.L. Bijnagte, H.J. Luger, GeoDelft, 2006
[16.] Elastic solutions for soil and roch mechanics, H.G. Poulos, E.H. Davis, 1974
[17.] Hollow sections in structural applications, J. Wardenier, bouwen met staal, 2002
[18.] Recommendations of the committee for waterfront structures harbours and waterways, EAU, 2004
[19.] NEN-EN ISO 19902, 2007
[20.] Constructieleer gewapend beton, ing R.Sagel, ing A.J. van Dongen, cement en beton, 2000
[21.] Probabilistisch ontwerp van een meer systeem voor grote zeeschepen, J.Oosting, 1984
[22.] grondmechanica, A.Verruijt, S.Baarss, 2004
[23.] Notitie: 'plooi stabiliteit en D/t verhouding', P.Heijndijk, 2006.
[24.] Laterally loaded pile, A. Verruijt, March 1999

6 The design of the reference model according to the standards

6.1 Introduction

In the original design of the berthing structure of the Lyondell jetty, the Blum method has been used. In this study the design of the soil is modeled according the API.

The original design was checked and it appeared that when using the p-y curves for soil modeling and to achieve sufficient fixity to develop a full plastic moment, the piles of the original design should be extended. From this check with help of the M-Pile software, the piles showed a tip displacement.

From this check it was decided to make a new design for the berthing structure referring to the API ground model. Consequently the geometry of the piles and the berthing beam are changed.

According to the PIANC it may be assumed that the point of collision of a vessel is at a ¼ of the total length. Because a simple hand calculation showed that the berthing structure could be too short, the berthing structure was lengthened with one pile (20 [m]).
The berthing structure is a slender structure and will distribute the energy to the piles according to the stiffness of the berthing beam. According to the method explained before, a unity factor is developed and with this the maximum load per pile is determined. The soil profile is assumed to be equal over the total length of the structure. Thus the ratio of the loading of the piles depends on the geometry itself. According to this method the inner piles are submitted to approximately an equal load. They will have the same geometry. In the next paragraph calculation of the berthing structure is shown.

Structure Limit State
In the design the limit states are copied from the terms of reference:
Service limit state: maximum deformation of approximately 0.70 [m]
Ultimate limit state: reaching the elastic yield stress of the steel and there is no point displacement allowed.

6.1.1 Energy Load

The design vessel in this design is copied from terms of reference of the Lyondell. By use of the equation of Saurin is the actual loading determined. This equation is introduced in an earlier chapter. The dimensions of the design vessel (Seagoing vessels) are:

- Length: 180.00 [m]
- Beam: 32.00 [m]
- Draft: 13.00 [m]
- Dead weight: 550000 [kN]
- Velocity: 0.15 [m/s]
- Angle of berthing: 12 [^{0}]

A safety factor of γ=1.5 [-] is used.
 This results in the following calculations:

$$k = (0.19 C_b + 0.11) L = (0.19 * 0.73 + 0.11) * 180 = 44.8$$

with:

$$C_b = \frac{M}{LBD\rho} = \frac{56065 * 10^3}{180 * 32 * 13 * 1025} = 0.73$$

the radius:

$$r = \sqrt{(\frac{L}{2} - L/4)^2 + (\frac{B}{2})^2} = \sqrt{(\frac{180}{2} - \frac{180}{4})^2 + (\frac{32}{2})^2} = 47.76[m]$$

angle:

$$\gamma = 90 - h.v.aanv. - \sin^{-1}(\frac{B}{2 * r}) = 90 - 12 - \sin^{-1}(\frac{32}{2 * 47.76}) = 58.43[^o]$$

calculating the eccentricity factor:

$$C_E = \frac{k^2 + (r\cos\gamma)^2}{k^2 + r^2} = \frac{44.8^2 + (47.76\cos(58.43))^2}{44.8^2 + 47.76^2} = 0.61$$

And Vasto da Costa equation:

$$C_m = 1 + \frac{2D}{B} = 1 + \frac{2 * 13}{32} = 1.81$$

insert all the parameters in to the equation:

$$E_{rep} = \frac{1}{2} M * v^2 * C_e C_m C_s C_c = 0.5 * 56065 * 0.15^2 * 0.61 * 1.81 * 1 * 1 = 696[kNm]$$

E_{rep} =representative energy (under normal conditions) to be absorbed by the berthing system (in kNm)

M   =mass of design vessel (displacement in tones), at chosen confidence level. Usually 95 % confidence level. (**M=56065 ton**)

v   = approach velocity of the vessel perpendicular to the berth (in m/s) (use 50% confidence   level) (**v=0.15 m/s**)

C_e = eccentricity factor (**C_e=0.61**)

C_m =virtual mass factor (**C_m=1.81**)

C_s = softness factor (**C_s=1**)

C_c = berth configuration factor or cushion factor (**C_c=1**)

With a design energy of (E_{rep}=690 [kNm]) E_d=1.5*690=1050 [kNm].

6.1.2 Structure

The berthing structure is a slender structure and so the distribution of the energy is dependent on the stiffness of the structure. The amount of energy per pile depends on the geometry of the structure. With the help of a unity factor the distribution of the energy over the piles is analyzed in percentages of the load. The normative load is taken for the design. In this design the soil model is taken equal over the length of the structure. The inner piles of the structure have about the same load and are taken all the same length.

For the design of the model the following material characteristics are used:

The used diameter for the profile of the tubes is:
Ø=1820 [mm]

The used yielding stresses of steel:
S355 (f_y=355 [N/mm^2])
X56 (f_y=380 [N/mm^2])
X65 (f_y=455 [N/mm^2])
X70 (f_y=480 [N/mm^2])

With a Young's modulus of E=2.1*10^5 [N/mm^2] and a material factor of γ=1.

The used wall thickness are coupled with the following yielding stresses (Table 4).

Wall thickness [mm]	22.2	25	28	30	38	40
Steel type	X56 (f_y=380 [N/mm^2])	X56 (f_y=380 [N/mm^2])	X65 (f_y=455 [N/mm^2]	S355 (f_y=355 [N/mm^2])	X56 (f_y=380 [N/mm^2])	X65 (f_y=450 [N/mm^2])
Length of elements	17 [m]	15 [m]	17 [m]	12 [m]	16,5 [m]	12 [m]

Table 4: pile characteristics

First an estimation is made of the geometry and is used as input for a calculation with the finite elements software "Scia-engineer". In the geometry of the berthing structure a horizontal beam has been assumed. The structure is loaded with a unit load of 1000 [kN]. From this calculation the normative load is determined per pile in percentage of the unit energy load.

$$E_{rep} = 0.5 * \alpha^2 * P_e * f_e \qquad 700 = 0.5 * \alpha^2 * 1000 * 0.28$$

The "a" is a magnifying factor in relation to the unit load. In the schematizing and developing of the magnifying factor the soil is modeled as a spring according to the API standard. Consequently the depth where the pile is considered to be fixed will vary depending on the load.

Because the berthing beam is solely loaded in the centre of the mass of the beam the resulting torsion moments are neglected. The normative absorbed energy per pile is found where the loading is near the point of the connection with the pile and the berthing beam.

Loading coordinate	Shear force [kN]-deformation [mm]	Shear force [kN]-deformation [mm]	Shear force [kN]-deformation [mm]	Shear force [kN]-deformation [mm]	Shear force [kN]-deformation [mm]	Energy of the unity load [kNm]
S1250	-	-	50/60 (2 [kNm])	270-180 (24 [kNm])	710-280 (99 [kNm])	140
S1250-S1300	-	11-25 (0.1 [kNm])	127-185 (12 [kNm])	340-185 (35 [kNm])	535-230 (62 [kNm])	
S1300	-	50-50 (1.3 [kNm])	230-130 (15 [kNm])	390-200 (40 [kNm])	343-170 (30 [kNm])	100
S1350-S1400	10-25 (0.12[kNm])	125-80 (5 kNm])	370-180 (33 [kNm])	345-170 (29 [kNm])	165-100 (8.5 [kNm])	
S1400	45-45 (1 [kNm])	230-126 (15 [kNm])	450-220 (50 [kNm])	235-130 (15 [kNm])	54-50 (1.35 kNm])	110

Table 5: Results of the unit load (F=1000 [kN])

After loading the third pile the distribution is approximately symmetrical and is considered to be representative for the other parts of the structure. Due to the geometry of the berthing structure the amount of energy will distribute over a couple of piles. The ratio (a^2) of energy per pile (see Table 5) is analyzed in the following equations.

Pile S1250

$$E = 0.5 * \alpha^2 * P_e * f_e = 0.5 * 0.71 * 1000 * 0.28 = 0.5 * 710 * 0.28 = 99.4 [kNm]$$

Pile S1300

$$E = 0.5 * \alpha^2 * P_e * f_e = 0.5 * 0.39 * 1000 * 0.2 = 0.5 * 390 * 0.2 = 39 [kNm]$$

Pile S1350

$$E = 0.5 * \alpha^2 * P_e * f_e = 0.5 * 0.45 * 1000 * 0.22 = 0.5 * 450 * 0.22 = 49 [kNm]$$

In the design of the piles, the piles are loaded with the normative energy loads. This ratio is used to design the piles on the actual amount of energy load and is taken as a measurement (a) for force and deformation in relation to the energy loading. This is checked for strength and deformation with help of the software of M-pile.

According to the NEN standards there are 4 cases of soil modeling used for checking the structure. The four cases consists of the higher and lower users limit state and the high and low ultimate limit state. The soil profile that is used for dimensioning the piles is taken from the geo-technical report of the Lyondell jetty (sounding CM628).

The resulting moments are shown in the figures below with the enveloping strength capacity of the profiles (see Figure 27 and Figure 28).
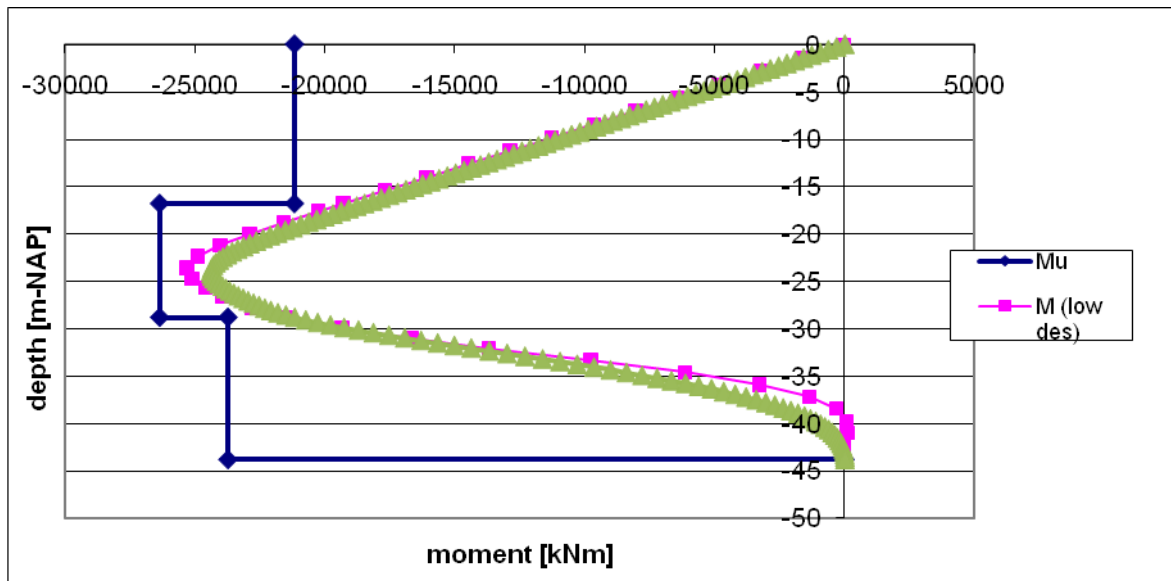
Figure 27: Resulting moment due to max load and moment capacity of inner piles
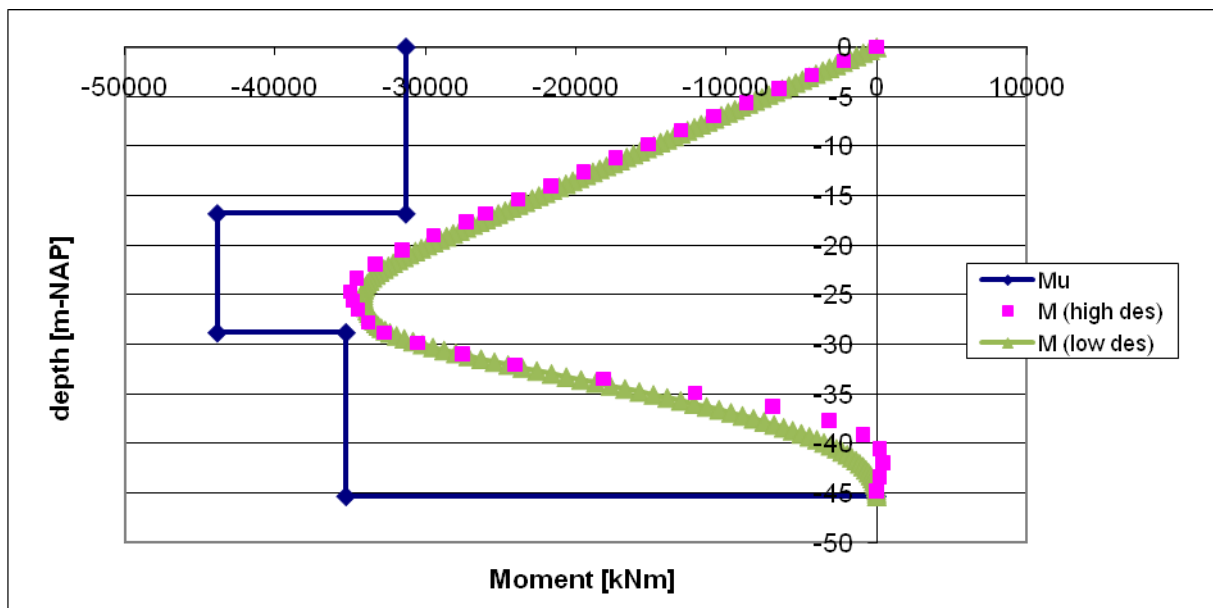
Figure 28: Resulting moment due to max load and moment capacity of outer piles

In the figures above both loading cases are normative for the pile. The low design value is normative for stability of the pile and the high design value is normative for the moment capacity of the pile.

The berthing beam is checked with a couple of load cases. The normative loads are used for dimensioning the strength for the entire beam (see Figure 29).
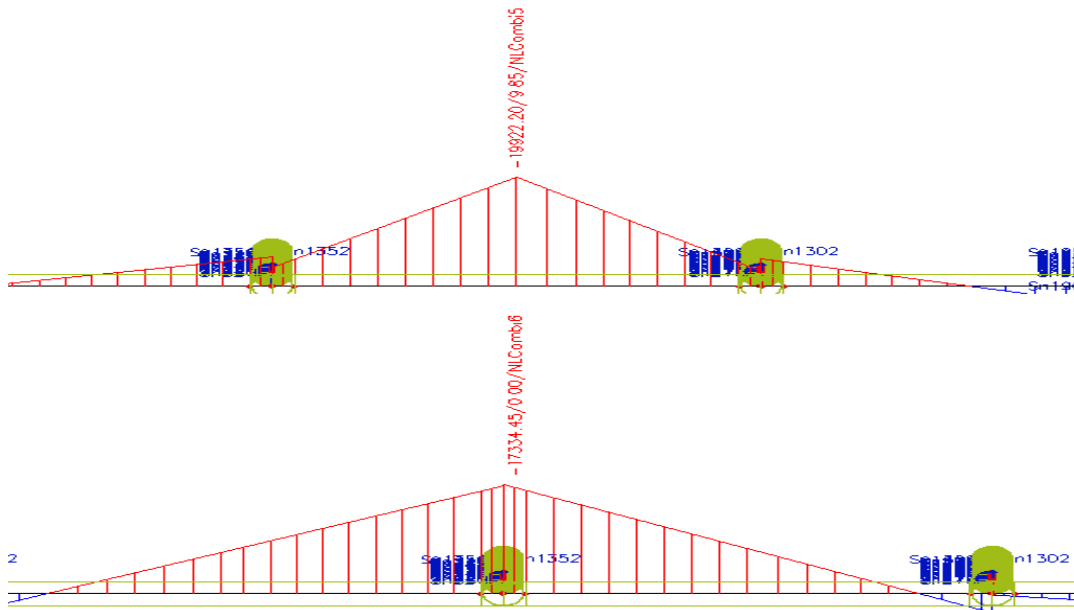
Figure 29: Overview of structure with normative loading for the berthing beam

The deflection of the total structure is checked (see Figure 30). For this check the lower representative values for soil are used. The exceeding of the service limit state is accepted (approximately 0.7 [m]).
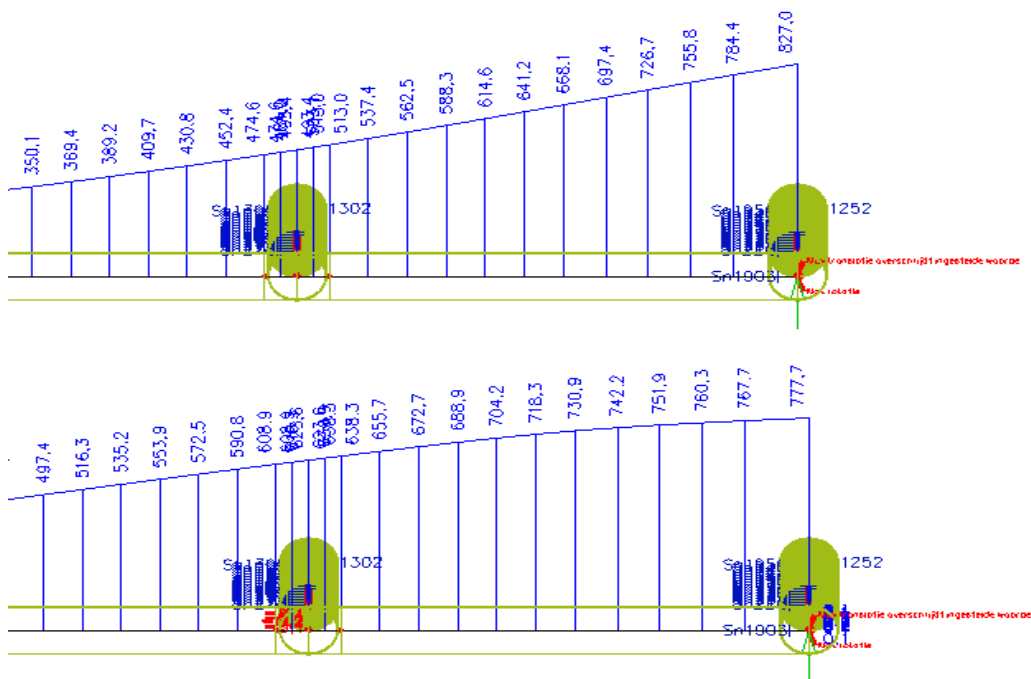
Figure 30: Normative deflection of the total structure due to representative load

7 The concept of probability

7.1 Introduction

The probabilistic design method starts off with making a definition for failure."A structure fails when it can no longer perform one of its principal functions.""A structure or a structural component collapses if it undergoes deformations of such magnitude that the original geometry and integrity are lost."[1.]

In the assessment of the safety of a system the probability of failure has to be calculated. The probability of failure is a function of strength and load, called a reliability function ('Z'). The reliability function makes use of variables. The variables with a stochastic character are called basic variables.[1.] Failure or collapsing with regard to principal functions is called the ultimate limit state. Failure with regard to the other functions is called the service limit state [1.].

When considering the safety of a structure, the system has to be considered as a whole. Failure of a component may or may not influence other components. When failure of a component can cause failure of one head event, this is called series connection. And with the failure of a component which will be compensated by another is called a parallel connection [1.]. To get insight in the total system, to order and define relationships in all failure mechanisms, a fault tree can be used. The relations between every mechanism is defined with an 'AND' (parallel system) and an 'OR' (series system) and everything in between.

7.2 Fault tree theory

Since the establishment of failure often can be done in different ways a fault tree can helps to get insight in the total system. The head event, which is the most important event to be considered, is placed in the top of the tree. The tree shows the relationship between the head event and the base events.

Every event is put in such a way that it can be described in a logical way using logical gates (in the appendix the most used gates are shown with the corresponding structure function). A logical gate has only one exit but one or more entries. The fault tree has a binary character, 'true' or 'false'.

Using the fault tree and determining the probability of failure it is possible to draw up a structure function ($\psi(y)$) of the system [2.].

$\psi(\vec{y}) = 0$ System fails
$\psi(\vec{y}) = 1$ System works

In which

$$\vec{y} = (y_1, y_2, ..., y_n);$$

y_i Is a binary indicator variable, which specifies whether or not the underlying event occurs. y_i=1 if the vase event 'i' occurs; y_i=0 if the base event 'i' does not occur.

	Mutual exclusive	Independent	Fully dependent
Series (or)	∑Pi (upper bound)	1-∏(1-Pi)	Max{Pi} (lower bound)
Parallel (and)	0 (lower bound)	∏Pi	Min{Pi} (upper bound)

Table 6: Relation between events

7.3 Serviceability limit state

The structure will be examined to excessive deformations with the Serviceability Limit State (SLS) using the design. The excessive deformations (u) should be limited by the causes of loss of functionality of the structure or the cause of damage to other structures and the comfort of users. Under these conditions (u_{admis}) fall:

- maximum deformations of the jetty
- maximum deformations of the berthing structure
- crack width of the concrete parts
- stresses and the maximum deformation in the transport pipes on the lower deck
- stresses and the maximum deformation in the loading arms

This will lead to the following equation:

$$Z = u_{admis} - u$$

with the following condition:

$$u_{admis} = \min|u|$$

In personal communication with ir. L. Groenewegen uses as guidance and first approximation, the maximum of deformation of the jetty should be taken 1/300 of the total height. According to dr. ir. J.G. de Gijt a guidance of 0.15 [m] is a first good approximation, which is comparable to the order of dimensions of the guidance rule of ir. L. Groenewegen. According to the 'NEN-EN 1993-1-1' the horizontal deformation should be defined by the owner. The 'NEN-EN 1992' gives as guidance for the vertical deformation a maximum deformation of 1/250 of the span for quasi-permanent loads.

The berthing structure is limited by a approximately maximum deformation of 700 [mm] [3.]. The EAU 2004 requires a maximum deformation of 1.5 [m][2.]. With larger deformations than 1.5 [m], the helmsman won't experience any resistance of the berthing construction. To secure the functionality of the devices located at the jetty a further analyses has been done. On the lower deck some pipes are located. These will be considered in the following text.

Transporting pipes

In personal communication with ir. Hufkes of "Gemeentewerken Rotterdam" , he assures that it can be assumed that the pipes are semi fixed mounted so they can expand when heated. And also the pipes are attached to each other with a flexible coupling.

The radius of the pipes always will be larger than the radius of the jetty, since the pipes do not have to follow the exact movements of the jetty. Test calculations (see the Appendix C) show that when this jetty is imposed to a load of 1000 [kN] the deformation will be 60 [mm] over the

whole length. Therefore the bending length of the pipes will be larger and the transport pipes can be assumed to be not indicative.

7.4 Ultimate limit state

The structure will be analyzed for the complete failure of each structural element using the limit state function (Ultimate limit state, ULS). For the ultimate limit state the moment will be considered as a function of stresses.

$$Z = M_{admis} - M$$

Under these conditions fall:

- Yielding stresses (M_y) of the steel parts
- Ultimate moment (M_u) of the concrete parts

In this thesis the soil stability is left out of the scope.

7.5 Safety considerations

For the design of a jetty or a berthing structure there are a couple of standards that are very common to use.

The PIANC does not give a failure rate but makes use of the Brolsma curves. In contrast to the "Manual of Quay Walls" the Brolsma curves use a reference period of 30 years[49][13.].

The EAU 2004 insinuates a service life of 50 to 60 years but recommends a economical analyses. Also for the limit states it refers to the DIN EN 1990. This would be in the Netherlands the NEN-EN 1990. If it is assumed that a jetty is considered to be in consequence Class 2 a β=3.8 in period of 50 years and β=4.7 in period of 1 year for the ultimate limit state is recommended. For the service ability a β=1.5 in a period of 50 years is advised and a β=2.9 in a year.

The description of consequence level 2 says:
Medium consequence for loss of human life economic, social or environmental consequences considerable.

This is not entirely true for the jetty. The economical damage is large and the loss of life will be small. The "Manual of Quay Wall" makes a distinction between normal safety considerations and economical importance. However the safety considerations are based on the NEN-6700 and this is replaced with the NEN-EN 1900. But the description of consequence level 2 says:

"Safety class 2 is applied when the chance of loose of life is small and the economical damage is large".

Also the economical importance of the jetty is of the same rate of a quay wall. Therefore the safety of the "Manual of Quay Walls" level 2 is assumed to be of the same rate. In this manual the lifetime of the structure is taken as lasting 50 years. The probability of failure is derived from the safety class 2 of the "Manual of Quay Walls":

β=3.4 for Ultimate Limit State probability of 3.369*10^{-4} over 50 years

β=1.8 for Service Limit State probability of 3.54*10^{-2} over 50 years

The API says that all loads of vessel collision should be calculated for a period of one year and recommends a chance of failure in the order of 10^{-3} or 10^{-4} per year. The service limit state is determined by the owner.

In the further analysis the safety considerations of the "Manual of Quay walls" is adopted. Even though the NEN 6700 is replaced by the NEN-EN 1900. The description of the NEN 6700 is more applied to the jetty. These safety considerations are more focused on the economical risk instead of the structural risk as the "Manual of quay walls" advices.

The intensity of use has a large influence on the probability of failure in a reference period and this is not known for this specific structure. This is therefore taken as a variable to consider. At first the frequency of berthing of once every week is assumed, secondly the frequency of twice a week is assumed.

The requirements are still somewhat high, because there are some specific differences between a quay wall and a jetty. The requirements are based on the economical consequences. And because the failure rate is based on economical risk the availability of the jetty is of great importance. For instance when failure of one part of the berthing structure occurs, the jetty has still the ability to operate.

Also the level of failure is not taken into account. In this model the structure is considered to fail when reaching the elastic stresses. But in practice it is possible to have a plastic deformation and by this there are some reserves (see chapter "Structural analysis"). There are different levels of failure of the berthing structure.

The NEN-EN 1900 suggests that it is allowed to replace a extreme distribution for a normal distribution (unless it concerns "fatigue").The replacement of extreme distribution for a normal distribution could lead to a smaller representative value. Also are all chances of failure calculated with a normal distribution.

7.6 Fault tree jetty

Here the total fault tree of the jetty is presented. High in the tree a distinction is made between service ability and ultimate limit state. The base events are further described in the appendix R .
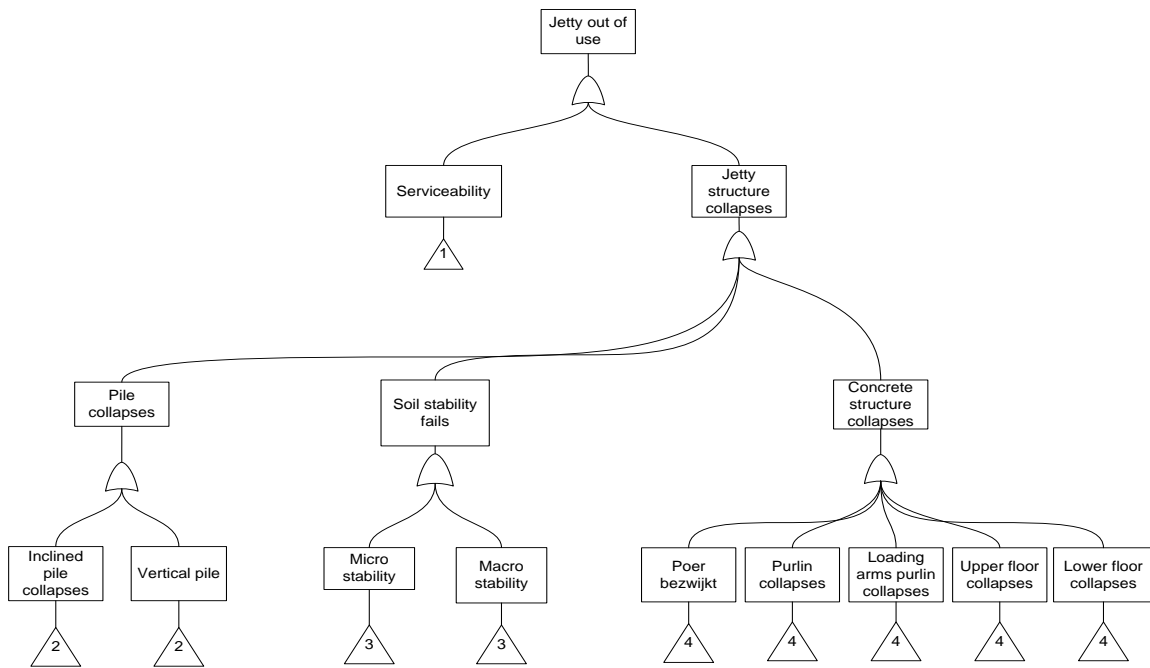
Figure 31: General fault tree
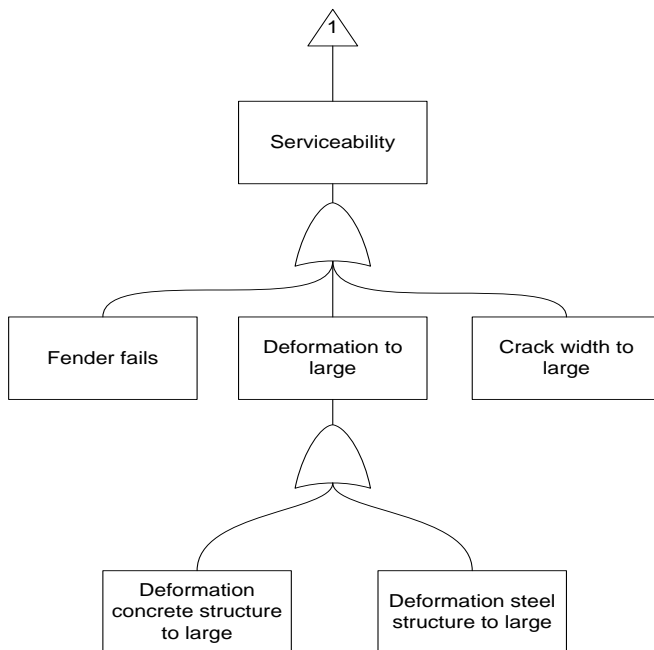
Figure 32: serviceability

7.7 Fault tree fender construction

The berthing structure is standing in front of the jetty self. When the berthing structure fails in the ULS the jetty cannot be taken in operation anymore. Therefore the failing of the berthing structure is called conditional failing.
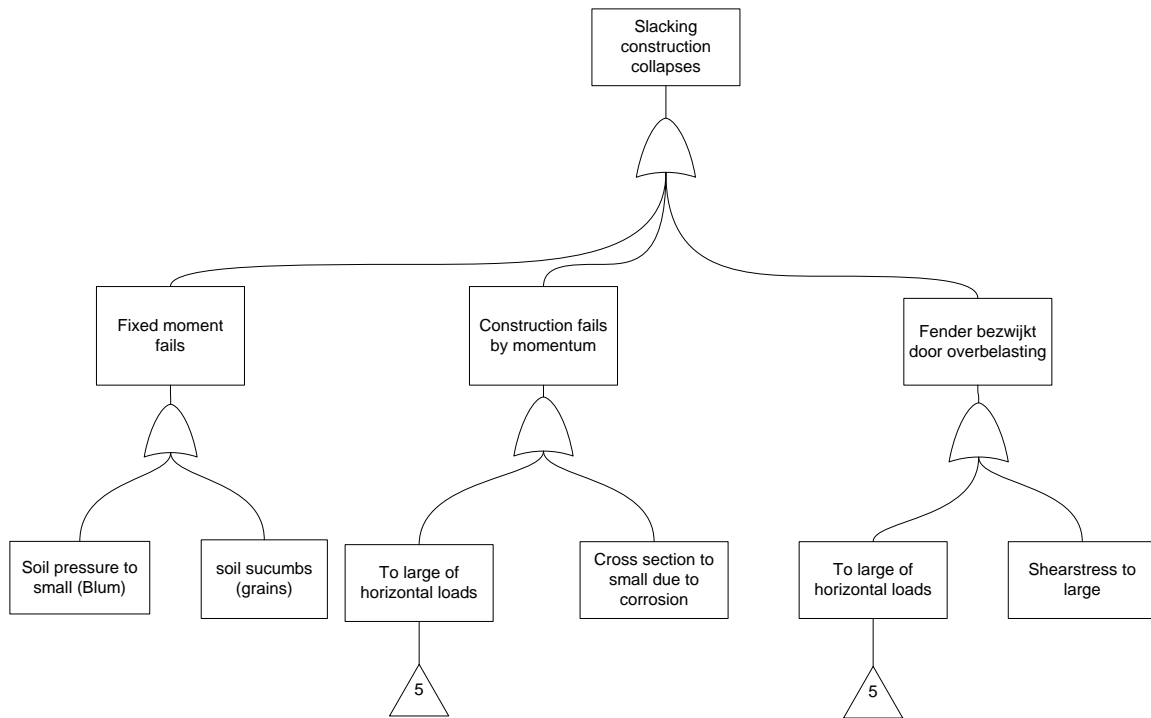
Figure 33: Slacking structure collapses

7.8 Probabilistic strength calculation

In the assessment of reliability of the structure there are three types of calculations. These calculations are divided in three different levels:

Level 1   characteristic value of strength and loads. Use of partial safety coefficients
Level 2   approach with a probabilistic method
Level 3   exact probabilistic method

In this thesis a comparison will be made between a structure which is designed with a level 1 method and a level 3 method. For analyses of the influence of all the variables a level 2 method is used.

7.8.1 Level 1

Level 1 method used by standards. A certain margin will be kept, between the representative strength and the representative loads [2.]. According to this method a representative value of the strength is divided by a partial safety factor and the load is multiplied by a safety factor (see equation and Figure 34).
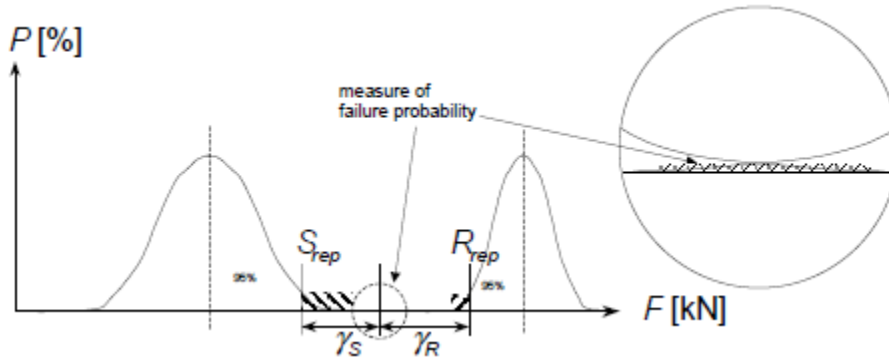
Figure 34: safety factors for strength and force[2.].

The representative values are calculated:

$$R_{rep} = \mu_R + k_R \sigma_R \qquad\qquad S_{rep} = \mu_S + k_S \sigma_S$$

The design point is the point in the failure space with the greatest joint probability density of the strength and the load:

$$R^* = \mu_R + \alpha_R \beta \sigma_R \qquad\qquad S^* = \mu_S + \alpha_S \beta \sigma_S$$

These equations result in the following condition:

$$\frac{R_{rep}}{\gamma_R} > \gamma_S S_{rep}$$

7.8.2 Level 2

In case of use of a non-normal distribution the reliability function will be a non-linear function. In this case the reliability function will have to be linearised using a Taylor polynomial:

$$Z = g(\vec{X}) \approx g(\vec{X}_0) + \sum_{i=1}^{n} \frac{\partial g}{\partial X_i}(\vec{X}_0)(X_i - X_{0i})$$

It is possible to determine the μ_z and the σ_z of this linear function. Using the following equations:

$$\mu_z \approx g(X_0) + \sum_{i=1}^{n} \frac{\partial g}{\partial X_i}(\vec{X}_0)(\mu_{X_i} - X_{0_i}) \qquad\qquad \sigma_z \approx \sqrt{\sum_{i=1}^{n} (\frac{\partial g}{\partial X_i}(\vec{X}_0)\sigma_{X_i})^2}$$

When the expected value and the standard deviation are known the reliability index can be approximated. In case of a liberalized reliability function the reliability index is determined by:

$$\beta = \frac{\mu_z}{\sigma_z} \approx \frac{g(\mu_{X1}, \mu_{X2}, ..., \mu_{Xn})}{\sqrt{\sum_{i=1}^{n} (\frac{\partial g}{\partial X_i}(\mu_{X1}, \mu_{X2}, ..., \mu_{Xn})\sigma_{X_i})^2}}$$

Determining the reliability index when, β is the minimum distance from origin to Z=0 (in the normalized space). When the design point is approximated, iteration will follow. Until the design point is determined.

7.8.3 Level 3

The base for using the Monte Carlo simulation is a simulation from the base events. These base events are first drawn 'random' numbers, between zero and one from uniform density function (see Figure 35).
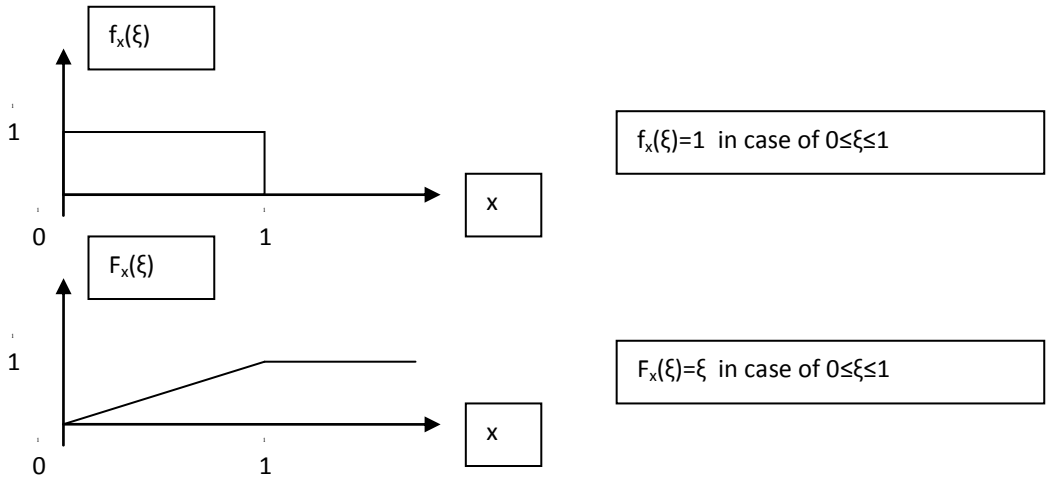
Figure 35: uniform distribution between 0 and 1

The drawn number from the uniform distribution can be used to generate a random number from the formula of an arbitrary distribution (base event). The drawn number will be transformed into a variable Y using $Y(x)=F_X(x)$ (see Figure 34). A given distribution random variable X with a distribution function $F_X(\xi)$ and a density function of $f_X(\xi)$.
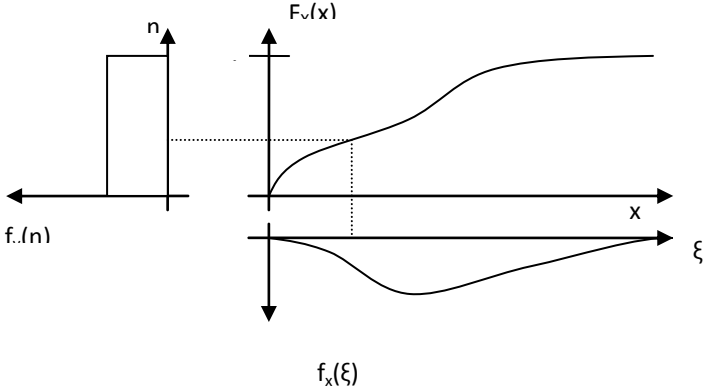
Figure 36: transformation relation between an uniform and a non-uniform distribution

For every distribution there is another different generator (see Appendix Q). The random generator is limited in the variety of sequence in numbers. This will result in a large amount of drawings that the numbers are not really independent.

Using a Monte Carlo simulation in a reliability problem, the relative error has to be considered. To make sure the relative error is small enough a minimum of calculations have to be made. A Monte Carlo method has a binomial character. With an enough large amounts of drawings, a normally distribution can be assumed and the change of failure can be expressed by:

$$P_f \approx \frac{n_f}{n}$$

In which

n   is the total number of simulations

n_f is the number of simulations, for which the limit state function is Z(X)<0

7.8.3.1   Random numbers

The random numbers are based on the uniform draws of figures between the zero and one. These are founded on the outcome of numerical errors. The quality of the uniform distribution depends on the used numerical scheme. The random generator of Excel is considered quit poor in comparison to the random generator of Matlab for instance.

7.8.4 Ditlevsen

An approximation method for failure probability of a serial system is that of Ditlevsen (see appendix S). In this method more limited boundaries of the failure probability are calculated. This method assumes a known correlation between the failure modes, expressed by a correlation coefficient ρ, and normally distributed reliability functions.

A system in serie of two elements will fail as soon as one element of the two elements will fail:

$$P\{systemfails\} = P\{Z_1 < 0 \cup Z_2 < 0\} = P\{Z_1 < 0\} + P\{Z_2 < 0\} - P\{Z_1 < 0 \cap Z_2 < 0\}$$

The influence of last term is determined by the correlation coefficient between the two

limit states. The correlation coefficient corresponds to independence -1≤ρ≤+1 (ρ=0

corresponds to independence).

$$\rho(Z_1, Z_2) = \sum_{i=1}^{n} \alpha_i^{(1)} \alpha_i^{(2)}$$

Where α_i influence coefficient is $\alpha_i = -\sigma_R / \sigma_Z$. The bounds of the failure probability are:

$$P\{Z_1 < 0 \, and \, Z_2 < 0\} \geq \max\{ \phi_N(-\beta_1)\phi_N(-\beta_2^*), \phi_N(-\beta_1^*)\phi_N(-\beta_2) \}$$

$$P\{Z_1 < 0 \, and \, Z_2 < 0\} \geq \phi_N(-\beta_1)\phi_N(-\beta_2^*) + \phi_N(-\beta_1^*)\phi_N(-\beta_2)$$

in which β_i^*

$$\beta_i^* = \frac{(\beta_i - \rho\beta_j)}{\sqrt{(1-\rho^2)}}$$

for the probability of failure of the serial system:

$$P(Z_1 < 0) + P(Z_2 < 0) + P(Z_2 < 0)\phi(-\beta_2^*) \le P\{systemfails\} \le P(Z_1 < 0) + P(Z_2 < 0) - P(Z_2 < 0)\phi(-\beta_1^*)$$

7.8.5 Model factor and Human failure

Because a model is a schematization and simplification of the real system and contains all kind of inaccuracies a model factor is introduced. The factor gives a ratio between the actual deterministic loads or strength and the value according to the calculation model based at random variables.

The chance that a human makes a mistake for regular labor is 0.01-0.001.

Reference:

[1.] Probabilistic design of flood defenses, report 141, technical advisory committee on water defenses, June 1990
[2.] Probability in civil engineering ct4130, TU-Delft, June 2006

8 Probability distribution functions design variables

8.1.1 Introduction

In this chapter all different variables in the design formulas are introduced as stochastic distributions. The variables are used initially for the deterministic design method. In order to use them in the probabilistic calculation they have to be written as a stochastic. Dependencies between variables are taken into account by expressing the dependent variables in each expression. In the next chapter all variables are written as a stochastic. From some of the distributions the back ground of the measurements are not taken in to account. For calculating the eventual failure chance this is of great importance. What is the time relation of the data to the reference period.

The distributions of the velocity, length, draft and width are all dependent of the vessel weight. In this thesis this relation is assumed solid. The distribution of the vessel weight consists out of 122 measurements, we assume that is equal to a time period of one or two years (one or two berthings a week).

The found distributions are investigated for their physical correctness. Some of them are replaced or bounded (see appendix FF).

In this chapter all the base variables are discussed. Some of them are eventually not taken into account of the calculations. Some extra attention was paid to discuss the Brolsma curves.

8.1.2 Berthing velocity

When designing berthing structures the berthing velocity of the design vessel will be defined. In practice the "Brolsma curves" are used. These curves give a relation between the displacement of the vessel and the difficulty of the berthing operation in accordance to the degree of exposure. These "Brolsma curves" are key components of BS6349 Pt. 4 1994 and the PIANC 2002. The data used to compose the distributions are collected at the '7th Petroleumport' and the 'Vingerpier'.

Brolsma curves

The Brolsma figure distinguishes five navigation conditions. These conditions are not precisely described and are suspected to be extrapolated from the selected data. From these figures a clear relation is shown between the dimensions of a vessel, the velocity and the type of berthing.

Considering the Brolsma curves there are some critical remarks:

- The amounts of measurements are very limited. About 150 measurements are used to extrapolate the curves. Even the measurements of Baker, Saurin and Brolsma together are very limited[2.]. Also the measurements were taken as extremes [1.].
- The 95% probability of maximum approach velocity is counting for 3.000 berthings (2 per week for 30 years) in a lifetime. This is extrapolated from the data using extreme probability graphs[1.].

- The Brolsma and Saurin's paper measurements (251 berthings) were 87% tankers with a weight in-between 36.000 [DWT] and 265.000 [DWT]. Therefore only the 3rd section is based on data. The others are probably extrapolated from the data.
- All vessels were tug assisted[1.]

Distribution of Velocity using the data of the "seventh Petrolport"

To construct a distribution of velocity the data collected from the 7th Petroleum port have been used. The data consists out of 85 measurements and were collected by Koopmans in 1998. The majority of the gathered measurements of the vessels that were monitored were tankers in between 30.000 [DWT] and about 150.000 [DWT].

The jetty, where these measurements were made, has an eastern and a western side where vessels are able to berth. The two outer piles are the more heavily dimensioned then the inner four. The piles are driven to a depth of NAP-33 [m], for the smaller berthing piles, and up to NAP-41 [m], for the more heavier outer berthing piles. The local depth is approximately 21 [m] and the water velocity is expected to be negligible.

To measure the velocities a recording system has been used. The recording system has to register the velocity of the vessel, the ability to brief the pilots about their current velocity. This is done with help of a sign.

- Green: velocity of < 7[cm/s]
- Yellow: velocity between 7 [cm/s] and 10 [cm/s]
- Red: velocity of >10 [cm/s]
- Alarm: velocity of >11 [cm/s]

During the berth it is possible that a vessel hits the pile multiple times. In this analyses only the maximum velocities are taken into account. The conditions are assumed to be comparable as that of the Lyondell jetty.

Velocity distribution

For velocity analysis only the group of vessels that are smaller than 168.000 [DWT] are taken into account. With every berth it is possible that the vessel hits the structure multiple times, the distribution only contains the maximum velocities (see Figure 37). From the data the average velocity as a function of the weight is constructed, the function (see Figure 37):

$$v_{average} = 1.925 * DWT^{-0.30} [m/s]$$
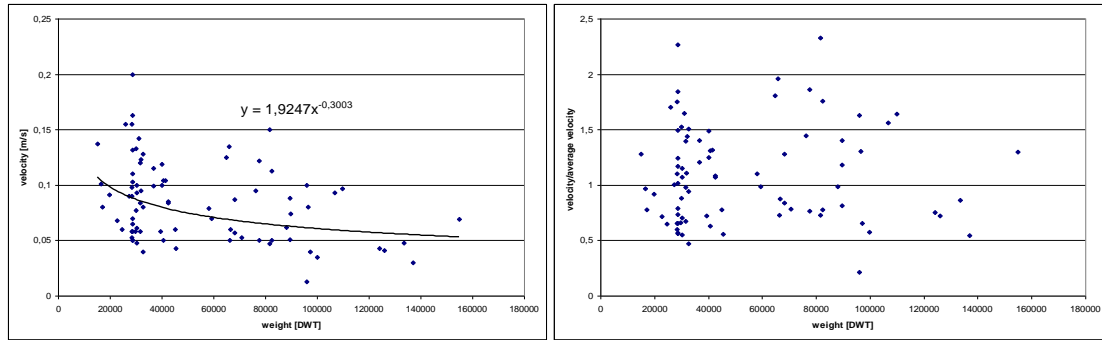
Figure 37: Left the maximum of the vessel velocities within the corresponding vessel weight. Right the average maximum velocity as a function of weight

The divided data by the average are plotted and shows the data beneath the average are very concentrated and the data higher than the average is more scattered. Also it concerns only maximum velocities indicating a Gumbel distribution.

Both Brolsma and Saurin suggested a Gumbel distribution, since the maximum velocity is normative. Using the data plotted in Figure 37 the distribution is calculated depending on the vessel weight:

$$v = v_{average} * Gumbel(\mu, \sigma^2) = (1.9247 * DWT^{-0.3003}) * Gumbel(1;0.44)[m/s]$$

A comparison of the different distributions are made, to get some insight in behavior of the distribution in relation to the actual data (see appendix U).

8.1.3 Distribution of vessel mass

To build a distribution for the mass, the collected data of the "Vingerpier, fith petrol port in the Europort" is used[2.]. The data of the "Vingerpier" consists of 257 measurements of vessels with a mass between 20.000 [DWT] and about 335.000 [DWT] and are the measurements of a period between 1985 and 1989 by ir. L. Groenewegen (1990). A very clear distinction is seen between a population with a weight less and higher than 168.000 [DWT] for both the dataset of the "7th Petrolport" and the dataset of the "Vingerpier" (see Figure 38). The design vessel of the Lyondell jetty has a value of 56.100 [DWT] and is put in the lower category.
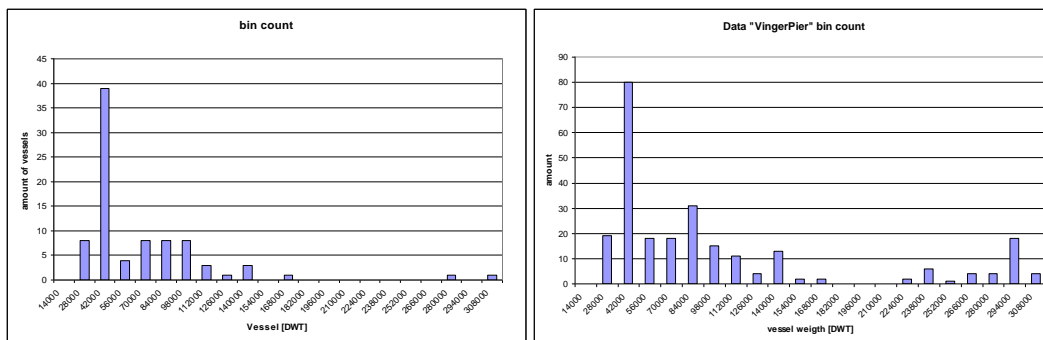
Figure 38: Bin count of the total monitored vessels at the '7th Petrol Port' and 'Vingerpier'

The design vessel has a weight of 56100 [DWT] and therefore the vessels larger than 60000 [DWT] are excluded. The data left are of 122 measurements.
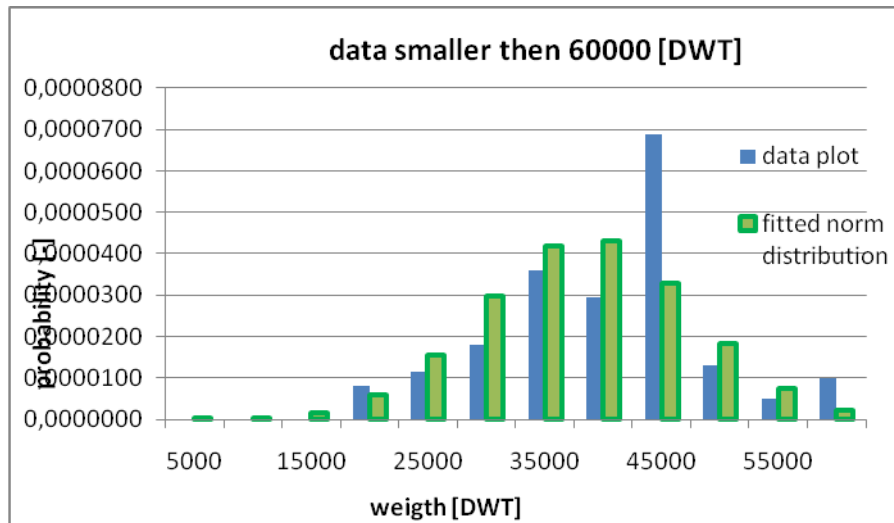
Figure 39: vessels smaller than 60000 [DWT] of the "Vingerpier"

From the data smaller than 60000 [DWT] a distribution is constructed with the outcome of:

$$DWT = N(38050;9025^2)$$

This is a distribution representative for 122 vessels.

8.1.4 Geometry of collision

Angle of berthing

The angle of berthing may assumed 5-10^0 with a confidence interval of 95 %[6.]. Using the rule of thumb that when using a normal distribution the variation can be assumed to be 2 (1.96) times the standard deviation. This will result in a distribution of:

$$\alpha = N(7.5;1.25^2)$$

According to the EAU 2004 berthing angle is generally less than 5^0 for a vessel with a deadweight of more than 50000 [DWT]. For smaller vessels which are not guided by tug boats, the EAU 2004 gives an angle of 10-15 ^{0}. So the angle of berthing is actually dependent on size and assistance.

When the stochastic of angles has a large variation it is possible that the angle becomes negative with a overshoot of more than 360 [^{0}]. This phenomenon is not taken in to account with a regular distribution.

Centre offset

The berthing tanker has to be positioned in the most favorable way in order for the loading arm to be operable. The coordinates of impact is concentrated. Assumed is:

$$berthingcoordinate = N(0;2,5^2)$$

The EAU 2004 gives an offset of the coordinates of 0.1*L<15 [m].

The coordinates are taken as independent of the function of the hull, the berthing beam and the length. This is not realistic. The aim of the helmsman is to berth as parallel as possible to the berthing line and when the vessel is berthing near the end of the berthing structure it may happen that the contact is not at the end of the vessel, but more in the middle. This will reduce the eccentricity and results in an increase of the energy. But for the sake of simplicity this is neglected.

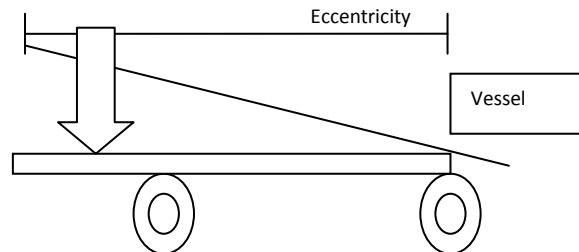**Figure 40: Overview of collision of berthing vessel at the end of the berthing structure**

Angel of velocity
The eccentricity factor of the method of Saurin is a function of the difference of the angle of the velocity vector and the berthing line. In this calculation the vector is assumed perpendicular to the berthing line and no velocity exists in line of the berthing line.

8.1.5 Vessel dimensions

The method of Saurin is also a function of parameters of dimensions. The dimensions of the vessels are strongly related to the vessel weight and the type of vessel. The data of the "Vingerpier" is used for construction of the distributions. The dimensions are assumed to be dependent of the weight [DWT] (see appendix U). This results in large inconsistencies in the relation:

$$C * L * B * D * \rho_{vessel} = DWT[tonnage]$$

In which

C   shape factor of the vessel

Van der Horst analyzed the sensitivity of using parameters only dependent of the weight or dependent of each other using the data of Clarkson (3000 measurements). Initially the dimensions are considered independent of each other and the results are compared with each other. If the dimensions are independent the results should be comparable. From this analysis was concluded that the length will not improve considerable by using more parameters and can be considered independent. However the accuracy of the width and draft will improve considerable. The recommended functions:

$$LOA = 9.2075 * DWT^{0.2861} * N(1;3.6094 * DWT^{-0.4020})$$

$$D = 1.2958 * (\frac{DWT}{LOA})^{0.4065} * N(1;0.2062 * (\frac{DWT}{LOA})^{-0.2235})$$

$$B = 3.1088 * (\frac{DWT}{LOA*D})^{0.7732} * N(1;0.7414 * (\frac{DWT}{LOA*D})^{-0.8610})$$

8.1.6 Soil

An estimation of the soil profile is constructed[3.] based on the geotechnical report of the Lyondell jetty. The uncertainties of soil properties are very large. The continuums of the properties vary continuously over distance and depth. There are continuous fluctuations around the average trend of variation.

The characteristics of geotechnical parameters are averaged by a trend of variation over depth and distance [4.]. The quality of the interpretation of the soundings depends on the skills and experience of the reader. Soil units with continuous spatial variability may be polluted with dislocations such as faults, lenses or fills, depending on the geological and morphological history. This variety can have large consequences for the stability of the structures. Geotechnical analysis of random field modeling of "point to point" variations forms the basis for quantitative assessment of uncertainties of averaged soil parameters. Even though there is a change over distance the profile is assumed strongly dependent in the horizontal plane but is taken independent in the vertical plane. This means over length the same parameters are used but in the depth the parameters are taken with a clear boundary.

In the model the Matlock and Reese soil modeling is used. These differ somewhat to the actual API soil modeling. However the Matlock and Reese is accepted by the API as well[5.]. The M-pile software uses the Matlock and Reese model as well and therefore makes it possible to compare and check the outcomes.

Description of the local profile
The soil properties at sounding location: Underneath the sprayed sandy material a mudflat sand formation is located, consecutively a layer of peat mixed with sand underneath of 1,5 to 2 [m] thick, a silty clay layer of 0,5 [m], a sand layer of 1,5 to 2,5 [m], a clay layer of 2,5 [m] and a peat layer with clay of 1 [m]. The Pleistocene layer starts of at a depth of NAP-22 [m].

Distribution type
It is very common to assume the properties of soil to fit a normal (Gaussian) probability distribution [4.]. This is supported by experimental evidence indicating that the normal fits the wide variety of soil properties. However in order to avoid physical inconsistencies the log-normal distribution is advised for soil properties. For instance the normal distribution will lead to physical inconsistencies, like negative values of shear strength

Soil property	Standard deviation [% of expected mean value]
Unit weight [kN/m^3]	5-10%
Internal Friction tan (φ') (drained)	10-20%
Drained Cohesion [kN/m^2]	10-50%
Un-drained Shearing Strength [kN/m^2]	10-40%
Stiffness [MN/m^2]	20-100%

Table 7: Indicative standard deviations of soil properties

Sand

The p-y curves according to the NEN-EN ISO 19902 are based on the functions of the effective soil pressure, the cohesion and the angle of the internal friction. These functions can be described as a function of internal angle of friction and the weight of the soil. In the JCSS the boundaries are given in which the parameters should be (see appendix W). In the CUR166 the parameters are given as a mean. From the CUR 166 is a clear relation found between the weight and the angle of internal friction. Using Table 7 will give a distribution that represents a percentage of the mean:

The unit weight is found:

$$\gamma_{soil} = \gamma_{saturated} * LN(1;0.075^2)$$

The angle of internal friction:

$$\varphi_{soil} = \varphi_{saturated} * LN(1;0.2^2)$$

The drained cohesion:

$$c_{soil} = c_{saturated} * LN(1;0.5^2)$$

The mean and the standard deviation are extracted from two representative values of angle of internal friction and drained cohesion given in the technical report. The soil stiffness is a function of the capacity and so on a function of the soil weight and the angle of internal friction.

After an further study about the spread of the resistance of the soil is decided to use a normal distribution instead of a log normal distribution (see appendix Z). All the draws were limited with a 2% lower bound and 98% upper bound. For every number drawn higher or lower a new draw is done.

Lateral capacity
The function describing the soil capacity makes use of dimensionless coefficients C1, C2 and C3.

These are a function of the angle of internal friction. Plotting these in excel and extracting a function (see appendix I):

$$C_1 = 0.1258 * e^{0.0903 * \varphi_{soil}}$$

$$C_2 = 0.5764 * e^{0.0508 * \varphi_{soil}}$$

$$C_3 = 0.6986 * e^{0.1241 * \varphi_{soil}}$$

For this the lateral capacity can be written as:

$$p_{rs} = (C_1 X + C_2 D)\gamma' X = (0.1258 * e^{0.0903 * \varphi_{sat} LN(1;0.2^2)} * X + 0.5764 * e^{0.0508 \varphi_{sat} LN(1;0.2^2)} D)\gamma_{sat} LN(1;0.075^2) * X$$

$$p_{rd} = 0.6986 * e^{0.1241 * \varphi_{soil}} * D * \gamma_{sat} LN(1;0.1) * X$$

The rate of increase with depth of the initial modulus of sub-grade reaction is advised to be based on the given values of:

φ	k [MN/m³]
25^0	5.4
30^0	11
35^0	22
40^0	45

Table 8: Rate of increase with depth of initial modulus of sub grade reaction

Using Figure 38 and describing these values as a function:

$$k = 0.1589 * e^{0.1411 \varphi_{soil}}$$

The lateral soil resistance-displacement p-y curves for sand are described as:

$$p = A * p_r * \tanh(\frac{k * X}{A * p_r} y) = A * p_r(\varphi_{soil}, X, \gamma_{soil}) * \tanh(\frac{k(\varphi_{soil}) * X}{A * p_r(\varphi_{soil}, X, \gamma_{soil})})$$

Clay

According to the NEN-EN ISO 19902 capacity of clay is given:

$$p_r = p_0' D + Jc_u X$$

This is limited by:

$$p_r = 9 * c_u * D \text{ for } X > X_R$$

J is an empirical constant with values ranging from 0.25 for weak clay up to 0.5 for stiff clayStandard Values for Soil. These values are determined by field testing, common practice being to use 0.5. It's not known how these values are distributed therefore the value of ir. C. Van der Horst is assumed:

$$J = N(\mu_j; 0.1\mu_j)$$

For the half strain the M-pile user manual recommends the use of the values:

c_u [kN/m^2]	ε_{50} [-]
5-25	0.020
25-50	0.010
50-100	0.007
100-200	0.005
200-400	0.004

Table 9: Determination of ε_{50} as a function of the un-drained cohesion

These values can be described with the relation:

$$\varepsilon_{50} = 0.0459 * c_u^{-0.4268}$$

In the API the shape of the soil resistance-displacement is not given as a function but defined as points (see appendix Y). These values can be described as a part of a continuous curve. The M-Pile manual gives:

$$p/p_u = \{ \begin{matrix} 0.5(y/y_{50})^{1/3} & for"y" < 3y_{50} \\ 0.72 & for"y" \geq 3y_{50} \end{matrix} \; forX > X_R$$

$$p/p_u = \{ \begin{matrix} 0.5(y/y_{50})^{1/3} & for & y < 3y_{50} \\ (0.06(y/y_{50}+0.54)(X/X_R-1) & for \; 15y_{50} \geq y \geq 3y_{50} \; forX < X_R \\ 0.72(X/X_R) & for & y > 15y_{50} \end{matrix}$$

In which:

X_R is the depth below soil surface of reduced resistance zone [m].

$$X_R = \frac{6D}{\gamma'D/c_u + J}$$

M-pile uses the mark points of 0.1y$_{50}$, 0.3y$_{50}$, y$_{50}$ and 3y$_{50}$ in the curve. The mark points will result in the relation:

y	Lateral resistance displacement relation
$0.1 * y_{50}$	$p = 0.5 p_u (0.1)^{1/3}$
$0.3 * y_{50}$	$p = 0.5 p_u (0.3)^{1/3}$
y_{50}	$p = 0.5 p_u (1)^{1/3}$
$3 * y_{50}$	$p = 0.72 p_u$

Figure 41: lateral resistance displacement relation of cyclic loading

8.1.7 Steel piles

IN the Monte Carlo simulation only the property of yield stress and wall thickness are taken as a variables. In this consideration of structural steel is only dealt with:

f_y yield strength [MPa]
t   wall thickness [mm]

However the distributions of the following properties are collected but not used (see the appendix). In chapter "Model analyses" the reason for excluding these properties from the calculation is explained :
f_u ultimate tensile strength [MPa]
E   Modulus of elasticity [MPa]
v   Poisson's ratio
ε_u ultimate strain
c_{co} corrosion
D_{dr} driving depth

Only specific points or parts of the full stress-strain curve are considered, thus the proposed model can only be used where these specific information is applicable. As distribution a multi-variety log-normal distribution is suggested[4.] . The mean value and coefficient of variation for the above vector are given in the Table 10.

Property	Mean value, E[..]	COV,v	VAR
f_y	$f_{ysp}*a*exp(-u*v)-C$	0.07	$0.07*(f_{ysp}*a*exp(-u*v)-C)$

Table 10: Mean and COVv values

In which:

The suffix (sp) is used for the code specified or nominal value for the variable considered
a   spatial position factor (a=1.05 for webs of hot rolled sections and a=1 otherwise)
u   factor related to the fractile of the distribution used in describing the distance between the code specified or nominal value and the mean value; u is found to be in the range of -1.5 to -2.0 for steel produced in accordance with the relevant EN standard.
C   constant reducing the yield strength. A value of 20 [MPa] is recommended.
B   =1.5   for structural carbon steel

=1.4   for low alloy steel
=1.1   for quenched and tempered steel

v   Poisson ratio= 0.27-0.30

The distribution is taken recommended as a Log-Normal distribution:

$$f_y = LN(f_{ysp} * \alpha * \exp(-u*v) - C; 0.07 * (f_{ysp} * \alpha * \exp(-u*v) - C))$$

$$f_y = LN(f_{ysp} * 1.52 - 20; 0.07 * (f_{ysp} * 1.52 - 20))$$

After analyses of the data generated by this function the outcome of the log-normal distribution was considered too wide. For high values of the mean a log-normal distribution shows similarities of a normal distribution. Therefore a normal distribution is used instead of the log-normal (see appendix Z).

Wall thickness

The tubular sections are fabricated out of a steel plate. It is assumed that per tubular section the wall thickness is constant. But the wall thickness per tubular section can differ from what was ordered. For this a normal distribution is used:

$$t_{wallthickness} = t_{ordered} * N(1; 0.1^2)[m]$$

8.1.8 Summary of distributions

Parameter	Type of distribution	Mean	Standard deviation
Vessel weight [DWT]	Normal	38050	9025
Berthing velocity [m/s]	Gumbel	$1.9247*m^{-0.3003}$	$0.44*1.9247*m^{-0.3003}$
Angle of berthing [^{0}]	Normal	7.5	1.25
Berthing coordinate [m]	Normal	0	2.5
Length [m]	Normal	$9.1647*DWT^{0.2861}$	$3.6094*DWT^{-0.4020}$
Width [m]	Normal	$1.2958*(DWT/LOA)^{0.4065}$	$0.2062*(DWT/LOA)^{-0.2235}$
Draft [m]	Normal	$3.1088*(DWT/LOA*D)^{0.7732}$	$0.7414*(DWT/LOA*D)^{-0.8610}$
Soil weight [kN/m^3]	Normal	$\gamma_{saturated}$	$0.01*\gamma_{saturated}$
Angle of friction [^{0}]	Normal	$\varphi_{saturated}$	$0.2*\varphi_{saturated}$
drained cohesion [kN/m^2]	Normal	$c_{u,calculated}$	$0.25*c_{u,calculated}$

Steel yielding strength [N/mm^2]	Normal	f_{sp}*1.52-20	0.07*(f_{sp}*1.52-20)
Wall thickness [mm]	Normal	$t_{ordered}$	0.1*$t_{ordered}$

Table 11: Overview of distributions (these variable is actually used in the Monte Carlo simulation)

Reference:

[1.] BR. Paper Review of berthing condition definitions, 2010
[2.] Prob som van een afmeer paal, C. van der Horst, 2000
[3.] Geotechnisch rapport, Lyondell steiger, Ingenieurs bureau Rotterdam, 1997
[4.] Soil Properties, JCSS-CI, revised version, 2006
[5.] M-Pile manual, J.L. Bijnagte, H.J. Luger, GeoDelft, 2006
[6.] Guidelines for the Design of Fender Systems, PIANC 2002

9 Model analyses

9.1.1 Introduction

The main purpose of this thesis is running a Monte Carlo simulation on a berthing structure. Normally the analytical Detlivsen method is used, this is introduced and described in chapter 4. For the Monte Carlo simulation a possibility using deterministic design formula's (Saurin) in combination with a finite element software Scia-engineer is investigated. Scia-engineer uses finite-element software to consider three dimensional constructions. Scia-engineer has the ability to use different methods for data input and output making it possible to communicate with other software. In this way a suit can be build around Scia-engineer, making it possible to put Scia in a loop and manipulate the used parameters.

Initially two of these methods were investigated (see appendix CC for a brief description of the second method) and eventually one of the methods was used and is considered in this chapter. A lot of effort is put in linking the software, because there was no experience with this method. The first method was favorite. It involved communicating with the COM-interface using Matlab. Because it was not possible to run Matlab at the network of GW this method was eventually excluded as a possibility. The second method consisted of using Excel (visual basic). This was initially considered as the "houtje touwtje" method. Because Excel is limited in calculation speed and size of the data input. Manipulating large quantities of data is very difficult and using calculation formula's in excel has a "black box" character.
 A model was build with use of the Scia-engineer software; this model is schematized at some points. The model, theory and reality differ in some points, these differences are discussed further in this chapter.

9.2 Implementation of Scia-engineer

The finite element software used in this analyses has the ability to consider the behavior of constructions under static loads. With normal use of the program the software provides a visual interface for the user. The user is able to build visually, with help of push buttons, a model for calculation. In a little sub window it is possible the define the elements characteristics and behavior. In the appendix BB is explained how external software can communicate with the Scia-software and makes it possible to run a Monte Carlo simulation. This is because of the specialized character of the matter.

In the next chapter is explained how the analyses deals with the problem that the Scia-software is only able to calculate the structure behavior on loads of forces [kN] and not loads of energy [kNm].

## 9.2.1 From force [kN] to energy [kNm]

The Saurin method is an energy [kNm] equation and the input of Scia-engineer is force [kN]. This makes it impossible to use the outcomes from the Saurin method directly in Scia-engineer.

Therefore the standard equation for energy with elastic deformation is applied at the Scia-engineer dataset. The data contains both the applied force and the caused deformation:

$$E = 0.5F\delta \qquad\qquad\qquad E = 0.6F\delta$$
or with some more plastic deformation

Using Scia-engineer to produce a linear function out of a dataset of F with the corresponding deformation and location. Of every location 24 runs will be made with forces of F_1=200 [kN] till F_{24} [kN] with steps of 200 [kN]. And from these drawings a data base is build for comparison with the drawings of the vessels energy loads. In total a library is build out of 2928 calculations for the structure.

However the real absorbed energy is also a function of the structure deformation and has a more curved function (see Figure 42). The absorbed energy can be calculated per location. Assigning every drawn result from the Saurin method to the best corresponding value in the produced dataset a relation is made.
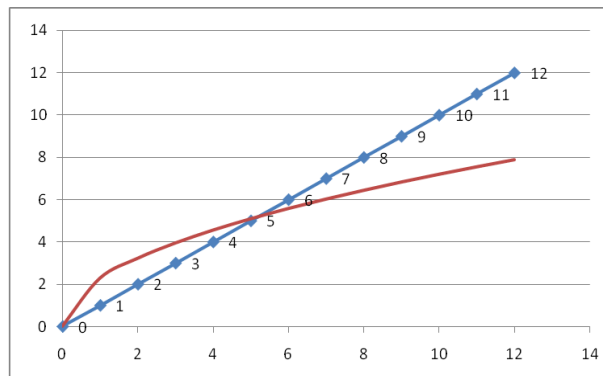
Figure 42: Relation between deformation, force and the surface under the line represents the amount of energy.

The real energy absorption is described by: $E = \int_{y_1}^{y_0} F(x)dx$

The model rounds the energy to a linear function and therefore is conservative in energy absorption. The fault of this selection procedure has a mean of 20 [kNm] and a standard deviation of 17 [kNm].

9.3 Structure

The simulation of the structure is the most important aim in the Monte Carlo simulation. This is the only part in this model that can fail. Because in this thesis it concerns a exploratory study and the capacity is limited, some of the structure characteristics are schematized. Also the measurements are limited. In this paragraph the consequences are discussed.

9.3.1 Fender rack

The actual berthing structure has an ongoing beam with a grid of vertical beams (berthing rack) for the first contact with the vessels. These vertical beams cause a torsion moment on the ongoing beam.
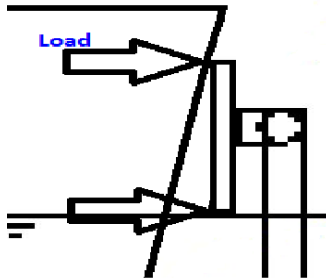

Figure 43: Berthing structure

As a result of the torsion moment the piles experience an additional head moment and they react more or less stiff. This depends on whether the vessel hits the top or the lower part of the berthing rack. This additional load is not considered in the model. Only loads applied direct in the centre of the mass of the horizontal beam are considered, leaving out the additional loads. The vessels skin is limited in strength capacity and is not considered in this analysis.

The horizontal forces parallel to the berthing structure are neglected. Later in this chapter some is explained about how Scia-engineer deals with spring modeling and will this topic be more worked out.

The fender rack is made out of wood and therefore has a friction coefficient of approximately of 0.5-0.6. The friction introduces an additional force in the plane of the structure self. The structure does not conform the shape of the hull resulting in very small interfaces. The local material will deform plastic. So the local stresses are very high but the additional forces on the structure remain limited. The structure reacts on force in the plane of the structure as a portal structure. Also the applied forces are smaller in comparison to the other plane and these are therefore neglected.
 Also is it possible for the vessel to touch the piles under water with large deformations. This failure possibility is left out of the scope as well.

9.3.2 Pile model

Because it is only possible to have one record point per element, the piles in the model are built out of short elements. The piles in the soil are schematized as a beam supported with springs. Because it is not known how the elements are calculated and what kind of numerical grid size is used, a test is done if there are differences in force distribution s with other modeling.

It appears that the way the springs and supports are attached to the piles have no influence on the distribution.
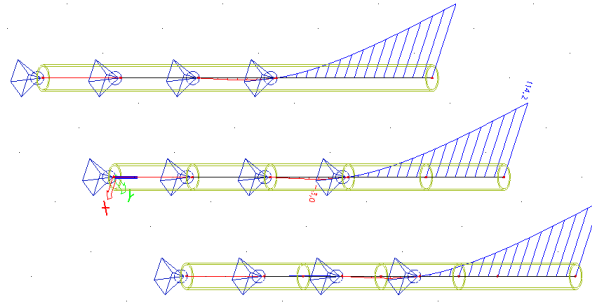
Figure 44: Continues beam supported, beam supported at transition of the elements, beam supported intern of the elements

In all the three methods the results are the same and can therefore be excluded as a possible factor of influence on the results.

9.3.3 Comparison of measurement grids

The amount of measurement points will influence the calculation time and the ratio of accurate measurement. And with use of excel 2003 there is some limited capacity of data storage.

Therefore a optimization analyses is done. There are three different measurement grids tested (2 (m), 1 (m) and 0,5 (m)). In this model three load cases are applied on the structure (see appendix FF).

Considering the maximum amount of force:

- 10066,44 [kNm] is given as the actual max moment by Scia-engineer.
- 10040,35 [kNm] with a grid of 0,5 [m] gives 0.2 [$^0/_0$]
- 10014,27 [kNm] with a grid of 1 [m] gives 0.5 [$^0/_0$]
- 9332,15 [kNm] with a grid of 2 [m] gives 7 [$^0/_0$]

The 0,5 [m] and the 1 [m] grid have a difference of 1 $^0/_0$ and between 1 [m] and 2 [m] is 7 [$^0/_0$]. The deformation is calculated due to a point load of 1000 (kN). Considering the maximum amount of deformation:

- 465.4 [mm] given by Scia-engineer as the absolute max deformation
- 461.8 [mm] with a grid of 0,5 [m] gives 0.7 [$^0/_0$]
- 456.6 [mm] with a grid of 1 [m] gives 1.8 [$^0/_0$]
- 435.7 [mm] with a grid of 2 [m] gives 6.4 [$^0/_0$]

The 0,5 [m] and the 1[m] grid have a difference of 1 $^0/_0$ and between 1[m] and 2 [m] is 5 $^0/_0$. To make sure the analyses will be sufficient accurate and the calculation time will be effective. From this analyses can be concluded that the grid of 1 [m] would be sufficient accurate.

9.3.4 Exploration of the berthing beam grid

Because the excel software processes very slowly large amounts of data, the amount of measurement points has to be limited. Therefore a measurement and loading tactic is developed for the berthing beam.

Within the limit state only the maximum moment and the deformation is important. In limiting

the amount of measure points, the behavior of this point is investigated. Using a couple of load cases [11 load cases] on different places on the berthing beam, the moment is considered. The load cases are engaged every 2,5 [m]. Because the current structure is symmetrical the behavior will be expected to be symmetrical. For these analyses only the half of the structure is considered.
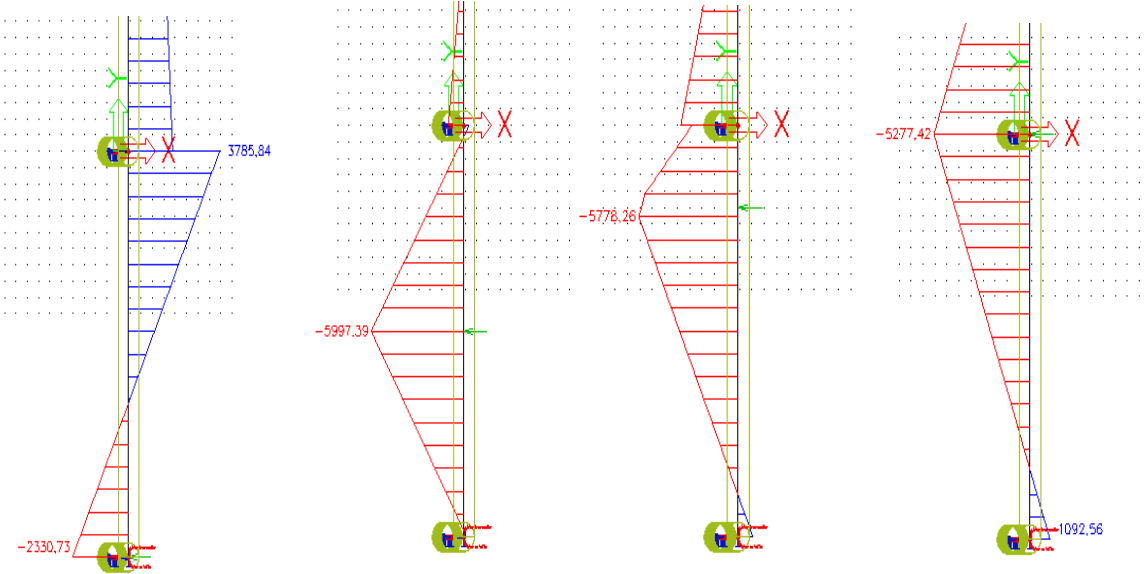
Figure 45: Moment due to 4 different load cases, in top-view.

From these cases the maximum moment is found at the coordinates of the applied forces and at location of the second pile. It can be concluded that when monitoring moment at the applied forces and at the second pile the maximum moment will be found.

9.4 Soil model

The soil is modeled by use of non linear springs. Initially the p-y curves provided by the API were considered. But for the simulation use is made by the Reese et al. curves. This is type of soil modeling is also used by M-pile software[2.] (see appendix GG and HH).

9.4.1 Reese et al.

The M-pile software makes use of the p-y curves of Reese et al.[2.] as well as the model used in this thesis does. Using the same curves makes it possible to have some controlling possibility. And the curves of Reese et al. are more easily to use analytically. Some remark has to be made about the difference between the two. In the thesis of ir. Ruigrok, there are two case studies to explain and show the differences. The results are presented and from these it can be concluded that the curves of the API are more optimistic than the curves by Reese in case of sand. In cohesive soils, the results are almost equal. The major difference is that the API is more stiff than the method of Reese et al.
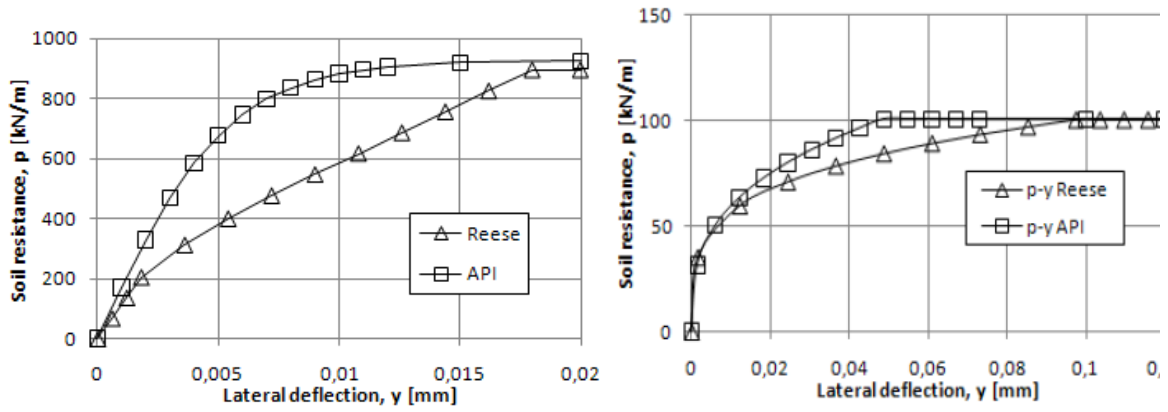
Figure 46: Comparison of soil modeling (left: non-cohesive soil at 3.36 [m] depth and right: cohesive soil at 0.86 [m])[4.].

Use of p-y curves in Dutch soils

The API curves are exclusive for sand and clay type of soils. The sand soils are very well described with an angle of internal friction and the clay soil could well be modeled with un-drained shear strength. But in practice some more type of soils are found which are not that well modeled by these methods. There is no p-y curve for peat soils developed. In un-drained loading conditions, it is possible that peat contributes a lot of resistance.

9.4.2 Cyclic soil behavior

The soil has elastic, with small soil deformation, and plastic, with large soil deformation, behavior. The P-Y curves have both tracks included but will not have any memory of previous events. Therefore the actual plastic deformation, that is irreversible, is not taken into account.
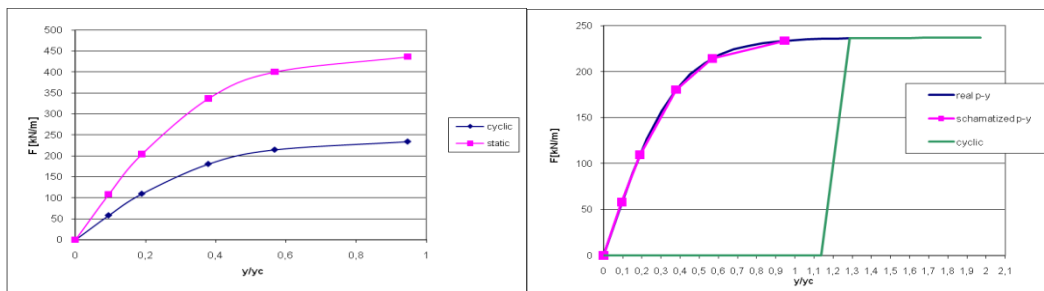
Figure 47: Left cyclic behavior according NEN-EN ISO 19902

and right schematized cyclic behavior according Prof. Verruijt[3.] after loading

The amount of absorbed energy will be calculated by the integral of the track of the P-y curve. Under the elastic deformation, the absorbed energy will directly be put back in the system after unloading. The energy will permanently be absorbed with crossing the plastic deformation (see the graph). The p-y curves add the passive and active soil pressure together [4.] from the Rankine theory.

The relation between the elastic Young's modulus and the cyclic Young's modulus according Plaxis-Hardening Soil model):

$$E_{ur} = 3 * E_{50}$$

In which;

E_{ur} Unloading/reload stiffness at engineering strains [kN/m^2]

E_{50} Elastic modulus with initial loading [kN/m^2]

Van der Horst investigated this phenomenon assuming the elastic behavior up to 0.3*y_c. Apply the Plaxis-Hardening Soil model to the p-y curve gives an additional track (see Figure 47). The second time the soil is loaded it will react a 3 times stiffer. So overall will the structure react stiffer resulting in larger forces.

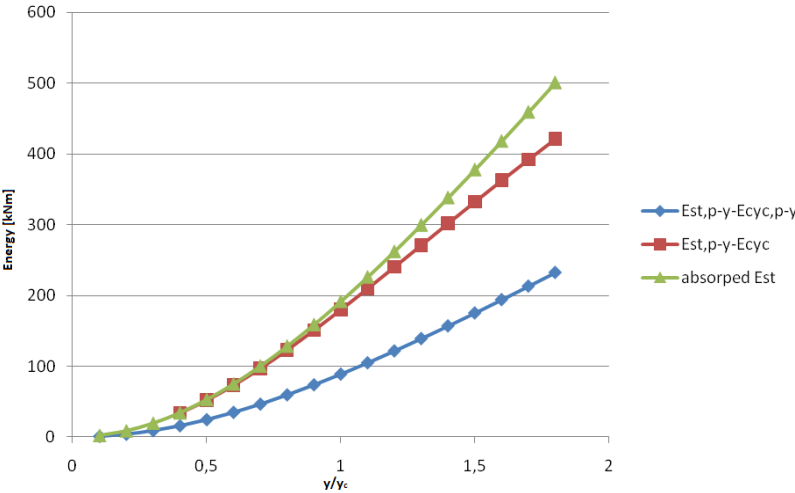**Figure 48: Energy that is absorbed over the relative deformation**

In the figure above the energy that is not put back in the system comparing the static p-y curve with the Hardening Soil model and the p-y cyclic curve. The NEN-EN ISO 19902 advises to use the reduction factor in case of cyclic behavior. But with a specific depth this factor is advised for every depth.

$$A = 3 - 0.8 \frac{X}{D} > 0.9 \qquad \frac{X}{D} < \frac{3 - 0.9}{0.8} = 2.625$$

From this depth on the cyclic resistance is larger than the static.
A note is made that over time a gap will develop next to the pile. But according to the cyclic behavior in Figure 47 the deformation always comes back to zero. The soil is modeled as it was cyclic loaded soil but any permanent deformations are not taken into account. Since the p-y curves are based on measurements on the top of the pile. The p-y curve describes the soil influence on the top of the pile instead of the soil behavior. Therefore it is more likely that cyclic behavior of the soil in p-y curves describes liquefaction of the soil. The soil will flow around the pile instead of the hardening theory. Because there is assumed equilibrium the pile will return to its original position.

9.4.3 Soil modeling due to spring behaviour

The soil is modeled as a supported beam on lose springs. In order to describe the deflection and the forces in the beam due to the horizontal loading on the head and the springs have a p-y behavior. The beam can be described by a differential equation (Euler-Bernoulli beam). This equation describes the deflection and the tensions over the whole length.

$$\rho A \frac{\partial^2 w(x,t)}{\partial t^2} + EI \frac{\partial^4 w(x,t)}{\partial x^4} + \frac{\partial}{\partial z}(H(z)\frac{\partial w(x,t)}{\partial z}) = o$$

$$\rho A \frac{\partial^2 w(x,t)}{\partial t^2} + EI \frac{\partial^4 w(x,t)}{\partial x^4} + \frac{\partial}{\partial z}(H(z)\frac{\partial w(x,t)}{\partial z}) + k_d w(x,t) = o$$

In which

$$\rho A \frac{\partial^2 w(x,t)}{\partial t^2}$$ is the force of inertia

$$EI \frac{\partial^4 w(x,t)}{\partial x^4}$$ is the force due to the bending stiffness

$$k_d w(x,t)$$ is the force imposed by the foundation (p-y curves)

$$H(z) = \rho A z$$

is the axial compressive force in the pile associated with the dead weight of the pile and has to be smaller than the buckling force.
With a relative small dead weight the expression H(z) is left out of the equation.

In Scia-engineering non-linear spring function is considered in behaviour against the reality. The pile will be loaded laterally which will give a load in the soil in the horizontal plane. The pile is surrounded by soil all around and should not differ in characteristics in the horizontal plane. The soil will have the same reaction to applied forces in every direction (see left of Figure 119). This will give the same deflection of the top from the centre in any direction.
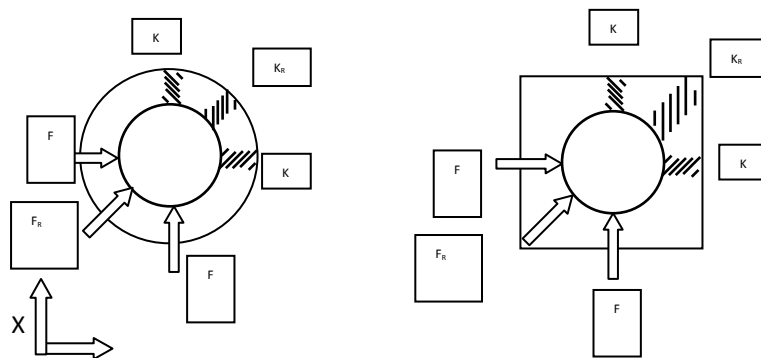
Figure 49: Schematization of the soil in Scia-engineering

The soil will be modeled as springs in two directions. This gives a difference in deflection when a force is applied out of the X or Y plane. Test are done with a model in both programs. A run is made with F=1000 [kN] and one run is done with a applied force F_R wchich will be applied in the x and y plane:

$$F_R = \frac{1000}{\sqrt{2}} = 707.1 kN$$
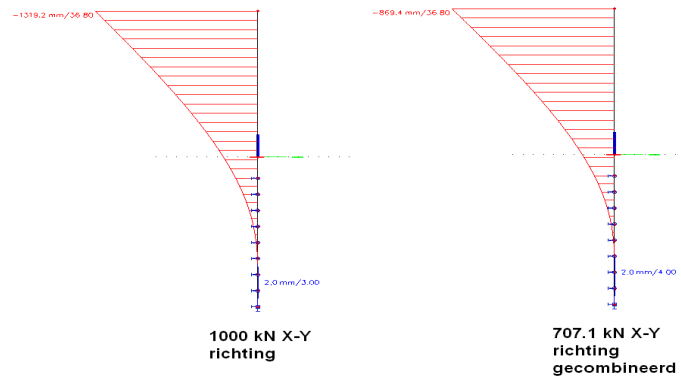
Figure 50: Deflection of model in Scia-engineering

When applying F_R the deflection of the model differs from the deflection of applied force F, the deflection is smaller, which will be the product of a stronger spring. This is in expectation with the right figure in Figure 49. The ratio between the two is 1319/869=1.5.

This approach of soil modeling is wrong, but since the mainly perpendicular character of the load this is acceptable.

Structure model

The measurement points are linked to each element and to the load. The elements are numbered in ranges of 50 for every separate column. Figure 51 shows each section indicated by corresponding elements and wall thickness according to the results of the deterministic design . The actual geometry of the elements and the measure points are discussed in chapter 6 "Model considerations". Conform the soundings mentioned before the elements beneath the NAP-17,6 [m] (elements higher then Sxx53 and Sxx03) are surrounded by land.
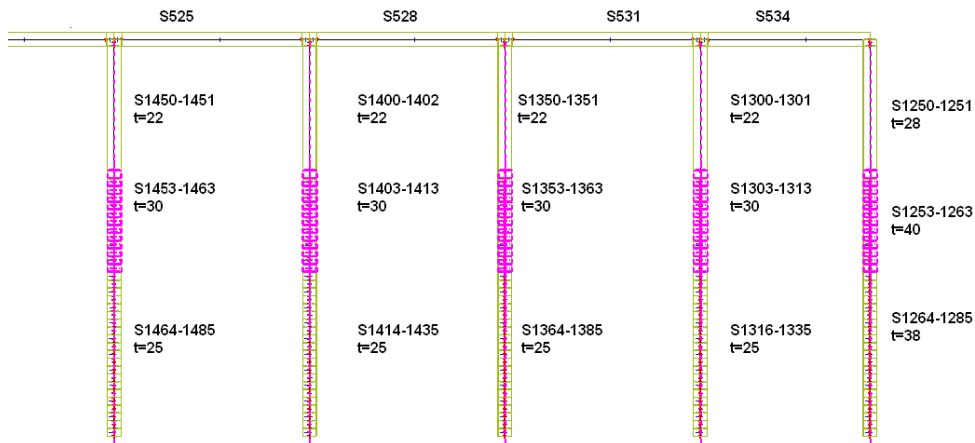
Figure 51: Geometry with element numbers

The deterministic design is taken as reference and from this design the first dimensions are taken (see reference design).

Reference:

[1.] Het berekenen van horizontal belaste paalgroepen, ir.J.L.Bijnagt, ir H.J. van der Graag, ir H.J. Luger, Geotechnical Institute, 1961

[2.] M-Pile manual, J.L. Bijnagte, H.J. Luger, GeoDelft, 2006

[3.] Grondmechanica, A.Verruijt, S. van Baars, 2005

[4.] Laterally Loaded Piles, Ruigrok, 2011

[5.] Material Models Manual Version 9.0, Plaxis 2D, Plaxis 2009

[6.] CUR 166 deel 2, 2005

10 Results and discussion

10.1 Introduction

The reliability function (Z) is used in the Monte Carlo simulation:

$Z=R(X_1, X_2, ...X_m) -S(X_1, X_2....X_n)$

The resistance (R) is a function of four variables (angle of internal friction, weight of volume of the soil, yield stress and the wall thickness of the tubes). The values of the variables of the resistance are the results of 122 drawings per variable.

The same method is used for the loading of the vessel (S). However this accounts for 7 variables (weight, length, depth, width, velocity, angle of berthing and the coordinates of centre offset). The values of all these variables are the result of 8000 drawings per variable.

By combining the random draws of variables from R with random draws of variables from S a distribution is build for Z since there were no draws Z<0. Using the distribution of Z the limit state is analyzed (Z=0). All results are based on the berthing of the design sea vessel on the second berthing point.

In the chapter "The concept of probability" the safety was considered. In this chapter the safety level of the "Manual of Quay Wall" was adopted. In this manual the lifetime of the structure is taken as lasting of 50 years. The probability of failure is derived from the safety class 2 of the "Manual of Quay Walls" (NEN 6700):

β=3.4 for Ultimate Limit State:

> $P_f=3.369*10^{-4}$ over 50 years
>
> $P_f=6.74*10^{-6}$ over a year
>
> $P_f=1.29*10^{-7}$ over a week

β=1.8 for Service Limit State:

> $P_f=3.54*10^{-2}$ over 50 years
>
> $P_f=7.09*10^{-4}$ over a year
>
> $P_f=1.364*10^{-5}$ over a week

The intensity of use has a large influence on the probability of failure in a lifetime and this is not known for this specific structure and is therefore taken as a variable to consider. The frequency of once and twice every week is assumed.

In this chapter the capacity and the safety level of the berthing structure of the Lyondell jetty are considered with the help of a three dimensional finite element software.

10.2 Loads (S)

In the original design the representative energy load is calculated with the equation of Saurin. From the representative value to the design value a safety factor of 1.5 is used. In this paragraph the results of the drawn variables are discussed. The variables of the loads are founded on collected data (see chapter " Probabilistic distributions"). Values directly taken from these data are representative for one berthing procedure. By running a Monte Carlo simulation of 8000 drawings a set of data is created (see Figure 52). The representative value that was found by use of the equation of Saurin has a value of E_{rep}=690-700 [kNm]. The values of the equation of Saurin (Brolsma curves) are based on two berthing procedures a week during a time of 30 years (instead of the assumed once a week over 50 years). There are 55 drawings done higher than the representative load. There are 3 drawings higher than the design value (E_d=1.5*700=1050 [kNm]).

The load is calculated according to the equation of Saurin and depends on 7 variables. The results of these variables are shown in Table 12. In this table all the characteristic values are shown including the extreme draws.

	Vessel mass [DWT]	Berthing velocity [m/s]	Vessel length [m]	Vessel width [m]	Vessel draft [m]	Angle of Berthing [°]	Centre offset [m]	Berthing coordinates [m]	E_d [kNm]
Max	82402	0.3	253	43	15.7	10.6	9.4	65.1	1373
Min	20426	0.01	134	18	8	34	-8.7	31.3	2
Mean	38023	0.1	187	29	11.2	7.5	0	46.7	136.26
stdv	8909	0.0352	15.4	3.2	1	1.2	2.5	4.6	126.83

Table 12: Results of 8000 drawings of the dimensions with the resulting energy

All the resulting drawings of the energy loading are included in a distribution and shown in Figure 52 . The maximum drawn energy has a distance of ten times of the standard deviation.
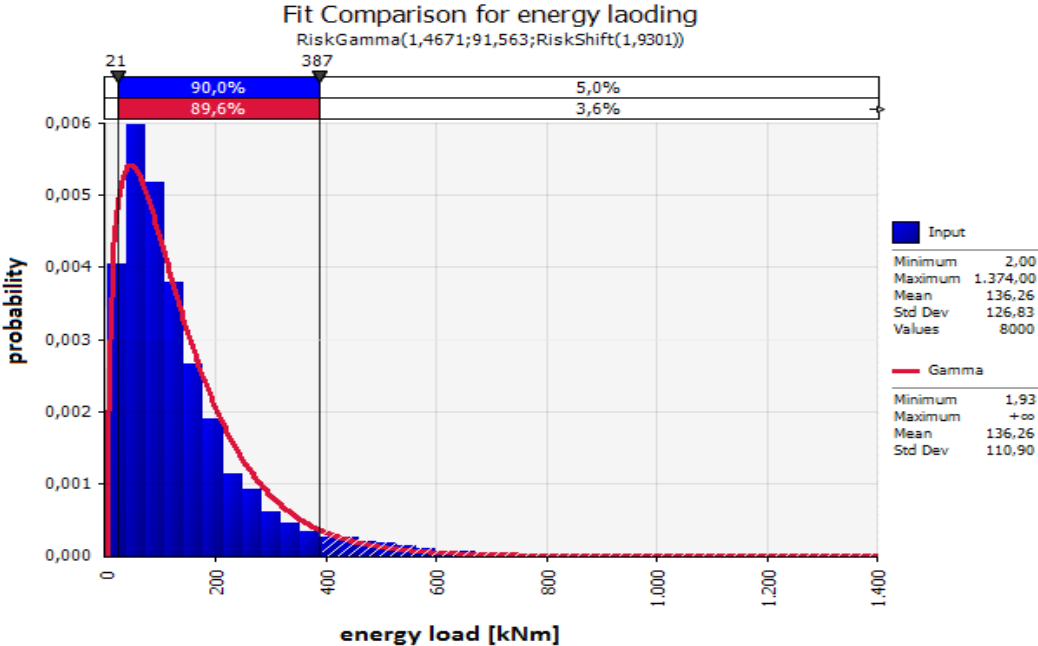
Figure 52: Distributions of the loading energy according to the equation of Saurin.

The resulting data represent a distribution for 100 times of berthing procedures (see Figure 52). There's nothing known about the intensity rate of berthing vessels of the Lyondell jetty. So therefore a rate of lower limit (once a week) and upper limit (twice a week) is assumed. Respectively 2600 berthings and 5200 berthings during a live time (Brolsma took 3000 times) or 52 or 104 times in a year.

In further calculations all the values are based on a frequency of berthing of two or one procedure a week with a failure chance of 5% over a 50 year period. Calculated with the equation:

$$P'_f = 1-(1-P_f)^m => P_f = 1-\sqrt[m]{1-P_f}$$

P_f=2.05*10^{-3} (once a week) with an representative energy load of 670 [kNm]

P_f=1.02*10^{-3} (twice a week) with an representative energy load of 735 [kNm]

The representative load calculated with help of Saurin (690 [kNm]) is in between both the values of representative energy load (P_f=1.6*10^{-3}) .

During the berthing procedure the vessel will be put in such a position that the connection of the vessel and the loading arms are after berth as close as possible. This maneuver is made before the vessel is berthed. The coordinate of the collision is taken as a function of the length and the offset of the vessel. The values for length and centre offset are also shown in Table 12. In Figure 53 the range of coordinates of impact are shown.

Figure 53: Location of impact marked at the berthing structure.

Discussion

The maximum realized energy has a distance of ten times of the standard deviation. With the used data it is not possible to distinguish the regular and the exceptional behavior due to, for instance, human failure. Therefore is this extreme value excepted.

The representative energy loading according to the equation of Saurin is based on values for berthing twice a week during a period of 30 years. In this thesis a reference period of 50 years are taken as period of lifetime with an intensity of berthing of once and twice a week.

The representative values of energy loading of the advanced level 2 simulation is compared with the equation of Saurin according to the PIANC and are found in the same range.

The point of impact with the vessel in to the berthing beam is limited with a minimum range of 31 [m] to the bow and stern (2*31=62 [m]) of the vessel. The part in-between is not used for direct reflecting of the vessel energy load according the collected data, but is dimensioned as such.

It is possible to design the less loaded part slimmer then the "hot-spots" or even completely leave it out of the design.

10.3 Relation of the results of the reliability function (Z)

The maximum resulting moment in the piles and the maximum moment in the berthing beam are strongly correlated (ρ=0.97) and show a strong relation with the energy loading (see Figure

54).
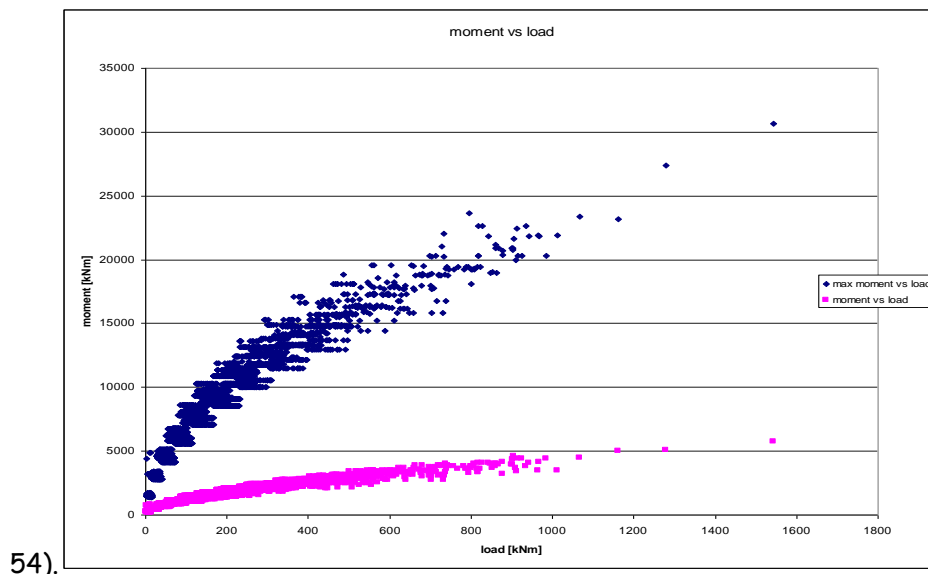
Figure 54: Resulting moment in the beam and the maximum resulting moment in het piles in relation to the energy laods

The boundary of 0.7 [m], from the terms of reference is crossed once (see Figure 55). The resulting deformation shows a almost linear relation with the resulting moment.
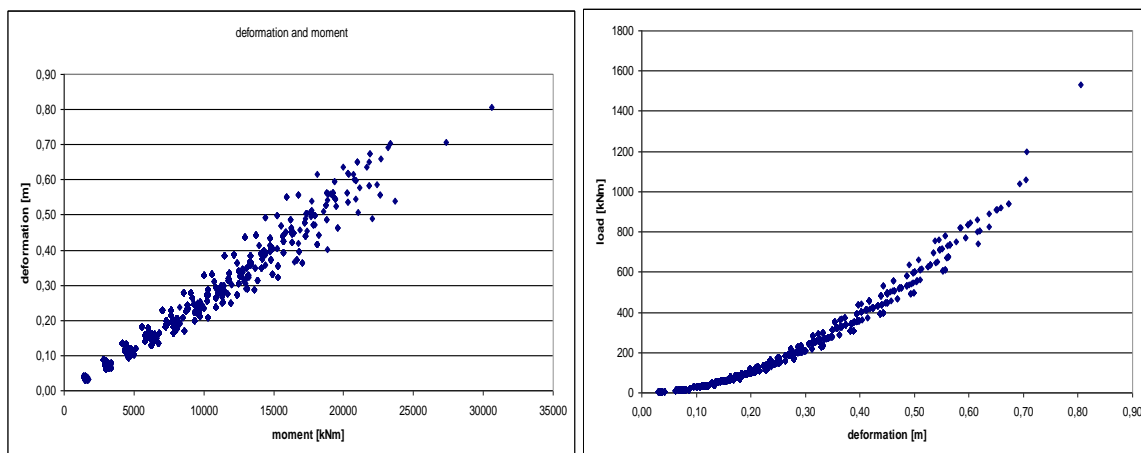
Figure 55: Left: resulting moment in the "berthing beam" in relation to the maximum deformation. Right: resulting deformation in relation to the energy loading

The resulting deformation due to the loading does not have a linear relation with the applied energy loading (see Figure 55).

Discussion

Because the pile is held with non linear springs the depth where the pile experiences moment of fixation will differ with the amount of loading (this relation is found in the Figure 55). There are no major deviations. The relations are conform the physical static relations introduced earlier in

this thesis. So it can be assumed that the model will simulate according the characteristic physical relations.

10.4 Results of the reliability equation (Z)

10.4.1 Failure of the reference model

As first the failure chance of the reference design is checked. The model is tested on two types of failure mechanisms. The first is the strength of the structure and is determined by exceeding the yield stress. The second is the maximum deformation of the structure and is set on 0.7 [m]. This boundary is defined in the terms of reference.

10.4.2 Strength

The strength of the structure depends on the earlier considered variables. The structure is considered in relation to the failure of the total structure and the failure of only the piles. In this consideration the chances are calculated with the help of the reliability equation.
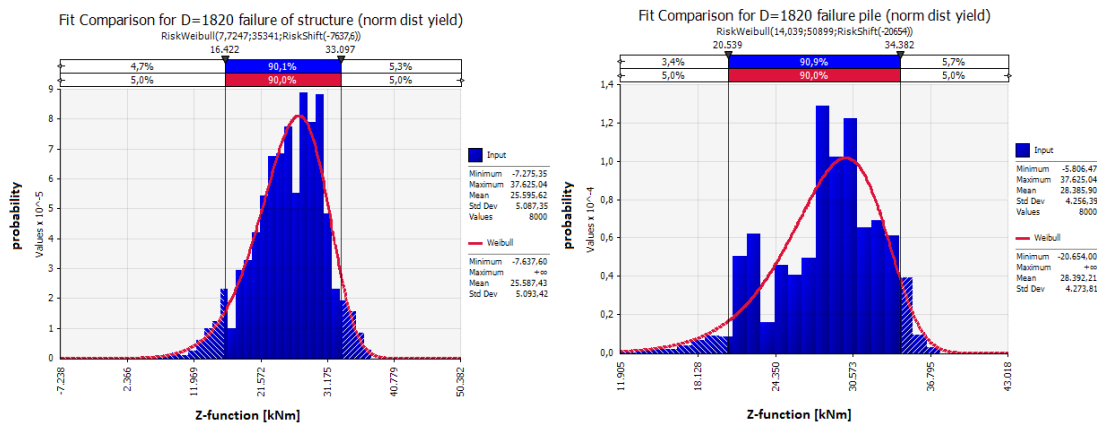
Figure 56: Results of the limit state equation of the collision with the bow of the vessel. Left the reliability function of the structure. Right the reliability function of the piles.

The chance of failure of the total structure by collision with the bow based on the reliability function is calculated on $P_f = 7.25 \times 10^{-6}$ per year. This is $P'_f = 3.63 \times 10^{-4}$ over a period of 50 years. The chance of failure of the piles, when failure of the berthing beam is neglected, is also calculated on $P_f = 3.17 \times 10^{-6}$ per year. This is $P'_f = 1.58 \times 10^{-4}$ over a period of 50 years (berthing frequency of once a wee

Failure	Distr type	Mean	Stdev	β^*	P_f (per year)	P'_f (50 years)	$\beta = -\Phi^{-1}(P'_f)$
Structure	Weib	25595	5087	5.03	7.25×10^{-6}	3.63×10^{-4}	3.4
Pile	Weib	28386	4256	6.67	3.17×10^{-6}	1.58×10^{-4}	3.6

Table 13: Results of the reliability function. Failure of the structure due to the collision with the bow of the vessel (β* is calculated direct from the assumed distribution type).

According to the "havenbedrijf van Rotterdam" a helmsman tries to berth as parallel as possible to the berthing line. Then there 's an equal chance on hitting the berthing structure first with the bow or with the stern of the vessel (see Table 14). From analyses of the data of the 5th Petrol port appears that the second contact can be normative over the first contact.

Failure	Distr type	Mean	Stdev	β^*	P_f (per year)	P_f (50 years)	$\beta = -\Phi^{-1}(P'_f)$
Structure	Weib	25245	3954	6.38	$4.23*10^{-5}$	$2.1*10^{-3}$	2.9
Pile	Weib	27765	3749	7.40	$5.12*10^{-7}$	$2.56*10^{-5}$	4.6

Table 14: Results of the reliability function. Failure of the collision with the stern of the vessel (β^* is calculated direct from the assumed distribution type).

The maximum capacity of the structure can be distributed out of the data of the library. This is combined with the drawn energy load for the collision with the bow of the vessel and displayed in Figure 57. However not from all the draws of the structure the capacity is known, some of them had more capacity than the chosen range of loadings. In that case the highest limit for the capacity of E_u= 3200 [kNm] is chosen for capacity.
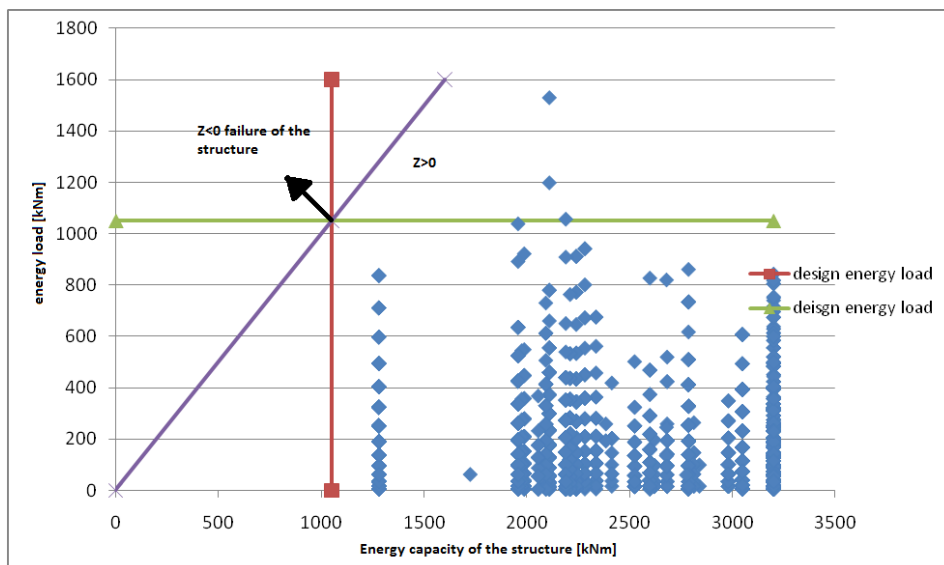
Figure 57: Drawn energy loads (vert.) in relation to the corresponding energy capacity of the structure (hor.) the capacity has a high boundary of 3200 [kNm].

The small amount of draws for the structure is obvious recognizable. There are 0 times a capacity lower than the design value. The rule for the amount of realization for a Monte Carlo simulation is based on the realizations over all. Not for a separate realization for the load or the resistance.

Discussion

In Figure 56 an obvious gap in the data can be recognized. A possible explanation can be that because the depth of maximum moment depends on the amount of load at the top (it fluctuates

over depth). The strength of the piles is fixed over depth per section. It is possible that when the belly of the maximum moment is at the depth of the transition of the strength sections corresponds with the loads were the gap in the data is. This means that there is too little safety taken in to account and a better transition between the different sections should be introduced. For instance an extra sections of pile. This phenomenon is not considered in the design procedure of the berthing structure.

The chance of failure due to collision of the stern is higher than the chance of failure due the bow. From the chance of exceeding of the deformation it is known that the part of the structure at the stern is more stiff then the part of the structure at the bow (see next paragraph). Therefore the forces are higher and the chance of failure will be increased.

As in Figure 57 is shown the limited amount of drawings for the structure. This results in an incidental distribution of capacity. Even though there is no real rule for the ratio of amounts of realizations between strength and load. Also the values of strength will not change over time as it will with the collisions. It is advised to do a sensitivity analyses. To change the amounts of realizations of strength, an optimum of realizations can be found. The amount of realizations will probably influence the answers. It is expected when the analyses is done with more realization, a better fit for the distribution can be found and also the failure can be distributed direct from the amount of failed drawings as well.

10.4.3 Deformation

In this design the maximum deformation prescribed by the terms of reference are not fixed. In the terms of reference is spoken about "approximately 0.7 [m]".

The data of the Monte Carlo simulation is analyzed and it occurs that the maximum deformation is set on 0.70 [m] and has a chance of exceeding of $P_f=3.13*10^{-4}$ per year of berthing. In a period of 50 years this results in a chance of failure of $P'_f=1.56*10^{-2}$.

And with a collision of the stern of the vessel the chance of failure is $P_f=2.8*10^{-4}$ per berthing year and $P'_f=1.4*10^{-2}$ per 50 years.

Because in the program of requirements the boundary is set on approximately d=0.7 [m]. The chance of exceeding the deformation of 0.8 [m] is also considered. The chance of failure is $P_f=5.85*10^{-5}$ per year. This has a failure chance of $P'_f=2.9*10^{-3}$ over 50 years period (berthing frequency of twice a week).

In the EAU 2004 a boundary of 1.5 [m] is advised and for this deformation a failure chance of $P_f=2.17*10^{-10}$ is found. With a failure chance of $P'_f=1.09*10^{-8}$ over a period of 50 years (berthing of twice a week).

Discussion
The boundary of 0.7 [m] of deformation is exceeded. But a deformation of 0.8 [m] has almost the same range of chance of failure as is adopted. The boundary of 0.7 [m] is probably introduced to make sure that the deformation near the bottom will not become too large. This was not analyzed any further. Therefore term "approximately" was probably introduced, so a

deformation of 0.8 [m] is excepted as well. The EAU 2004 gives as reason for the boundary that they prefer, that the helmsman can't berth only on sight and looses the feeling of the collision with deformation large than 1.5 [m]. And this deformation has a chance of failure which is very small.

10.4.4 Lower boundary

Because the distribution of the yield stress is considered very large, the same analyses is done using the representative values of yield stress. A distinction is made between failure of the total structure and failure of the piles.
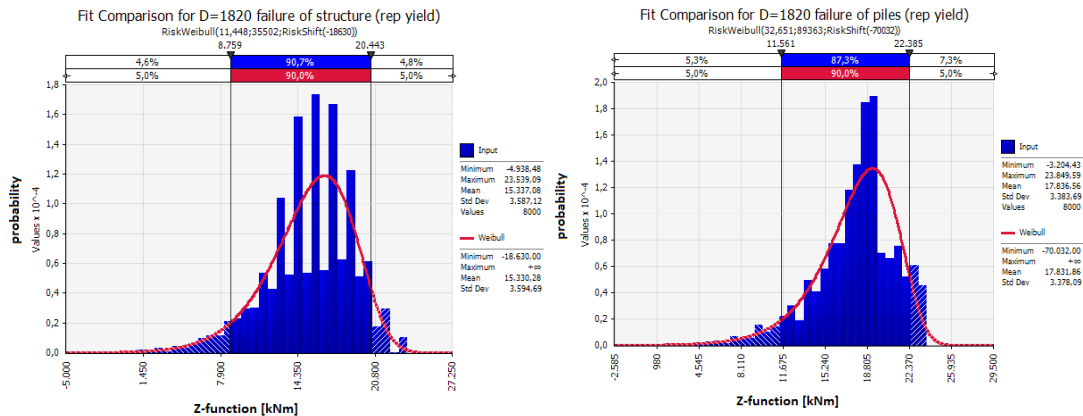

Figure 58: Results of the reliability equation. Left: the failure of the structure. Right : failure of the piles.

The chance of failure of the total structure is $P_f=6.22*10^{-4}$ per year. This is a $P'_f=3.11*10^{-2}$ over a period of 50 years. The chance of failure of the piles is $P_f=3.17*10^{-6}$ per berthing procedure. This is $P'_f=1.58*10^{-4}$ over a period of 50 years.

Discussion

When the distribution for yield stress is replaced with the value of the representative yield stress, the chance of failure is higher due to the replacement of the normal distribution instead of the log-normal distribution of the yield stress. The found value of chance of failure is an upper limit.

10.5 Required depth of the piles

In the reference design are the piles designed with a single point load. This load will be applied over the whole length of the berthing beam. In the previous paragraph is determined that a vessel will hit the berthing beam on very specific places (see Figure 53).

In this paragraph the depth of the different piles is calculated based on the data from the Monte Carlo simulation. To guarantee the soil stability in the model of the Monte Carlo simulation, the length is extremely exaggerated. Based on the theory of Blum a relation is assumed between the depth where the moment of a continuous pile is 0 [kNm] (t_0) and the final length of the pile, where still a stability of the pile in the soil is assumed to exist. In this

analyses only the 5 piles that were loaded the most are examined (see Figure 59).

In the figures the measurements points are clearly recognizable every meter of depth.
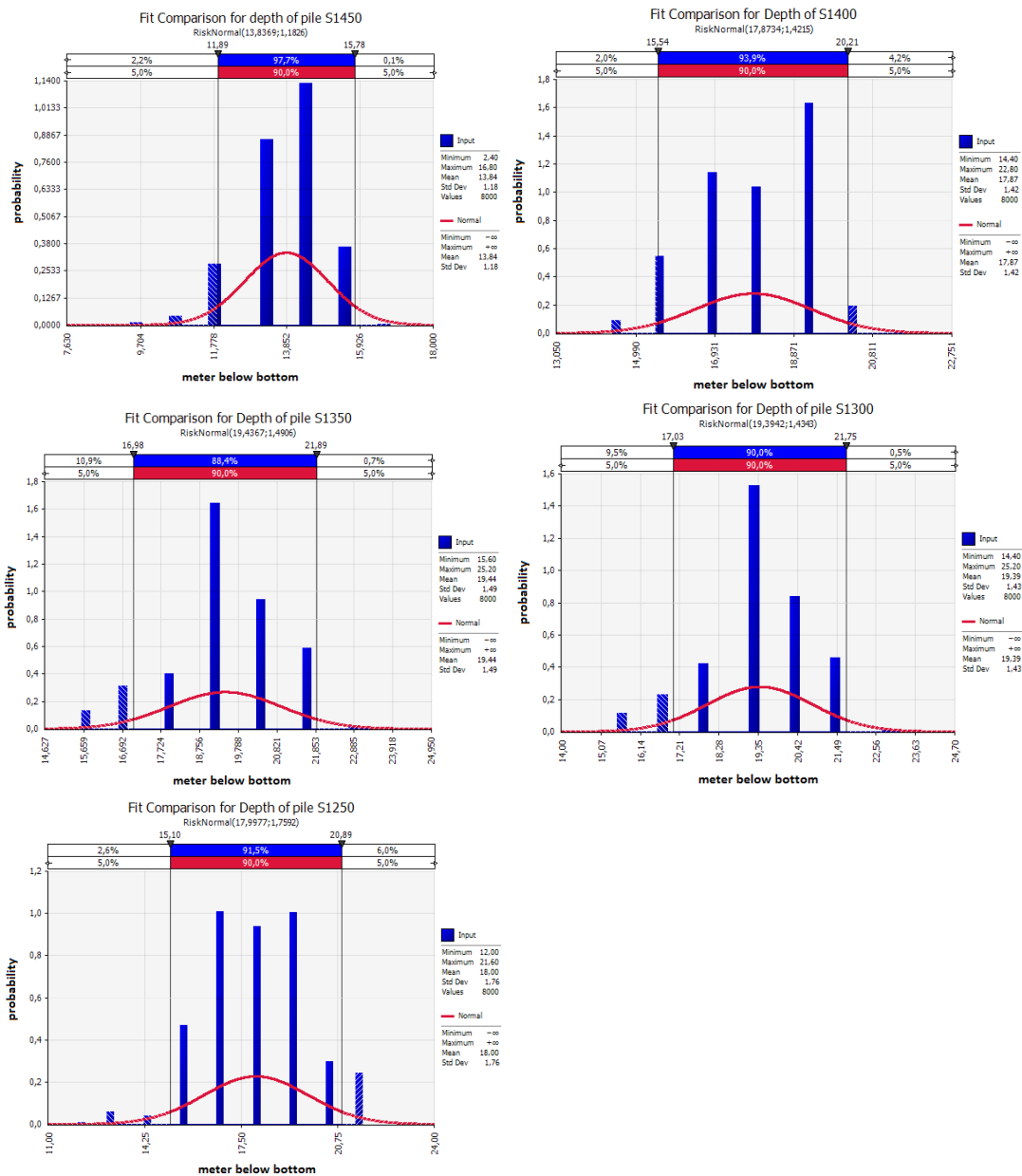
Figure 59: Depth analyses of piles S1250 to S1450 as result of collisions with the bow of the vessel (meters of depth from the bottom on).

The ultimate depth for the piles is calculated according the chance of failure conform the safety requirements adopted from the quay manual (see Table 15).

Pile	Distr	Mean	St dev	Length one year	Length 50 year
S1250	Norm	17.9577	1.7592	25.5	26.5
S1300	Norm	19.3942	1.4343	26	26.5
S1350	Norm	19.4367	1.4215	26	27
S1400	Norm	17.8734	1.4215	24.5	25
S1450	Norm	13/8369	1.1826	19.5	19.5

Table 15: Depth of the piles from the bottom on (NAP-16.8 [m]).

To make the comparison with the depth of the reference design that was calculated 28,5 [m] for S1250 and 27[m] for S1300 and S1350 (the inner piles).

A big portion of the total costs is consumed by the amount of material used. The length of the piles are of great influence on the amount of the material used. In the design a depth is found of 27 [m] beneath the bottom for the inner piles and 28.5 [m] beneath the bottom for the outer piles.

From the results of the Monte Carlo simulation an estimation is made of the depth of the 5 most loaded piles where the pile is clamped, when the vessel berths with his bow. At this point it is possible to calculate the minimum of depth according to the adopted safety level of Ultimate Limit State and assuming that a normal distribution can be used for plotting the data.

Pile code	S1250	S1300	S1350	S1400	S1450
Det	28.5 [m]	27 [m]	27 [m]	27 [m]	27 [m]
Prob	26.5 [m]	26.5 [m]	27 [m]	25 [m]	19.5 [m]
Length dif.	-2 [m]	-0.5 [m]	-0 [m]	-2 [m]	-7.5 [m]

Table 16: Comparison of the found depth of the piles beneath the bottom.

Discussion

In the reference design all the lengths of the inner piles are assumed to be equal. As can be noticed the minimum of depth of the piles in the Monte Carlo simulation are decreasing fast (see Table 16). The capacity of the piles of the reference model are not fully used. From the analyses can a reduction be found of approximately 9% (see Table 16). An analyses of the collision with the stern of the vessel should point out exactly where is too much capacity.

## 10.6 Level 2 Optimization of the structure

By adopting the failure rate of the quay walls, failure of a jetty is considered as a large economical risk. In the paragraph "failure of strength" is concluded that the chance of failure of the reference structure meets the required chance of failure (see the introduction of this chapter).

The chance of failure and the amount of material use of the total structure is strongly determined by the diameter of the piles. So to make a comparison an Monte Carlo simulation is done with different diameters, only for a collision with the bow of the vessel. The diameter is varied with the following diameters:

- 1620 [mm]
- 1820 [mm]
- 2200 [mm]

In this analyses only the failure due to the collision with the bow of the vessel is taken into account.
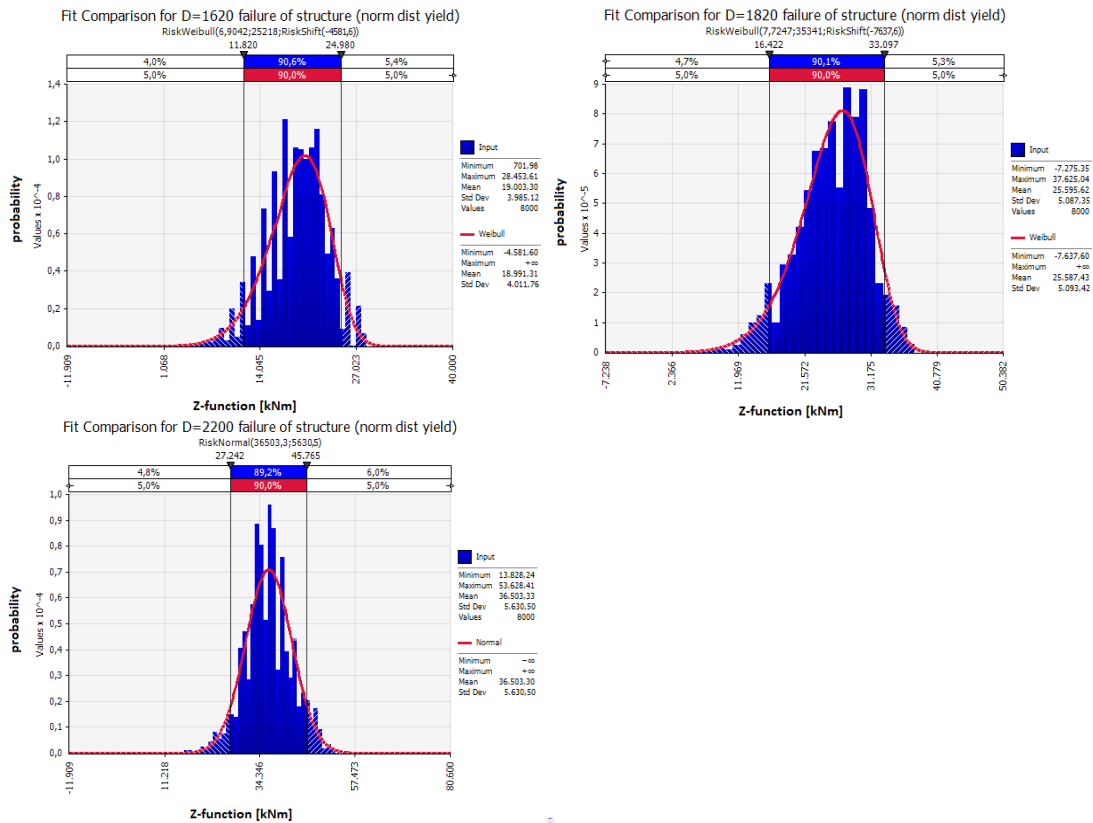
Figure 60: Results of limit state (Z) function for strength

From the constructed distributions a chance of failure is calculated (Z<0) per year of berthing and for a period of 50 years (with a berthing intensity of twice a week). The distributions are analyzed with a statistical tool that recommends a distribution based on the chi-square test, however some of the distributions are chosen over practical reasons or with the focus on the feet of the distribution.

Pile diameter (mm)	Distr type	Mean	St dev	β^*	P_f (per year)	P'_f (per 50 years)	$\beta = -\Phi^{-1}(P'_f)$
1620	Weib	19003	3985	4.76	$7.69*10^{-6}$	$3.85*10^{-4}$	3.3
1820	Weib	25595	5087	5.05	$7.25*10^{-6}$	$3.63*10^{-4}$	3.4
2200	Norm	36503	5630	6.4	$4.49*10^{-11}$	$2.25*10^{-9}$	5.9

Table 17: Structure failure per used diameter (β^* is calculated direct from the assumed distribution type).

In the resulting chance of failure a decreasing trend is visible. Also the chance of failure is calculated when the failure of the berthing beam is ignored (see Table 18).

Pile diameter (mm)	Distr type	Mean	St dev	β^*	P_f (per year)	P'_f (per 50 years)	$\beta = -\Phi^{-1}(P'_f)$
1620	Norm	21273	3753	5.67	$7,15*10^{-9}$	$3.58*10^{-7}$	4.9
1820	Weib	28386	4256	6.67	$3.17*10^{-6}$	$3.17*10^{-6}$	4.5
2200	Weib	41496	5131	8.09	$3.06*10^{-16}$	$1.53*10^{-14}$	8.1

Table 18: Failure of the piles per used diameter (β^* is calculated direct from the assumed distribution type).

The decreasing chance of failure paired with the increasing diameter of the profile is recognized. From a diameter of 2020 [mm] that chance of failure reaches a chance of failure that meets the adopted safety requirements based on economical risk.
The transformation of the Weibel to the Normal distribution and the use of a Normal distribution for the d=1620 [mm], gives a change in the trend of the chance of failure. It appears to disturb the outcomes. Logically the smallest diameter should have the smallest beta.

Deformation
The second failure mechanism is the exceeding of the maximum deformation of the berthing structure. Initially the maximum deformation is taken 0.7 [m]. with this a failure chance is calculated per berthing procedure and taken over a period of 50 years (see Table 19).

Pile diameter (mm)	Distr type	Mean [m]	St dev [m]	β^*	P_f (per year)	P'_f (per 50 year)	$\beta = -\Phi^{-1}(P'_f)$
1620	Gam	0.225	0.114	1.97	$1.7*10^{-3}$	$8,5*10^{-2}$	1.4
1820	Gam	0.193	0.097	1.99	$3.1*10^{-4}$	$1.5*10^{-2}$	2.1
2200	Gam	0.157	0.0773	2.03	$1.2*10^{-5}$	$6*10^{-4}$	3.2

Table 19: Chance of failure of the maximum deformation of 0.7 [m] .

From the diameter of 2200 [mm] on a chance of failure of P_f=1.2*10^{-5} is found. The chance of failure when a normal distribution is used instead of the Gamma distribution is much smaller. Going on this diameter of 1720 [mm] would be sufficient.

Discussion

In all the cases the berthing beam is the weak link. There is a logical relation found with the increasing diameter and the decreasing chance of failure. A distinction is made between the optimization of service limit state or ultimate limit state. The found diameters with the best fitted distribution are selected from the chance of failure:

Ultimate limit state   d=1820 [mm]
Service limit state   d=1820 [mm]

By calculating the beta of the normal distribution a relation can be found with the diameters and the chance of failure. The transformation of the Weibel to the Normal distribution and the use of a Normal distribution for the d=1620 [mm], gives a change in the trend of the chance of failure. It appears to disturb the outcomes. Logically the smallest diameter should have the smallest beta.
Nevertheless the beta's are used to calculate the new diameters for the structure.

The exact found diameters with the normal distribution (trend of the found β) are:
Ultimate limit state   d=1760[mm]
Service limit state   d=1720[mm]

These diameters are not really an option but the nearest larger diameter (d=1820 [mm]) should be used.
The costs and duration that it takes to repair the beam is much lower than it takes for the piles. Therefore an indication of the used diameter of the piles is also calculated with the help of the trend of the beta's. the found diameter for the piles is d=1470 [mm] (see appendix). In that case the β=2,33 is calculated for the structure overall, a β=3,4 for the ultimate limit state and a β=1,1 for the service limit state of the piles. An economical analyses should be done to consider the possible benefits of this outcome.
*From the analyses in paragraph "loads" it occurs that the vessel will only load the area 31 [m] till 64[m] from the loading arms. This goes both directions and will exclude a length of about 2*31=62 [m] of direct reflection. It is possible to remove this part of the berthing beam.*
In that case the analyses has to be done again since the system is then totally changed.

10.7 Factor of influence

From the results of the Monte Carlo simulation the influence of the separate variables on the chance of failure cannot directly be established. Therefore an α-factor is calculated using the classical sensitivity analysis. The α-factor is a measure for the contribution of every basic variable to the variation of the reliability function.

The size of the a-factor shows that the basic variables play a more or less important role in the total deviation of the distribution of the reliability function.

variable	Gam	Phi	T	f_y	Coor	Mass	vel	W	L	D	angle
Alfa^2	0.19	$3.1*10^{-4}$	0.2	0.19	$7*10^{-4}$	0.02	0.4	0.01	$7*10^{-4}$	0.01	0.01
σ/μ	0.075	0.25	0.1	0.07	∞	0.24	0.44	0.06	0.052	0.06	0.16

Table 20: Alfa factor of analysis of strength (sigma Alfa^2=1,03)

Discussion
Especially the velocity is of great influence. The parameters of strength of the volume weight of the soil, the wall thickness and the yielding stress also have a reasonable influence on the deviation of the distribution.
The centre-offset and the length have an equal influence. It can be noticed that the histogram of these variables show an asymmetrical behavior.
*From additional analyses the length of the vessel and the centre offset appear to give an almost equal deviation over the coordinates of the impact on the structure. In this respect the centre offset has no influence on the magnitude of the kinetic energy. The influence of the length of the vessel on the deviation of the kinetic energy is very small and the magnitude of kinetic energy shows a negative relation with the length.*
The soil parameters (volume weight and the angle of internal friction) are calculated over the total depth. In the previous chapter can be seen that all the soil variables have the same variance coefficient. This is actually not right since the influence of the soil on the surface should have a much more influence then the much deeper soil.

Histogram of the influence of length
In the classical sensitivity analysis all the results are taken as a normal distribution. In most cases this is reasonably applicable because the results show a somewhat symmetrical distribution. But this assumption does not count concerning the results in which the coordinates of impact play a role (see Figure 61).
The coordinates of impact itself are fitted as a normal distribution but the mean of the distribution coincide with the middle of the bridging of the berthing beam. Because of the symmetrical shape of the energy load relatively large amounts of larger moments are found in relation to smaller moments (see Figure 61). In the calculation for the a-factor the distribution is assumed to be a normal distribution in order to simplify.
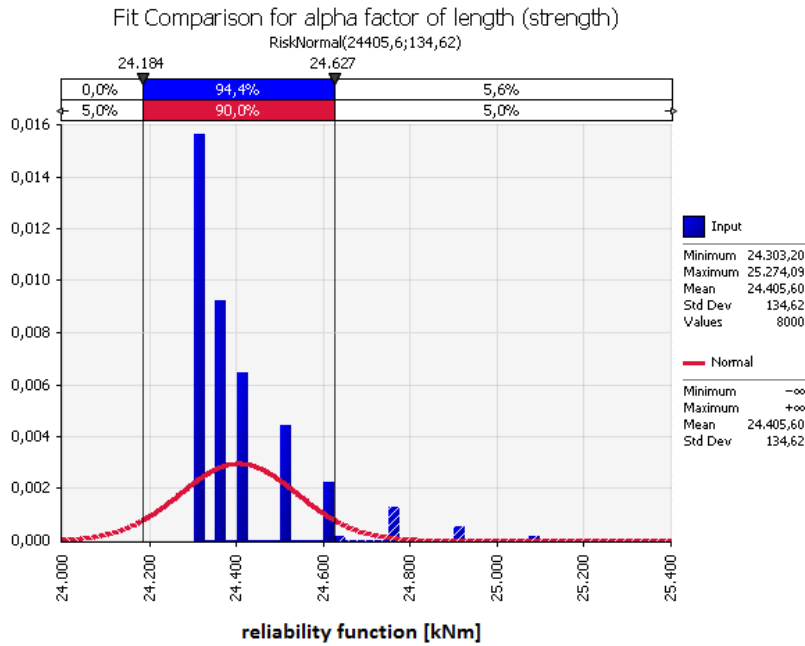
Figure 61: Results of the reliability equation (Z)

Even though it is clearly not a normal distribution. In this comparison the distribution is fitted in correspondence of the normal distribution. In practice the normal distribution would be fitted in exact correspondence with the interested area of the distribution. Because of simplicity this is neglected.

10.8 Safety factors

According to the information obtained from the Monte Carlo simulation and the alfa-factors, it is possible to calculate an indication of the design values. In determining the design values, it is assumed that all the distributions can be replaced with normal distributions. This results in the earlier found β=3.4 for the analyses of the ultimate limit state.

So, all variables of strength are assumed to be normally distributed and the design values are calculated according to equation (see Table 21):

$$X_d = \mu_X + \alpha_X \beta_Z \sigma_X$$

Variable of strength	γ'(volume weight) (layer 1)	φ (angle of int friction) (layer 1)	t (wall thickness) (22,2 [mm])	f_y (yield stress) (355 [N/mm²])	Width [m]	Length [m]
Rep values	19	25-27	22.2	355	32	180
Des values	16.1	25.7	18.8	465	27.9	185
Safety factor	1.2	0.97-1.05	1.18	0.76	1.08	0.97

Table 21: Calculated design values with corresponding safety factors for strength.

In the calculation of the design values the action variables are assumed to be normally distributed as well (see Table 22).

Variable of action	Mass [DWT]	Velocity [m/s]	Centre offset [m]	Draft [m]	Angle [^{0}]
Rep value	56065	0.15	+15-15	13	12
Des value	42162	0.16	0.23	11.65	8.27
Safety factor	0.75	1.07	0.02	0.89	0.69

Table 22: Calculated design values with corresponding safety factors for load.

The results of the centre-off set and the length of the vessel have a more characteristic shape of a extreme distribution than that of the assumed normal distribution (see Figure 61).

This result is only an indication, since all the values are derived direct from the reliability function. If we put the found design values in the equation of Saurin the found energy is E_d=495 [kNm]. Instead of the calculated E_d=1050 [kNm]. This has an overshoot (see Figure 52) of P=0.012.

Discussion
The width and the length are taken as variables of strength instead as load. The length gives a larger eccentricity with a larger value and the width is a part of the rule of Vasto Costa and this term decreases with growth of width.

The found design value is smaller than the representative value. This would indicate too little reliability. From Table 21 and Table 22 can be noticed that a couple of the variables of strength and loading have a safety factor smaller than 1. The values used in the calculation are distributed direct from the analyses. This is probably because of the non linear character of the reliability function and the correlations between the variables.

The design value of draft should be larger than the representative value, since the added mass of water should increase with a smaller space between the bottom and the keel. The eccentricity of the vessel will decrease with a larger angle of berthing causing a larger energy loading and the energy loading will increase with more weight.

10.8.1   Level 3 sensitivity analysis

Following the classical sensitivity method an analysis is made of the correlation. A correlation is determined between the reliability equation and the basic variables.

Variable	Mass [DWT]	Vel [m/s]	L [m]	W [m]	D [m]	Angle [^{0}]	Coor [m]	E [kNm]
ρ	-0.12	-0.55	-0.102	0.055	-0.099	0.004	-0.016	-0.57
ρ^2	0.01	0.3	0.01	0.003	0.001	$1.6*10^{-6}$	$2.5*10^{-4}$	0.32

Table 23: Correlation coefficient between basic variables of the energy loading of the vessel and the reliability function.

The influence of the negative correlation of the energy is clearly recognizable from the results (see Table 23). A negative correlation means that when one variable (for instance energy) becomes larger the other variable will decrease (Z- value). In other words when a larger energy is applied the value of the reliability function will become smaller (Z→0).

The speed as well as the thickness of the wall and the yielding stress show a clear correlation with the reliability function (see Table 23 and Table 24). The wall thickness of 22.2 [mm] and 30 [mm] has a positive relation with the reliability function.

Variabele	t=22,2 [mm]	T=30 [mm]	T=38 [mm]	T=40 [mm]	f_y =380[mm]
ρ	0.68	0.44	-0.37	-0.25	0.68
ρ^2	0.46	0.19	0.14	0.06	0.46

Table 24: Correlation coefficient between basic variables of strength (wall thickness and yielding stress) and reliability function.

The horizontal beam of the berthing structure was recognized before in this chapter as being the weak link. It appeared that the wall thickness and the yielding stress of the beam of the berthing structure are 22.2 [mm] and 380 [N/mm^2].This is in accordance with the positive correlation.

The wall thickness of 38 [mm] and 40 [mm] are the thicker parts of the piles. From the negative correlation it appears that these are designed too thick. But the values of the correlation are very small.

The variables of the resistance have a big influence because they are assumed to be equal over the whole structure. In reality this will not be the case.

The correlation of d=1620 [mm] is shown in Table 25.

variable	Gamma layer 1	Phi layer 1	Gamma layer 2	Phi layer 2
ρ	-0.01	-0.29	0.27	-0.07
ρ^2	$1*10^{-4}$	$8*10^{-2}$	$7*10^{-2}$	$5*10^{-3}$

Table 25: Correlation of the soil properties

The relation of the velocity with the reliability function is put in Figure 62. As can been seen there is a negative relation. The grid for the coupling of energy and forces are very recognizable.
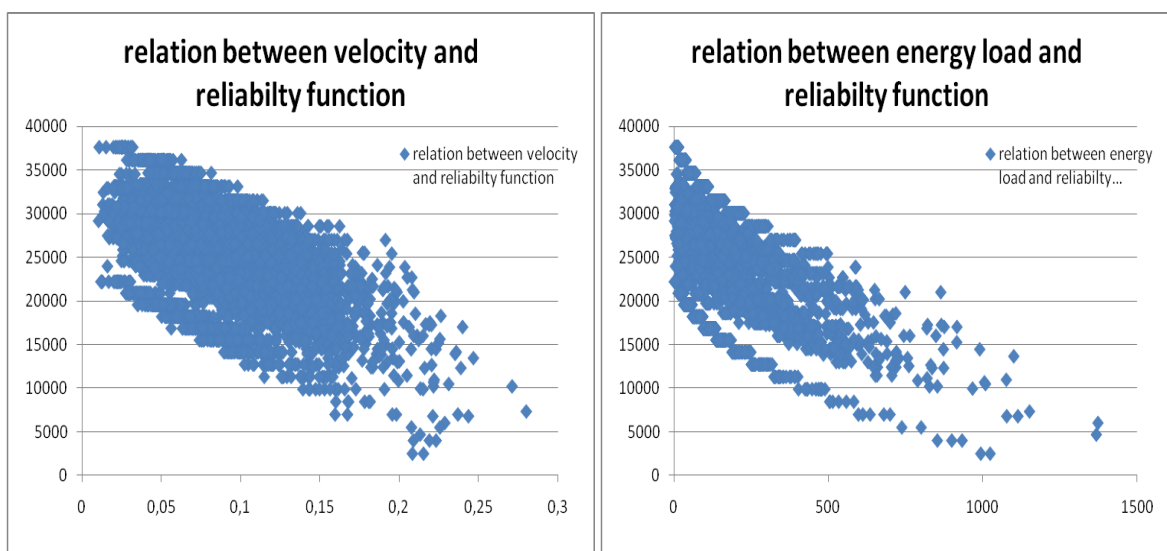
Figure 62: Graph of the reliability function in relation to the velocity.

Discussion

The earlier found characteristic behavior of the structure are very clear seen in Table 24. From the positive correlation it can be concluded that the two wall thicknesses t=22.2 [mm], t=30 [mm] and the yield stress of 380 [N/mm^2] are chosen too small. The wall thickness and the yield stress are both indicators for the berthing beam. The negative correlation of t=38 [mm] and t=40 [mm] are probably indicating that the parts are too stiff and makes the moment concentrate more around these parts. This causes the weaker parts around them to fail at the transition between the pile sections.

The parameters of the soil are very small and not logical. It is impossible to make any assumptions from these. Because of the size of the values, they are very small value, it could be just noise. It is advisable to do more sensitivity analyses.

10.9 Calculation of the total failure according to a fault tree analysis

In the chapter "Principle of probability" the fault tree of the jetty is introduced. The fault tree represents the relation of all base failure mechanisms in relation to the head event. In this theses several of the basic failure mechanisms are considered. In this tree it appeared that the failure of the berthing structure is the conditional for the functionality of the jetty. In the next paragraph the calculated chances of the reference structure of failure (d=1820 [mm]) for the base failure mechanisms are filled in the fault tree.

The chance of failure in relation to the strength of the structure and the exceeding of the maximum deformation both are related to a high energy load. Both chances are dependent on the same energy load. In the next calculation the extreme boundaries are investigated for independent chances and fully dependent chances. As base failure mechanisms are taken the exceeding of the yield stress and the deformation limit due to collision of the bow or the stern of a vessel (see Figure 63).
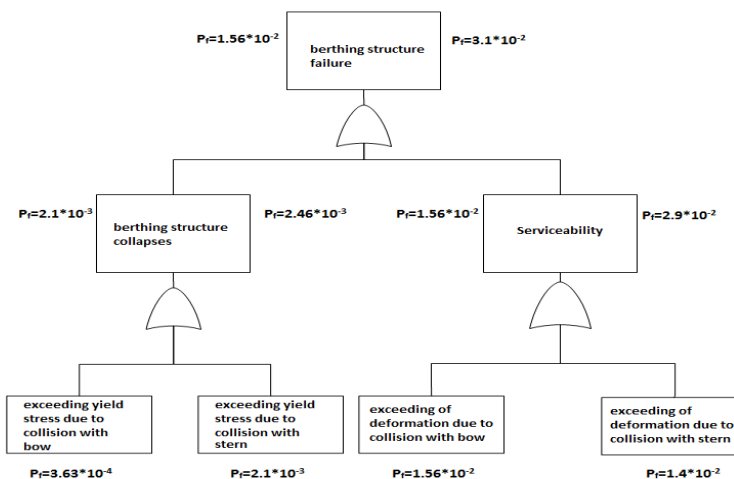

Figure 63: Fault tree of the berthing structure with ref. period of 50 years. On the left side of the text the dependent failure chance on the right side the independent failure chance.

When one of the four failure mechanisms occurs, the structure is considered to have been failed.

Discussion

The deformation is the dominant failure mechanism in both cases. The deformation is a logical indicator for total failure. Even though, as was mentioned earlier in the results, the assumed deformation limit was considered as very small. If the limit for deformation would be somewhat larger, the chance on failure of the head event would be lower.
Reference

[1.] JCSS, Prof Vrouwenvelder, 10-11-2000
[2.] C. van der Horst, 2004

11 Conclusion and Recommendations

Before discussing the conclusion the research question are repeated again. With the berthing of a vessel the structure will be loaded by kinetic energy. This load must be absorbed. In this research the deterministic and the probabilistic method are compared in relation with the accepted chance of failure of the berthing structure and the reference period.

11.1 Risk analysis

The risk is a function of chance of occurrence of a event during a period and the expected consequences. In this risk evaluation the risk is appreciated as a global estimation of chance and the consequences are appreciated according to a short description.

The costs of the structure are many times less than the cost of dysfunction in production and transport. The consequences of failure of the structure has many levels. The consequences of dysfunction of the jetty itself is considered to be the most severe. When the jetty itself becomes damaged all four berthing sites are taken out of production. Let alone the possibility that a part of the port has to be closed down. In case of small local damage of the berthing structure it can be repaired easily and in worst case scenario one berthing point has to be taken out of production.

The structure has been designed to absorb a certain energy. The considerations of local circumstances and the dimensions of the expected vessels are included in the design energy. These variables can be verified before any berthing procedure will take place. During the berthing procedure two variables are unique in every berthing procedure, the angle and the velocity of berthing. They will have to be determined at the spot and are influenced by the local circumstances. Because the aim is pursued of berthing parallel to the berthing structure as much as possible the berthing angle can be expected to be limited. When the angle is very wide it is probably caused by a human or mechanical error. It is known that the velocity has the greatest influence on the energy load. When there is a matter of hurry, carelessness, bad sight or human or mechanical error a higher velocity is easily the consequence.

Local damage to the fender structure and consequent failure of a berthing site

can be intercepted by another berthing site. The time needed to repair the damage will be relatively short. When there is local damage to the berthing structure the damage will take place on different levels. In case of little overload the wooden facing will be damaged.

In case of damage of the berthing beam, the berthing beam can be replaced locally. Depending on the design on the structure the deformation can reach such a value that the vessel makes direct contact with the piles. In case of damage to the berthing pile it needs to be cut loose from the berthing beam and has to be pulled in order to put another pile in its place. Where failure of the wedge of the soil, the soil can be disturbed in such a way that it cannot be expected to have any resistance for a

considerable time. The soil will need to be repaired or in worst case the pile must be positioned in another place.

In more severely cases of total failure of the berthing structure the structure will run out of energy absorbing capacity and the jetty itself has to absorb the kinetic energy. The jetty itself is very stiff and will have only little deflection, reaching high reaction forces fast.

With only little energy loading the concrete will show larger cracks and the fixed pile-concrete plug that makes the connection with the foundation piles will become joints. In case of only a little movement the equipment will be damaged and has to be repaired.

In case of more energy loading the high reaction forces cause the concrete structure to fail and probably to rupture the skin of the vessel. Depending of the nature of the cargo, but with leakage or a fire break out of the chemicals the functioning of a part of the port will be disturbed.

The risk is a function of chance times consequences. In the next part of the paragraph the chance of failure and everything involved in the process is weighted and all the factors that have a role in the whole process are mentioned. In the last part of this paragraph the consequences are discussed listed.

The berthing process is put in a list based on the risk factors presented in the "Aanvaarrisico's voor remmingwerken" written by G. Van Driel and A. Vrijburcht commissioned by "Rijkswaterstaat" :

- Vessel characteristics
- Fairway features
- Human action
- External circumstances

The energy capacity of the structure depends on the following factors:

- Proper construction building
- Correctness of determination of the soil profile
- Repairing possibilities
- Consequences

This study is conducted for sea vessels. Factors relating to the vessel that are important for berthing and the load on the berthing structure are:

- Size
  A larger vessel will less manageable than a smaller vessel.
- Velocity
  A vessel with a larger velocity will make a greater effort to brake than a vessel with a smaller velocity.
- Mass with loading
  A loaded vessel will brake less easily than an empty vessel. The location of berthing can be determined by the load.

- Power of the propeller
  While berthing the power of the propeller and the time to reverse of great importance.
- Ability to maneuver
  The possibility of the use of thrusters is of great importance
- Technical reliability of the vessel
    - Main engine; it is important that the reverse clutch or the reversibility of the engine functions appropriately.
    - Engine of a possible thruster; in every situation a thruster must be able to get started quickly.
    - Rudder; possible causes of rudder defects are defects in the lines, valves or in the autopilot that runs the rudder.
    - Mari phone; failure can cause miscommunication between the helmsman and the jetty/tug personnel.

Port geometry

- Geometry
    - Length and width of the port
    - Berthing structure consisting of a freestanding piles, open or continuous berthing structure or closed wall (cushion effect)
    - Possibility to make a curve near the jetty
- Location
- The location and orientation of the port and the jetty in relation to the wind and possible shelter.

Human failure that can occur during the berthing procedure:

- Steering
  A helmsman can make a error caused by inattention, inexperience, hurry or physical/mental condition:
    - Mistaking forwards vs. reverse
    - Wrong use of thrusters
    - Berthing at an greater angle then design
- Judgment
    - Wrong judgment of the distance
    - Sailing at a high speed
    - Wrong judgment of the robustness of the berthing structure
- Communication
    - Miscommunication between the helmsman and the sailor in the prow, or between the jetty personnel and the helmsman.

Also the fact that the personnel is owner of the vessel or not is a important risk factor since in case of ownership they will be more careful. Also the experience and acquaintance of the helmsman with certain locations will play a role in the risk-seeking or risk-avoiding behavior.

These aspects are included implicitly in the analyses. The human error is translated in a wrong berthing angle or velocity.

External factors
Factors that are originate from external circumstances:

- Wind

  A strong cross wind can cause an empty or high vessel, to be berthed on a relatively too high velocity.

- Sight

  A risk factor is the sight of a helmsman has during the berthing process. It can be influenced by the darkness, fog and rain.

- Stream and waves

  Stream and waves in the port can cause unexpected vessel movements near the jetty, such as:
  - Wind waves
  - Translation waves
  - Waves caused by propeller of another vessel

Structure

The energy capacity of the structure depends on several factors.

Assembly quality

- Placing the piles
  - Accurate positioning (top and bottom)
  - Sequence
  - Accurate depth
  - Avoiding of damage during driving of the piles
- Quality of the welds
  - Because of the location just above the water there is some risk of contamination of the weld
  - Difficult access of the location of weld
  - Experience of the welder
- Coating
  - To avoid corrosion due too rapid alternation of salt water and air, sanding due to running water with sand
  - Type of coating
  - Quality and method of coating assembling

Correctness of the determination of the soil profile and model depends on:

- Number of soundings for a representative soil profile.
- The quality and experience of the geotechnical
- Local erosion surrounding shallow founded piles.

Design criteria

- Applicability of the p-y curves
  - Based on elasto-plastic soil behavior, modeled as springs over the total length of the piles creating a large interaction.
  - Applicability of Dutch soil characteristics.
  - Negligent with possible point displacement leaving out the shear force at the point and the additional vertical force caused by the rotation of the point.
  - Loss of information of soil behavior through the grid of the spring modeling.
  - No direct interaction of the springs

- o The method of p-y curves is laborious since the answer is determined iteratively
- o Availability use of software (M-pile)
- Applicability of Blum
  - o Blum is ultimate strength model
  - o Modeling of one large soil wedge. Causing one point load.
  - o Impossible to simulate the soil characteristics over depth as springs
  - o In principle only non cohesion soil (sand)
  - o Inaccurate assumption of the horizontal distribution of the wedge
  - o Impossible to calculate the deformation of the pile
  - o Does not represent the actual pile-soil interaction behavior
  - o Quick estimate of the final pile design
- Material (steel) fatigue due to large changes of stress throughout the structure
- Failure mechanisms caused by local buckling and ovalisation
- Neglecting capacity of energy absorption due to plastic deformation.

Disassembly

- Replacement of the wooden facing elements
- The repair or replacement of piles

Consequences of overloading

- When a separate fender structure is used
  - o An overcapacity of 200% in deformation according to the PIANC 2002 causing an extra reserve capacity of 400% of the berthing structure
    - ▪ Limited plastic deformation to the steel elements is no reason to shut down the mooring point
    - ▪ Depending on the distortion/plastic deformation of the soil if the mooring point has to be shutdown
- When a fender system has been placed directly on the jetty
  - o Little to no reserve capacity can be used when overloading. The concrete deck does not allow big deformations and in the least bad case larger cracks will occur
  - o Due to overloading and the stiffness and robustness of the deck of the jetty the connection with the piles and the deck will become a joint.
- Damage of the hull of the vessel and possibly loss of content of the vessel due to contact with the pile.
- In case of total collapsing of the separate and direct placed fender system
  - o In case of damage to the equipment, possible spill of cargo which can be collected in the "basin" /lower deck
  - o In case of damage to the equipment and large damage to the jetty, the "basin"/lower deck is damaged as well and the cargo will be spilled in the water. Depending on the nature of the cargo this could result in a total shutdown of (a part of) the port
  - o In case of damage to the equipment it is possible that a fire will break out on the jetty or the vessel. Causing possible shut down of productivity in the port because of risk of inhaling harmful smoke and risk of explosion. In the Netherlands there is a dominant South-West wind causing a possible shut down of the head entrance of the port resulting a large queue of vessels.

11.2 Limitations

- The amount of observations where the berthing structure has failed is very low. The constructed chances of failure are therefore based on very few observations.
- Not all possible scenarios of failure are applied in the Monte Carlo simulation. All causes of failure like human error, hard wind, failure of equipment are implicitly included by the used data and distributions of the basic variables.
- To construct the stochastic model of energy load limited amount of vessel- types has been used. It is assumed that all vessel were assisted by tugs. Vessels that could berth independently were not considered.
- Based on the large dependency of the soil profile in the horizontal plane the used soil profile is taken equal over the entire length of the berthing structure. In reality there will be differences along the length of the berthing structure and will contain local discontinuities.
- As input of the cross sections of the tubular sections in the structure a limited amount of cross sections characteristics per realization has been used. Therefore is the influence of the section characteristics considerably larger.
- By increasing the capacity of stability of the piles the only failure mechanism for strength is reaching the yielding stress. The plastic deformation/failure of the soil is not taken into consideration.
- The reaching of the yielding stress means the failure in relation to strength. However by allowing plastic deformations the capacity of the structure is enlarged approximately 400 %. Also there is no distinction is made between smaller and larger deformations
- The failure of the vessel hull is not taken in to account as a failure mechanism
- The berthing of a vessel at one mooring point is considered in the calculations. It concerns the most heavily loaded part of the structure.

11.3 Research questions in this thesis

In this thesis two primary objectives will be assessed:

1. "Is the developed technique applicable for running a Monte Carlo simulation?"

In order to answer this question it is necessary to consider the following sub-questions:

1.1. Is it possible for Scia to simulate the soil model?

1.2. Are the reactions and relations of the model physically correct?

2. "The difference in amount of material necessary between a jetty designed according to the standardized method in comparison to a jetty designed according to the probabilistic method, assuming the same terms of reference and natural conditions as the Lyondell jetty (the reference jetty)".

An analysis will be made of the magnitude of reliability of each component in the total failure system. In order to answer the stated question the following sub questions are investigated:

2.1. What is the most prominent basic failure mechanisms and what are the relations to the head event?

2.2. What is the actual live expectance of the Lyondell jetty and at what safety level is the Lyondell jetty built according to the standards?

2.3. What is the actual safety level of the Lyondell jetty by means of a probabilistic analysis?

2.4. What is the relation between the safety level and the use of amount of material by means of a probabilistic analysis?

2.5. What is the most critical base variable in the design of the berthing structure?

The main interest of this investigation is a possible reduction of costs but this will not be explicitly examined. The costs are taken as a direct relation with the amount of used material. This question will be answered with the second research question.

But to answer the second question first is investigated if the first research question " is it possible to run a Monte Carlo simulation with the developed model" can be answered positive.

11.4 Conclusion

In this thesis there are actually two main questions to answer. The first target is to answer the question:

" Is the developed technique applicable for running a Monte Carlo simulation?"

To answer the stated question, there are two sub questions made.

1.1.   *By comparing the results of a model in both programs M-pile and Scia engineer the results show great similarities. Only the model in M-pile reaches the plastic state sooner than the model in Scia. However by reaching this state the model is already considered to be failed. So it is possible to simulate the soil model in Scia engineer.*

1.2.   *The simplified model shows the characteristic behavior of the structure and can be measured sufficiently. By analysis of the relations of the deformation and the energy loading and the resulting moments, it appeared that the relations are expressed according to the known mechanical rules. Thus the relations of the model are physically correct.*

The two sub questions are replied positively. The first objective with the corresponding research question is answered with " the developed technique is fitted to use for a Monte Carlo simulation" .

The second objective was stated to answer the actual main question:

"Is there a difference in amount of capacity needed between a jetty designed according to the deterministic method in comparison to a jetty designed according to the probabilistic method, assuming the same terms of reference and natural conditions as the Lyondell Jetty (the reference jetty)?".

An analysis will be made of the magnitude of chance of failure based on the reliability function of each component in the total fault tree. In order to answer the stated question the sub questions are investigated:

2.1. A fault tree of the total failure/non functioning of the jetty is built. It shows that the most prominent basic failure mechanism is the failure of the berthing structure, which is conditional for the failure of the jetty in a collision of a vessel.

2.2. The Lyondell jetty is according the "terms of reference" designed with help of the EAU and the NEN codes. The EAU 2004 refers for safety level to the DIN EN 1900, in the Netherlands this is the NEN-EN 1900. Knowing this, it can be concluded that the Lyondell jetty is built according to the Dutch used safety rules. The NEN 6700 are more economical orientated then the NEN-EN 1900. The safety considerations of the NEN 6700 are adopted.

2.3. Considering the best fitted distribution the chance on failure of strength during berthing of the large sea vessel is in the range of the adopted safety rules. The service limit state of 0.7 [m] is chosen small, it would be better to use a maximum deformation of 0.8 [m].

2.4. In the analysis of minimum of capacity of the used model the overcapacity in length of the piles shows a strong relation with the location of the energy loading. From this analyses an overcapacity of 9% is found over the 5 most loaded piles. Reasoning from the resulting trend there is material to be saved.

2.5. Reaching the yield stress or large deformations large values of velocities are found. A high energy load is mainly caused by high velocity. Thus the most critical base variable is the velocity in addition the wall thickness of the berthing beam appeared also to be an important base variable.

11.5 Recommendations

In relation to the first research question it can be concluded that the developed method for a probabilistic analysis can be considered as appropriate. The method makes it possible to determine the used total capacity within the structure.

By use of this method the structure can be designed in a more efficient way. In other words the capacity is applied exclusively at locations where it is necessary in order to meet the assumed chance of failure.

The use of a three dimensional finite element software with an users interface by Scia-engineer offers the possibility to consider complex structures with a probabilistic method.

Recommendations in relation to the application of external executer:
First recommendation:
In this thesis for practical reasons use was made of Excel. Excel has a rather black box character and is a relatively bad executer. Excel also can generate and process only a limited amount of data. In order to work at a reasonable rate the processing has been divided over several Excel files. It would be preferable to replace Excel by a more clear and handier program.

Second recommendation:

The use of Matlab is advised. It is possible to connect to the finite element software by means of the COM-interface. The Matlab program offers a possibility for this. Matlab is a more advanced and stronger executer and has also a better random number generator than Excel. Because of the use of the random number generator of Excel several adaptations were made. By means of Matlab the whole procedure can be hosted in one program.

Third recommendation:

By making use of energy loads a lot of time has been spend in setting up a library. When structures are tested with forces instead of energy the simulation can be used more efficiently.

Recommendations concerning the second mean research question.

First recommendation:

With the help of the three dimensional finite element software only the possibilities of determining overcapacity was investigated at the berthing site 2. Through testing the remaining berthing sites it is possible to develop a new geometry. This geometry can make use more efficiently of the distribution of materials and still meets the assumed chances of failure and terms of reference.

Second recommendation:

The developed fault tree concerning the failure of the jetty contains more basic failure mechanisms that were not considered in this report. They can be further elaborated. In accordance with an accurate economical analysis a specific chance of failure and reference period of a jetty can be assessed. The chances of failure and reference period in the Dutch codes are very generally stated.

Third recommendation:

The results show that the energy load are applied very local. It is possible to reduce the capacity and design the structure more efficient in relation to the loads and still maintain the same chance of failure.

Fourth recommendation:

The critical variable is the velocity. If the distribution of the velocity can be reduced consequently the distribution of the loading will be reduced and so the structure can be designed to be more slender and cheaper.

Fifth recommendation:

The p-y curves are only developed for a limited amount of different soil types limiting the application of the p-y curves. With developing of more curves for different soil types the application can be more widely.

Sixth recommendation:

In the Monte Carlo simulations 122 realizations were run for the structure. In the analysis it became clear that the resistance was accidental distributed. It is advised to perform a sensitivity analysis. By running tests with greater amount of realizations for the structure, an optimum can be found. By reducing the size of the grid it is possible to run more drawings. It is advised in accordance with an earlier recommendation to use an alternative program for Excel.

Seventh recommendation:

The safety limits are calculated with help of the reliability index. It appeared that the values of the chances are so small that the translation from other distribution types to a normal distribution disturbs the logical outcome. Also reaches the normal distribution faster smaller values of failure in contrast to the other distributions. Comparison of chances with different distributions has many disadvantages.

Advised is to do more realizations in the Monte Carlo simulations so the chance of failure can be calculated directly from the amount of fault realizations. Secondly, it is advised to use a chance of failure calculated from the actual best fitted distributions and not calculated from the normal distributions or reliability index.

Eight recommendation:

The design points calculated in the results are indications. Advised is to explore the more use of a more advanced method such as "nearest to the mean", "angles" or "centre of gravity".

Ninth recommendation:

By use of a finite element software it is possible to consider different structures in a three dimensional way. It would be interesting to try this technique also in relation to other structures for instance bridges and overpasses.

APENDICES

A. Working procedure of placing the piles

The piles were placed according the following principle (see figure below). First the metal rings are welded into the pile. The piles will then be driven or vibrated into the soil. After placement the upper 3 [m] are placed on top. The pile will be filled with water up to the top and keep it filled. The soil in the pile will be excavated till 3 [m] from the pile base. To make a stop in the pile concrete will be poured in the pile. And the upper part of the pile will be filled with sand.
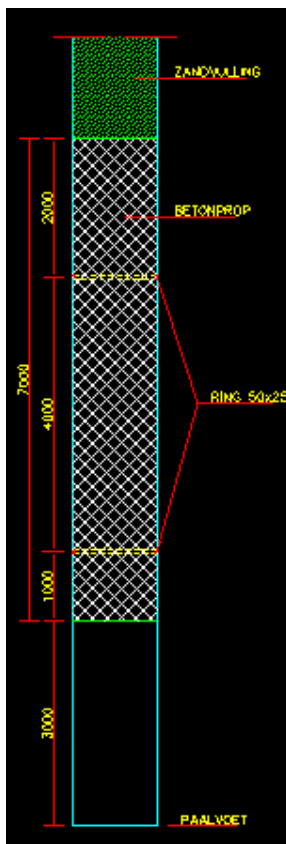
Figure 64: schematization of the pile feet

B. Concrete structure part

The upper concrete structure consists out of two levels. On the lower level the transport pipes are situated. On the upper level the operating equipment is realized and there is room left for traffic (vehicles) to maneuver.

There are for each loading/unloading spot four loading arms available. They have a separate supporting structure, instead of the slabs, which consists out of one beam which spans over 3 supporting grids (see Figure 68). To make sure the concrete can expand enough due to temperature differences, there are five expansion joints.

Construction method

The part where the steel piles and the concrete part meet will have to transfer all the loads from one and another. After driving the steel piles, a steel plate will be welded on the outer side of the piles. The welded plate will serve as supporting for a prefabricated girder. The prefabricated girder will bridge the length between two or three piles (see figure below).

Figure 65: Photo made during construction of the Lyondell jetty

In the prefabricated girder some space is left, to be filled later with concrete, to make the connection with the steel pile. After placement of the reinforcement about 2 meters of the upper part of the steel pile and the space left in the girder is filled with concrete.

After the construction of the supporting grid, prefabricated slabs will be placed on top. The reinforcement of all elements will be placed in such a grid that these will fit in to each other. After placement all elements, the joints will be casted together with concrete. Therefore the deck can be considered as one monolithically element.
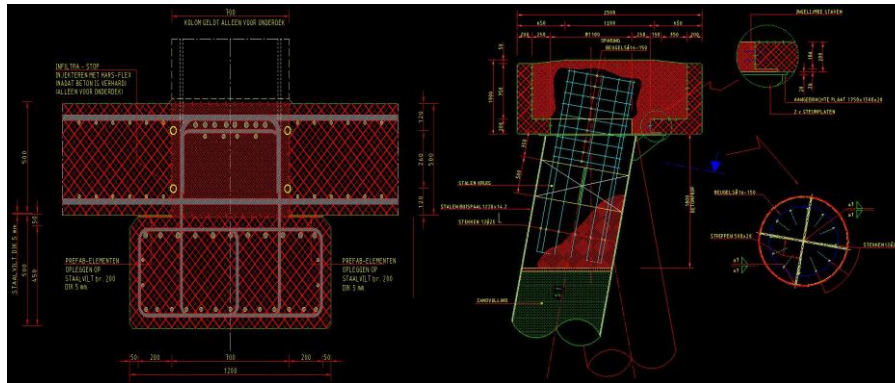
Figure 66: left: cross section of the connection of the prefabricated floor slabs, with the reinforcement. Right: connection of the steel piles and the concrete beam

The column that supports the upper deck is prefabricated and is string over the reinforcement sticking out of the joint. To make a solid connection the space around the reinforcement is grouted after placement (see Figure 66 and Figure 67). On top of the column a girder is realized, these will function as a support for the upper deck. The deck self is constructed with prefab elements and after placement they will be casted together.

Figure 67: Photo made during construction of the deck.

The upper part of the pile is filled with reinforced concrete. Here the connection between the concrete upper construction and the piles is made which is quite similar as the lower level connection. To support the loading arms a separate concrete girder is fabricated (see Figure 68). For every two loading arms one girder is made.
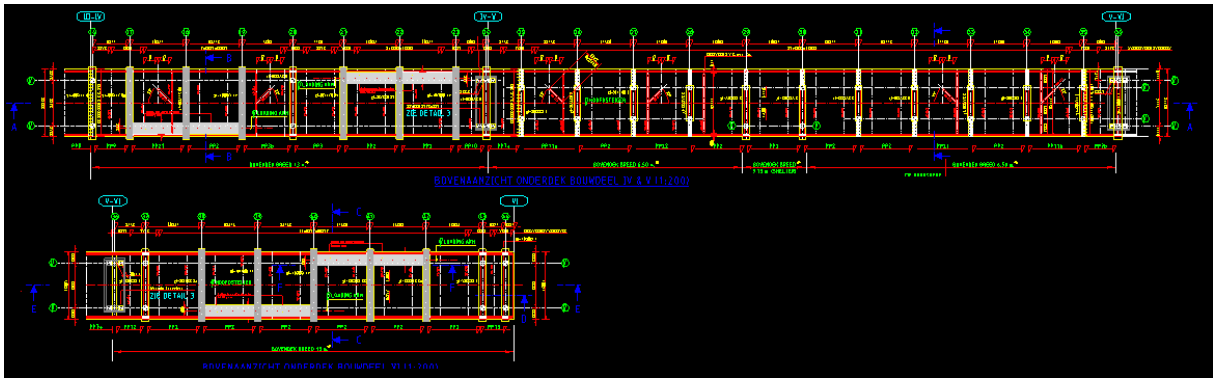
Figure 68: jetty overview, with the supporting beams (grey) for the loading arms
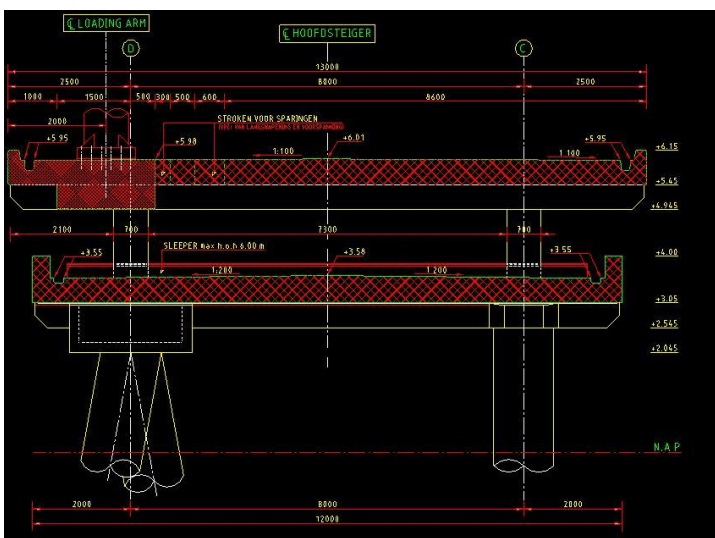
Figure 69: upper part of the fender construction in front of the jetty

C. Test calculations behavior of the transport pipes.

In this analyses the structure is schematized and build in the finite element software 'Scia engineer'. The deck is modeled as a ongoing beam over the length of the jetty. The piles are implemented in concrete girders. With this model the deck will not support the stiffness of the girders.

Construction dimensions:

- With*Thickness lower floor   :12.00*0.5   [m]
- With*Thickness upper floor (thin)   :6.50*0.5   [m]
- With*Thickness upper floor (wide)   :13.00*0.5   [m]
- Length steel pipes   : 35.65   [m]
- Section properties   :1219*14.2   [mm]

The steel pipes are clamped at the lower end and are all exact horizontal.

A load of 1000 kN is applied. This gives a deformation of 60 [mm] spread out over the total length of the jetty.

Beneath the horizontal displacement is shown, caused by the applied load.
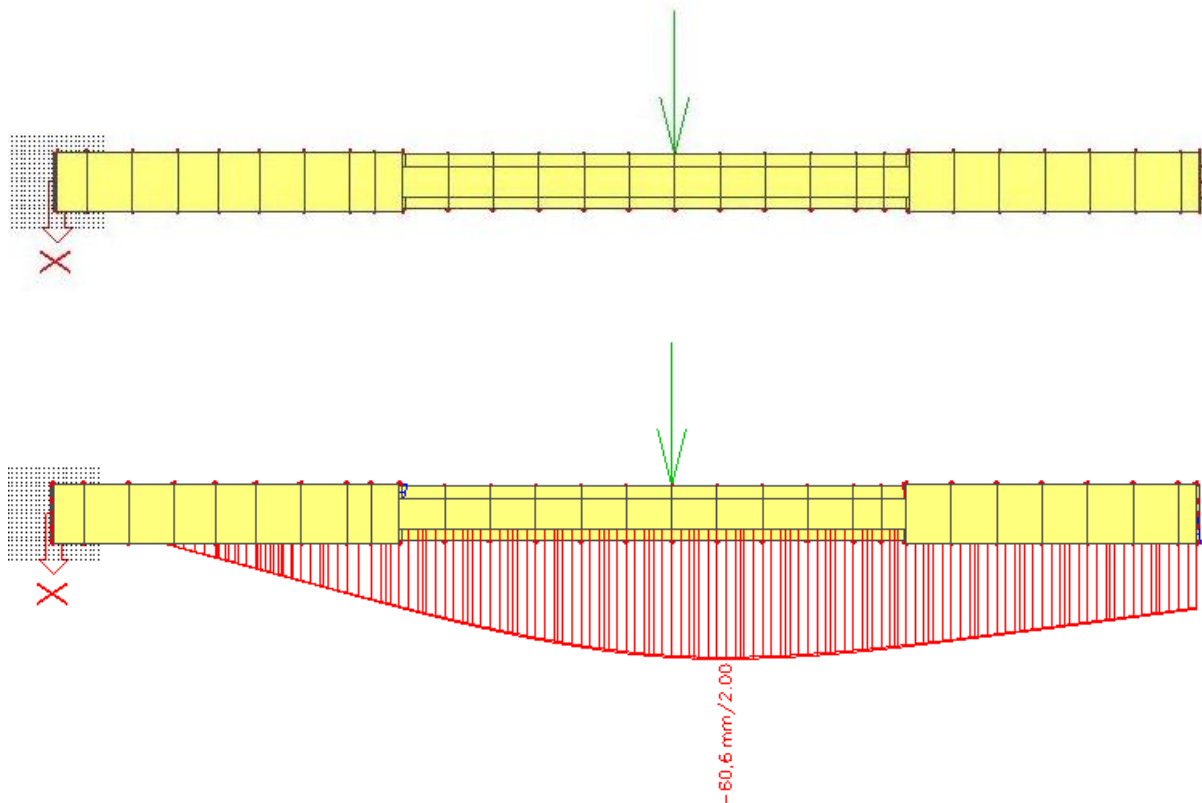
Behavior of a moored vessel

During the process of a berthing vessel, the vessel is subjected to a large of different elements. A large vessel is almost rudderless when at low speed [2.]. This is why the vessels are guided in the harbor self. Tugs are applied to keep the movements of the ship in line.
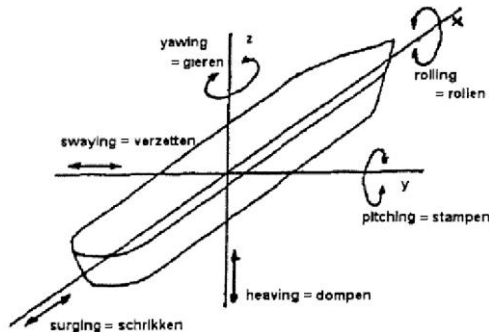
Figure 70: different degrees of freedom of a vessel

In the model the ship is assumed to be infinite stiff. The water is assumed to be a liquid with constant parameters of temperature, salt, sediment and has no elastic volume. Two equations can be established using the second law of Newton[1.]. To make an appropriate description of the movement it is important to know the external forces behavior in time. A force causes acceleration in line with the force. And due to exocentric forces a moment will be created.

This causes the following equations:

For translation:

$$m_s \frac{d^2 y}{dt^2} = F_{constructie} + F_{sleepboten} + F_{wind} + F_{stroming} + F_{hydrodinanisch}$$

For rotation:

$$I_s \frac{d^2 \psi}{dt^2} = M_{constructie} + M_{sleepboten} + M_{wind} + M_{stroming} + M_{hydrodinanisch}$$

D. Ship hydrodynamics

Wave forces

To derive the wave force[2.] computer computations are done with a model of a vertical elliptical cylinder with dimensions L_s, B and D as a constant. The wave force was determined for the longitudinal (X) and lateral (Y) direction.
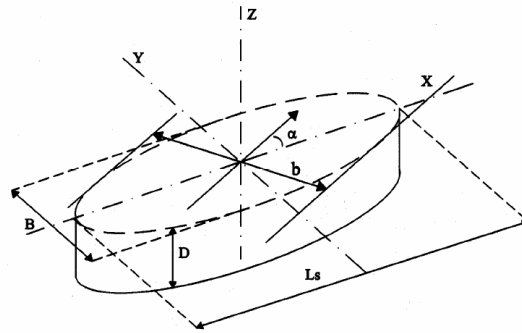
Figure 71: schematization of vessel with incident wave[2.]

The direction of the incident waves, with wave length L and height H, is taken a. Goda, 1972 has produced a graph were the coefficients of C_{mx} and C_{my} can be determined.

$$F_{x,\max} = C_{mx} \frac{\sinh(2\pi \frac{h}{L}) - \sinh(2\pi \frac{h-D}{L})}{\cosh(2\pi \frac{h}{L})} \frac{\pi \sin \alpha}{8} b^2 wH$$

$$F_{y,\max} = C_{my} \frac{\sinh(2\pi \frac{h}{L}) - \sinh(2\pi \frac{h-D}{L})}{\cosh(2\pi \frac{h}{L})} \frac{\pi \sin \alpha}{8} b^2 wH$$

in which:

C_{mx} C_{my} = virtual mass coefficients [-]

H   = water depth at the berth location [m]

b   = sheltering width in the wave direction [m] (B+(L$_s$-B)sin a

w   = specific weight of seawater (=10.25 [kN/m^3])

Current forces

The current forces on a vessel are proportional to the cross-sectional area under water and the average current velocity squared. The coefficient C depends on the angle of current direction with the ship axis, the keel clearance, the shape of the ship bow. Example of the ship bow is a conventional or a bulbous bow.

Forces of the currents on the vessel

$$F_{xc} = C_{xc} (\frac{\rho_w}{7600}) V_c^2 DL_{pp}$$

$$F_{yFc} = C_{yFc}\left(\frac{\rho_w}{7600}\right)V_c^2 DL_{pp}$$

$$F_{yAc} = C_{yAc}\left(\frac{\rho_w}{7600}\right)V_c^2 DL_{pp}$$

in which:

C_{xc} = longitudinal current force coefficient
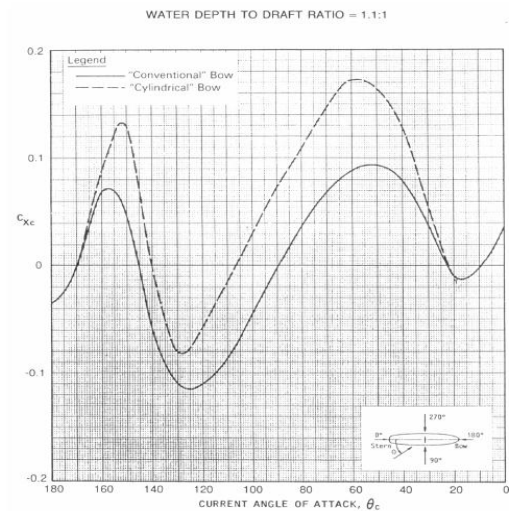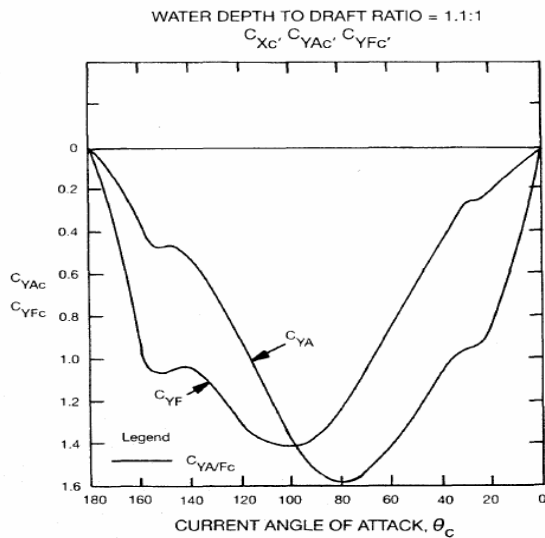
C_{yFc} = transverse current force coefficient force

C_{yAc} = transverse current force coefficient aft

ρ_c =density of sea water (=1025 [kg/m^3])

V_c = average current velocity over the under water part of the keel [kn]

D   = ship draught (for condition considered)

The values of the current force coefficient are produced on base of experiments and are found in the OCIMF publication "Prediction of wind and current loads on VLCC's (1977).

Figure 72: Left: lateral current force coefficient at the forward and aft perpendiculars loaded tanker and Right: Longitudinal current force coefficient, loaded tanker

Wind forces

A port is an open area where the wind founds hardly any obstacle. During the mooring process the wind can influence the vessel in his way to the berthing place. The vessel has to be corrected to avoid drifting and rotating.

The wind forces[2.] are calculated with

$$F_{xw} = C_{xw}(\frac{\rho_w}{7600})V_c^2 A_T$$

$$F_{yFw} = C_{yFw}(\frac{\rho_w}{7600})V_c^2 A_T$$

$$F_{yAW} = C_{yAw}(\frac{\rho_w}{7600})V_c^2 A_T$$

in which:

F_{xw}	= longitudinal wind force	[kN]
F_{yFw}	= lateral wind force fore	[kN]
F_{yAw}	= lateral wind force aft	[kN]
C_{xw}	= longitudinal wind force coefficient	[-]
C_{yFw}	= lateral wind force coefficient fore	[-]
C_{yAw}	= lateral wind force coefficient aft	[-]

ρ_w = density of air (1.223)   [kg/m^3]

V_w = wind velocity at 10 m elevation   [kn]

A_T = transverse above water area   [m^2]

A_L = longitudinal above water area   [m^2]

The coefficients and the forces are depended on the size and the shape of the area of the vessel that is above the seawater. In the graphs below the coefficients are shown (Figure 73 and Figure 74) .
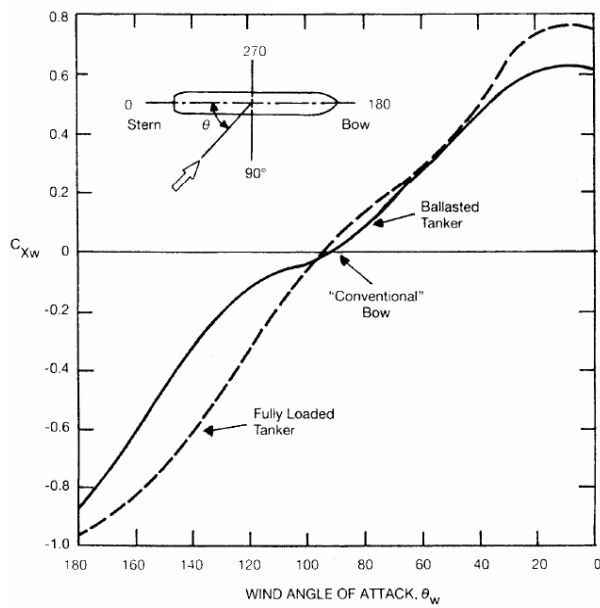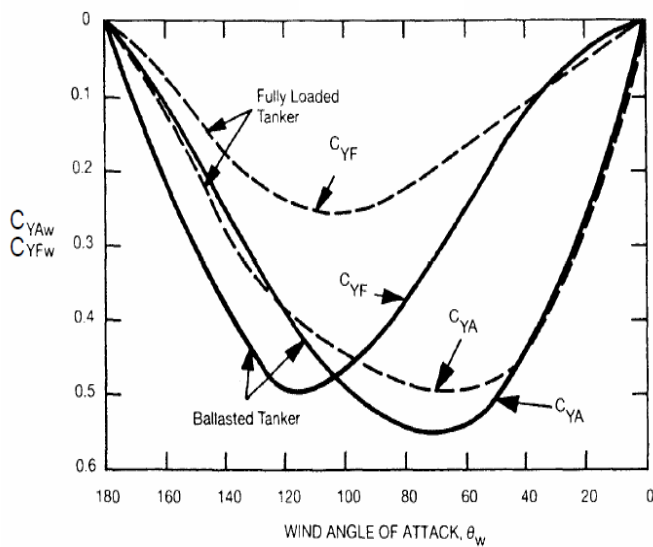

Figure 73: longitudinal wind force coefficient

Figure 74: Lateral wind force coefficient at the forward and aft perpendiculars

E. Basic maneuverability

The dimensions within a port are relatively small comparing to the vessels. Accurate maneuvering of the vessel is necessary in order to prevent damage. Earlier this chapter is found that a large vessel is almost rudderless when at low speed. The vessels maneuvering characteristics are determined by several properties belonging to the vessel. The maneuvering ability[2.] is determined by the ship's hull shape, the rudder system and dimensions, its mass, the propulsion system and the power.

The maneuvering characteristics are:

- The vessel reaction to the rudder and to changes in propeller revolutions
- Turning ability
- Stopping ability

These maneuverability are very complicated to describe and are not taken in account in this investigation. But are discussed in the following paragraphs to understand the whole process.

Rudder efficiency
When the rudder is turned while sailing, the vessel will experience a moment. The flow of the propeller will increase the influence of the rudder. The length/beam ratio and the block coefficient together with the beam/draft ratio, the mass/propulsive power and the rudder area determine the maneuvering characteristics.

The lecture notes[2.] give a definition of the dynamically unstable and stable condition. When a vessel experiences a moment by the rudder and counteracts the movement of the ship caused by the initial disturbance, a vessel has a dynamical stable condition. When the vessel continues turning even after a new equilibrium has been reached, the condition is called dynamical unstable.

Turning maneuver
By the use of twin propeller arrangement or bow thrusters or a combination of the two the turning capability at low speed is improved. The operation of the rudder is influenced by the screw and vice versa.

Stopping distance
There are several influences when a ship is coming to a halt which determine the accuracy and the distance. The stopping distance[2.] is affected by:

- The size of the vessel and the relation propulsive power-displacement (mass)
- The speed at which the vessel starts the procedure
- The kind of stopping procedure
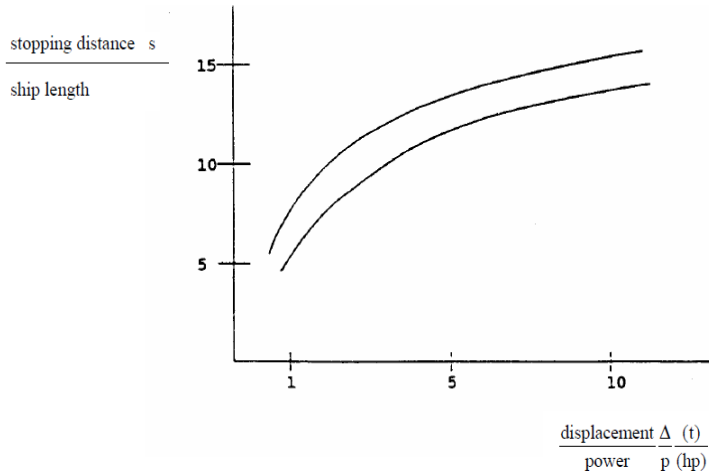
Figure 75: relation of stopping distance and length of the ship to displacement and engine power

Relatively the power available of decelerating decreases with the increasing ship size. Also the astern power depends on the system that is used in the vessel (see Figure 75).

The two extreme stopping procedures are the crash stop and the fully controlled stop. In the crash stop, the distance is relatively short. But there is no prediction of the course of the vessel. In the fully controlled stop the course of the vessel is relatively known but the distance is very long. See results of experiment below (Figure 76).

number		A2	A3	A4	A5	A6	A7	A8	A9	J1	J2	J3
rudder	deg.	0	0	0	0	0	0	0	0	30	30	30
speed	kt	9	4.9	14.8	4.2	15	2.4	13	5	16.2	11	14.4
revs		55.2	31.6	85.4	31	83	33.4	77.1	32	85.8	63.4	84
ast. revs		42	44.7	42.5	48.8	47.5	46.7	48.3	48.3	42.9	47.7	47.6
h/T		∞	∞	2.1	2.2	1.7	1.5	1.3	1.4	∞	∞	1.7
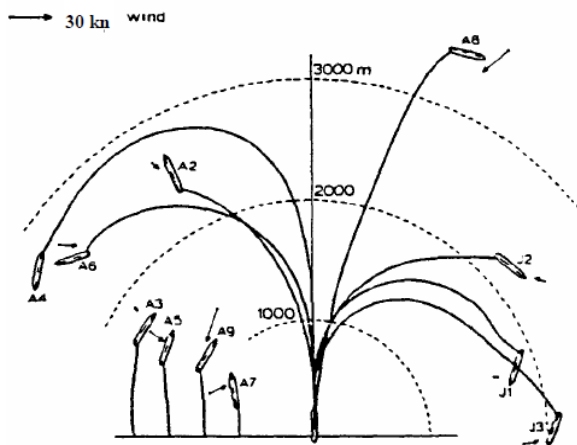
Figure 76: published in IAHP, 1981 'stopping manoeuvres of tanker MAGDALA, 220.000 [dwt]'[2.]

F. Soil Model

Plastic springs

In the approach Verruijt developed the elastic part is minimized, like the originally developed by Blum (1931).
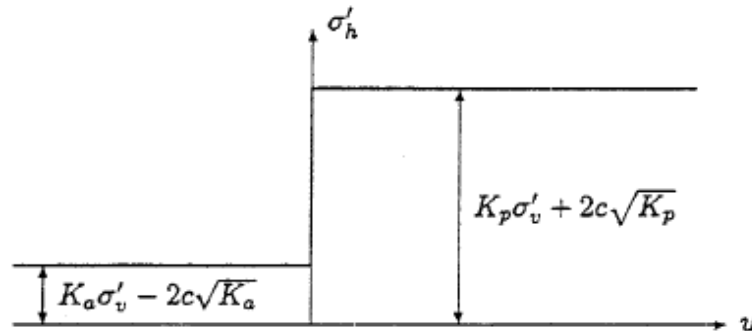

Figure 77: perfectly plastic soil response

With any displacement the response will be either maximum or minimum. When a force is applied on a pile as in the situation below, the response is given by:

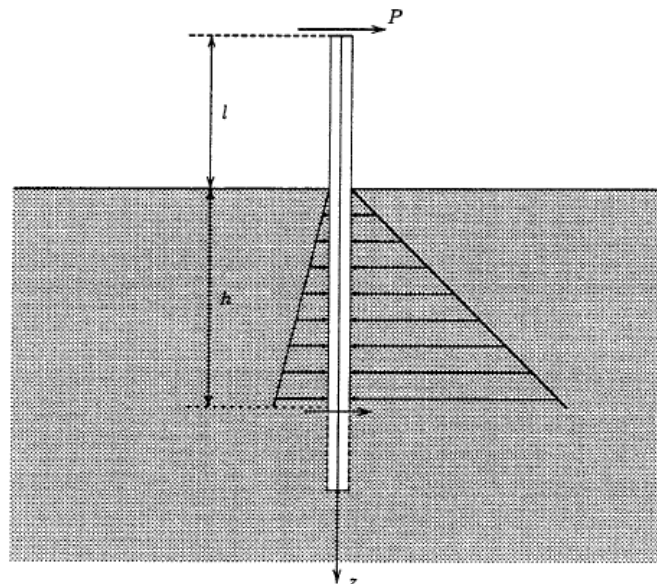$$f = -(K_p - K_a)D\sigma'_v - 2cD(\sqrt{K_p} + \sqrt{K_a})$$

Figure 78: Blum's schematization

When the influence of depth is taken in to account, the function of the vertical effective stress increases linearly with depth.

$$f = -(K_p - K_a)D\gamma'z - 2cD(\sqrt{K_p} + \sqrt{K_a})$$

γ'=10 kN/m², this is the submerged unit weight of the soil.

As is shown in the figure a force is applied on the top of the pile, towards the right. This will give a displacement of the pile to the right. Because of the soil reaction forces, equilibrium will occur, where the displacement is zero. Because of the angular distortion the lower part of the pile will deform towards the left.

The differential equation is, assuming that the soil is cohesion less sand (c=0).

$$EI\frac{d^4u}{dz^4} = f = -(K_p - K_a)D\gamma'z$$

The three dimensional effects are taken into account by taking the width D somewhat larger.

At the value of parameter h, where the pile is clamped is unknown.

The boundary conditions in z direction are:

z = 0: $Q = -EI\frac{d^3u}{dz^3} = -P$ z =h: $u = 0$

z =0: $M = -EI\frac{d^2u}{dz^2} = -Pl$ z =h: $\frac{du}{dz} = 0$,

z =h: $\frac{d^2u}{dz^2} = 0$

The general solution of the differential equation is:

$$u = \frac{\sigma_0 z^5}{120EI} + C_1 z^3 + C_2 z^2 + C_3 z + C_4$$

where σ₀=(Kp-Ka)γ'D

The integration constants can be determined from the boundary conditions.

Boundary conditions:

$$C_1 = \frac{P}{6EI}, \quad C_2 = \frac{Pl}{2EI}$$

follows from the fifth boundary condition:

$$P = \frac{\sigma_0 h^2}{6(1 + l/h)}$$

when this equation is rewritten:

$$\sigma_0 h^2 = 6P(1 + l/h)$$

It now follows from the first and second boundary conditions that

$$C_3 = \frac{-Ph(h + 3l)}{4EI}$$

$$C_3 = \frac{Ph^2(4h + 9l)}{30EI}$$

When the parameters are entered in the general solution

z =0: $u = u_0 = \dfrac{Ph^2(4h + 9l)}{30EI}$ z =0: $\phi = \phi_0 = -\dfrac{du}{dz} = \dfrac{Ph(h + 3l)}{4EI}$

The displacement of the top of the pile (for z=-l) consists of three terms,

z =-l: $u = u_t = u_1 + u_2 + u_3 = u_0 + \phi_0 l + \dfrac{Pl^3}{3EI}$

Using the method of Brinch Hansen[11.] the cohesion has to be replaced for a notional value of cohesion, given by the equation:

$$c_{fic} = c * \frac{K_c}{2 * \sqrt{K_{a,p}}}$$

The values of K_q and K_c are derived from the graphs created by Brinch Hansen (see graphs below).
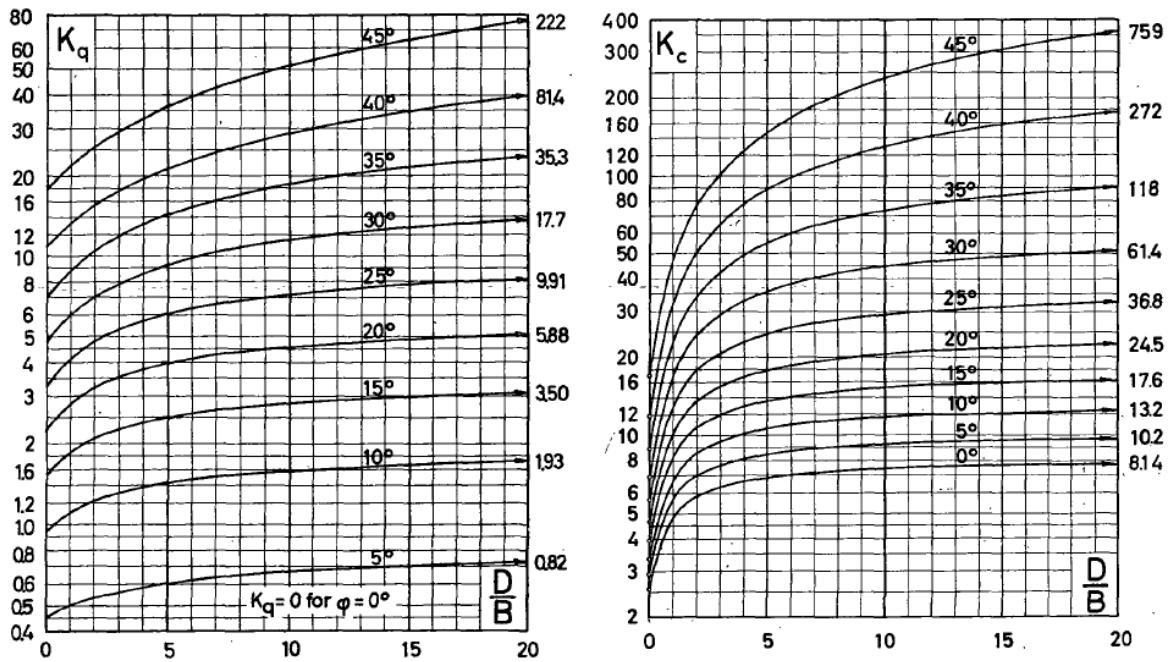
Figure 79: Earth pressure coefficient for overburden pressure (left) and Earth pressure coefficient for cohesion (right)[12.]

G. Consolidation theory

The berthing of a vessel can be considered as relative short and sudden loading. Due to sudden loading of wet soil, the deformation can be delayed caused by a volume reduction in which the contained water is pushed out, this is called consolidation. Instead of describing the soil deformation only as a function of stress the behavior of soil has then an obvious time depended element (Grondmechanica, A.Verruijt, S. Baars, 2004).. This consideration will be limited to an brief and one dimensional case. The elastic coefficient is assumed to be linearly elastic. Therefore it is assumed that the amount of stress difference is very small.

The grains are assumed non compressible so the volume of soil is only reduced when the porosity is reduced or by extracting water. In theory the consolidation process is an infinitely long process . In practice only the 99% of the settlement is reached. In this case:

$$t_{99\%} = \frac{1.784h^2}{c_v} \approx \frac{1.8h^2}{c_v} = \frac{1.8h^2(m_v + n\beta)\gamma_w}{k}$$

In which

c_v Consolidation coefficient

k Permeability coefficient $k = \gamma_w m_v c_v$

m_v Compressibility coefficient $\quad m_v = \dfrac{\Delta h_\infty}{hq}$

Δh_∞ Infinite settlement

The elastic coefficient is assumed to be linear elastic. There for it is assumed that the amount of stress difference is very small.

The strain and stress relation is written as:

$$\varepsilon = m_v \sigma'$$

with $m_v = \dfrac{1}{E_{oed}}$

considered the elementary volume V of soil. Within the volume of water:

$$V_w = nV$$

In which:

n   porosity

the volume of grains

$$V_k = (1-n)V$$

The grains are assumed to be non compressible. From this the volume of the soil is only reduced when the porosity is reduced. The whole problem can be split in to two problems.

The first possibility for volume reduction is compression of the water as a function of the water pressure.

$$\Delta V_1 = \beta V_w \Delta p = \beta n V \Delta p$$

In which the β is the compressibility of water. Water is considered as almost incompressible (β=0.5*10^{-9} [m^2/N]).

The second possibility of volume change due to extracting of water. As a function of time:

$$\Delta V_2 = (\nabla * q)V\Delta t = (\frac{\partial q_x}{\partial x} + \frac{\partial q_y}{\partial y} + \frac{\partial q_z}{\partial z})V\Delta t$$

When $\nabla * q$ is taken positive the water is flowing out of the taken volume of soil.

The change of volume strain in a time mote:

$$\Delta \varepsilon_{vol} = \frac{\Delta V}{V} = \frac{\Delta V_1 + \Delta V_2}{V} = n\beta\Delta p + (\frac{\partial q_x}{\partial x} + \frac{\partial q_y}{\partial y} + \frac{\partial q_z}{\partial z})\Delta t$$

When the time is taken out of the right term the storage equation is retained:

$$\frac{\partial \varepsilon_{vol}}{\partial t} = n\beta\frac{\partial p}{\partial t} + (\frac{\partial q_x}{\partial x} + \frac{\partial q_y}{\partial y} + \frac{\partial q_z}{\partial z})$$

Using the law of Darcy the equation can be turned in:

$$\frac{\partial \varepsilon_{vol}}{\partial t} = n\beta \frac{\partial p}{\partial t} + \nabla(\frac{k}{\gamma_w}(\frac{\partial p_x}{\partial x} + \frac{\partial p_y}{\partial y} + \frac{\partial p_z}{\partial z}))$$

To solve this three dimensional equation the equilibrium-, the compatibility- and the kinematic equation as well the initial and the boundary conditions has to be known.

To make equilibrium:

$$(\frac{\partial \sigma_{xx}}{\partial x} + \frac{\partial \sigma_{yx}}{\partial y} + \frac{\partial \sigma_{zx}}{\partial z}) - f_x = 0$$

$$(\frac{\partial \sigma_{xy}}{\partial x} + \frac{\partial \sigma_{yy}}{\partial y} + \frac{\partial \sigma_{zy}}{\partial z}) - f_y = 0$$

$$(\frac{\partial \sigma_{xz}}{\partial x} + \frac{\partial \sigma_{yz}}{\partial y} + \frac{\partial \sigma_{zz}}{\partial z}) - f_z = 0$$

Introducing the related to the compression modulus (K) and shear modulus (G), λ and μ elastic coefficient of the material (Lamé's constants).

$$\lambda = K - \frac{2}{3}G \text{ and } G = \mu$$

Using the law of Hooke and taken as an isotropic material

$$\sigma'_{xx} = -\lambda \varepsilon_{vol} - 2\mu \varepsilon_{xx}, \ \sigma'_{xy} = -2\mu \varepsilon_{xx}, \ \sigma'_{xz} = -2\mu \varepsilon_{xx}$$

$$\sigma'_{yy} = -\lambda \varepsilon_{vol} - 2\mu \varepsilon_{yy}, \ \sigma'_{yz} = -2\mu \varepsilon_{yz}, \ \sigma'_{yx} = -2\mu \varepsilon_{yx}$$

$$\sigma'_{zz} = -\lambda \varepsilon_{vol} - 2\mu \varepsilon_{zz}, \ \sigma'_{zx} = -2\mu \varepsilon_{zx}, \ \sigma'_{zy} = -2\mu \varepsilon_{zy}$$

The volume strain is given by:

$$\varepsilon_{vol} = \frac{\Delta V}{V} \varepsilon_{xx} + \varepsilon_{yy} + \varepsilon_{zz}$$

In case of a homogenous material $\nabla^2 = \frac{\partial^2}{\partial x} + \frac{\partial^2}{\partial y} + \frac{\partial^2}{\partial z}$:

$$(\lambda + \mu)\frac{\partial \varepsilon_{vol}}{\partial x} \mu \nabla^2 u_x + f_x - \frac{\partial p}{\partial x} = 0$$

$$(\lambda + \mu)\frac{\partial \varepsilon_{vol}}{\partial y} \mu \nabla^2 u_y + f_y - \frac{\partial p}{\partial y} = 0$$

$$(\lambda + \mu)\frac{\partial \varepsilon_{vol}}{\partial z} \mu \nabla^2 u_z + f_x - \frac{\partial p}{\partial z} = 0$$

The boundary condition are the pressure and the three components of the deformation at time (t). This leaves 4 equations and 4 unknown. This can be solved.

Undrained deformations

When the soil layer is poorly permeable, the deformation will be undrained. The water can flow away fast enough and the pores between the grains can't reduce in volume. In this case the storage equation can be integrated over a small time window:

$$-\frac{\partial \varepsilon_{vol}}{\partial t} = n\beta \frac{\partial p}{\partial t} + (\frac{\partial q_x}{\partial x} + \frac{\partial q_y}{\partial y} + \frac{\partial q_z}{\partial z})$$

This will become

$$\Delta \varepsilon_{vol} = n\beta\Delta p + \int_0^{\Delta t} (\frac{\partial q_x}{\partial x} + \frac{\partial q_y}{\partial y} + \frac{\partial q_z}{\partial z})dt$$

The because of the small time window the second term can be neglected (order Δt). Because we assume that the volume strain and pressure just slightly differ over time:

$$-p = \frac{\varepsilon_{vol}}{n\beta}$$

Using this equation, will lead to the equilibrium equation:

$$(\lambda^* + \mu)\frac{\partial \varepsilon_{vol}}{\partial x} + \mu\nabla^2 u_x + f_x = 0$$

$$(\lambda^* + \mu)\frac{\partial \varepsilon_{vol}}{\partial y} + \mu\nabla^2 u_y + f_y = 0$$

$$(\lambda^* + \mu)\frac{\partial \varepsilon_{vol}}{\partial z} + \mu\nabla^2 u_z + f_z = 0$$

With $(\lambda^* = \lambda + 1/n\beta)$

The total of pressure and deformation shall be written according the elasticity theory but the λ has to be replaced with λ*. The other coefficients are still the same. The compression modulus (K) and shear modulus (G):

$$K^* = K + \frac{1}{n\beta} \text{ and } G^* = G$$

When the water and the grains are taken as incompressible and the soil is loaded fast, the soil becomes incompressible.

H. Poulos

Poulos developed influence factors for the displacement and rotation at the top of a pile in a uniform semi-infinite elastic mass [14.]. Based on integral calculations where the interaction is based on the elasticity modulus of the soil, the axial and bending stiffness of the pile and the position of the piles. In this method the displacements, strains, and stresses are expressed in terms of integrals of products of trigonometric functions [16.].

For instance the eventual displacement of the pile heads of a group of fixed piles is the sum of their own displacement and the sum of the interaction effects[4].
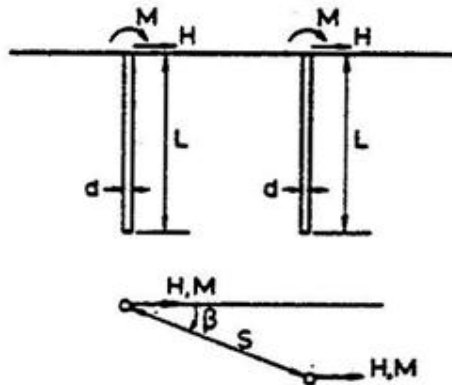

Figure 80: schematization of the piles

The horizontal displacement of a pile 'i', for free headed piles, in a group of k piles is given:

$$\rho_i = \rho_h (\sum_{\substack{j=1 \\ j\neq 1}}^{k} H_j \alpha_{\rho Hij} + H_i) + \rho_M (\sum_{\substack{j=1 \\ j\neq i}}^{k} M_j \alpha_{\rho Mij} + M_i)$$

in which:

H_j =horizontal load in pile j

$\alpha_{\rho Hij}$ =value of $\alpha_{\rho H}$ for spacing and value of β between piles i and j

ρ_H =horizontal movement of single pile due to unit applied horizontal load

M_j =moment in pile j

α_{MHij} =values of $\alpha_{\rho M}$ for spacing and values of β between piles i and j

ρ_M =horizontal movement of single pile due to unit applied moment

For this method a pile is schematized as it was a stroke with a bending stiffness (see Figure 80). Because of this the shear stresses along the pile are neglected. The paper in the 'geotechniek' makes any comments on the method Poulos[14.] in an elastic medium:

- The method is developed for pile groups with a little distance centre to centre.
- The method provides values only at the pile head, along the pile shaft there are no values given.
- A pile is schematized as it was a strip with a bending stiffness. The shear stresses along the pile are neglected. This results into deviations up to 20 [%] in soil pressure.
- The method is based on fully elastic behaviour. With a symmetrical pile group there is no difference found between the piles in the front or the one at the back.
- It is not possible to simulate more than two layers.
- Only forces that are in the load plane are considered. This approach is approximate because of the spreading of load in the soil to the other poles, there will arise forces perpendicular to the direction of loads. In the maximum moment this will cause deviations up to 20%.
- The method can only be applied to flexible piles. A considerable length of the pile has to be free of influence of the moved pile head.
- When higher forces and larger deformations are applied the soil still reacts elastic.

Plasticity

Later a method was developed to take the plasticity in to account as well. Focht and Koch [14.] added a plasticity factor in the original displacement equation (see Figure 81). The horizontal displacement of a pile 'i', for free headed piles, in a group of k piles with plasticity effects added is given by:

$$\rho_i = \rho_h (\sum_{\substack{j=1 \\ j \neq 1}}^{k} H_j \alpha_{\rho Hij} + H_i) + P_{Hi} H_i + \rho_M (\sum_{\substack{j=1 \\ j \neq i}}^{k} M_j \alpha_{\rho Mij} + M_i)$$

in which:

H_j =horizontal load in pile j

$\alpha_{\rho Hij}$ =value of $\alpha_{\rho H}$ for spacing and value of β between piles i and j

ρ_H =horizontal movement of single pile due to unit applied horizontal load

M_j =moment in pile j

α_{MHij} =values of $\alpha_{\rho M}$ for spacing and values of β between piles i and j

ρ_M =horizontal movement of single pile due to unit applied moment

P_{Hi} =plasticity factor

A zone just around the pile has a plastic reaction. This plastic factor reduces the stiffness of the pile and furthermore of the whole pile group.

To calculate the whole deformation the separate contributions of the elastic and plastic influence, will be calculated and added together.
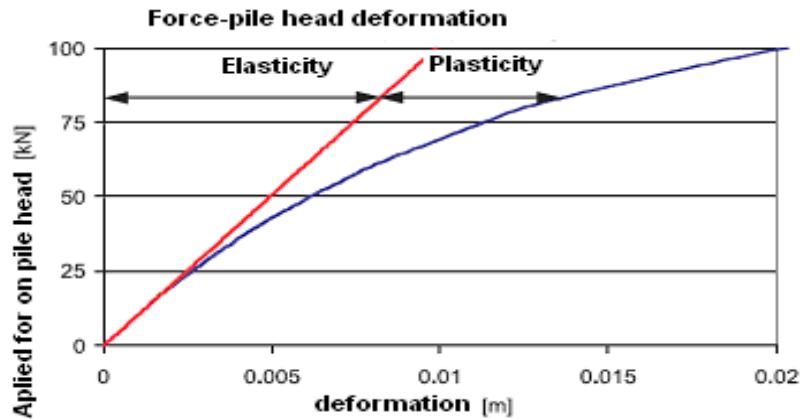
Figure 81: plasticity effects according to Focht and Koch for a single pile

The paper in the 'geotechniek' makes some comments on the method Poulos [14.] in a elastic medium with plastic factor:

- In the original article of Focht and Koch the factors are actually not really compatible with the Poulos method.
- The factor reduces strength and stiffness over the whole length equal. This is not realistic.
- For small loads the soil behaviour is entirely elastic. Plasticity only occurs with high loads and only very locally. The surrounding piles only feel the elastic deformation.

I. P-Y curve

To make use of the elastic track that soil has, the use of P-Y curves is recommended. The **PIANCError! Reference source not found.** recommends for pile analysis in an elastic approach the use of p-y curves according to the 'American Petroleum Institute' standards (Or when there is enough specific soil data fabricated a three dimensional finite element model).The same method is used by the NEN-EN ISO 19902.

In the NEN-EN ISO 19902 a distinction is made in three different types of soil. The types of soil described here are 'sand soil', 'soft clay' and 'stiff clay'.

The soundings (see annex), made for the original Lyondell jetty, show that the ground is not homogeneous. So instead of only one type of soil all the layers shall have to be considered.

Sand soil

In this method it is assumed the strength of sand is depth depended. According to Reese, Cox and Koop[11.](1974) the soil behaviour can be modelled by a force-displacement graph.

There is assumed that two failure mechanisms will occur:

- a wedge of soil provides a horizontal resistance. A straight sliding surface is assumed.
- The soil flows around the pole to the sides where a gap is likely to occur as a result of horizontal displacement.

It is possible to calculate the depth where both mechanisms equal each other.

The determination of the representative capacity of sand soil makes distinction of deep and shallow depth.

For shallow

$$p_{rs} = (C_1 X + C_2 D)\gamma' X$$

For deep

$$p_{rd} = C_3 D\gamma' X$$

In which

s   Signifies shallow

d   Signifies deep

p_r The representative lateral capacity in units of force per unit length

γ' The submerged unit weight of soil

X   The depth below the sea floor

$C_1, C_2,$

C_3 Dimensionless coefficients

D   Pile diameter

$$C_1 = \tan\alpha\tan\beta(\frac{\tan\beta}{\tan(\beta-\varphi)} - K_0) + K_0\sin\beta\tan\varphi(\frac{\cot(\beta-\varphi)}{\cos\alpha} + \tan\beta)$$

$$C_2 = \frac{\tan\beta}{\tan(\beta-\varphi)} - K_a$$

$$C_3 = K_a(\tan^8\beta - 1) + K_0\tan\varphi\tan^4\beta$$

With

$$K_a = \tan^2(45^0 - \varphi/2)$$

$$K_0 = 0.4$$

$$\beta = 45^0 - \varphi/2$$

$$\alpha = \varphi/2$$

Φ   Angle of internal friction [^{0}]
X   Depth below soil surface [m]
D_H Average pile diameter from surface to depth X [m]
γ'   Effective unit weight of the soil [kN/m^3]

The lateral soil resistance and the associated displacement is a non-linear relation and can be approximated, for any specific depth, with the equation:

$$p = A * p_r \tanh(\frac{k * X}{A * p_r} * y)$$

In which:

A   Factor to make distinction between static and cyclic actions

$$A = (3.0 - \frac{0.8X}{D}) > 0.9 \text{ for static actions}$$

$$A = 0.9 \text{ for cyclic actions}$$

p_r Representative lateral capacity at depth X in units of force per unit of length

k
per   Rate of increase with depth of the initial modulus of sub grade reaction, in units of force volume (see **Error! Reference source not found.**).

X   The depth below the sea floor.

y   Lateral displacement at depth X

ϕ'	k	
	MN/m³	(lb/in³)
25°	5,4	(20)
30°	11	(40)
35°	22	(80)
40°	45	(165)

Figure 82: Rate of increase with depth of initial modulus of sub grade reaction[3]

Soft clay

The failure lateral actions of soft clay, when charged with statically forces is assumed to be between $8C_uD$ and $12C_uD$. Cyclic actions cause a reduction of the lateral capacity as compared to static forces.

As the depth increases from 0 to X_R, p_r will increase from $3c_uD$ to $9c_uD$

Calculating the force in shallow depth ($X<X_R$)

$$p_r = 3*c_u*D = p_o'*D + J*c_u*X$$

Calculating the reaction force in deep soil ($X>X_R$)

$$p_r = 9*c_u*D$$

in which:

p_R The representative lateral capacity, in units of force per unit length

c_u The undrained shear strength of undisturbed clay soil samples, in stress units

D   The pile diameter

P_o' The effective overburden stress at depth, X.

J   A dimensionless empirical constant with values ranging form 0.25 to 0.5. (common taken 0.5)

X   Depth below the sea floor

X_R Depth below the sea floor to the bottom of a reduced resistance zone for uniform soils

The shallow soil reacts different than the more deeper soil, and the depth can be calculated

$$X_R = \frac{6c_u D}{\gamma' D + Jc_u}$$

In which:

γ' Submerged unit weight of soil in weight density units

According a rule of thumb can be assumed that X_R is at least 2,5 times the pile diameter.

Like the sand curve the clay strength curve is not linear. For statically forces the resistance will first be high and decreases when deformation increases.

For dynamic loads the strength will increase with the depth. Below the depth of X_R the strength will be constant.

p/p_r	y/y_c
0.00	0.00
0.23	0.1
0.33	0.3
0.50	1.0
0.72	3.0
1.00	3.0
1.00	∞

Table 26: mobilized lateral resistance-displacement data for short-term static actions

$X > X_R$		$X < X_R$	
p/p_r	y/y_c	p/p_r	y/y_c
0	0	0.0	0
0.23	0.1	0.23	0.1
0.33	0.3	0.33	0.3

0.50	1.0	0.50	1.0
0.72	3.0	0.72	3.0
0.72	∞	0.72X/X_R	15.0
		0.72X/X_R	∞

Table 27: Mobilized lateral resistance-displacement data for equilibrium conditions of cyclic actions

In which:

X   Depth below sea floor

X_R Depth below the sea floor to bottom of reduced resistance zone for uniform soils

p_r Representative lateral capacity, units of force per unit length

p   Mobilized lateral resistance, units of force per unit length

y   Local lateral displacement

y_c 2.5 ε_c D

D   Pile diameter

ε_c Strain at one-half maximum deviator stress in laboratory undrained compression tests of undisturbed soil samples.

Stiff clay

The representative unit lateral capacity, p_r, of stiff clay is similar to that for soft clay. Stiff clay (c>96 kPa) has also a non-linear stress strain relationship as the soft clay does. Only stiff clay is more brittle than soft clay is. This will lead to possibly fast deterioration of the lateral capacity at large displacements and cyclic actions. For this the representative lateral capacity shall be reduced[19.].
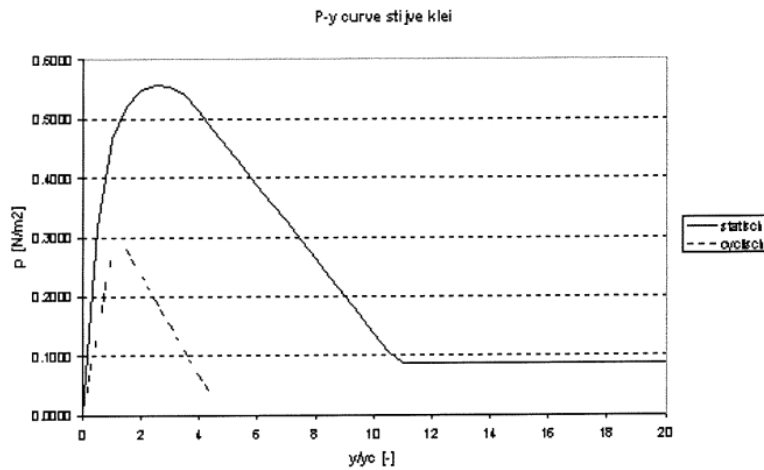
Figure 83: p-y curve of stiff clay[5.]

But in the origenal paper p-y curve is found for stiff clay (see Figure 19)[5.]. The ultimate soil resitance at the surface is described as a function of

$$p_{ct} = 2c_{u,gem}D_{paal} + \gamma' D_{paal}H + 2,38c_{u,gem}H$$

The soil will be pushed out as a wedge at the surface.

At a surten depth the stresses near the pile are as high that the soil will fail and the soil will "flow" horizontally around the pile:

$$p_{c2} = 11c_{u,gem}D_{paal}$$

The undrainded shear force, in the equation, is given at a surten depth. As with sand the lowest of the two equations is hte normative ultimate strength of the soil. The calculated values are somewhat higher then the values of the experiments. This is why is the ultima emperical strength is adjusted. The observed ultimate strength is divided by the calculated ultimate strength:

$$A = \frac{(p_u)_s}{p_c} \quad \text{and} \quad B = \frac{(p_u)_c}{p_c}$$

Wher A is included for statical loads and B for cyclic loads.

To make it possible to describe the behavior analytical, the track is diveded in a couple pieces.

The p-y curve of stiff clay for static load can be described with the following expresion:

$$p = 0.5p_c(\frac{y}{y_c})^{0.5} \quad \text{for} \quad y < Ay_c$$

$$p = 0.5p_c\left(\frac{y}{y_c}\right)^{0.5} - 0.055p_c\left(\frac{y - Ay_c}{Ay_c}\right)^{1.25} \qquad Ay_c < y < 6Ay_c$$

for

$$p = 0.5p_c(6A)^{0.5} - 0.411p_c - \frac{0.0625}{y_c}p_c(y - 6Ay_c) \qquad 6Ay_c < y < 18Ay_c$$

for

$$p = 0.5p_c(6A)^{0.5} - 0.411p_c - 0.75p_cA \qquad 18Ay_c < y$$

for

A P-y curve for stiff clay under cyclic loading is expreced:

$$p = kxy \qquad 0 < y < 0.45y_p$$

for

In which the stiffness of k is read from the table

Mean undraind shear force [kN/m^2]	53-106	106-211	211-422
K_s (static) [kN/m^3]	$136*10^3$	$272*10^3$	$543*10^3$
K_s (cyclic) [kN/m^3]	$54*10^3$	$109*10^3$	$217*10^3$

Table 28: Stiffness of the statically and cyclic loading

And the value of y_c and y_p can be calculated with $y_c = \varepsilon_c D_{pile}$ in which ε_c is dependent of the undreamed shear strength and $y_c = 4.1 Ay_c$

Mean undrained shear strength [kN/m^2]	53-106 [kN/m^2]	106-211 [kN/m^2]	211-422 [kN/m^2]
ε_c [-]	0.007	0.005	0.004

Table 29: Stiffness of the statically and cyclic loading

$$p = Bp_c\left(1 - \left(\frac{y - 0.45y_p}{0.45y_p}\right)^{2.5}\right) \qquad 0.45y_p < y < 0.6y_p$$

for

$$p = 0.936Bp_c - \frac{0.085}{y_c}p_c(y - 0.6y_p) \qquad 0.6y_p < y < 1.8y_p$$

for

$$p = 0.936Bp_c - \frac{0.102}{y_c}p_cy_p \qquad 1.8y_p < y$$

for

Calculation modeling P-y curves

Calculating lateral loaded piles, M-pile uses the Matlock approach. For this method the soil resistance is described by a so-called "P-Y curve".

For vertical loads a comparable method is used. Using the T-Z curve and besides the "negative skin friction" is possible.

In the API, the P-Y curves for clay is given by a continues curve. The P-Y curve generated by M-Pile is modelled by five parallel elasto-plastic springs. The multi-linear spring characteristics are correct at displacements:

- $0.1 * y_{50}$
- $0.3 * y_{50}$
- y_{50}
- $3 * y_{50}$
- $8 * y50$

These points result in a approach of the continues P-Y curve (see figure below).
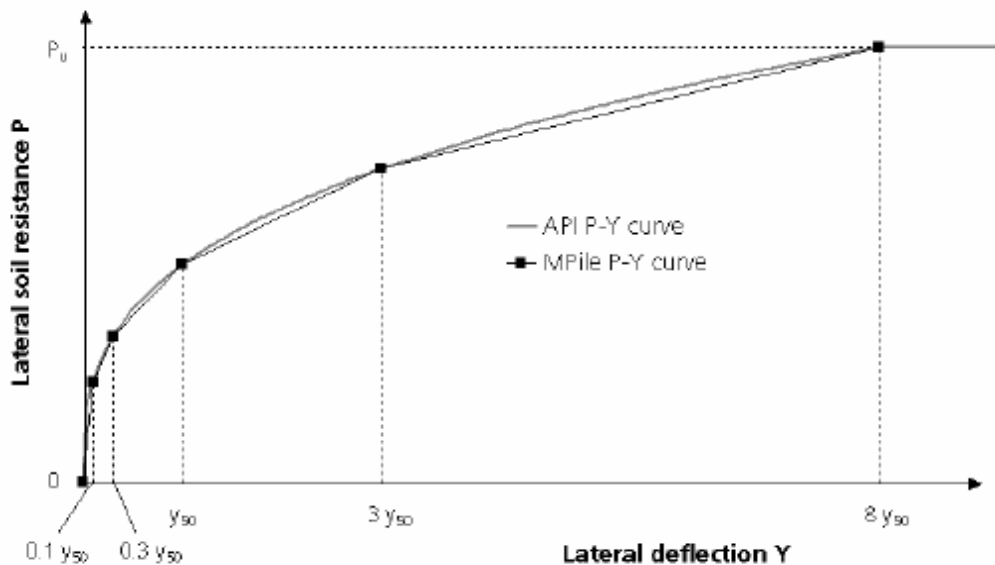

Figure 84: Modeling of the P-Y curve (API) for clay and static loading (M-Pile manual)

The points in the table are part of the continuous curve given by the formula:

$$p = 0.5 * p_u (y / y_{50})^{1/3} \; for : y < 8 * y_{50}$$

$$p = p_u \, for : y > 8 * y_{50}$$

In which:

P Actual lateral soil resistance at depth H [kN/m^2]

p_u Ultimate lateral soil resistance at depth H [kN/m^2]

y Actual lateral deflection [m]

y_{50} $2.5*\varepsilon_{50}*D$

ε_{50} Strain which occurs at one-half the maximum stress on laboratory undrained compression tests of undisturbed soil samples [-]

D Pile diameter [m]

Because the initial stiffness of the curve is relatively high compared to the stiffness at larger strains.

 These specific points result in a correct description of the stiffness at small strains. Which will influences the overall results.

C_u [kN/m^2]	ε_{50} [-]
5-25	0.020
25-50	0.010
50-100	0.007
100-200	0.005
200-400	0.004

Table 30: Determination of ε_{50} as a function of the un-drained cohesion

The P-Y curve for sand is also modeled by five parallel elasto-plastic springs.

The ultimate resistance p_u is calculated depth dependend. Therefore the shallow and deep behavior are compared and the smallest is taken into account.

These springs are chosen such that the resulting multi-linear spring characteristic is correct at displacements:

- $0.25*y_{max}$
- $0.5* y_{max}$

- y_{max}
- $1.5* y_{max}$
- $2.5* y_{max}$

With:

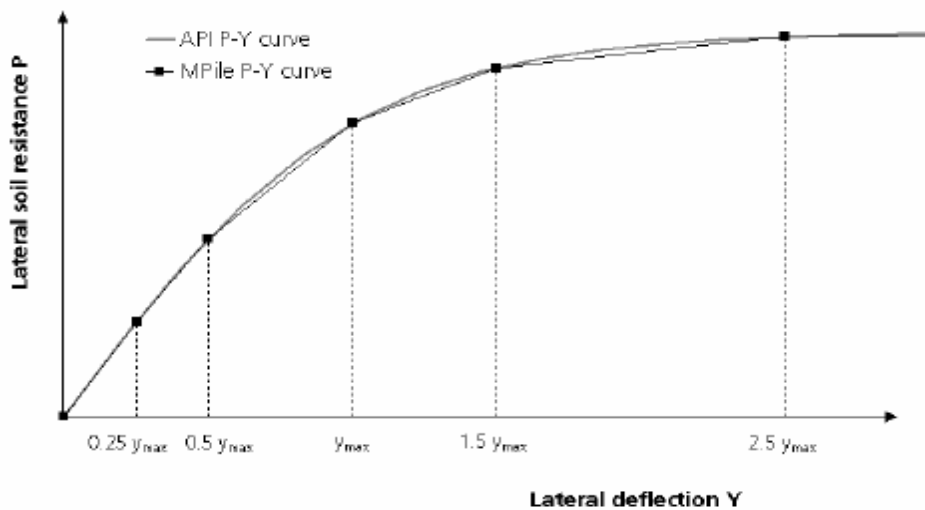$$y_{max} = \frac{A * p_u}{k * H}$$

Resulting in the following figure:

Figure 85: Modeling of the P-Y curve (API) for sand (M-Pile manual)

J. Drag force coefficient

The circular hollow section also has the advantage of very low drag coefficients if exposed to wind or water forces, in comparison with other shapes (see **Error! Reference source not found.**).

Section	Drag coefficient
Circular	0.5-1.2
rectangular	0.6-2.0
I-shaped	2.0

Table 31: Drag coefficients for I-profiles and hollow sections

In the structure the cylindrical pile/girder are used as foundation of the jetty and berthing structure and for the berthing beam.

K. Stiffness of the berthing beam

The way the berthing beam distributes the loads over the piles depends on the relative stiffness of the beam. With a rigid beam the loads will be distributed over a lot more piles than using a flexible beam. How a beam is classified is shown in **Error! Reference source not found.**.

Name	Criteria	Calculation method
Flexible	$\dfrac{\pi}{\lambda} < a$	N lose piles, without any influence of the beam
Medium 1	$a < \dfrac{\pi}{\lambda} < 4a$	Frame work
Medium 2	$4a < \dfrac{\pi}{\lambda} < L$	Elastically supported beam, infinite length
Medium 3	$L < \dfrac{\pi}{\lambda} < 4L$	Elastically supported beam, finite length
Rigid	$4L < \dfrac{\pi}{\lambda}$	Infinite rigid

Table 32: Classification of the berthing beam[21.]**. With:** $\lambda = \sqrt[4]{\dfrac{k_{pile}}{4EI_{beam}}}$ **, a='distance between piles', L=beam length, k$_{pile}$=pile stiffness, EI$_{pile}$= EI-value of beam**

L. Member check

The tubular members have to be checked[19.] on the stresses that occur due to the applied loads. A distinction is made between axial stresses and bending stresses. The shear stresses are left out of this scope. Since the normal stresses are much larger than the shear stresses.

There are two different types of tubular members underneath the jetty, completely vertical and tilted piles. These piles are loaded with normal forces in combination of moment forces (see Figure 20). The members of the fender structures are checked for moment forces.
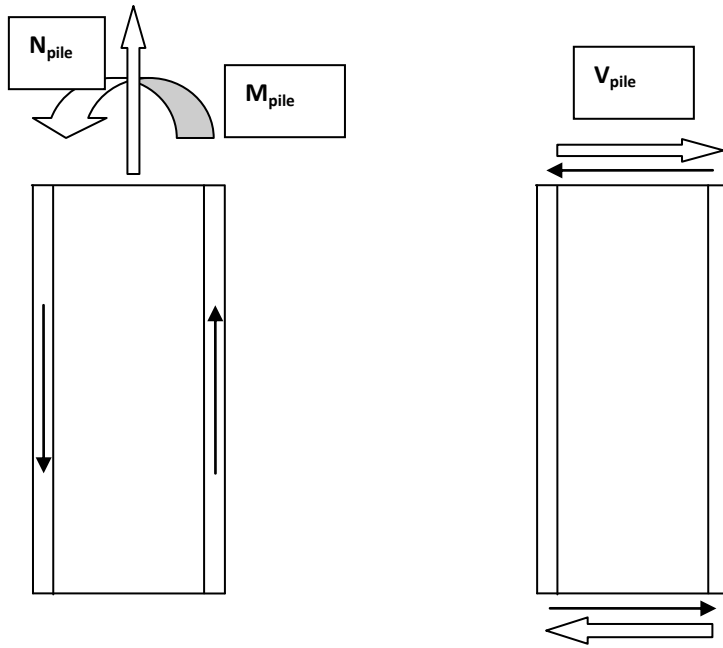
Figure 86: pile subjected to normal and bending force

Using the standard the different checks are presented here.

Tubular members that are subjected to axial tension stresses have to satisfy:

$$\sigma_{pile} \leq \frac{f_y}{\gamma R_t}$$

σ_t is   the   axial   tensile   stress   due   to   forces   from   factored   actions

f_t is the representative axial tensile strength, $f_t = f_y$

f_y is the representative yield strength, in stress units

$\gamma_{R,t}$ is the partial resistance factor for axial tensile strength, $\gamma_{R,t} = 1.05$

Tubular members subjected to axial compressive stresses have to satisfy

$$\sigma_c \leq \frac{f_c}{\gamma R_{R,c}}$$

in which

σ_c is the axial compressive stress due to forces from factored actions

f_c is the representative axial compressive strength, in stress units

$\gamma_{R,c}$ is the partial resistance factor for axial compressive strength, $\gamma_{R,c} = 1.18$

For members that are subjected to bending moments have to satisfy:

$$\sigma_b = \frac{M}{Z_e} \leq \frac{f_b}{\gamma R_{R,b}}$$

in which

σ_b is the bending stress due to forces from factored actions

f_b is the representative bending strength, in stress units

$\gamma_{R,b}$ is the partial resistance factor for bending strength, $\gamma_{R,b} = 1.05$

M is the bending moment due to factored actions

M_y is the elastic yield moment

Z_e is the elastic section modulus, $Z_e = \frac{\pi}{64}(D^4 - (D-2t)^4)/(\frac{D}{2})$

There are 3 different representative bending stresses to distinguish when a member is loaded by moment:

- fully elastic and plastic hinge development
- fully elastic and then partly plastic hinge development
- fully elastic and the local buckling failure

The representative bending strength for tubular members depends on the ratio between the width and the wall thickness and is determined by:

$$f_b = (\frac{Z_p}{Z_e})f_y \qquad \text{for } \frac{f_y D}{Et} \leq 0.0517$$

$$f_b = [1.13 - 2.58(\frac{f_y D}{Et})](\frac{Z_p}{Z_e})f_y \qquad \text{for } 0.0517 < \frac{f_y D}{Et} \leq 0.1034$$

$$f_b = [0.94 - 0.76(\frac{f_y D}{Et})](\frac{Z_p}{Z_e})f_y \qquad \text{for } 0.1034 < \frac{f_y D}{Et} \leq 120\frac{f_y}{E}$$

inwhich

f_y is the representative yield strength, in stress units

D   is the outside diameter of the member

T   is the wall thickness of the member

Z_p is the plastic section modulus, $Z_p = \frac{1}{6}[D^3 - (D-2t)^3]$

From an interview with Mr. Plugge, of the 'Ingenieursbureau Gemeentewerken Rotterdam', shows the use of the rule of a limitation of the wall thickness of 1/80 of the diameter. Following this rule should rule out the change of buckling.

The foundation tubular members are checked for the combination of moment and normal forces.

These tubular members shall be designed to satisfy the following condition at all cross-sections along their entire length:

$$\frac{\gamma_{R,c}\sigma_c}{f_c} + \frac{\gamma_{R,b}}{f_b}\left[\left(\frac{C_{m,y}\sigma_{b,y}}{1-\sigma_c/f_{e,y}}\right)^2 + \left(\frac{C_{m,z}\sigma_{b,z}}{1-\sigma_c/f_{e,z}}\right)^2\right]^{0.5} \leq 1,0$$

And

$$\frac{\gamma_{R,c}\sigma_c}{f_c} + \frac{\gamma_{R,b}\sqrt{\sigma_{b,y}^2 + \sigma_{b,z}^2}}{f_b} \leq 1,0$$

in which:

$\sigma_{b,y}$ is the bending stress about the member y-axis (in-plane) due to forces from factored actions

$\sigma_{b,z}$ is the bending stress about the member z-axis (out of plane) due to forces form factored actions

$C_{m,y}, C_{m,z}$ are the moment reduction factors corresponding to the member y- and z- axes,

respectively (see annex)

$f_{e,y}, f_{e,z}$ are the Euler buckling strength corresponding to the member y- and z-axes, respectively, in stress units

$$f_{e,y} = \frac{\pi^2 E}{(K_y L_y/r)^2}$$

$$f_{e,z} = \frac{\pi^2 E}{(K_z L_z/r)^2}$$

In which

K_y, K_z are the effective length factors for the y- and z-directions

L_y, L_z are the unbraced lengths in the y- and z-directions

R   is the radius of gyration, $r = (I/A)^{1/2}$

I   is the moment of inertia of the cross-section

A   is the cross-sectional area

For a fast first guess an estimation of both the connections at the ends of the poles are made. Since the upper structure is relatively very stiff the upper connection is rolled. The lower part will be considered as clamped in to the soil. Knowing this the following mechanical scheme can be made.
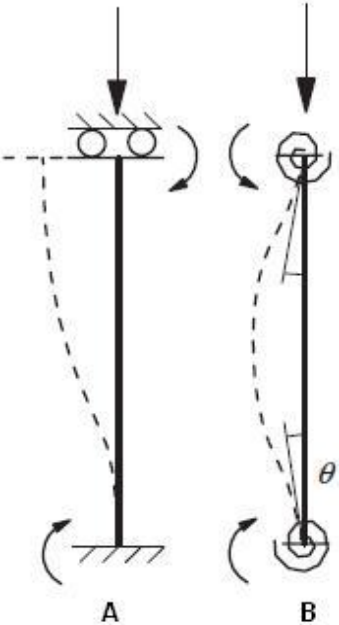
Figure 87: A is a clamped member in unbraced frames (l_0=l) and B is a member with spring support ($l/2 < l_0 < l$).

Total column buckling[19.], for segments under the sea floor, is normally not considered as a problem. The surrounding soils inhibit overall column buckling.

M.Local Buckling according to Prof. Gresnigt

However the according to the NEN 3650 developed by Prof Gresnigt the critical strain of tubes (D/t<120) depends on geometric shape[23.] :

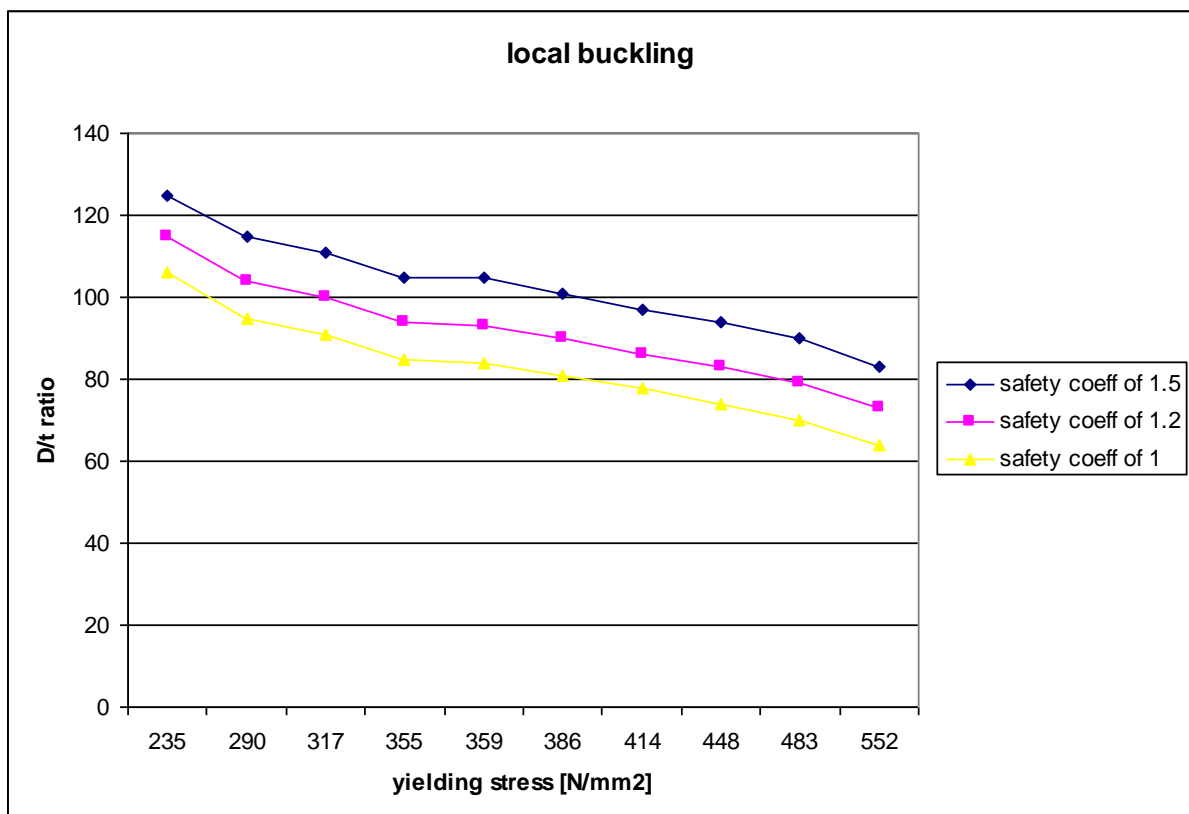$$\varepsilon_{cr} = 0.5 * (\frac{t}{D}) - 0.0025$$

Using the linear elastic rule of Hooke:

$$\varepsilon_y = \frac{f_y}{E_{steel}}$$

to make sure this will stand in the ultimate limit state a coefficient of γ_{plooi}= 2 is used.

$$\gamma_{ploot}\varepsilon_{rep} \leq \varepsilon_{cr}$$

from this can be concluded that the with a decreasing steel quality a smaller allowable D/t ratio is found (see appendix)

N. Concrete upper structure

The concrete upper structure is build partly out of concrete prefabricated parts and partly in-situ concrete combining best of both. Using prefab elements will speed up the building process. The quality of the concrete of the prefab units will be higher than the in-situ concrete. By use of in-situ it is possible to make up for the inaccuracies of the foundation piles. This would not be possible in the use of only prefab units.
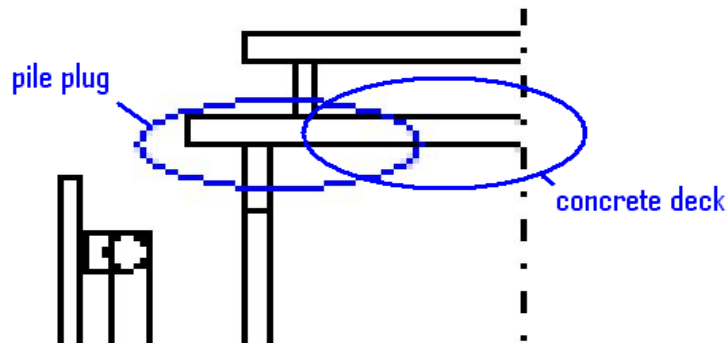

Figure 88: schematization of a cross-section of a jetty

The concrete structure must meet 'Ultimate Limit State' (ULS) and the 'Service Limit State' (SLS).

Due to the geometry the loads will be distributed over some of the width of the deck. This distribution and the way it can be included into the calculations are discussed.

Concrete failure

The concrete consists out of two components, the aggregate (sand and gravel) and lime (cement and water). High compression forces will lead to high transverse forces trough the lime causing for micro cracks between the aggregate and the lime. These micro cracks will develop into macro cracks. When the concrete is loaded by tensile forces, all the stresses will be transferred through the contact area. In comparison to the lime, the aggregate has a high strength resulting in crack development only around their surface. The stresses can no longer be transferred by the contact surfaces in the grain skeleton and the strength of the contact surface will be normative. Because the grain skeleton can't be used efficiently with tensile stresses, the tensile strength is about a factor 10 or 15 lower than the compression strength.

Concrete check

All the concrete elements in the jetty are reinforced with steel. The concrete will be checked (EN1992 (part1-1)) for strength capacity (ULS) and crack width (SLS). When the width of the cracks is too large the salt will intrude the concrete and makes the reinforcement corrode. Because of the wet and salty environment the cracks are of big importance for the life time of the concrete.

The characteristic compressive strain of concrete is related to the characteristic (5%) cylindrical strength f_{ck}, or cubical strength $f_{ck,cube}$ determined 28th day after casting. The characteristic strength used in the Lyondell jetty is B35 and an environmental class of 5a. The concrete strength representative for B35 is C 28/35.

Concrete strength	f'_{ck} (N/mm^2)	f'_b (N/mm^2)	f_b (N/mm^2)	f_{bm} (N/mm^2)	E'_b (N/mm^2)
B35	35	21	1.40	2.8	31000

Table 33: concrete characteristics according to NEN-code

Concrete strength	f_{ck} (N/mm^2)	f_{cd} (N/mm^2)	f_{ctd} (N/mm^2)	f_{ctm} (N/mm^2)	E'_b (N/mm^2)
C 28/35	28	18.7	1.29	2.8	32000

Table 34: Concrete characteristics according to EN-code

f'_{ck} Characteristic cube pressure stress [N/mm^2]

f'_b Calculation value for pressure stress [N/mm^2]

f_b Calculation value of tensile stress [N/mm^2]

f_{bm} Mean value of tensile stress [N/mm^2]

E_b Elasticity modulus [N/mm^2]

f_{ck} Characteristic cylindrical pressure stress [N/mm^2]

f_{cd} Calculation value for pressure stress [N/mm^2]

f_{ct} Calculation value of tensile stress [N/mm^2]

f_{ctm} Mean value of tensile stress [N/mm^2]

Acting width

The acting width of a floor part varies over the length of de girder (see Figure 89). The acting width (b_e) will expand with the increase of the span. To simplify the calculation, the acting width is taken as a constant over the length of the girder [1.](see Figure 89). The calculation value of the compressive stress (f'_b) occurs at the moment of failure in the outer fibre of the acting width.

Real track of concrete stresses
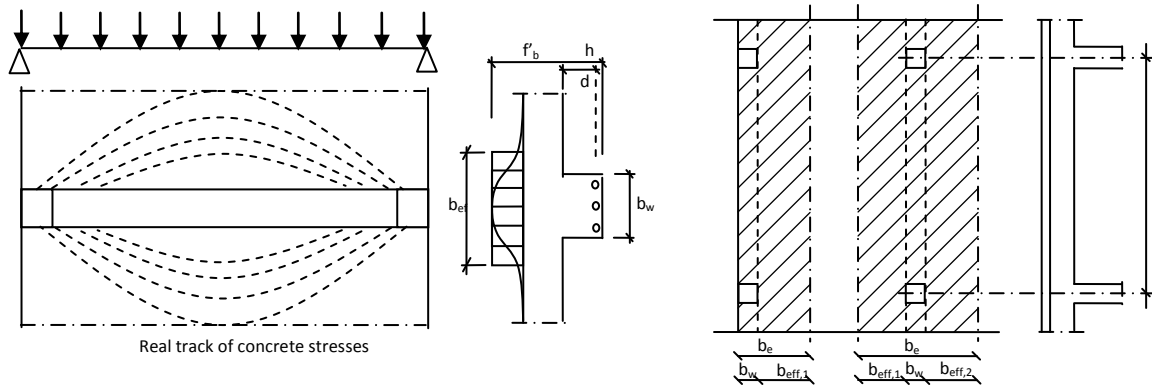
Figure 89: The acting width acting and the schematised width by a T- and a Γ-floor

For the calculation of a T- and Γ- girders the acting width have to be determined.

With the T-girder: $b_e = b_w + b_{eff,1} + b_{eff,2} < b$

With the Γ- girder: $b_e = b_w + b_{eff,1} < b$

In which:
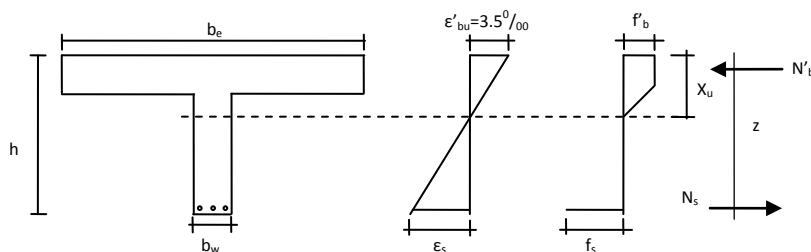
b_e Acting width

b_w Web width

$b_{eff,i} = 0,2b_i + 0,1l_0 < 0,2l_0$ and $b_{eff,i} < b_i$

Strength calculation of a reinforced concrete crossing

For the calculation of the ultimate moment resistance, the shape of the pressure zone depends on

the height of the neutral axis (see Figure 90) .

Figure 90: stress pattern

In this calculation the ultimate moment capacity is determined. The concrete will deform only plastic from a deformation of ε'_{bpl}= 1,75^0/$_{00}$. The maximum moment capacity (M_u) will be given by:

$$M_u = N_c * z$$

in this

N_s The ultimate tensile force that can be obtained by the cross section of reinforcement steel

z The lever arm. With a value of z=d-0.39 X_u

Where:

$$X_u = \frac{A_s f_s}{0.75 f'_b b}$$

In which

A_s Surface of reinforcement

f_s Yielding stress of reinforcement steel

Crack width

To make sure the reinforcement steel is safe for environmental influences the width of the cracks in the concrete are limited. The demands for width of the cracks are determined by environmental conditions. The crack width of the concrete is calculated using:

$$w_k = s_{r,\max} (\varepsilon_{sm} - \varepsilon_{cm})$$

in which:

$s_{r,max}$ The maximum crack width

ε_{sm} The average strain in the applied reinforcement.

ε_{cm} The average concrete strain between the cracks

The difference in strain is calculated:

$$\varepsilon_{sm} - \varepsilon_{cm} = \frac{\sigma_s - k_t \dfrac{f_{ct,eff}}{\rho_{p,eff}}(1+\alpha_e \rho_{p,eff})}{E_s} \geq 0.6 \frac{\sigma_s}{E_s}$$

in which:

σ_s The stress in the reinforcement, assuming a cracked cross section

α_e The ratio E_s / E_{cm}

$\rho_{p,eff}$ $(A_s + \xi_1^2 A_p') / A_{c,eff}$

A_p' and $A_{c,eff}$

ξ_1

k_t The collision of the vessel is considered as a short-term load

in situation where the adhesive reinforcement is placed close enough to each other (distance < 5(c+Φ/2)) the following formula is used:

$$s_{r,max} = k_3 c + k_1 k_2 k_4 \phi / \rho_{p,eff}$$

in which:

Φ   The diameter of the reinforcement bar.

C   The longitudinal reinforcement cover

k_1 The coefficient that takes the surface properties of the reinforcement into account

  =0.8 for bars that have a rough surface

  =1.6 for bars that are very smooth

k_2 The coefficient that takes the stress distribution into account

  =0.5 for bending

  =1.0 for pure normal stress

The values of k_3 and k_4 differ in every country. In the Dutch standards the k_3=3.4 and k_4=0.425 is recommended.

[1.] NEN-EN ISO 19902, 2007

O.Results of sounding CM628

Chosen partial factor for soil characteristics retaining structures and embankments:

Partial factor for soil characteristics (γ_m)	Ultimate state (favourable)	Users state
$\gamma_{m;\phi}$ tangent of the angle of internal friction	1.2	1
$\gamma_{m;c2}$ cohesion	1.5	1
$\gamma_{m;cu}$ undrained shear strength	1.5	1

Table 35: partial factors (NEN 6740)

Here is chosen to use only the $\gamma_{m;cu}$ instead of the $\gamma_{m;\phi}$ and the $\gamma_{m;c2}$. Using the partial factors of the internal friction and cohesion would be very conservative compared to the factor for undrained shear strength.

The soil characteristics are based on the result of the soundings. The high and the low representative values are given (see Table 36). Since replacement of a pile after failing is easier than repairing the soil after failing, the lower representative values of the soil are used (see Table 37). From these results the design value is calculated (see Table 38).

b.k. layer [m NAP]	Soil type	Expected value	Lower representative value			Higher representative value		
		γ_{sat} [kN/m^3]	ϕ' [^{0}]	δ' [^{0}]	c' [kPa]	ϕ' [^{0}]	δ' [^{0}]	c' [kPa]
-17.6	Sand I	19	25	16.6	0	27	18	0
-24.7	Clay, sandy I	18	22.5	15	0	25	16.6	0
-26.5	Peat	12	15	0	5	15	0	10
-27.3	Clay, sandy II	18	22.5	15	0	25	16.6	0
-27.8	Sand II	20	32.5	20	0	35	20	0
-32.0	Sandy III	20	35	20	0	40	20	0

Table 36: soil characteristics of sounding CM0628

Soil	Dry unit weigth	Wet unit weight	Phi [^{0}]	K_o [kN/m^3]	Cone resistance [kN/m^2]	Dz at 100%	Factor alpha
Sand I	19	19	25	0.58	3000	0.001	0.006
Sand II	20	20	32.5	0.43	22000	0.001	0.006
Sandy III	20	20	35	0.43	30000	0.001	0.006
			C_u [MPa]	Emp. Cons. J	Strain at 50% fail. load		
Clay Sandy	18	18	69.9-86.4	0.25	0.02	0.01	
Peat	12	12	80.3-90.9	0.25	0.05	0.01	
Clay, Sandy II	18	18	92.6-93.1	0.25	0.02	0.01	0.006

Table 37: soil characteristic used for the M-pile calculations, lower rep value

Soil	Dry unit weigth	Wet unit weight	Phi [°]	K_o [kN/m³]	Cone resistance [kN/m²]	Dz at 100%	Factor alpha
Sand I	19	19	20.8	0.58	3000	0.010	0.006
Sand II	20	20	27.1	0.43	22000	0.010	0.006
Sandy III	20	20	29	0.43	30000	0.010	0.006
			C_u [MPa]	Emp. Cons. J	Strain at 50% fail. load		
Clay Sandy I	18	18	58.25-57.6	0.25	0.02	0.01	
Peat	12	12	53.5-60.6	0.25	0.05	0.01	
Clay, Sandy II	18	18	61.7-62	0.25	0.02	0.01	0.006

Table 38: lower des value

P. Prob relations

Below is shown the most used gates with corresponding structure function.

Gate	Symbol	Operation	ψ
AND		Ψ=1 ⇔ all ψᵢ=1	$\Psi = \prod_{i=1}^{n} \varphi_i$
OR		Ψ=1 ⇔ at least one ψᵢ=1	$\Psi = 1 - \prod_{i=1}^{n}(1-\varphi_i)$
PRIORITY-AND		Ψ=1 ⇔ all ψᵢ=1 and if they occurred in sequence	$\Psi = \{\prod_{i=1}^{n}(\varphi_i)\} \cap \{\prod_{i=1}^{n-1}(t_{\varphi_i} < t_{\varphi_{i-1}})\}$
EXCLUSIVE OR GATE		Ψ=1 ⇔ precisely one ψᵢ=1	$\Psi = \{\sum_{i=1}^{n}\varphi_i = 1\}$
VOTING		Ψ=1 ⇔ at least 'm' times ψᵢ=1	$\Psi = \{\sum_{i=1}^{n}\varphi_i \geq m\}$

INHIBIT GATE		Like the AND-gate	φ_2 is a contingency, which only can occur when φ_1 occurs

Q.Random number generators

Distribution type	Probability density function	Transformation of uniformly distributed random variable X_u
Normal	$f_x(x) = \dfrac{1}{\sqrt{2\pi}\sigma_x} e^{-\frac{1}{2}(\frac{\mu_x - X}{\sigma_X})^2}$	$X = \mu_X + \sigma_X(-2\ln X_{u,1})^{\frac{1}{2}}\cos(2\pi X_{u,2})$
Lognormal	$f_x(x) = \dfrac{1}{X\sqrt{2\pi}\sigma_x} e^{-\frac{1}{2}(\frac{\mu_x - \ln(X)}{\sigma_X})^2}$	$X = e^{\mu_X + \sigma_X(-2\ln X_{u,1})^{\frac{1}{2}}\cos(2\pi X_{u,2})}$
Exponential	$f_x(X) = \lambda e^{-\lambda(\mu_X - X)}$	$X = -\dfrac{1}{\lambda}\ln(X_u) + \mu_X$
Weibull	$f_x(x) = \dfrac{\beta}{\alpha_x}(\dfrac{X}{\alpha})^{\beta-1} e^{-\frac{1}{2}(\frac{X}{\alpha})^\beta}$	$X = -\alpha(\ln(1 - X_u))^{\frac{1}{\beta}}$
I-max	$f_x(X) = \alpha e^{(-\alpha(X-u)-\exp(-\alpha(X-u)))}$	$X = \mu_X - \dfrac{1}{\alpha}\ln(\ln(\dfrac{1}{X_u}))$
II-max	$f_x(X) = (\dfrac{k}{u})(\dfrac{u}{X})^{k+1} e^{(-\frac{u}{X})}$	$X = \mu_X(\ln(\dfrac{1}{X_u}))^{\frac{-1}{k}}$
III-max	$f_x(X) = (\dfrac{k}{u-\varepsilon})(\dfrac{X-\varepsilon}{u-\varepsilon})^{k+1} e^{((-\frac{X-\varepsilon}{u-\varepsilon})^k)}$	$X = \mu_X(\ln(\dfrac{1}{X_u}))^{\frac{1}{k}}$
I-min	$f_x(X) = e^{(-\exp(-\alpha(X-u)))}$	$X = \mu_X + \dfrac{1}{\alpha}\ln(\ln(\dfrac{1}{(1-X_u)}))$
II-min	$f_x(X) = 1 - e^{(-(\frac{u}{X})^k)}$	$X = \mu_X\ln(\dfrac{1}{(1-X_u)})^{\frac{-1}{k}}$
III-min	$f_x(X) = 1 - e^{(-(\frac{X-\varepsilon}{u-\varepsilon})^k)}$	$X = \mu_X\ln(\dfrac{1}{(1-X_u)})^{\frac{1}{k}}$

R. Fault tree

Here the total fault tree of the jetty is presented. High in the tree a distinction is made between service ability and ultimate limit state. The base events are further described in the appendices. The berthing structure is standing in front of the jetty self. When the berthing structure fails in the ULS the jetty cannot be taken in operation anymore. Therefore the failing of the berthing structure is called conditional failing.
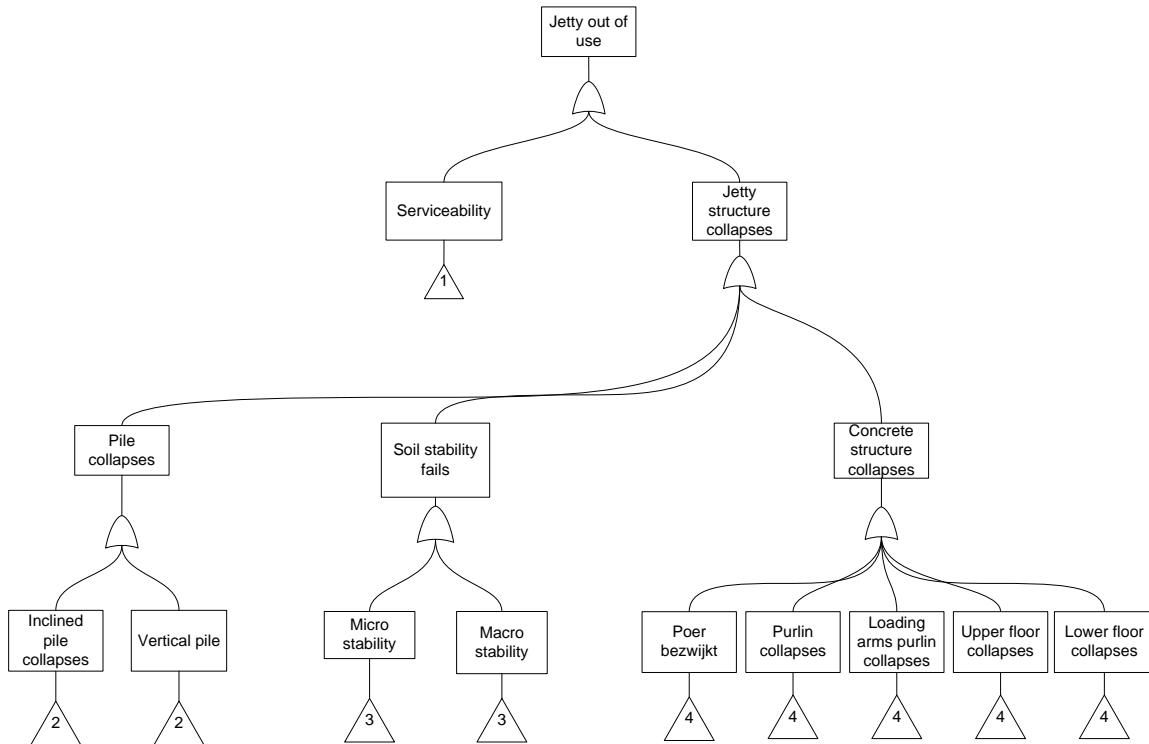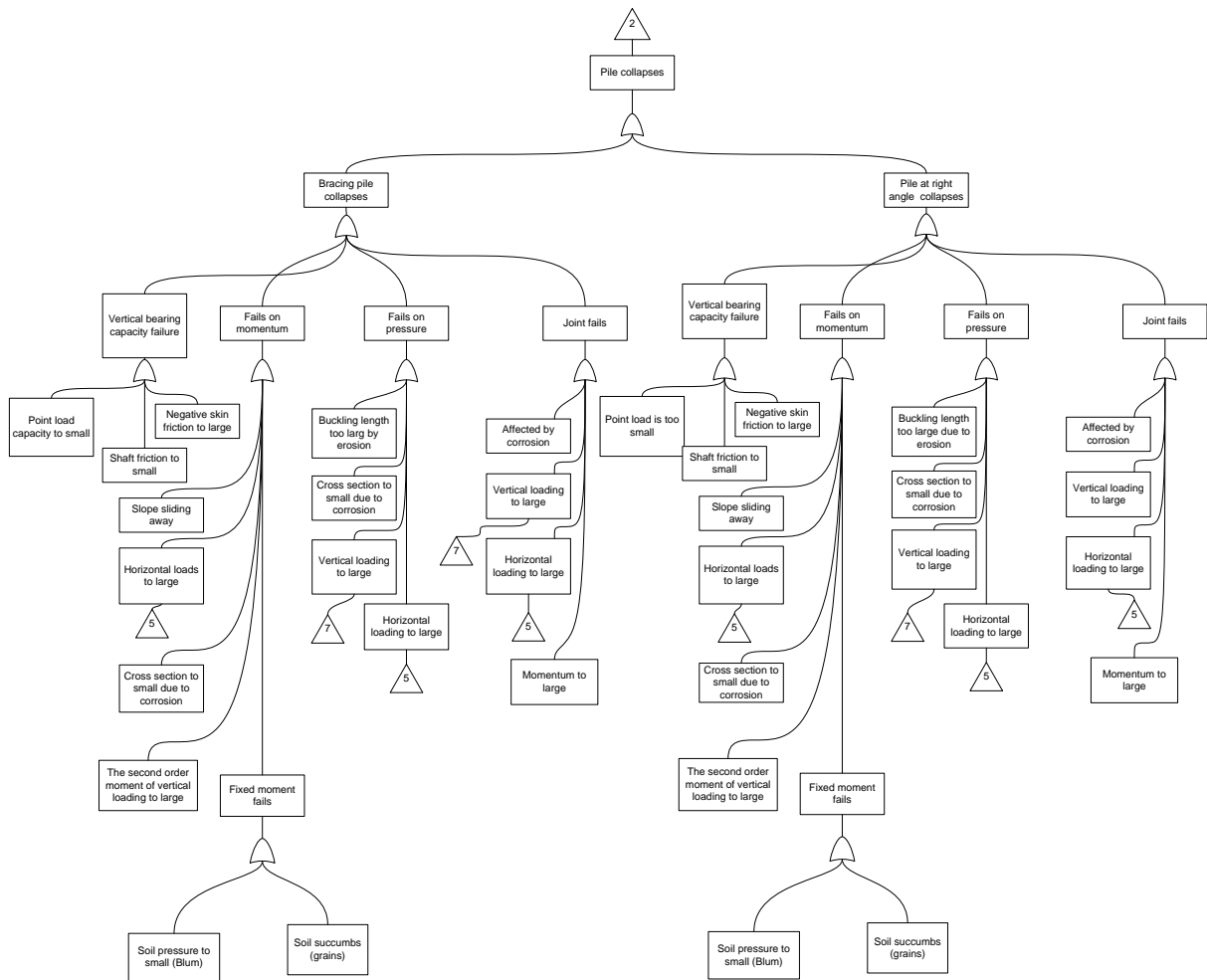

Figure 91: general fault tree

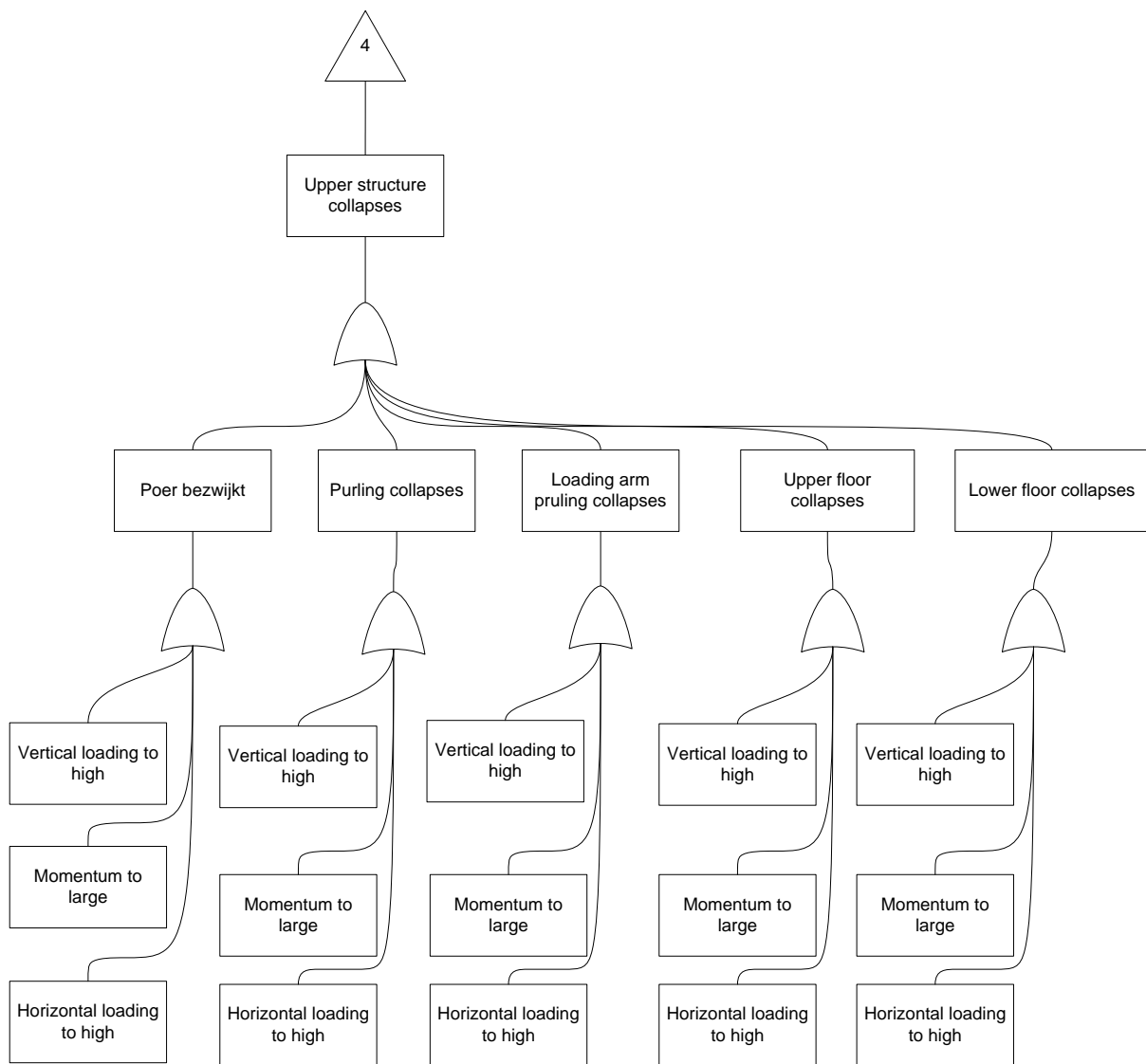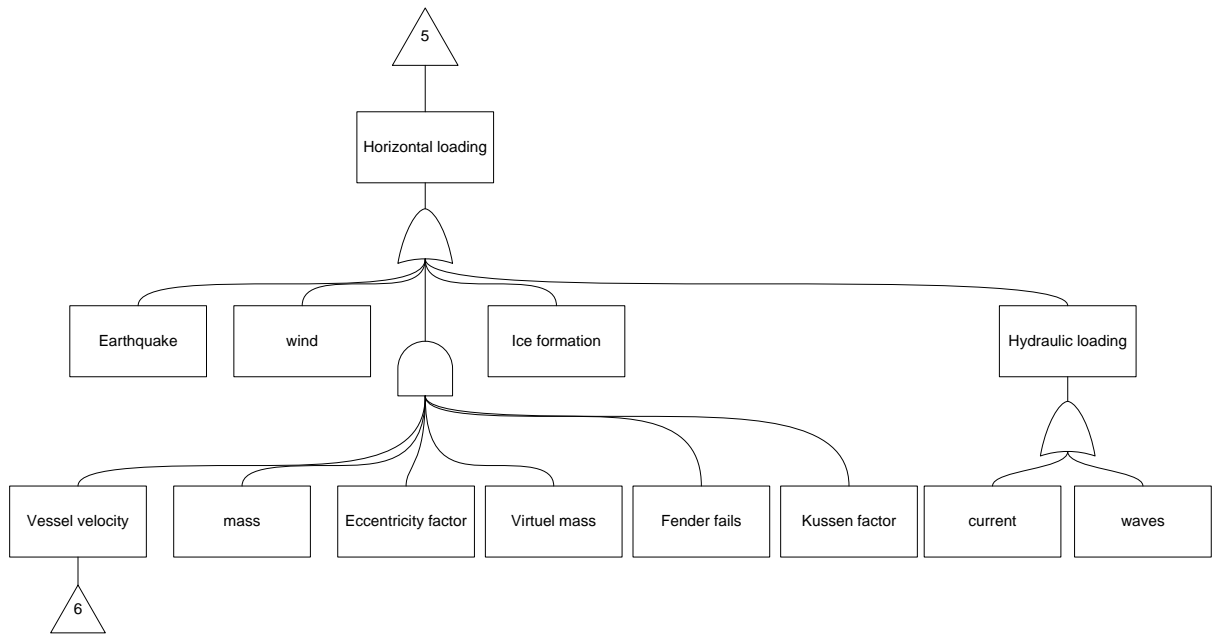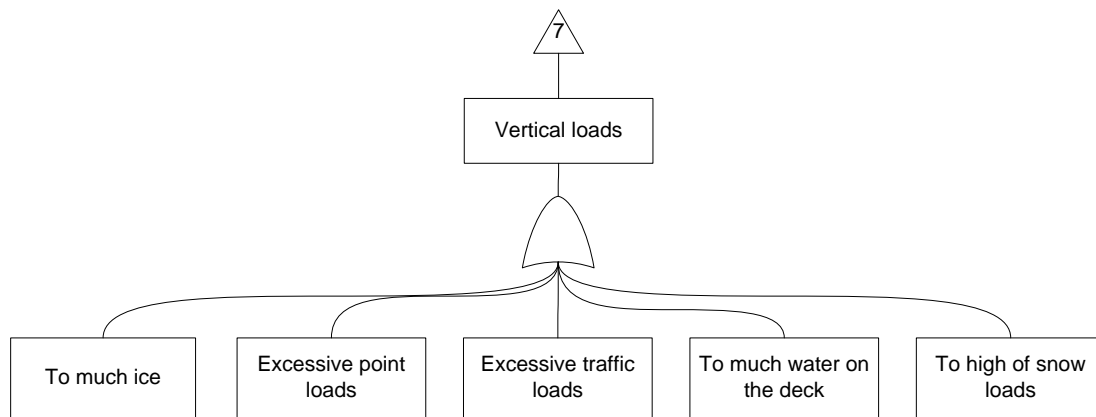**Figure 92: pile foundation fails**
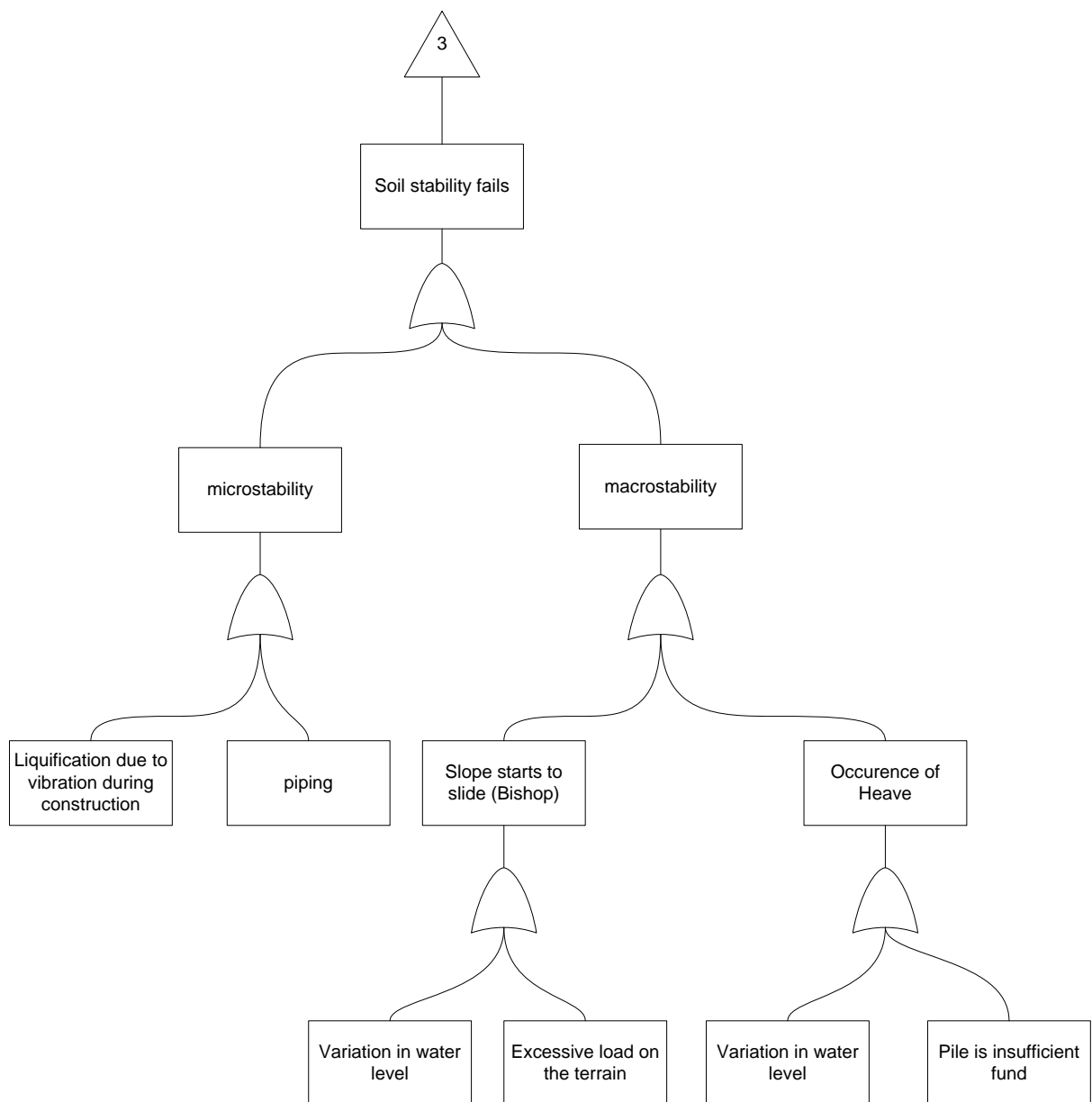
Figure 93: soil stability

Figure 94: upper structure fails

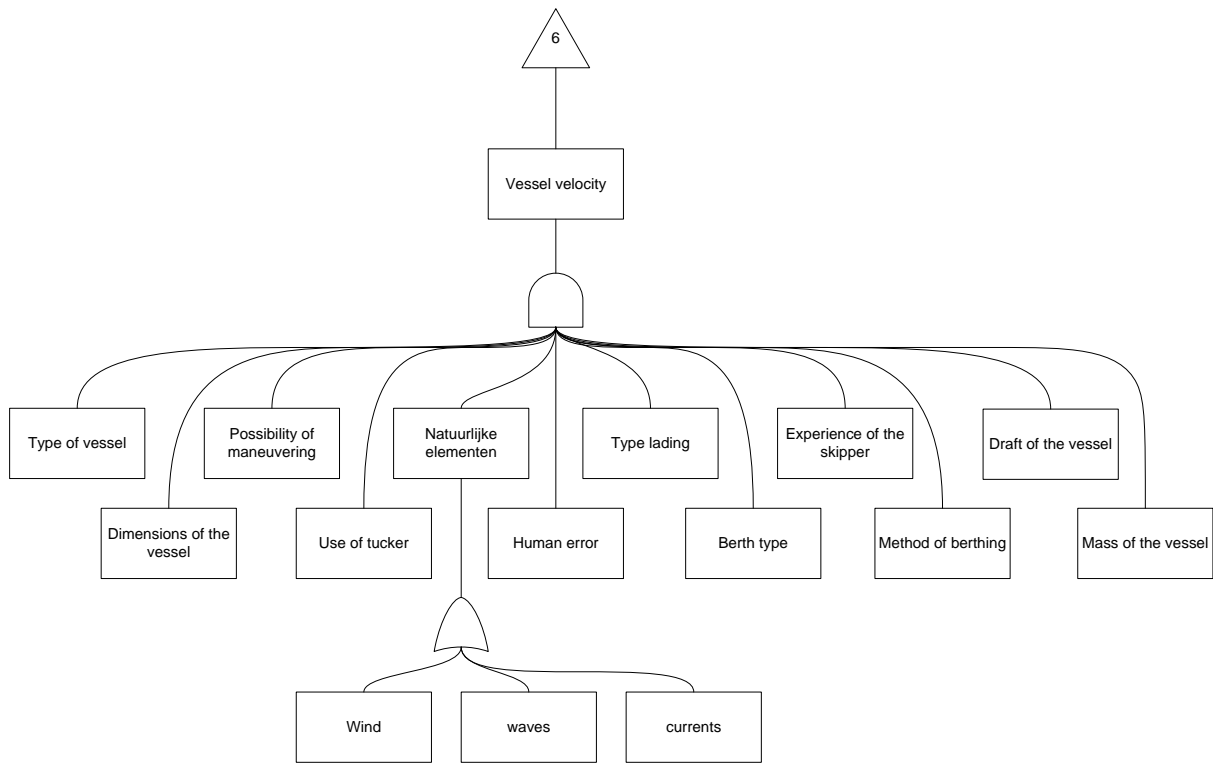**Figure 95: horizontal loads**

Figure 96: vertical loading

Figure 97: relation with vessel velocity

S. Ditlevsen

Calculation example:

In the problem below a system is considered by means of the virtual work principle. The system Ditlevsen bound and the probability of failure are calculated.

There are three failure modes found in the portal construction when the yield hinge mechanism is applied. This gives the following systems and equations:
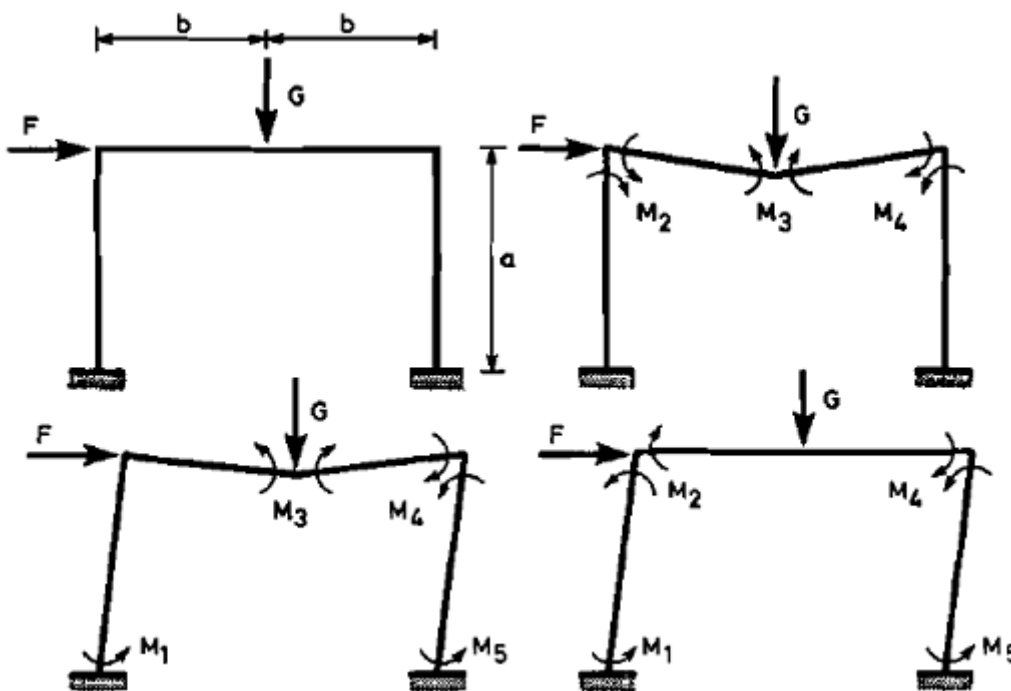

Figure 98; portal construction with imposed forces and the failure modes

Equation:

$$W_1 = M_1 + 2*M_3 + 2*M_4 + M_5 - F*a - G*b$$

$$W_2 = M_2 + 2*M_3 + M_4 - G*b$$

$$W_3 = M_1 + M_2 + M_4 + M_5 - F*a$$

There is assumed that the yield moments M_1 to M_5 are uncorrelated random quantities with common mean μ and standard deviation σ. In this case all 3 modes reliability indices are equal ($\beta_1 = \beta_2 = \beta_3 = \beta$).

The correlation coefficients $\rho(W_i, W_j)$ for i,j=1,2,3:

$$Cov(W_1, W_2) = Cov(M_1 + 2M_3 + 2M_4 + M_5, M_2 + 2M_3 + M_4) =$$

$$Cov(2M_3, 2M_3) + Cov(2M_4, M_4) = 4\,var(M_3) + 2\,var(M_4) = 6\sigma^2$$

$$var(W_1) = var(M_1) + var(2M_3) + var(2M_4) + var(M_5) = (1 + 4 + 4 + 1)\sigma^2 = 10\sigma^2$$

Correlation coefficients:

$$\rho(W_1, W_2) = \frac{6\sigma^2}{\sqrt{(10\sigma^2 + 6\sigma^2)}} = 0.77$$

$$\rho(W_1, W_3) = \sqrt{\frac{4}{10}} = 0.63$$

$$\rho(W_2, W_3) = \sqrt{\frac{1}{6}} = 0.41$$

Ditlevsen bounds:

$$D_{system} = P(W_1 < 0 \cup W_2 < 0 \cup W_3 < 0)$$

$$\phi(-\beta)\phi(-\beta\sqrt{\frac{1-\rho}{1+\rho}}) < P(W_i < 0 \cap W_j < 0) < 2\phi(-\beta)\phi(-\beta\sqrt{\frac{1-\rho(W_i, W_j)}{1+\rho(W_i, W_j)}})$$

$$P_{system} > \phi(-\beta)(3 - 2(\phi(\beta_{1,2}^*) + \phi(-\beta_{1,3}^*) + \phi(-\beta_{2,3}^*)) <$$
$$\phi(-\beta)(3 - 2(\phi(\beta_{1,2}^*) + \phi(-\beta_{1,3}^*) + \phi(-\beta_{2,3}^*)) + \min(\phi(-\beta_{1,2}^*), \phi(\beta_{1,3}^*), \phi(-\beta_{1,3}^*))$$

For β=4 → 3.74<P$_{sys}$<3.76

For β=5 → 4.78<P$_{sys}$<4.30

In case of independence:

$$P_{sys} = 1 - (1 - \phi(-\beta))^3 \approx 3\phi(-\beta) =$$

P$_{sys}$=3.73 for β=3

P$_{sys}$=4.78 for β=4

Sensitivity of safety margins to system reliability is smaller then sensitivity of basic variables to system reliability.

T. Number of simulations

Using a Monte Carlo simulation in a reliability problem, the relative error has to be considered.

To make sure the relative error is small enough a minimum of calculations have to be made. A

Monte Carlo method has a binomial character. With an enough large amounts of drawings, a

normally

distribution can be assumed and the change of failure can be expressed by:

$$P_f \approx \frac{n_f}{n}$$

In which

     n is the total number of simulations

     n_f is the number of simulations, for which the limit state function is $Z(X){<}0$

The simulation's relative error is given by:

$$\varepsilon \approx \frac{\dfrac{n_f}{n} - P_f}{P_f}$$

When the expectation of the relative error can be assumed to be zero. The standard

deviation is

$$\sigma_\varepsilon = \sqrt{\frac{1 - P_f}{n P_f}}$$

When the amount n is sufficiently large, based on the central limit theorem the error

can be assumed to be normally distributed. Estimation of the n requires that the

relative error is smaller than E=kσ_ε for the reliability of Φ(E/σ_ε). Than the number of

simulations has to meet:

$$n > \frac{k^2}{E^2}\left(\frac{1}{P_f} - 1\right)$$

From this can be concluded that the minimum amount of simulations are independent

of the number of random variables. But depend on k, P_f and ε.

A high accuracy (ε<<1), a large reliability (k>>0) and a small probability of failure

(P$_f$<<1) results in a large amount of simulations.

U. Dimension distribution

The method of Saurin makes use of parameters of dimensions. The dimensions of the vessels are strongly related to the vessel weight and the vessel function. Developing the distributions the data of the "vingerpier" has been used. The dimensions are assumed to be independent. This will result in some inconsistencies in the relation:

$$L*B*D*\rho_{vessel} = DWT[tonnage]$$

Length

The data of the "Vingerpier" has been used to analyze the mean length in relation of the vessel weight.

First the data is plotted in relation to the weight and then the mean is calculated as a function of the DWT:
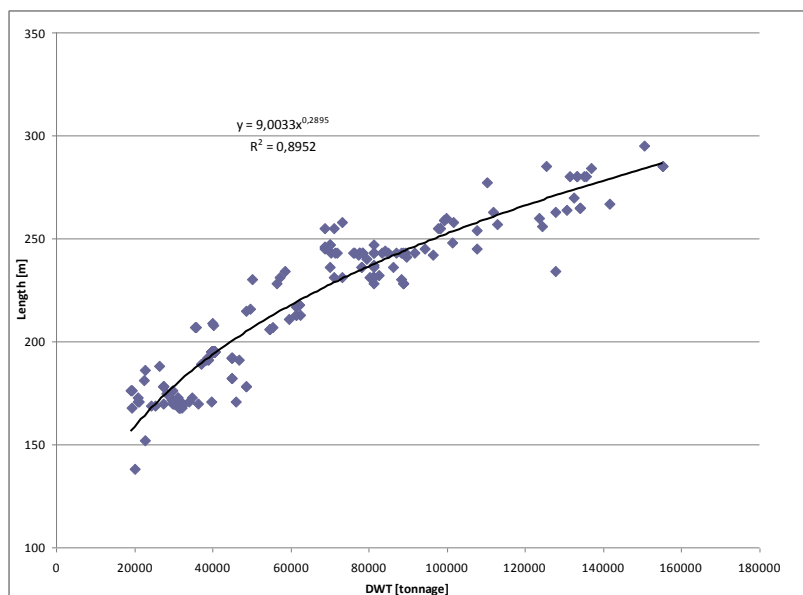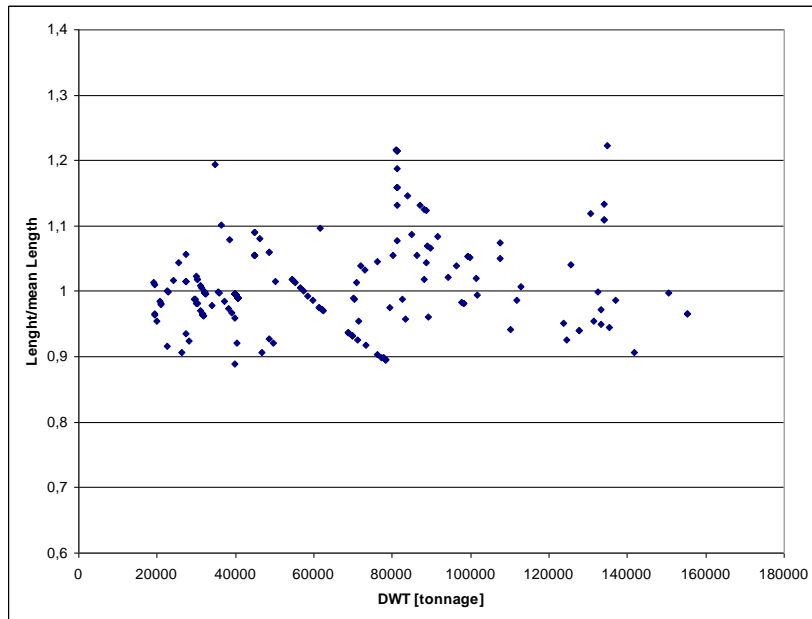
$$L_{mean} = 9.003*DWT^{0.2895}$$

Figure 99: The length of the vessel in relation to the DWT

Figure 100: Length divided by the mean length in relation to the DWT

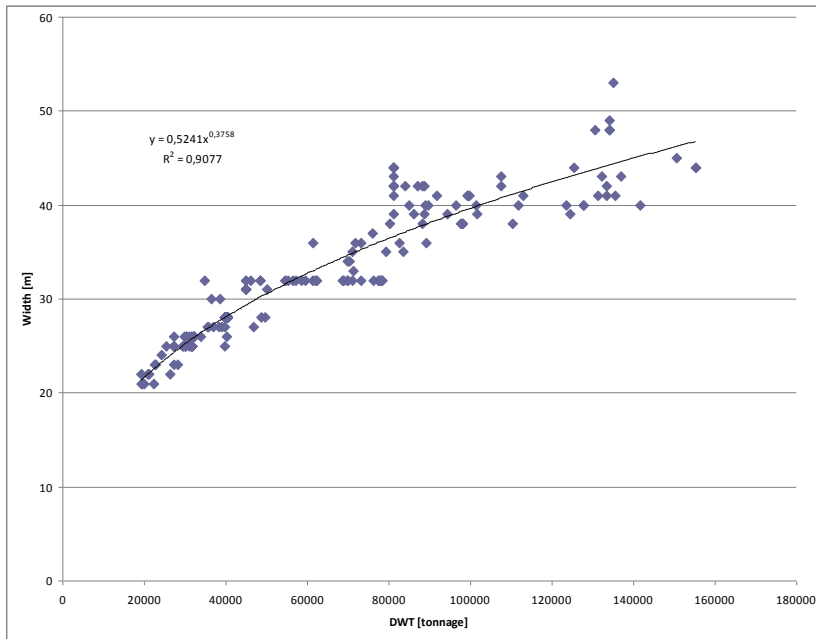The distribution is chosen to be normal. The expression of the length will be a normal distribution, with a mean of 1, times the mean. The mean is a function of the weight:

$$L = 9.003 * DWT^{0.2878} N(1;0.052^2)$$

Width

The width of the vessels is plotted in **Error! Reference source not found.**. In this figure the mean is calculated as a function of the weight and drawn:

$$W_{mean} = 0.5241 * DWT^{0.3758}$$

Figure 101: The width in relation to the DWT

Figure 102: The width divided by the mean width in relation to DWT

The distribution of the data shown in **Error! Reference source not found.** is based on regular data instead of data of extreme. For this a normal distribution is used with a mean of 1:

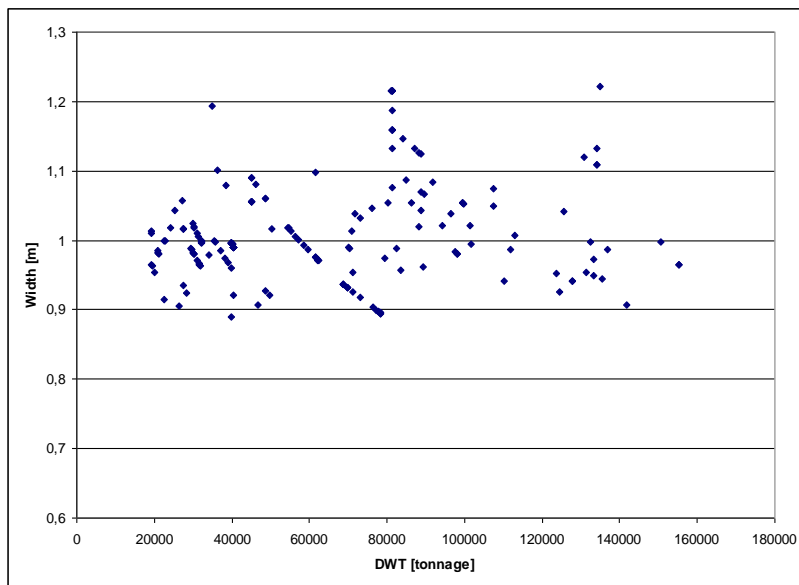$$W = 0.5241 * DWT^{0.3758} * N(1;0.067^2)$$

Draft

The draft of the vessels is plotted in **Error! Reference source not found.**. In this figure the mean is calculated as a function of the weight and drawn:
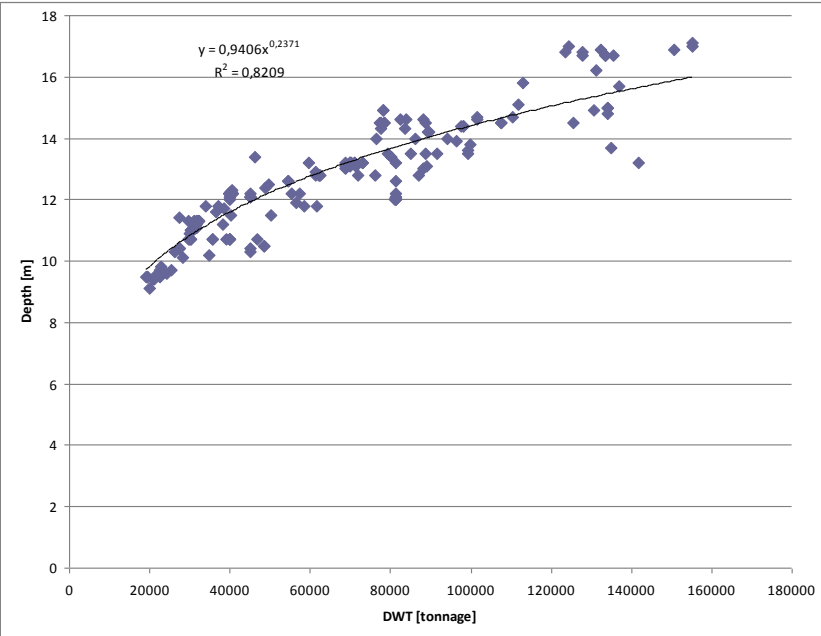
$$D_{mean} = 0.9406 * DWT^{0.2371}$$

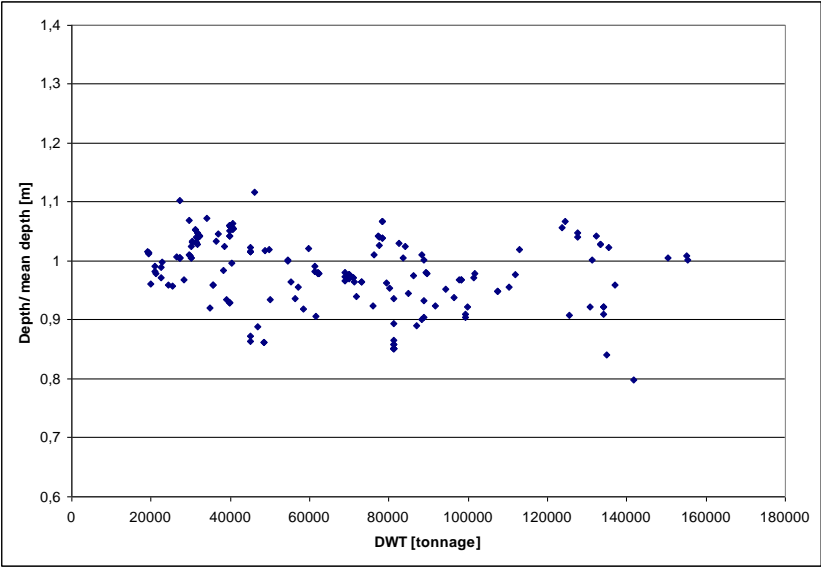
Figure 103: The depth in relation to the DWT

**Figure 104: The depth divided by the mean depth in relation to the DWT**

The distribution of the data shown in **Error! Reference source not found.** is based on regular data instead of data of extreme. For this a normal distribution is used with a mean of 1:

$$D = 0.9406 * DWT^{0.2371} * N(1;0.062^2)$$

Velocity distribution

For velocity analysis only the group of vessels that are smaller than 168.000 [DWT] are taken into account. With every berth it is possible that the vessel hits the structure multiple times, the distribution only contains the maximum velocities (see Figure 37). From the data the average velocity as a function of the weight is constructed, the function (see Figure 37):

$$v_{average} = 1.925 * DWT^{-0.30} [m/s]$$
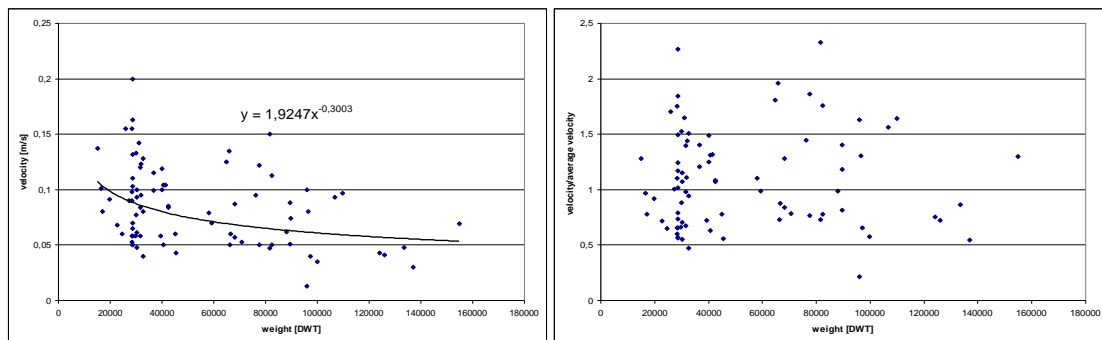
Figure 105: Left the maximum of the vessel velocities within the corresponding vessel weight. Right the average maximum velocity as a function of weight.

The divided data by the average are plotted and shows the data beneath the average are very concentrated and the data higher than the average is more scattered. Also it concerns only maximum velocities indicating a Gumbel distribution.

Both Brolsma and Saurin suggested a Gumbel distribution, since the maximum velocity is normative. Using the data plotted in Figure 37 the distribution is calculated depending on the vessel weight:

$$v = v_{average} * Gumbel(\mu, \sigma^2) = (1.9247 * DWT^{-0.3003}) * Gumbel(1;0.44) [m/s]$$

A comparison of the different distributions are made, to get some insight in behavior of the distribution in relation to the actual data.

Figure 106: Comparison of Normal and Gumbel distribution over the data

In **Error! Reference source not found.** it is shown that the Gumbel distribution fits the data better than the normal distribution. shows that a normal distribution is more likely to draw negative values for the velocities.

V. Steel piles

In the consideration of steel members the following properties of structural steel are dealt with:

f_y yield strength [MPa]

f_u ultimate tensile strength [MPa]

E   Modulus of elasticity [MPa]

v   Poisson's ratio

ε_u ultimate strain

Only specific points or parts of the full stress-strain curve are considered, thus the proposed model can only be used where these specific information is applicable. As distribution a multi-variety log-normal distribution is suggested**Error! Bookmark not defined.**. The mean values and coefficients of variation for the above vector are given in the Table 10.

Property	Mean value, E[..]	COV,v	VAR
f_y	$f_{ysp}*a*exp(-u*v)-C$	0.07	$0.07*(f_{ysp}*a*exp(-u*v)-C)$
f_u	$B*E[f_u]$	0.04	$0.04*(B*E[f_u])$
E	E_{sp}	0.03	$0.03*(E_{sp})$

Table 39: Mean and COVv values

In which:

The suffix (sp) is used for the code specified or nominal value for the variable considered

a   spatial position factor (a=1.05 for webs of hot rolled sections and a=1 otherwise)

u   factor related to the fractile of the distribution used in describing the distance between the code specified or nominal value and the mean value; u is found to be in the range of -1.5 to -2.0 for steel produced in accordance with the relevant EN standard.

C   constant reducing the yield strength. A value of 20 [MPa] is recommended.

B   =1.5   for structural carbon steel

           =1.4   for low alloy steel

           =1.1   for quenched and tempered steel

v   Poisson ratio= 0.27-0.30

The distribution is taken recommended as a Log-Normal distribution:

$$f_y = LN(f_{ysp} * \alpha * \exp(-u*v) - C; 0.07*(f_{ysp}*\alpha*\exp(-u*v) - C))$$

$$f_y = LN(f_{ysp} * 1.52 - 20; 0.07*(f_{ysp}*1.52 - 20))$$

After analyses of the data generated by this function. The outcome of the log-normal distribution was considered too wide. Therefore because of practical reasons a normal distribution is used.

Driving depth

The depth of driving is assumed to be normally distributed with the aim of depth as the mean**Error! Bookmark not defined.**. The expected change of deviation more than 0.5 [m] is assumed to be 0.10. This will result in a standard deviation of 0.1:

$$D = N(D_{aimeddepth}; 0.1^2)[m + NAP]$$

Wall thickness

The tubular sections are fabricated out of a steel plate. It is assumed that per tubular section the wall thickness is constant. But the wall thickness per tubular section can differ from what was ordered. For this a normal distribution is used:

$$t_{wallthickness} = t_{ordered} * N(1; 0.1^2)[m]$$

Elasticity modulus

The elasticity modulus is normal distributed and has a COVv of 0.03:

$$E = E_{sp} * N(1; 0.03^2)$$

In which

E_{sp} nominal Young's Modulus

Corrosion

The thickness of the wall will be impacted by the environment. Due to corrosion the wall thickness will decrease. The amount of corrosion will be environmental dependent**Error! Bookmark not defined.**.

- Above MLWS-1.0 [m]   0.003 [m]
- Between MLWS-1.0 [m] and bottom – 1.0 [m]   0.002 [m]
- Underneath bottom-1.0 [m]   0.001 [m]

For the corrosion a uniform distribution is used.

W.   Standard Values for Soil

Non cohesive Soil type	Density	Dry Unit Weight [kN/m^3]	Saturated Unit Weight [kN/m^3]	Internal Friction tan(φ')	Stiffness [MN/m^2]
Coarse gravel, Boulders	Loose medium dense	15-17 17-18 18-20	19-20 20-21 21-23	0.65-0.73 0.70-0.83 0.78-0.90	150-300 150-300 250-350
Sand, gravel Uniform grain Size	Loose Medium Dense	15-16 17-18 18-19	19-20 20-21 21-22	0.58-0.65 0.65-0.73 0.70-0.83	30-100 50-150 100-200
Sand, gravel Non-uniform Grain size	Loose Medium Dense	17-19 18-20 20-21	20-22 21-23 22-24	0.57-0.70 0.62-0.75 0.70-0.85	30-100 50-150 150-250
Sand Slightly Silt Silt		18-20 18-20	20-21.5 19.5-20.5	0.50-0.65 0.45-0.60	25-50 20-40

Table 40: Indications of soil properties of non cohesive soils

Cohesive Soil type	Consistency	Saturated Unit Weight [kN/m^3]	Internal Friction Tan(φ') (drained)	Cohesion (drained) [kN/m^2]	Undrained Shearing Strenght [kN/m^2]	Stiffness (normally Consolidated) [MN/m^2]
Inorganic Cohesive	Soft Stiff	16-18 17-19	0.27-0.36	0-5 5-15	10-20 20-50	1-2 2-4

soils, Plastic	Very stiff	20-22	0.27-0.36 0.27-0.36	15-30	50-100	4-10
Inorganic Cohesive soils, Medium plastic	Soft Stiff Very stiff	17-19 18-20 19-21	0.35-0.42 0.35-0.42 0.35-0.42	0-5 5-10 10-20	0-10 15-30 40-100	1-2 2-4 4-10
Inorganic cohesive soils, Weakly plastic		18-20	0.40-060	0-5	0-10	2-5
Boulder clay		20-24	0.52-0.64	20-30	-	200-700
Organic cohesive soils, Silt	Soft Stiff	13-18 14-19	0.24-0.28 0.24-0.28	0-5 5-10	5-20 15-30	0.2-0.5 0.5-1

Table 41: Indications of soil properties of cohesive soils

X. Concrete properties as a stochastic

The concrete properties can be described as a function of the reference strength of concrete:

In situ compressive strength:

$$f_c = \alpha(t,\tau) * f_{co}{}^{\lambda} [MPa]$$

Tensile strength:

$$f_{ct} = 0.3 * f_c{}^{2/3} [MPa]$$

Modulus of elasticity:

$$E_c = 10.5 * f_c{}^{1/3} (\frac{1}{1 + \beta_d \varphi(t,\tau)} [GPa]$$

Ultimate compressions strain:

$$\varepsilon_u = 6*10^{-3} * f_c{}^{-1/6}(1 + \beta_d \varphi(t,\tau))[m/m]$$

In which:

λ   is a factor taking into account the systematic variation of in situ compressive strength and strength of standard tests. Assumed a log-normal variable with mean of 0.96 and variation of 0.005*0.96=4.8*10^{-3}.

a(t,τ) is a deterministic function which takes into account the concrete age at the loading time t [days] and the duration of loading τ [days]. The function is given by:

$$\alpha(t,\tau) = \alpha_1(t)\alpha_2(t)$$

in which

$\alpha_1(t) = \alpha_3(\infty) + [1 - \alpha_3(\infty)]\exp[-a_\tau \tau]$ with $\alpha_3(\infty) \approx 0.8$ and $a_\tau = 0.04$

$\alpha_2(t) = a + b * \ln(t)$

In most applications $\alpha_1(\tau) = 0.8$ can be used. The type of cement and the climatically environment influence the coefficients 'a' and 'b' in $\alpha_2(t)$ (under normal conditions a=0.6 and b=0.12).

Assuming that the t>28 days is the lower boundary:

$$\alpha_2(t) = 0.6 + 0.12 * \ln(28) = 0.99$$

When these parameters are used:

$$\alpha(t,\tau) = \alpha_1(t)\alpha_2(t) = 0.8 * 0.99 = 0.79$$

$\varphi(t,\tau)$ the creep coefficient according to some modern code assumed to be deterministic.

β_d the ratio of the permanent load to the total load and depends on the type of the structure; generally β_d is between 0.6 and 0.8.

For the strength of concrete a log-normal distribution is recommended. The strength of concrete at a particular point I in a given structure j as a function of standard strength f_{co} is given as:

$$f_{c,ij} = \alpha(t,\tau)(f_{co,ij})^{\lambda} Y_{1,j}$$

$$f_{co,ij} = \exp((U_{ij}\Sigma_j + M_j))$$

in which

$f_{c0,ij}$ log-normal variable, independent of $Y_{i,j}$, with distribution parameters M_j and Σ_j

M_j the logarithmic mean at job j

Σ_j the logarithmic standard deviation at job j

$Y_{1,j}$ a log-normal variable representing additional variations due to the special placing, curing and hardening conditions of in situ concrete at job j.

U_{ij} a standard normal variable representing the variability within one structure

λ lognormal variable with mean 0.96 and coefficient of variation 0.005; generally it suffices to take λ deterministically

Using the function from strength in relation to tensile strength, strain and modulus of elasticity:

$$f_{ct,ij} = 0.3 * f_{c,ij}^{2/3} * Y_{2,j}$$

$$E_{c,ij} = 10.5 * f_{c,ij}^{1/3} * Y_{3,j}(1 + \beta_d \varphi(t,\tau))^{-1}$$

$$\varepsilon_{u,ij} = 6*10^{-3} * f_{c,ij}^{-1/6} * Y_{4,j}(1 + \beta_d \varphi(t,\tau))$$

The variables $Y_{2,j}$ to $Y_{4,j}$ mainly reflect variations due to factors not well accounted for by concrete

Compressive strength (like gravel type and size, chemical composition of cement and other

ingredients, climatically conditions).

Variable	Distribution type	Mean	Coefficient of variation	Related to
$Y_{1,j}$	LN	1.0	0.06	Compression
$Y_{2,j}$	LN	1.0	0.30	Tension
$Y_{3,j}$	LN	1.0	0.15	E-modulus
$Y_{4,j}$	LN	1.0	0.15	Ultimate strain

Table 42: Data for parameters Yi

If no specific information is given the values can be based on **Error! Reference source not found.**.

Concrete type	Concrete grade	Parameters			
		m'	n'	s'	v'
Ready mixed	C15	3.40	3.0	0.14	10
	C25	3.65	3.0	0.12	10
	C35	3.85	3.0	0.09	10
	C45	3.98	3.0	0.07	10
	C55	-	-	-	-
Pre-cast elements	C15	-	-	-	-
	C25	3.80	3.0	0.09	10
	C35	3.95	3.0	0.08	10
	C45	4.08	4.0	0.07	10
	C55	4.15	4.0	0.05	10

Table 43: Parameters for concrete strength distribution (f_{co} [MPa])

Under the condition that n'*v'> 10, a log-normal distribution can be assumed:

$$f_{co} = LN(m'; s' \sqrt{\frac{n'}{n'-1} \frac{v'}{v'-2}})$$

For the "Lyondell jetty" the quality of C28 has been used. Since the this is not taken into account in

Error! Reference source not found. this is calculated:

Ready mixed

$$m' = 2.2962 * x^{0.1447} = 2.2962 * 28^{0.1447} = 3.72$$

$$s' = -0.0024 * x + 0.177 = -0.0024 * 28 + 0.177 = 0.11$$

pre-cast elements

$$m' = 2.6351 * x^{0.1139} = 2.6351 * 28^{0.1139} = 3.85$$

$$s' = -0.0013 * x + 0.125 = -0.0013 * 28 + 0.125 = 0.09$$

Using these interpolations:

Ready mixed concrete:

$$f_{co} = LN(3.72;0.11\sqrt{\frac{3}{3-1}\frac{10}{10-2}}) = LN(3.72;0.15)$$

Pre-casted elements:

$$f_{co} = LN(3.85;0.09\sqrt{\frac{3}{3-1}\frac{10}{10-2}}) = LN(3.85;0.12)$$

Compression strength:

$$f_{c,ij} = 0.79 * f_{co,ij}^{LN(0.96;4.8*10^{-3})} * LN(1;0.06)[MPa]$$

Tensile strength:

$$f_{ct,ij} = 0.3 * f_{c,ij}^{2/3} * LN(1;0.3)$$

Modulus of elasticity:

$$E_{c,ij} = 10.5 * f_{c,ij}^{1/3} * LN(1;0.15)$$

Ultimate compression strain:

$$\varepsilon_{u,ij} = 6 * 10^{-3} * f_{c,ij}^{-1/6} * LN(1;0.15)$$

Y. Clay p-y curve

Clay

According to the NEN-EN ISO 19902 capacity of clay is given:

$$p_r = p_0'D + Jc_u X$$

This is limited by:

$$p_r = 9 * c_u * D \text{ for } X > X_R$$

J is an empirical constant with values ranging from 0.25 for weak clay up to 0.5 for stiff clay**Error! Bookmark not defined.**. These values are determined by field testing, common practice being to use 0.5. It's not known how these values are distributed therefore the value of van der Horst is assumed:

$$J = N(\mu_j; 0.1\mu_j)$$

For the half strain the M-pile user manual recommends the use of the values:

c_u [kN/m^2]	ε_{50} [-]
5-25	0.020
25-50	0.010
50-100	0.007
100-200	0.005
200-400	0.004

Table 44: Determination of ε_{50} as a function of the undrained cohesion

These values can be described with the relation:

$$\varepsilon_{50} = 0.0459 * c_u^{-0.4268}$$

In the API the shape of the soil resistance-displacement is not given as a function but defined as points (see **Error! Reference source not found.**).

X>X$_R$		X<X$_{R0.3}$	
p/p$_r$	y/y$_R$	p/p$_r$	y/y$_c$
0	0	0	0
0.23	0.1	0.23	0.1
0.33	0.3	0.33	0.3
0.50	1.0	0.50	1.0
0.72	3.0	0.72	3.0
0.72		0.72X/X$_R$	15.0
		0.72X/X$_R$	

Table 45: Mobilized lateral resistance-displacement data for equilibrium condition of cyclic actions

These values can be described as a part of a continuous curve. The M-Pile manual gives:

$$p/p_u = \begin{cases} 0.5(y/y_{50})^{1/3} & for" y" < 3y_{50} \\ 0.72 & for" y" \geq 3y_{50} \end{cases} forX > X_R$$

$$p/p_u = \begin{cases} 0.5(y/y_{50})^{1/3} & for y < 3y_{50} \\ (0.06(y/y_{50}+0.54)(X/X_R-1) & for15y_{50} \geq y \geq 3y_{50} \\ 0.72(X/X_R) & for y > 15y_{50} \end{cases} forX < X_R$$

In which:

X$_R$ is the depth below soil surface of reduced resistance zone [m].

$$X_R = \frac{6D}{\gamma'D/c_u + J}$$

M-pile uses the mark points of 0.1y$_{50}$, 0.3y$_{50}$, y$_{50}$ and 3y$_{50}$ in the curve. The mark points will result in the relation:

y	Lateral resistance displacement relation
$0.1 * y_{50}$	$p = 0.5 p_u (0.1)^{1/3}$
$0.3 * y_{50}$	$p = 0.5 p_u (0.3)^{1/3}$
y_{50}	$p = 0.5 p_u (1)^{1/3}$
$3 * y_{50}$	$p = 0.72 p_u$

Figure 107: lateral resistance displacement relation of cyclic loading

The range of the distribution of the yield stress has a larger range than expected. The influence of this distribution has been subjected to further study. The JCSS suggests a lognormal distribution.

Z. Analyses of distributions

The yield stress of f_y= 455 [N/mm^2] varies between 262 to 1647 [N/mm^2]. The yield stress of f_y=480 [N/mm^2] has a range of 203 to 1274 [N/mm^2]. And for a yield stress of f_y=355 [N/mm^2] a range of 277 to 1740 [N/mm^2] is found. This is a very wide distribution.

$$f_y = LN(f_{ysp} *1.52 - 20;0.07*(f_{ysp}*1.52 - 20))$$

In which

f_{ysp} is the nominal value of a variable according the standards[Error! Reference source not found.]

The representative value of yield stress has a undershoot of 2.5%. After a quick check a undershoot of 7% is found. Also a max/min ratio of 6 is found.

Depending of the type of certificate the producer sells the steel, there will be no undershoot in relation to the representative yield stress.

The log normal distribution tends to show a similar shape as the normal distribution for higher values of the mean. Therefore the normal distribution is taken instead of the log normal. In the normal distributions no values are drawn lower than the representative yielding stress.

The yield stress of f_y= 455 [N/mm^2] varies between 505 to 832 [N/mm^2]. The yield stress of f_y=480 [N/mm^2] has a range of 533 to 880 [N/mm^2]. And for a yield stress of f_y=355 [N/mm^2] a range of 390 to 643 [N/mm^2] is found. This is a very wide distribution.

The distribution of the wall thickness is taken in to account in the Monte Carlo simulation (see Table 12) and determines partly the stiffness of the pipes (see Table 46). The values that were found here are considered to be very wide.

t [mm]	22.2	25	28	30	38	40
Max	0.0278	0.031965	0.0369874	0.0374	0.04636	0.049544
Min	0.016648	0.01887	0.01915	0.023337	0.02976	0.030429

mean	0.022558	0.025038	0.027798	0.02982	0.03824	0.04006

Table 46: Wall thickness of 122 drawings.

Making a brief calculation for comparison between the moment of inertia (D=1820 [mm]):

$I(t=40 \text{ [mm]})= 8.8633*10^{10} \text{ [mm}^4\text{]}$

$I(t=30 \text{ [mm]})= 6.7586*10^{10} \text{ [mm}^4\text{]}=0.76* I(t=40 \text{ [mm]})$

$I(t=50 \text{ [mm]})= 1.0696*10^{11} \text{ [mm}^4\text{]}=1.21* I(t=40 \text{ [mm]})$

Soil model

The soil depends of the volume weight and the angle of internal friction. An additional analyses is done to these variables. Based on this additional analyses is decided to change the type of distribution and limit the distribution to more physical correct values.

In the exploratory analyses the characteristics of the soil behavior is analyzed. In this analyses the soil stiffness is considered at a depth of NAP- 21 [m] and NAP -31 [m]. Per base variable the influence on the p-y curve is analyzed.

In first a classical sensitivity analyses is done, in which the soil characteristics are assumed to be lognormal.

In the model is a spring build every two meters. As determined earlier the spring stiffness is described as a tanh(X) function (see chapter "structure analyses").

Angle of internal friction values	Sand (NAP-17,6) [^{0}]	Clay, Sandy (NAP-24.7) [^{0}]	Peat (NAP-26.5m) [^{0}]	Clay Sandy (NAP-27.3m) [^{0}]	Sand (NAP-27.8 m) [^{0}]	Sand (NAP-32 m) [^{0}]
Gem	26.15	24.5	15..2	24.5	34.3	37.9
Stdev	2.8	6.9	2.6	6.8	6	6.5
Min	18.9	10.1	8.7	10.2	20.2	22.2
max	35.9	51.6	24.4	53.9	60.3	85.6

Table 47: Results of 8000 draws of angle of internal friction for all soil layer from a lognormal distribution.

Volume weight values	Sand (NAP-17,6) [kN/m^3]	Clay, sandy (NAP-24.7) [kN/m^3]	Peat (NAP-26.5m) [kN/m^3]	Clay Sandy (NAP-27.3m) [kN/m^3]	Sand (NAP-27.8 m) [kN/m^3]	Sand (NAP-32 m) [kN/m^3]
Gem	19.2	18.2	12.4	18.2	20.1	20.1
Stdev	2.8	2.7	3.6	2.7	1.99	2
Min	11.6	11.5	4.9	11.7	15.1	13.2
max	30.6	26.3	25.2	30.6	28.3	26.9

Table 48: Results of 8000 draws of Volume weight for all soil layer from a lognormal distribution.

These values are very wide and don't meet the physical expected values. Therefore new drawings are done with help of a normal distribution instead of the lognormal and the number are bounded with 2-98%. This results in values that meet the physical values and these are used for soil modeling (see Table 49 and Table 50).

Angle of internal friction waarden	Sand (NAP-17,6) [^{0}]	Clay, Sandy (NAP-24.7) [^{0}]	Peat (NAP-26.5m) [^{0}]	Clay Sandy (NAP-27.3m) [^{0}]	Sand (NAP-27.8 m) [^{0}]	Sand (NAP-32 m) [^{0}]
Gem	26.00	23.7	15	23.7	33.7	37.5
Stdev	0.44	0.55	0.22	0.56	0.55	1.12
Min	24.2	22	14.3	22	32	34.3
max	27.2	25.4	15.7	25.5	36	41.1

Table 49: Results of 8000 draws of angle of internal friction for all soil layer from a normal distribution.

Volume gewicht Waarden	Sand (NAP-17,6) [kN/m^3]	Clay, Sandy (NAP-24.7) [kN/m^3]	Peat (NAP-26.5m) [kN/m^3]	Clay Sandy (NAP-27.3m) [kN/m^3]	Sand (NAP-27.8 m) [kN/m^3]	Sand (NAP-32 m) [kN/m^3]

Gem	19.0	18.0	12.1	18.1	20.0	20.0
Stdev	0.44	0.44	1.1	0.44	0.22	0.22
Min	17.5	16.7	8.8	16.4	19.4	19.2
Max	20.5	19.6	15.2	19.2	20.8	20.7

Table 50: Results of 8000 draws of Volume weight for all soil layer from a lognormal distribution.

The resistance of the soil at a depth of Nap-21 [m] and at a depth of NAP-31[m] is analyzed. The points of measurement are a function of the ultimate soil strength (see chapter "structural analyses"). The amount of distribution per point is getting wider when reaching the ultimate values.

Angle of internal friction	P(y1) [N/m]	P(y2) [N/m]	P(y3) [N/m]	P(y3) [N/m]	P(y4) [N/m]
Gem	113426	214014	352708	419190	456919
Stdev	3654	6894.9	111363	13505	14720
Min	99698	188112	310018	368454	401616
max	123630	233265	384434	456896	498019

Table 51:Results of resistance of the 8000 drawings for angle of internal friction

Volume gewicht	P(y1) [N/m]	P(y2) [N/m]	P(y3) [N/m]	P(y3) [N/m]	P(y4) [N/m]
Gem	113449	214058	352779	419046	456762
Stdev	5669	10696	17629	20952	22837
Min	94489	178284	293822	349205	380635
max	132285	249598	411351	488887	532889

Table 52: Results of the resistance of the 8000 drawings for Volume weight

When the track of the p-y curve is further of the origin is removed the standard deviation becomes larger. The share of the stiffness of both the variables is almost the same, considering the resistance there is no major differences. Due to the volume mass the standard deviation becomes larger.

Conclusion and recommendations

Because of a wide range of results the yield stress with the log-normal distribution, knowing that the producer of steel will sort out the lower yielding stress, and that the log-normal is almost similar to the normal distribution at high values of the mean, the distribution is replaced with a normal distribution. After verification with Prof Bijlaard he gave a mean of $1.1628*f_{y,rep}$. This in contrast to the mean chosen from the

JCSS. Also in previous analyses is concluded that the log-normal distributions of Excel give unexpected wide range of numbers.
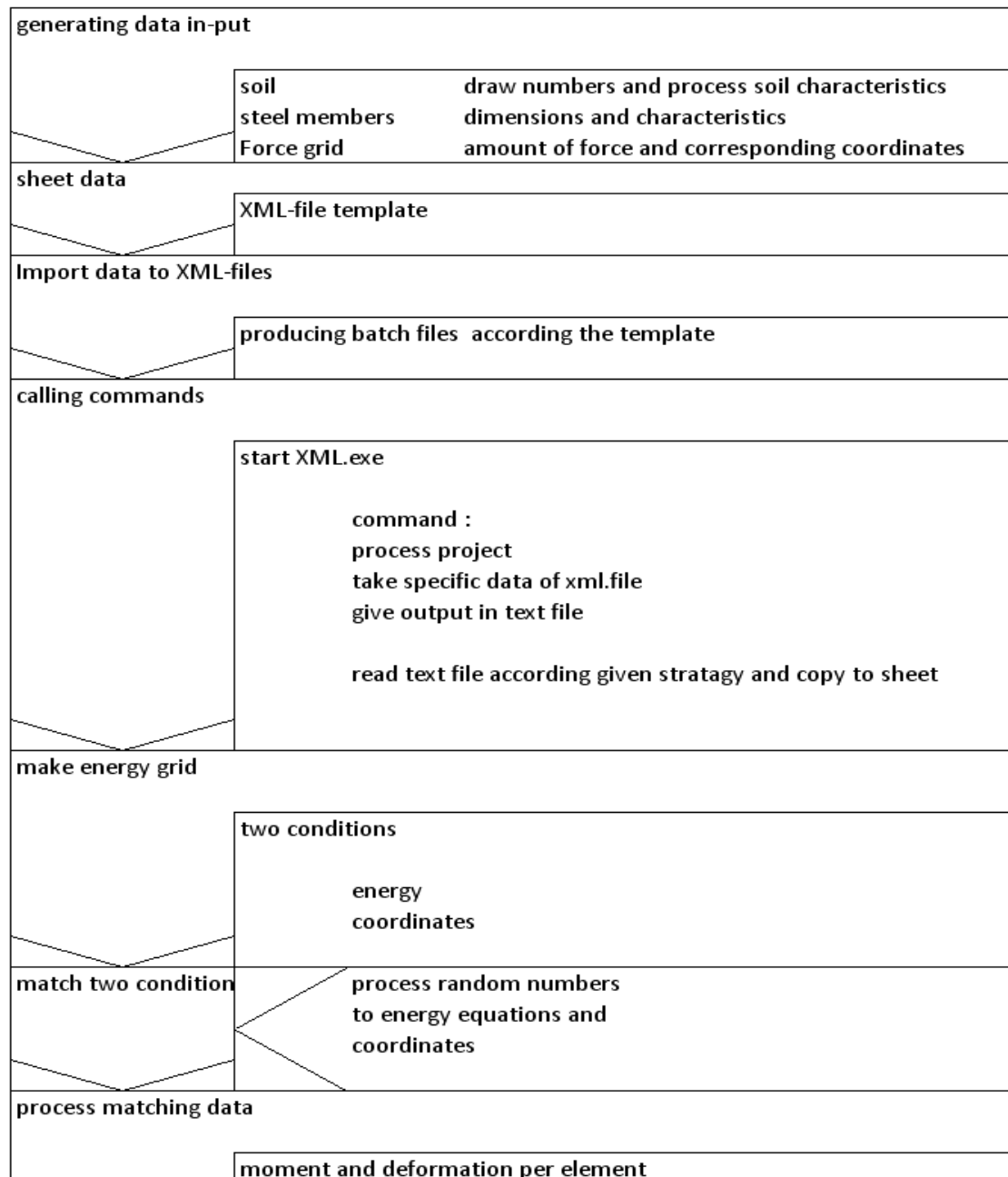
The wall thickness of the tubes have a deviation of 25% in relation to the mean. This will give approximately a deviation of 20% of the mean stiffness. According to the certificate of the a tube manufacturer the outer diameter will have no larger deviation than +0.5 of -0.5 [mm]. So this is considered to be very wide range.

In practice the mean of the wall thickness is taken as representative value. In contrary to the other variables of strength were a lower limit is maintained. If a lower limit would be maintained would this effect the stiffness. In structures were a curtain stiffness is expected a lower limit would not be desirable.

The distributions of the variables of soil can be disrobed with a normal distribution according to the JCSS. But one must be aware for non-physical values. The deviation of angle of internal friction and volume weight resulting from the adopted distribution have a non physical wide range. Therefore a normal distribution is adopted and the range of drawn numbers is bounded.

AA. Flow chart of data and commands

To come to the Monte Carlo results some events have to take place in specific order. These events edit the in-put data and process them to the results. The whole system is described beneath.

```
generating data in-put

                    soil                draw numbers and process soil characteristics
                    steel members       dimensions and characteristics
                    Force grid          amount of force and corresponding coordinates
sheet data
                    XML-file template

Import data to XML-files

                    producing batch files  according the template

calling commands

                    start XML.exe

                            command :
                            process project
                            take specific data of xml.file
                            give output in text file

                            read text file according given stratagy and copy to sheet


make energy grid

                    two conditions

                            energy
                            coordinates

match two condition         process random numbers
                            to energy equations and
                            coordinates

process matching data

                    moment and deformation per element
```

BB. Excel linked with a XML-file

Scia-engineer has the ability to use different methods for data input and output. It is possible to regulate this from outside the Scia-executer making it possible for other software to communicate with Scia-software. In this specific case excel is using visual basic (see for a flow chart the appendix). Scia-engineer software implements data saved in a XML-file of the '.esa' project as a batch file. Specific data from a model is saved according to a specific structure (the syntax). The XML-files are a platform for external software to manipulate the model. With excel-macro (Visual Basic) the executer is triggered and the XML-files are manipulated making it representative for the project. The processed data are put in text files, one for every run, and stored in a specific map, by using a loop in the syntax. After all runs are done the data is read from these text files. The events with their relation are specified in Figure 108.
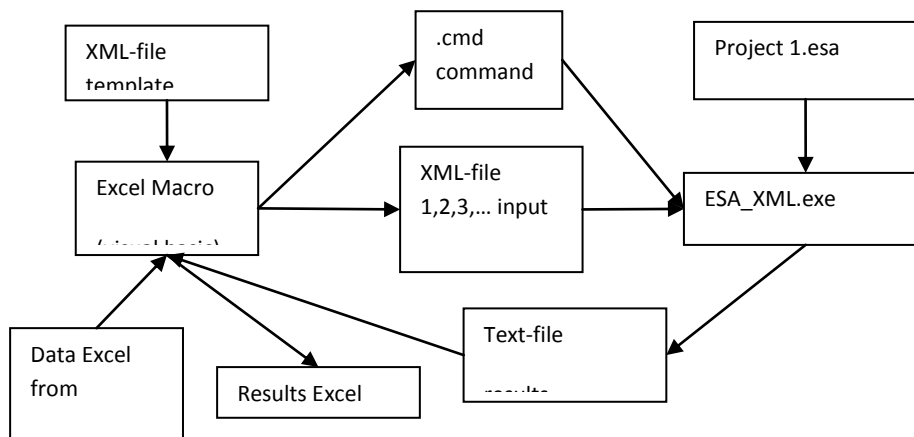
Figure 108: Relation diagram of data storage and processing

In the XML-file some specific structure is used. In this syntax an object including the project characteristics are defined. Normally these characteristics are fixed, but with the indication of "_&A&_" the macro create batch files. After setting up the XML-files to run the excel macro will produce a .cmd file for commanding the XML_ESA.exe (executer) to:

- start running.
- load in the XML-file and the .esa file and run the calculation.
- After the calculation the .cmd file demands the XML_ESA.exe to put the result in a .txt file.
- The macro of the excel file is able to read in the .txt files and sort out the results.

To recognize the data of the results the visual basic uses marks, column and row numbers (Figure 109).

```
Niet-lineaire berekening, Extreem : Snede, Systeem
Zie tabel 1

Tabel 1
Staaf   Mx  [kNm]      My  [kNm]       Mz  [kNm]
S221    175,11  611,27  -0,29
S221    175,11  611,27  -0,29
S222    175,11  591,00  -0,12
S222    175,11  591,00  -0,12
S223    175,11  519,62  -0,08
S223    175,11  519,62  -0,08
S224    175,11  412,72  -0,05
S224    175,11  412,72  -0,05
S225    175,11  291,34  -0,05
```

Figure 109: Fragment from result in the text file

The excel visual basic will screen the text files for a specific word (first mark), for instance "Tabel 1". From this mark on the next mark will be found (see Figure 109). For instance the beam name "S222" (second mark). The column is specified by 'the second' and from this the value will be read (591.00).

CC.   Com-interface using Matlab

Using the COM-interface makes it possible to communicate for software to each other. The COM-interface makes it possible to use another interface. Direct behind the COM-interface is a library. This library can be called on by commands. When calling on the library directly the commands have to be made recognizable with the header file (see the appendix for the list of commands).
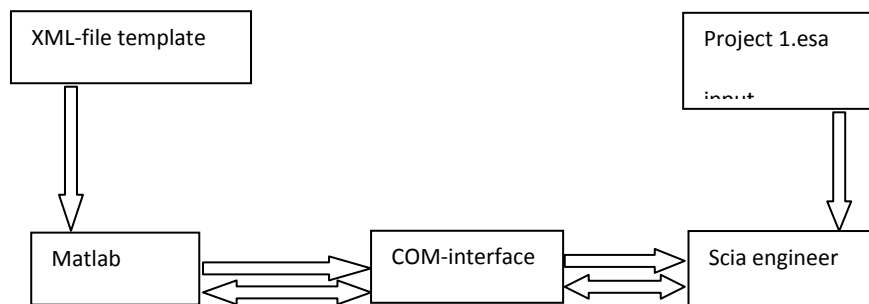
Figure 110: relation diagram of data storage and processing

Using the COM-interface the header file is unnecessary. The commands can directly be reclaimed.

From these commands the function can be called. So the program can be started, the saved model can be opened and run.

Using the XML-syntax the project can be described. From this the model can be manipulated by changing some of the parameters, in the XML-syntax and the type of calculation can be specified (linear or nonlinear).

The result can be asked back, processed and saved by Matlab. The data output of Scia is put in several different possible files (xml, text or esa-file).

Using Matlab has the advantage that Matlab is able to handle large quantities of data. Next to this the generator for random numbers is more reliable.

DD.   M-Pile

M-pile is a collection and a combination of several different methods of soil modelling in one interface. The program makes it possible to find out how a single pile and a pile group react on horizontal and vertical applied forces.

The program offers five different types of calculations modes (see Figure 111):

- Poulos
- Plasti-Poulos
- Cap- model
- Interaction Cap-model
- Dynamic model

Interaction and calculation models are schematized in the figure below[14.].

Poulos

In this mode[15.] the soil is modelled as it were fully elastic and the calculations are made according Poulos/Randolph[16.]. There is only interaction through the cap, not through the soil.

Plasti-Poulos

In the soil behaviour track the plasticity is included. A plasticity factor is added in the original Poulos calculations.

Cap model

In this mode the pile-soil interaction is modelled by a Tilly program. Soil is assumed elasto-plastic and the interaction of the piles are only by the cap. The soil is only modelled as it were springs that do not inflict with each other.

Cap soil interaction model

The pile-soil interaction is modelled by a Tilly progam, with soil that is assumed elasto-plastic. The pile-soil-pile interaction is modelled according to Mindlin, with a constant Young's modulus assumed over the depth.

Cap layered soil interaction model

Soil is assumed to be elasto-plastic. The pile-soil-pile interaction for layered soil is performed. Calculation are made by a finite element method and the Tilly program.

Dynamic model

This mode is a dynamic analysis based on the cap model. A collision of a ship is simulated in the this mode.

No interaction through the soil (Infinitely stiff environment)

Interaction through the elastic soil with local plastic soil behavior

Interaction through the elastic soil (two layers)

Interaction through the elastic soil with a possible local plastic behavior of the soil (two layers)
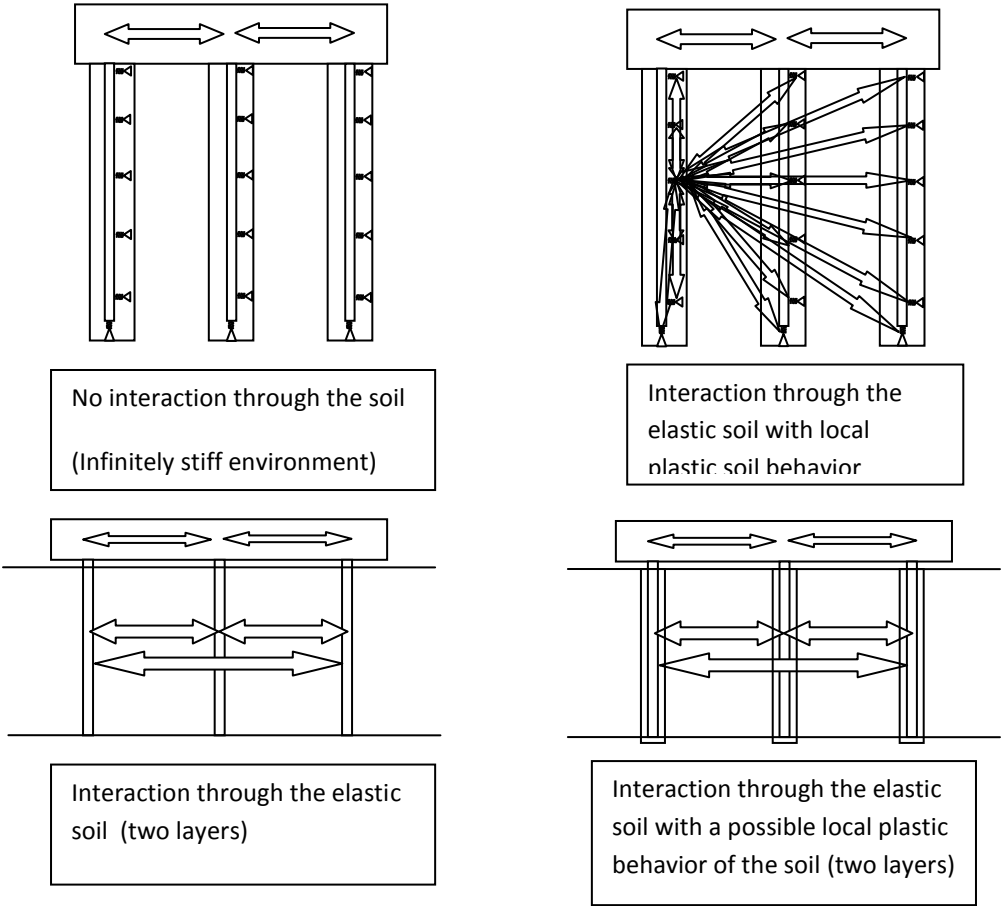
Figure 111: schematization of the different interaction models and analyses

EE. Interaction of piles through the soil

In several cross sections of the jetty the piles are standing in row and very near each other. Due to the horizontal soil pressure this can have an influence on the deformation and strength of the jetty.

To have some idea of the influence of the interaction between the piles through the soil, a basic calculations is done. In order to explore the possible influence of elastic interaction between the piles.

The elastic soil pressure is approximated using a hand calculation. Based on the force calculations using M-pile (see Figure 112)
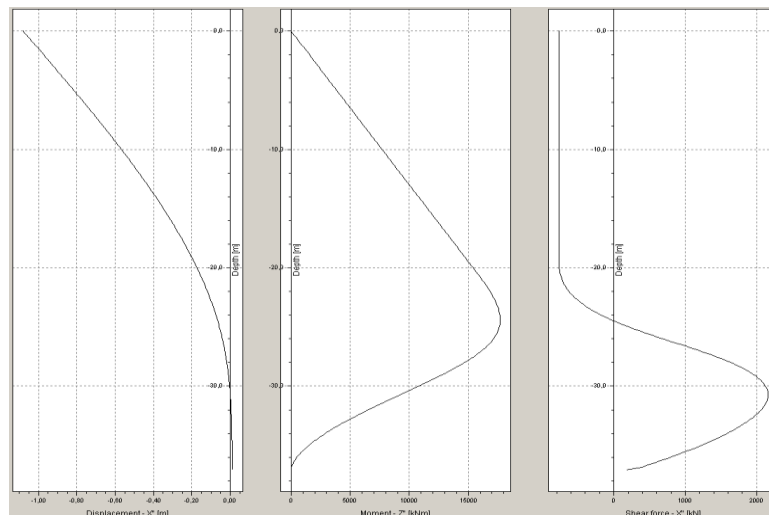
Figure 112: width of the pile is 1.82 [m] and wall thickness is 0.0142 [m] applied force of 770 [kN].
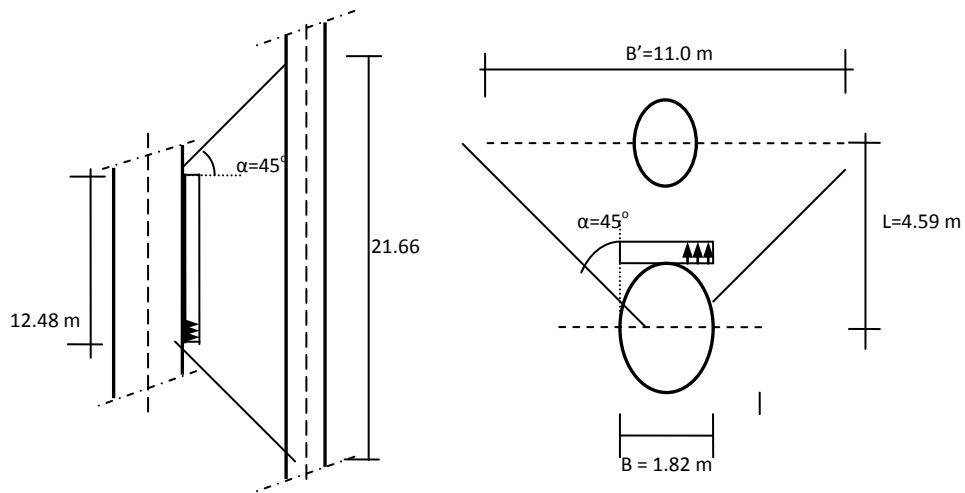
Figure 113: left, elastic distribution in horizontal plane and right: elastic distribution in vertical plane

The original shear forces in the fender beam converted into a point load.

$$F_1 = 0.5*2160*12.5 = 13478.4[kN]$$

After converting into a point load, the load is even distributed over the length.

$$q_1 = \frac{F_1}{l} = \frac{13478.4}{12.48} = 1080.7[kN/m]$$

Line load equal distributed across the width of the pile:

$$q_1' = \frac{q_1}{b} = \frac{1080.7}{1.82} = 5593.8[kN/m^2]$$

The two areas near the piles:

$$A_1 = 21.66*11 = 238.26[m^2]$$

$$A_2 = 1.82*12.48 = 22.7[m^2]$$

Horizontal soil pressure near the second pile:

$$q_2 = \frac{13478.4}{238.26} = 56.57[kN/m^2]$$

Surface that the soil is inflicting the pile:

$$A_2' = 21.66*1.22 = 26.42[m^2]$$

$$F_2 = 56.57*26.42 = 1495[kN]$$

Percentage of the initial pressure:

$$\frac{F_2}{F_1} = \frac{1495}{13478.4} = 0.11 \rightarrow 11[\%]$$

FF.   Model behaviour

The soil will be modelled using two different software programs. To make a reliable model these programs will be considered in their similarities, differences and their boundaries.

Comparison of model in 'Scia-engineering' and 'M-pile'
To make a comparison between both software programs a model will be made (see Figure 114). The model will be loaded by the same loads and the deflection of the top will be monitored. From these results an analyses will be made about the behaviour of the models, if they show comparable behaviour or different behaviour.

The model of the pile will first be run in M-pile for the characteristic p-y curve values. The characteristic values of the soil will then be used in non linear springs of the model in Scia-engineering.

The characteristics for soil of sand are (γ_{sat}=19 kN/m^3, c'=0 kPa, φ'= 27^0)
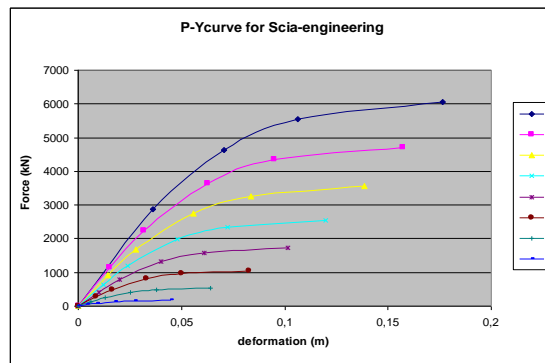
Figure 114: The P-Y characteristics derived from the M-pile model

Scia-engineering has the ability to simulate a bed with non-linear soil characteristics.

In this analysis a comparison is made between both programs with a similar model. The applied force varies and the comparison deflection is measured.

The Scia-model has non linear springs every two meters from the base on. With the same p-y curve characteristics as the model in M-pile. The dimensions of the pile are d=1820 mm with a width of t=14 mm.
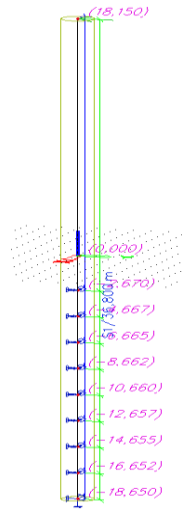
Figure 115: model of pile in Scia-engineering
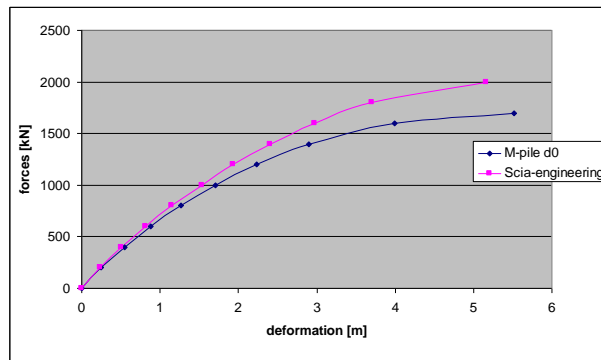
Figure 116: graph of the deflection of the pile top with applied forces

The two curves are comparable for the first meter. The M-pile model has a very recognizable plastic deformation that sets in at a load of 2000 [kN]. In the results of M-pile there is a very recognizable part where the failing of the pile starts. The soil is deforming plastic and has reached its capacity. In the Scia-engineering model there is only al little plastic deformation recognizable. For further loading it still shows no sign of fully plastic deformation, which one would expect.

Since the range of allowable deformation is about a half a meter to a meter. Both the models react comparable.

GG.   Comparison of the used sheet for soil modeling and M-pile

Sheet is made for introducing the p-y curves in the finite element model. The curves at the some shallow soil differ. The curve of the sheet are more stiff then the M-Pile. For the more deeper soil the curves get more in the similar. The difference of the curves are accepted because the contribution of the realy shallow soil is very small in comparison to the more deeper. For further studies this should be better optimized.
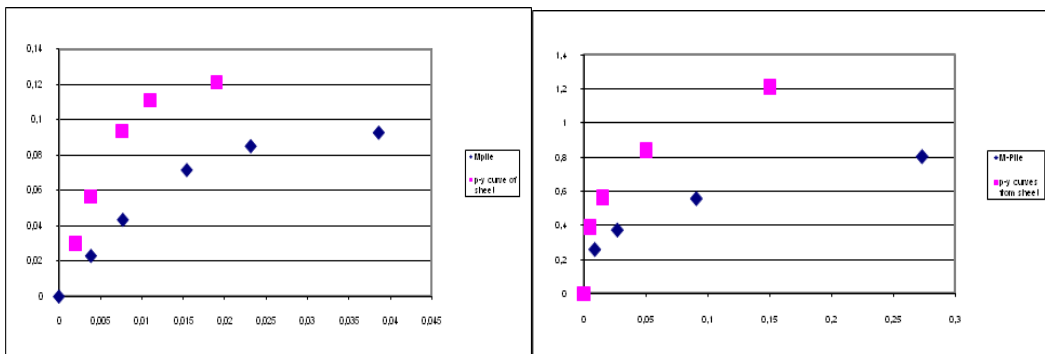
Figure 117: left p-y curves at a depth of NAP-25 [m] right p-y curves at a depth of NAP-19 [m]
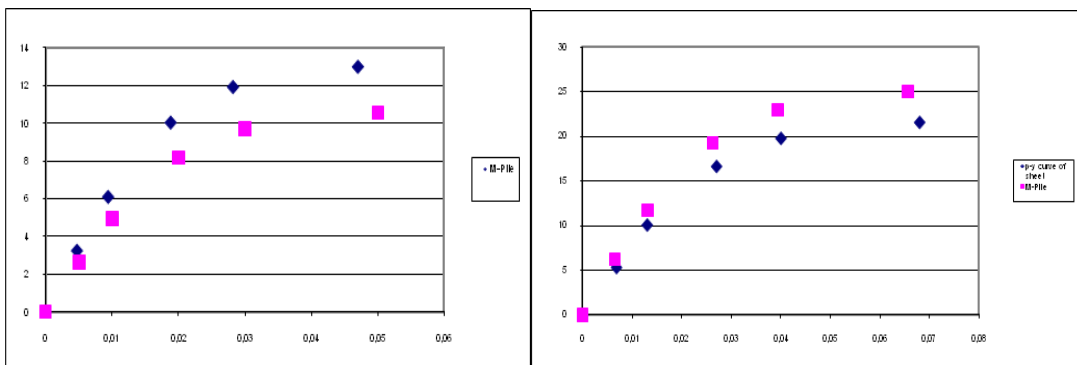
Figure 118: Left: p-y curves at a depth of NAP-33 [m] RIgth: p-y curves at a depth of NAP-39 [m]

HH.   Soil modelling due to spring behaviour

When using M-pile and Scia-engineering for modelling should be considered the behaviour of the models against reality. The pile will be loaded laterally which will give a load in the soil in the horizontal plane. The soil will be all around the pile and will not differ in characteristics in the horizontal plane. The soil will have the same reaction to applied forces in every direction (see left of Figure 119). This will give the same deflection of the top from the centre in any direction.

X
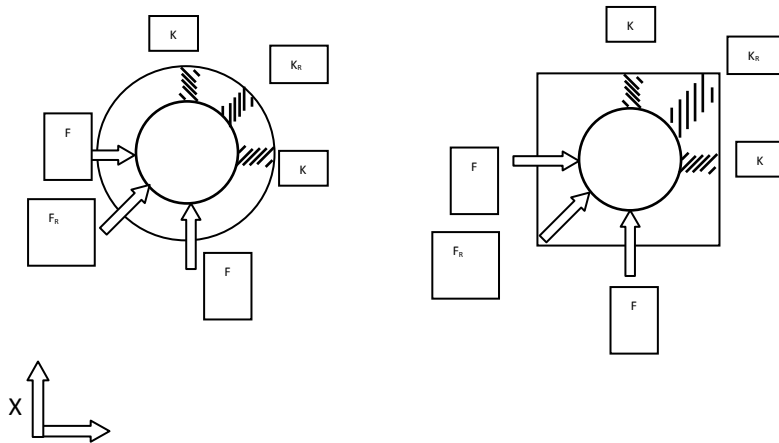
Figure 119: schematization of the soil in M-pile and Scia-engineering

Using M-pile and Scia-engineering model the soil will be modeled as springs in two directions.

This will give a difference in deflection when a force is applied out of the X or Y plane. Test is done with a model in both programs.
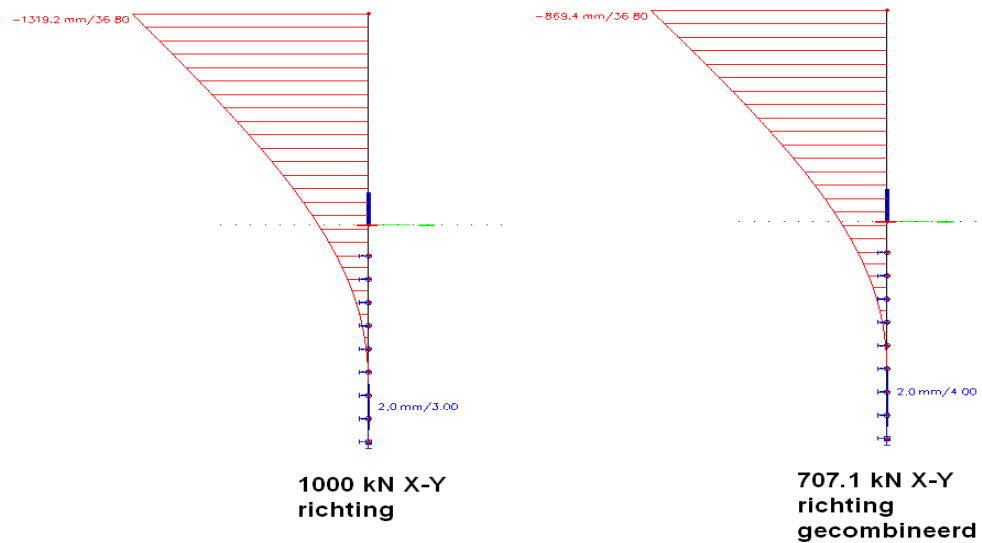
A run is made with F=1000 kN and one run is done with a applied force F_R.

The F_R will be applied in the x and y plane:

$$F_R = \frac{1000}{\sqrt{2}} = 707.1 kN$$
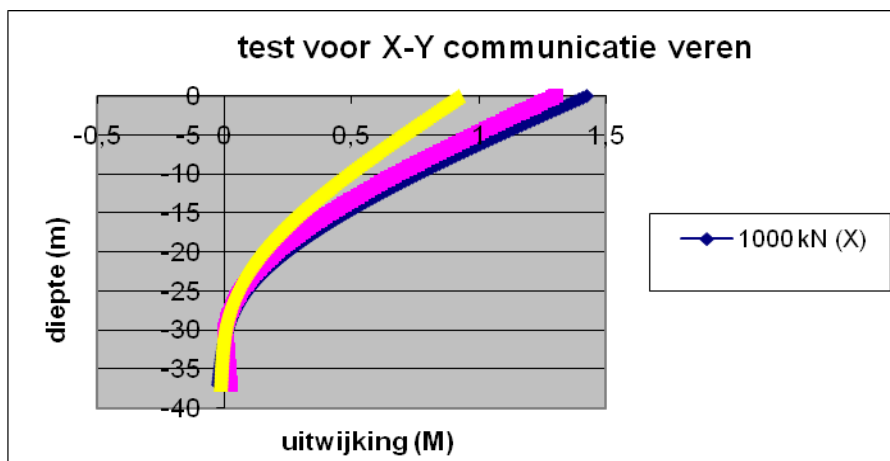
Figure 120: deflection of model in M-pile

Figure 121: deflection of model in Scia-engineering

When applying F_R de deflection of the model differs from the deflection of applied force F, the deflection is smaller, which will be the product of a stronger spring.

Since the probabilistic model is only loaded in one plane, the model will have to rule out any influence of forces in the other planes.

II. Comparison of results grids

The amount of measurement points will influence the calculation time and the ratio of accurate measurement. For this three different grids are tested (2 (m), 1 (m) and 0,5 (m)).

In this model three load cases are applied on the structure.
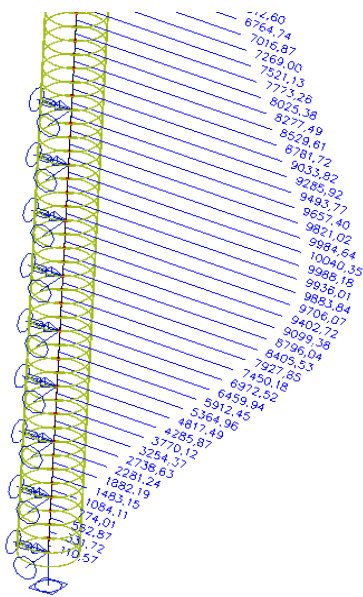
Figure 122: Grid of 0,5 (m)
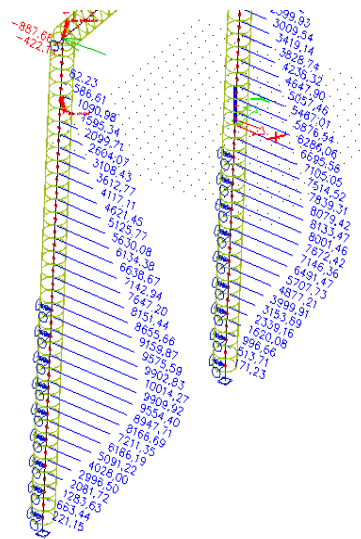
Figure 123: Grid of 1 (m)

Figure 124: Grid of 2 (m)
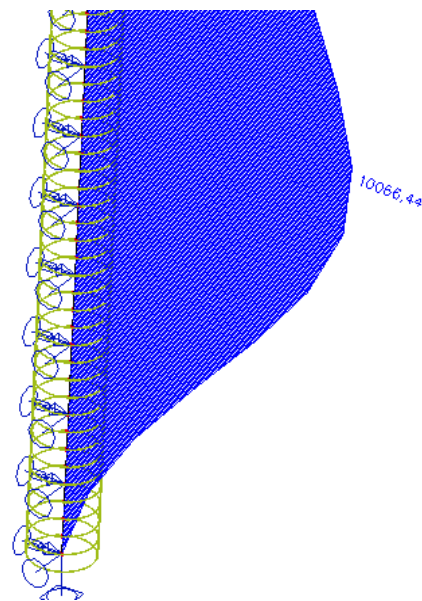
Figure 125: Actual max moment given by Scia-engineer

Considering the maximum amount of force:

- 10066,44 (kNm) actual max moment by Scia-engineer.
- 10040,35 (kNm) with a grid of 0,5 (m) 0.2 $\%$
- 10014,27 (kNm) with a grid of 1 (m) 0.5$\%$
- 9332,15 (kNm) with a grid of 2 (m) 7$\%$

The 0,5 (m) and the 1 (m) grid have a difference of 1 $\%$ and between 1 (m) and 2 (m) is 7 $\%$.

Considering the deformation:

The deformation is calculated due to a point load of 1000 (kN).
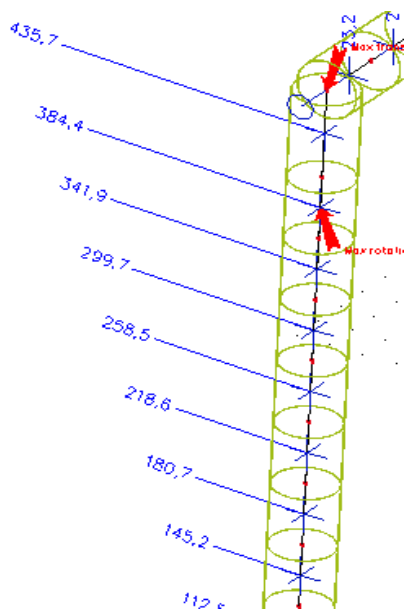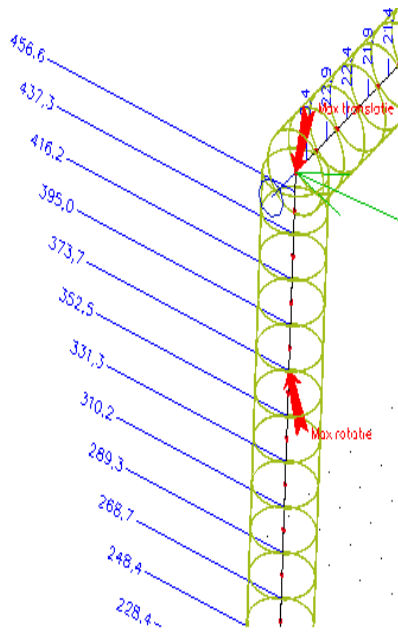

Figure 126: grid of 2 (m)
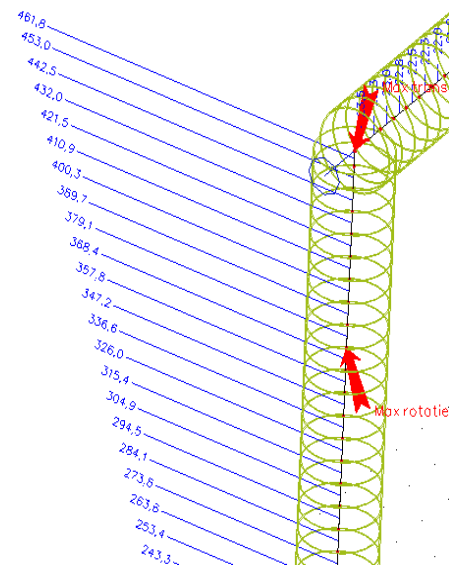
Figure 127: grid of 0,5 (m)

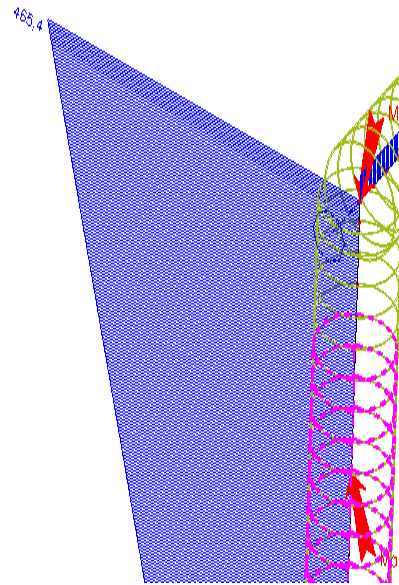**Figure 128: grid of 1 (m)**

**Figure 129: value of deformation at the end
of the bar (actual max deflection)**

Considering the maximum amount of deformation:

- 465.4 (mm) given by Scia-engineer as the max deformation
- 461.8 (mm) with a grid of 0,5 (m) $0.7^0/_0$
- 456.6 (kNm) with a grid of 1 (m) $1.8^0/_0$
- 435.7 (kNm) with a grid of 2 (m) $6.4^0/_0$

The 0,5 (m) and the 1 (m) grid have a difference of $1^0/_0$ and between 1 (m) and 2 (m) is $5^0/_0$. To make sure the analyses will be sufficient accurate and the calculation time will be effective. From this analyses can be concluded that the grid of 1 m would be sufficient accurate.

JJ.   Exploration of the berthing beam grid

Within the limit state only the maximum moment and the deformation is important. In limiting the amount of variables the behavior of this point is investigated.

Using a couple of load cases [11 load cases] on different places on the berthing beam, the moment is considered. The load cases are engaged every 2, 5 [m]. Because the current structure is symmetrical the behavior will be expected to be symmetrical. For this only the half of the structure is considered.

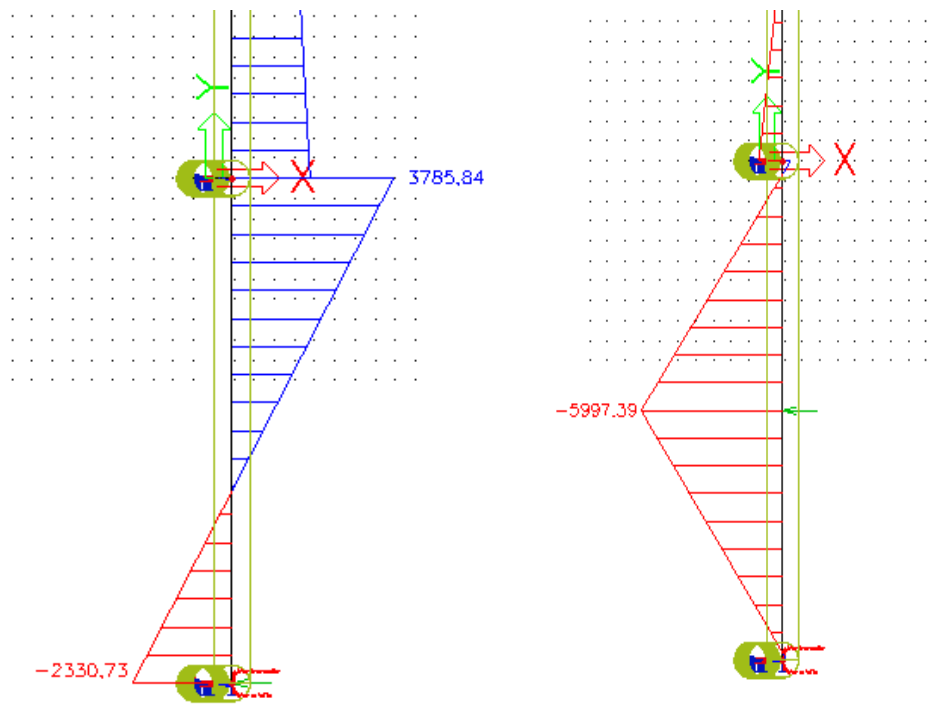In the following figures the moment due to the load cases are displayed.

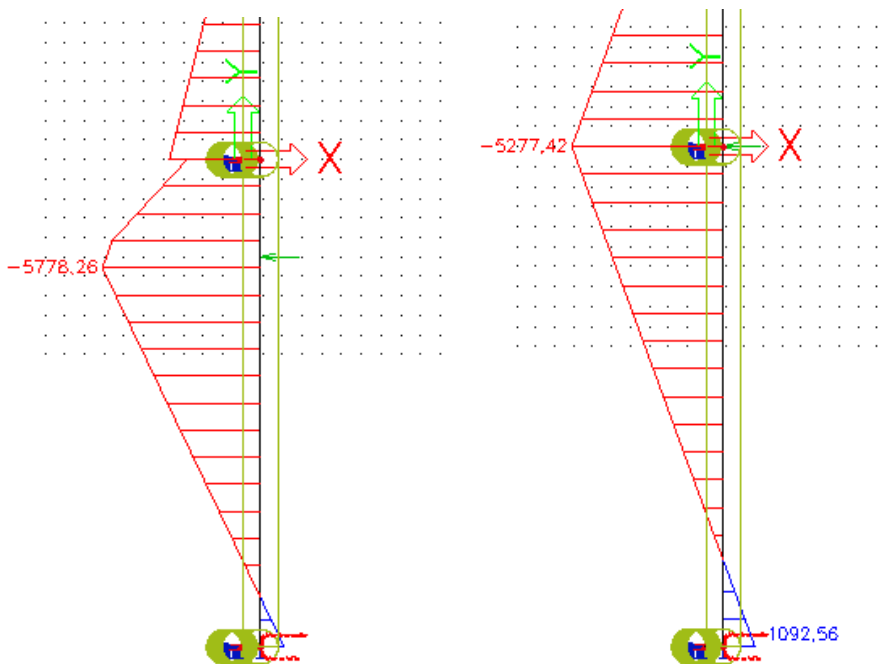**Figure 130: Moment due to load case 1 and 9, in top-view.**

Figure 131: Moment due to load case 8 and 10, in top- view.

From these cases the maximum moment is found at the coordinates of the applied forces and at location of the second pile.

It can be concluded that when monitoring moment at the applied forces and at the second pile the maximum moment will be found.

KK.   Overall distributions

In the early stages of this study there is a comprehensive study done on various parameters which are used in the design of a jetty. The results of this study is shown in the table below.

Parameter	Type of distribution	Mean	Standard deviation
Vessel weight [DWT][*]	Normal	38050	9025
Berthing velocity [m/s] [*]	Gumbel	$1.9247*m^{-0.3003}$	$0.44*1.9247*m^{-0.3003}$
Angle of berthing [^{0}][*]	Normal	7.5	1.25
Berthing coordinate [m][*]	Normal	0	2.5
Length [m][*]	Normal	$9.1647*DWT^{0.2861}$	$3.6094*DWT^{-0.4020}$
Width[m] [*]	Normal	$1.2958*(DWT/LOA)^{0.4065}$	$0.2062*(DWT/LOA)^{-0.2235}$
Draft[m] [*]	Normal	$3.1088*(DWT/LOA*D)^{0.7732}$	$0.7414*(DWT/LOA*D)^{-0.8610}$
Soil weight[m] [*]	Normal	$\gamma_{saturated}$	$0.075*\gamma_{saturated}$
Angle of friction [^{0}] [*]	Normal	$c_{saturated}$	$0.25*c_{saturated}$
Undrained shear strength [N/mm^2] [*]	Normal	$c_{u,calculated}$	$0.5*c_{u,calculated}$
Half strain [N/mm^2]	Normal	$8*10^{-6}*c_u+0.0036$	$0.25*(8*10^{-6}*c_u+0.0036)$
Coefficient J [-]	Normal	0.5	0.05
Steel yielding strength [N/mm^2] [*]	Normal	$f_{sp}*1.52-20$	$0.07*(f_{sp}*1.52-20)$
Steel ultimate strength [N/mm^2]	Normal	$B*E[f_u]$	$0.04*B*E[f_u]$
E-modulus [[N/mm^2]	Normal	E_{sp}	$0.03*E_{sp}$

Driving depth [m]	Normal	$D_{aimeddpeth}$	0.1
Wall thickness [m] (*)	Normal	$t_{ordered}$	$0.1 * t_{ordered}$
Corrosion [m]	Uniform	0.003/0.002/0.001	0.00086/0.00058/0.00029
Basic concrete insitu mixed concrete [N/mm^2]	Log-Normal	3.72	0.15
Basic concrete ready mixed concrete [N/mm^2]	Log-Normal	3.85	0.12
In situ compression strength [N/mm^2]	Log-Normal	$0.97 * f_{c,ij}{}^{\wedge}$	$0.06 * 0.97 * f_{c,ij}{}^{\wedge}$
Tensile strength [N/mm^2]	Log-Normal	$0.3 * f_{c,ij}{}^{2/3}$	$0.3 * 0.3 * f_{c,ij}{}^{2/3}$
Modulus of elasticity [N/mm^2]	Log-Normal	$10.5 * f_{c,ij}{}^{1/3}$	$0.15 * 10.5 * f_{c,ij}{}^{1/3}$
Ultimate compression strain [N/mm^2]	Log-Normal	$6 * 10^{-3} * f_{c,ij}{}^{-1/6}$	$0.15 * 6 * 10^{-3} * f_{c,ij}{}^{-1/6}$
Variation of in situ strength of standard test [N/mm^2]	Log-Normal	0.96	$4.8 * 10^{-3}$

Table 53: Distributions of variables ((*) are the variables that are used in the simulation).